The Use of Coated Piezoelectric Crystals for the Determination of CO and CO_2

by

Christine Anne Pankhurst M.Sc.,D.I.C.

A thesis submitted for the degree of Doctor of Philosophy of the University of London.

September 1976

Department of Chemistry,
Imperial College of Science and Technology,
South Kensington,
London.
SW7 2AY

Abstract

The development of the quartz crystal microbalance and its modification to the piezoelectric sorption detector are reviewed and discussed, following a brief review of air pollution and the current methods of monitoring inorganic air pollutants. The fundamental equations relating the change in frequency to added mass are developed according to Sauerbrey, Lostis and Stockbridge. A complete analytical system is described based on a 9.0 MHz AT Cut crystal operated in its fundamental mode in a flowing gas stream. The equipment used is described in detail and consists of:- oscillator circuits and associated power supplies, and oxygen-free-nitrogen gas flow system, detector cells and coated crystals, digital counter for monitoring the frequency, and a digital/analogue converter for voltage readout. The parameters of the system, mass,are and bleed rate of coating, temperature, carrier gas flow rate and pressure etc. are discussed The main coatings used are triethanolamine and diethanolamine and these proved capable of determining CO_2 . A system for CO determination is described and is based on the mercuric oxide reduction with subsequent analysis of the liberated CO_2. The gases can be determined below their threshold limit values. A brief study is made of the high frequency effect, generally encountered with solids and suggestions as to its cause are made.

60 tables, 71 figures and 131 references are given.

"Buckminster Fuller's analogy with a spaceship is exact: a small, vulnerable, delicately balanced mechanism that is, above all, finite. Nothing we have is indestructable or inexhaustable - not the air we breathe, not the land we use, not the water we drink - they all have an end, an increasingly foreseeable end. The strongest impression I got from the photographs brought back from space was of a very small, very lonely planet. And so it is, and so it must be treated."

Lynette Hamblin

Acknowledgements

I should like to thank: my supervisor, Professor T.S.West for his help and guidance throughout this study; the Science Research Council for financial assistance; and my colleagues for helpful discussions and comments.

The Research work presented in this thesis was carried out in the Department of Chemistry, Imperial College of Science and Technology, from September 1974 to September 1976. It is entirely original except where due reference is made. No part of this work has been submitted previously for any other degree.

Contents

Tables

Figures

69. Peak Profiles for Liberated Mercury.
70. Peak Profiles for Liberated CO_2.
71. Effect of Carrier Gas Pressure on the Response.

Chapter 1 Air Pollution

The atmosphere has always been polluted to some extent, and since the late 1940's and early 1950's, pollution disasters have become more frequent and hazardous to life. Public awareness is on the increase and governments are seeking legislation to control the amount of pollutants discharged into the atmosphere, rivers and oceans. As these requirements become more stringent, the methods of analysis must develop accordingly and be able to offer the desired sensitivity for both discrete and continuous samples.

The object of this thesis is to investigate the application of the piezoelectric quartz crystal to atmospheric pollution monitoring and, in particular, its use in the determination of carbon monoxide and carbon dioxide.

1.1 History of Air Pollution

Man-made pollution has existed on a local scale since man invented fire for cooking his food and warming his ill-ventilated caves. Crude oil combustion in Persian shrines is reported as early as 500 B.C., and Horace, in his poetry, deplors the smoke-blackened temples of Rome in 100 B.C..(1)

The medieval towns of Europe suffered air pollution from wood smoke and odours of many domestic activities, of trades such as tanning, and the decaying rubbish in the streets. Public disatisfaction began to arise from the beginning of the 14th century and man-made pollution became such a nuisance that British kings decreed that the fouling of London air by smoke, was an offence punishable by the death penalty. In 1300, a royal proclamation prohibited the use of coal in London. An

English diarist in 1661 declared in a tract entitled "Fumifugium, or the inconvenience of Aer and Smoak of London", that the city of London "resembles the face Rather of Mount Aetna, the Court of Vulcan,Stromboli, or the Suburbs of Hell,than an Assembly of Rational Creatures and the Imperial seat of our Incomparable Monarch." (2)

By 1600 it was well known that the sulphur in coal was responsible for the unpleasant smell and irritation to the throat and nose, which accompanied the burning of coal, and methods of coking coal to remove some of the sulphur began to be developed.(3)

About 1800 with the development of the chemical industry, hydrochloric acid was recognised as a pollutant from the production of sodium carbonate from common salt. Other pollutants introduced at this time, were hydrogen sulphide, nitrogen dioxide, hydrogen fluoride and fumes from such metals as lead, arsenic, zinc and copper.(3)

Until about 1940 air pollution meant for most people, smoke and sulphur dioxide, and upto this time, pollution control had had little widescale effect. In 1943 Los Angeles began to experience a new type of pollution - smog - the word being a contraction of smoke and fog. The problem was characterised by an atmospheric condition which appeared and disappeared, sometimes remaining for several days. The visibility was reduced by a light blue haze and many suffered from sore throats,running noses and eyes, and headaches. The cause was found to be petroleum hydrocarbons reacting with nitrogen dioxide in the lower atmosphere to produce lachrymatory compounds,and measures were made to control their production into the atmosphere by reducing the output of the parent compounds.

1948 saw the Donora, Pennsylvania ,disaster.Effluents from a number of industries, such as a sulphuric acid plant, a steel mill and

a zinc production plant, became trapped in a shallow valley inversion to produce an unbreathable mixture of fog and pollution. About 6000 people, or 43% of the population, were affected, and over the three day period, the number of deaths was 20, and increase of 18 over the normal expectation. It has been suggested that the sulphur dioxide reached peak values of about 5500 $\mu g/m^3$. (1)

In 1952 it was the turn of London with the worst air pollution disaster ever reported. The meteorological conditions were ideal for a pollution build-up, and low average daily temperatures for December, meant an increase in pollutants from space heating and power plants.(1) The highest daily smoke values reached 4460 $\mu g/m^3$ and the highest daily sulphur dioxide values 3830 $\mu g/m^3$, which was nine and five times the normal concentration for the November- December period. Over the four day period, 4000 people died as a result of the pollution. As a result of this, the Clean Air Act was introduced in 1956 mainly to control the visible pollution from smoke.

Pollution disasters are still occurring in spite of the experiences of Los Angeles, Donora, New York, London etc.. Accidental man-made disasters occur, the most recent at the time of writing, being at Seveso,Italy in July 1976, with the escape of poisonous gas from a chemical factory producing herbicides.

1.2 Composition of Clean Air

Table 1 gives the composition of clean,dry air near sea level. The levels for sulphur dioxide,nitrogen dioxide,ozone,carbon monoxide and methane can be seen to be low.

Table 1.Composition of Clean Air (1)

Component	Concentration (vpm)	Component	Concentration
N_2	780900	CH_4	1.5
O_2	209400	H_2	0.5
Ar	9300	CO	0.1
CO_2	318	O_3	0.02
Ne	18	NO_2	0.001
He	5.2	SO_2	0.0002

1.3 Composition of Polluted Air

The composition of polluted air, varies considerably with location and time. Table 2 shows data for three cities and it can be seen that the levels of the major pollutants have increased over the clean air values.

Table 2. Composition of Polluted City Atmospheres

1962-1963 CAMP data (1)

Component		Concentration in vpm		
		Chicago	Cincinnati	New Orleans
SO_2	a)	0.135	0.029	0.010
	b)	0.344	0.056	0.020
	c)	0.79	0.011	0.06
NO_2	a)	0.042	0.030	0.019
	b)	0.064	0.043	0.031
	c)	0.13	0.09	0.05
Total Oxidant	a)	0.004	0.014	0.019
	b)	0.010	0.040	0.038
	c)	0.07	0.09	0.08
Total Hydrocarbon	a)	3.2	3.3	1.8
	b)	4.3	4.6	3.1
	c)	6.0	10.0	5.0

CO	a)	7.6	6.9	4.4
	b)	9.6	10.4	4.8
	c)	19.0	16.0	13.0

a) is the 2 year mean concentration

b) is the maximum monthly concentration

c) is the maximum hourly concentration.

1.4 Atmospheric Concentrations of Carbon Monoxide and Carbon Dioxide.

1.4.1 Carbon Monoxide

The world's total CO production per year is 232 million tons, of which 80% is produced by automobiles.(1) If this amount was evenly spread over the lower atmosphere it would increase the CO content by 0.03 vpm per year, a significant amount since CO is a very stable gas. Under experimental conditions a CO - O mixture exposed to sunlight, remained unchanged after seven years.However, the background concentration of CO remains at about 0.1 vpm, and four possible ways of removal of CO from the atmosphere have been suggested.

1) Escape into the general atmosphere.

2) Oxidation to CO_2

3) Use of by metabolising bacteria.

4) Absorption by the oceans.

A comprehensive study of the global distribution of atmospheric CO, by Seiler and Junge (4) found the following concentrations of CO.

a) Upper troposphere of the northern hemisphere 0.10 - 0.15 vpm

b) Planetary boundary layer over the N.Atlantic 0.16 - 0.30 vpm

c) Mid-tropospheric data from subtropics showed no difference between the hemispheres

d) Surface waters of Atlantic compared to atmospheric equilibrium values. The CO concentration was 10 - 40 times higher.

e) Tropopause region showed rapid decrease of CO above tropopause.

Certain portions of the oceans may act as CO sinks, but because of the low solubility of CO in water, this mechanism would be rather ineffective. The decrease of the CO above the tropopause suggests that the stratosphere is the major sink for tropospheric CO.

The concentration of CO in city streets varies with the density of motor traffic. In Cincinnatti, in 1952, the concentration in the commercial and industrial districts ranged from 0 to 55 vpm with an average of 9.5 vpm, as compared to 4.0 vpm in the residential area.(3) In Los Angeles in 1954 the concentration reached a diurnal mean peak of 8.8 vpm at 8.30 am. dropping sharply to about 3.5 vpm in the early afternoon, and rising to about 7.0 vpm at 4.30 pm.. In December 1957 the maximum concentration of CO in the centre of Los Angeles was reported to be as high as 72 vpm.(3)

Transient CO levels of 50 vpm are not uncommon in city streets and several hundred vpm can be found in tunnels and garages.(5) Levels of about 360 vpm have been reported in Oxford Street, London.(6)

1.4.2. Carbon Dioxide

The concentration of CO_2 in clean air is 318 vpm and in industrial areas, levels have reached the 1000 vpm level. Increased CO_2 levels produce the so-called greenhouse effect which raises the temperatures in cities, by allowing sunlight to reach the earth's surface, but limiting re-radiation of the resulting heat into space. Between 1860 and 1960 the combustion of fuels added nearly 14% to the CO_2 content of the air. At a concentration of 600 vpm the earth's temperature

would increase by 1.5°C (6) and a report by the U.S. Government found that the extra heat due to fuel-produced CO_2, accumulated in the air by the year 2000, might be sufficient to melt the Antartic Ice Cap in 400 to 4000 years according to the method of calculation.(7)

1.5 Sources of Pollution with emphasis on Carbon Monoxide and Carbon Dioxide

This section will deal briefly with the sources of CO and CO_2 from man-made pollution, since that from natural causes, eg. forest fires, volcanoes, should be reasonably constant.

Table 3. Natural and Man-made Trace-gas Cycles (5)

Component	Natural (Tonnes)	Man-made (Tonnes)
O_3	2×10^9	small
CO_2	7×10^{10}	1.5×10^{16}
H_2O	5×10^{14}	1×10^{10}
CO	?	2×10^8
S	1.42×10^8	7.3×10^7
N	1.4×10^9	1.5×10^7

The U.S. Public Health Service has catalogued the five major sources of pollutants and these are given in the table below.(1)

Table 4. Major Sources of Air Pollutant Emissions in the U.S. in 1965

Source	S oxides	CO	Hydrocarbons	N oxides	Particulates
Motor vehicles	1	66	12	6	1
Industry	9	2	4	2	6
Power Plants	12	1	1	3	3
Space Heating	3	2	1	1	1
Refuse Disposal	1	1	1	1	1
Total	26	72	19	13	12

The data is given in million of tons per year.

A) Motor Vehicles

From the above table, it can be seen that the largest amount of pollutants (60%) were emitted by the 90 million motor vehicles that were registered in 1965 in the United States. By 1970 the 100 million mark had been reached. About 80% of the world's total CO is produced by automobiles, and the hydrocarbons and nitrogen dioxide emitted, contribute to photochemical smog.

Parker, in 1954, estimated that the total annual emission of CO into the air of Great Britain was 24 million tons, of which petrol vehicles were responsible for 4 million.(8) The situation is far worse in the United States - in Los Angeles in the early 1960's, 3.5 million vehicles were burning about 7 million gallons (21500 tons) of gasoline per day, and emitting 1800 tons of unburned hydrocarbons, 500 tons of nitrogen oxides and 9000 tons of CO daily.(2)

In the United States by 1976, the CO and hydrocarbon emissions from new cars are to be reduced by 96-97% of the levels from uncontrolled cars.(9). Standards agreed upon within the European Economic Commission, call for reductions in CO and hydrocarbon emissions of about 35% from uncontrolled levels.

In Marseilles, an experimental ban on parking in the city centre, resulted in a lowering of the CO concentration by 10-60% depending on the time of day. The average reduction, based on 502 samples at 4 locations was 40% (9).

One obvious remedy to the pollution from vehicles is to use diesel engines, rather than petrol, since they emit less than 1/20 th CO and less than 1/7 th hydrocarbons.

Every time a jet crosses the Atlantic it has been found to consume 35 tons of oxygen and produce about 70 tons of CO_2, large

amounts of water vapour and fine particles.(6)

B) Industry

Industry in the United States produces about 20% of the total pollution. According to Parker, industry and domestic fires, emitted 10 million, of the 24 million tons annually of CO.(8)

In the United States in 1972 more than 90% of the electrical energy was generated by burning coal and oil with increasing pollution by SO_2. Open fires, oil fired central heating and bonfires all contribute to the pollution levels, and in high risk areas smokeless zones have been introduced in order to minimise the pollution danger.

The annual production of waste material in the United States is about 150 million tons, the majority being burned in municipal, industrial and commercial incinerators.

1.6 Effects of Carbon Monoxide and Carbon Dioxide on Man

1.6.1 Carbon Monoxide

CO is a colourless, odourless and lethal gas which combines with the haemoglobin of the blood and interrupts the normal oxygen supply to the body tissues. The CO preferentially combines with the haemoglobin and gives a bright cherry red colour to the blood.

The effects of CO are given below and range from headaches, collapse and eventual death depending on the exposure.(10)

Table 5 Symptoms caused by various amounts of CO-Haemoglobin in blood

Blood Saturation % CO-Haem	Symptoms
0 - 10	No symptoms
10 - 20	Slight headache
20 - 30	Headache and throbbing in temples
30 - 40	Severe headaches, dizziness, nausea, collapse
40 - 50	As above, increased possibility of collapse
50 - 60	Coma and poor respiration

Henderson and Haggard (11) proposed the following equations as a rough guide in estimating the probable effect of CO.

Hours x ppm	= 300	No perceptible effect
Hours x ppm	= 600	Just perceptible effect
Hours x ppm	= 900	Headache and nausea
Hours x ppm	= 1500	Dangerous to life

Every smoker, and those exposed to cigarette smoke, inhales a certain amount of CO. Cigarette smoke, as inhaled, contains 200 to 800 ppm CO and cigar and pipe smoke considerably more. A smoker's blood may become saturated with CO to the extent of 5% within a period of 2 hours. Jones and co-workers studied the effects of cigarette smoke.(12)

The maximum allowable concentration for an 8 hour exposure is 100 ppm. (10) An exposure of 1 hour to 120 ppm CO is classed as a 'serious' level and to 240 ppm as an 'emergency' level.(2) In New York studies have indicated that exposure to 50 ppm can affect the mental processes drastically, as measured by visual performance and ability to discriminate time intervals.(5,6)

These levels of CO pollution are frequently encountered in city streets. In a street in Prague with heavy traffic (1000 cars/hr, 10-20 mg CO/m^3), the increase of the level in the carboxyhaemoglobin was monitored in persons spending some time there.(13)In a group of 8 non-smokers a 2 hour stay gave an increased level of CO in the expired air by almost 3 mg CO/m^3; and after 4 hours the increase was 4 mg CO/m^3. This corresponds to an increase of carboxyhaemoglobin in the blood of almost 2%. In the city of London during 1957, the level of CO was found to be 360 vpm on a calm day.(14) Lawther et al analysed continuously the CO concentrations at Oxford Circus,London in 1958. Average concentrations over 10 minute periods were found to

vary from 10 to 55 ppm, and the mean concentration for an 8 hour period was 36 ppm. A maximum concentration of 155 ppm was recorded during the evening rush hour. The same workers found a mean hourly concentration of 295 ppm in the Blackwall tunnel, and a transient peak of 500 ppm in the Rotherhithe tunnel. The concentrations were found to decrease in high wind conditions, and with height above the road.

It was found that the level of CO in cars, can reach the 100 ppm mark. Lawther reports that the concentration of CO in a car, in traffic with the air intake on, was 110 ppm, which in a traffic jam would greatly increase.

An exposure of 8 hours to 30 ppm by volume would give a blood saturation of 5% (2) and exposure to 100ppm 13% (14).

1.6.2 Carbon Dioxide

Whereas CO_2 is not generally considered to be a pollutant, in excess concentrations it can contribute a danger by causing oxygen deficiency. The initial effect of inhalation of excessive concentrations is noticed at 2% (20,000 vpm) when the breathing becomes deepened. At 4% the depth of respiration is markedly increased, and at 4.5-5% the breathing is laboured as the CO_2 controls the rate of respiration. Concentrations up to 8-10% have been inhaled by men for periods upto 1 hour with no evident, harmful effects.

The maximum concentration for an 8 hour exposure period is 5000 ppm.(10)

1.7 Analysis of Atmospheric Pollutants

There are two approaches to the analysis of atmospheric pollutants, continuous monitoring with sampling followed closely by

analysis (sometimes referred to as 'real-time' analysis), and discrete monitoring with a time delay between the sampling and subsequent analysis. Both these methods are used and have certain advantages. The continuous method is obviously of more value to the monitoring of a build-up of a pollutant during the day, eg. the increase in CO levels with traffic congestion; however, should only a few measurements be required over a specific time interval then discrete sampling is adequate. The latter method does have the disadvantage that it gives retrospective data which is of little use in the monitoring of rapidly increasing poisonous pollutants.

1.7.1 Sampling Methods

1.7.1.1 Continuous Sampling

For continuous sampling, the air is drawn through the apparatus by a pump at the desired flow rate which influences the concentration presented for analysis. Filters may be incorporated in the air stream in order to eliminate interferents, eg. moisture,hydrocarbons.

1.7.1.2 Discrete Sampling

Discrete sampling systems, as has already been mentioned, have the disadvantage of a time interval between collection and analysis, which may be further lengthened by the need for a preconcentration or pretreatment stage, thus introducing further errors. On the other hand, preconcentration techniques permit lower levels to be determined than obtained by most real time techniques.

1.7.1.3 General Considerations of Sampling

There are several parameters that must be taken into consideration when sampling the atmosphere.

a) Size of sample - this must be large enough to provide sufficient

material for analysis.

b) Changes in the sample during and after sampling - care must be taken not to introduce any contaminants or to lose sample during storage eg. onto the walls of the container.

c) Sampling rate - this must be optimised to ensure efficient sampling.

d) Sampling duration - this is a function of the sampling rate and the change of the pollutant with time.

e) Collection efficiency- this must be as high as possible and reproducible.

The methods of sample collection are varied and can be chosen with regard to the subsequent method of analysis.

Grab samplers rely on a container of an inert material being filled with the polluted air, either by suction of a pump, or by filling a container which has been evacuated. The method is efficient and reproducible.

Gases can be sampled by means of a suitable absorption reagent. A glass tube is filled with liquid reagent and fitted with a porous glass partition so that the air passes through the reagent in the form of fine bubbles.The amount of pollutant collected is limited by the reagent. An allied method is collection by adsorption where the air is passed through an adsorption column containing a solid medium such as silica gel or activated charcoal. The pollutant is the removed from the column for analysis.An indicator may be added to the adsorption column to give a quantitative analysis in situ.

Another method is to use a condensation trap to condense the volatile constituents.Control of the temperature ensures a degree of specificity although some interference from moisture is often encountered.

1.7.2 Methods of Analysis for Carbon Monoxide and Carbon Dioxide

1.7.2.1 Carbon Monoxide

a)Continuous Measurement

1) Non-dispersive Infra -red

This is the most common and reliable method and is used for the calibration of other instruments.The air is usually dried prior to aspiration through the analyser at a flow rate of 0.7 l/min..(14) Radiation is absorbed in the sample tube and is dependent on the concentration of the gas.The minimum dection limit is reported to be 0.8 ppm (v/v). (15)

2)Electrochemical

a) Galvanic

This method relies on the reaction of CO with I_2O_5.

$$5\ CO + I_2O_5 \xrightarrow{150^\circ C} 5\ CO_2 + I_2$$

The liberated I_2 is dissolved by an electrolyte and transferred to the cathode of the galvanic cell where it is reduced and the resulting current measured. This current is related to the concentration of CO. The method can be used for both discrete and real time analysis.

b) Coulometric

The principle of this method is that the titrating agent is formed in situ by electrolysis in the titration cell. The above reaction is used and CO can be determined at the 1 ppm level. Interferences are caused by mercaptans,hydrogen,hydrogen sulphide, olefins,acetylenes and water.

3) Mercury Vapour Analyser

This method is based on the reaction of CO with hot red mercuric oxide and subsequent measurement of the liberated mercury.

$$HgO + CO \xrightarrow{175\text{-}200^{\circ}C} CO_2 + Hg$$

The mercury can be determined photometrically using the 253.7 nm Hg emission line.(16) The range of the instrument is 0 to 50 ppm and a minimum detectable concentration has been reported as low as 30 ppb (34 $\mu g/m^3$) with a stoichiometric analyser having an 18 cm optical cell. Another study reported a sensitivity of 5 ppb. The interferents are hydrogen, hydrocarbons and olefins.

The mercury can also be determined by flameless atomic absorption spectroscopy.(17)The range quoted is 0 to 20 ppm and the sensitivity less than 0.5 ppm.

4) Gas Chromatography

Many different types of column have been used to ensure separation of the components of air. CO can be detected in the low ppm range after conversion to methane and detection using a flame ionisation detector.(18)

b) Intermittent Measurement of Carbon Monoxide

There are a great many methods for the intermittent measurement of CO and these will only be reviewed briefly.

1) Colorimetric Indicators

This is a popular method where air is drawn through a tube filled with a solid support impregnated with a reagent sensitive to CO, and which will produce subsequently a colour change. One example is palladium chloride on silica gel - the air is passed through the tube at 3 l/min and within 15 to 30 minutes the colour changes from yellow to grey.(19) The range quoted is 85 to 200 ppm CO, with no discernible effect at concentrations less than about 14 ppm.The

interferents are hydrogen, hydrogen sulphide, ammonia and some hydrocarbons. Other reagents are crystalline haemoglobin mixed with either ascorbic acid or methylene blue.(20)Changes in the colour or infra-red absorption of these media can be used to monitor the CO concentration. Silver p-sulphamoyl benzoic acid gives a range of 2-80 ppm,(21,31) and a mixture of silica gel, ammonium molybdate, palladium sulphate and sulphuric acid will detect less than 10 ppm CO.(10,24,25)CO will reduce Pd(II) to Pd. (23)

2.Conversion to Carbon Dioxide

Another well used method is to convert the CO to CO_2 with subsequent analysis.Reagents used for this are, solid siver permanganate mixed with zinc oxide at 11-40°C (26);decomposed silver permanganate, with a detection of 0.1-1.5% on a 500 cm^3 sample at a temperature of 450-500°C (22);conversion over Hopcalite and measurement of the rise in temperature, which is proportional to the gas concentration.(27)

3. Absorption of Carbon Monoxide

A review of absorbents was published soon after the First World War and is detailed in its treatment.(28) Finely divided nickel has been reported to absorb CO,(29)also manganous chloride and activated charcoal (30); a mixture of cuprous sulphate, β-naphthol and sulphuric acid is good for small samples.(10)

4. Spectrophotometric Method

A spectrophotometric method for the analysis of CO is to react it with iodine pentoxide at 110°C and to absorb the liberated iodine with an indicator paper impregnated with choline iodide. The concentration of CO is assessed from the colour of the paper. The range is 2 to 20 µg CO/l air.(32)

1.7.2.2. Carbon Dioxide.

The most popular method for CO_2 analysis is absorption followed by a titrimetric analysis. Reagents used are numerous and a selection is sodium hydroxide, strontium hydroxide (33), barium hydroxide in an ethanol,aniline and water mixture (34), 2-amino-2 (hydroxymethyl) 1,3 propanediol (35), ethylenediamine (36), and a mixture of sodium bicarbonate and potassium chloride (38).

The heat of the reaction between CO_2 and lithium hydroxide has been used to detect picomole amounts of CO_2 (37).

CO_2 has been dissolved in pyridine and monoethanolamine to give hydroxyethylcarbamic acid which is titrated with sodium methanolate hydroxyethylcarbamic acid.(39) The colour change can be monitored photometrically.

CO_2 can be determined by non-dispersive infra-red spectroscopy in the range 0 to 10% v.v. (15).It can also be monitored using gas chromatography and indicator tubes.

1.8 Summary

From the above brief review it can be seen that many of the methods for gas analysis rely on discrete sampling and a preconcentration stage prior to analysis, Continuous methods require complicated and expensive instrumentation.

In the following chapters an attempt is made to study the applicability of the piezoelectric effect to atmospheric pollution analysis for CO and CO_2 . The effect is produced by coating the electrode of a suitable crystal with an absorbent for CO or CO_2. When the pollutant is absorbed on the coating there is an accompanying decrease in the frequency of the crystal. This decrease in frequency is

directly related to the mass absorbed from the gas stream.

The technique is potentially very sensitive - responding to mass changes of 10^{-12}g.Instrumentally it is simple and economical and more important, combines both the sampling and measurement stages.

As will be shown, the piezoelectric quartz crystal did not offer sensitivities as low as some other continuous methods, but it was able to analyse, at, and below, the recommended threshold levels for an 8 hour exposure and therefore it has potentiality as a pollution monitor for the CO/CO_2 system.

Chapter 2 Piezoelectricity

Piezo is derived from a Greek word meaning 'to press' and, therefore, literally piezoelectricity is 'pressure electricity'. Cady(40) defines piezoelectricity as 'electric polarisation produced by mechanical strain in crystals belonging to certain classes, the polarisation being proportional to the strain and changing sign with it.' This defines the direct piezoelectric effect and closely related to it, is the converse effect whereby 'a piezoelectric crystal becomes strained, when electrically polarised, by an amount proportional to the polarising field.'

2.1 History and Development of Piezoelectric Crystals

The piezoelectric effect was discovered experimentally by Pierre and Jacques Curie in 1880, when they found that some crystals when compressed in particular directions show positive and negative charges on certain portions of their surfaces. These charges are proportional to the pressure and disappear when it is withdrawn. They found that the effect is present in many crystals including quartz, rochelle salt and tourmaline. The converse piezoelectric effect of a crystal, that is an applied voltage producing a displacement, was predicted theoretically by Lippman in 1881 and later verified by the Curies.(41)

The effect remained a scientific curiosity until World War I, during which Langevin, initiated work on the utilisation of piezoelectric devices for picking up compressional waves from the sea.(42) He developed an echo system employing supersonic waves, with both the supersonic emitter and the pick-up consisting of quartz plates.

By 1917, Nicolson experimenting with rochelle salt, had

constructed loudspeakers, microphones and phonograph pick-ups. He also controlled a vacuum tube oscillator by means of a crystal of rochelle salt,and holds the primary crystal oscillator patent.(42)

Cady, in 1921, showed that quartz crystals could be used to control oscillators, which gave greater stability.After Cady's publication Pierce devised a number of circuits and showed that it was possible to construct oscillators with quartz as the piezo-electric element, and a single electron tube, as Nicolson had done, but without using the electrical resonant circuits employed by Cady. (42)

By 1927, Marrison had obtained a quartz crystal with a low temperature coefficient by cutting a 'doughnut' shaped crystal from a slab cut parallel to the natural side face. As a result of this, other quartz crystals were discovered and developed,notably the AT and BT cuts, as well as CT,DT,ET,FT and GT.The GT crystal was,and is, the crystal with the flattest temperature-frequency curve so far developed and has found extensive use in clocks and watches.

2.2 Theory of Piezoelectricity

Piezoelectricity only appears in insulating solids and in crystals which do not have a centre of symmetry. A pressure which deforms the crystal lattice causes a separation of the centres of the positive and negative charges thus generating a dipole moment in each molecule.(42) How this separation can cause a coupling to an electrical circuit is shown in Figure 1, where a crystal is shown with metal electrodes normal to the direction of charge separation. Short circuiting the electrodes applies a stress causing the centres of the charges to separate,excess negative charges in the wire flow toward the electrode in the direction of positive charge separation,

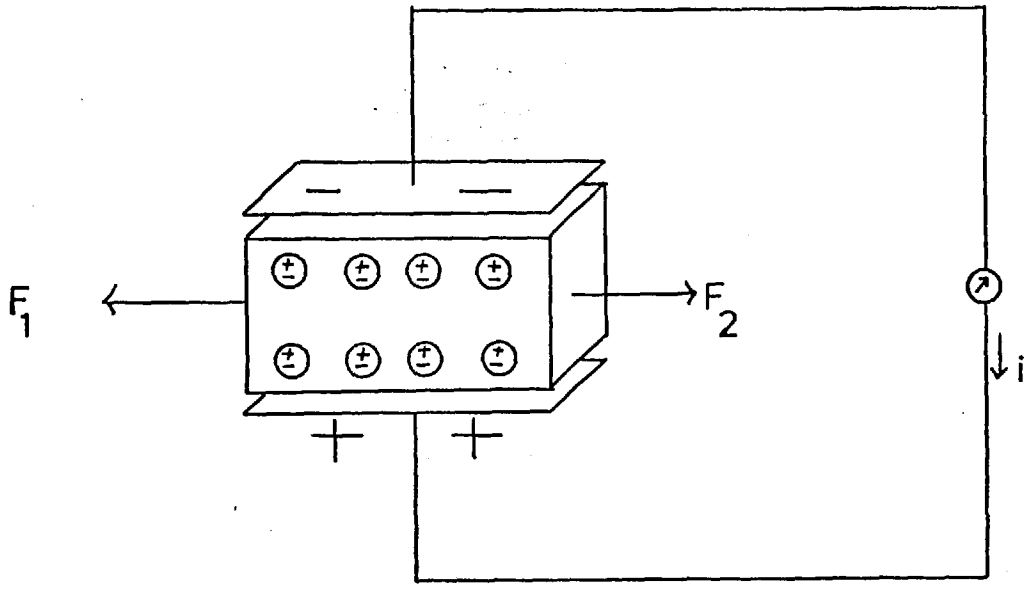

Figure 1.

Method for Transforming Mechanical Energy into Electrical Energy in a Crystal (42)

and excess positive charges flow to the negative electrode until the crystal is electrically neutral to external tests. Releasing the stress causes a similar pulse to occur in the opposite direction. Thus, placing a resistance in the connecting wire and applying a sinusoidal stress to the crystal will produce an alternating current flowing through the load, and will be converting mechanical power to electrical. Conversely an alternating voltage will produce an alternating stress in the crystal, so converting electrical into mechanical energy.

Quartz is a crystalline mineral found mainly in the α-quartz form and consists of silicon dioxide. It occurs as two enantiomorphs both the right and left hand crystals being found in nature. Only the right handed quartz crystals are used since the left handed quartz produces a piezoelectric strain in the opposite direction to that of normal quartz.(43)α-quartz belongs to the D_3 trigonal system with one three-fold symmetry axis, and three two-fold symmetry axes. A quartz crystal is shown in Figure 3.

Figure 2 represents the approximate arrangement of silicons and oxygens in a quartz molecule, with the silicon atoms represented by a plus (+) and the oxygen atoms by a minus (-). If a longitudinal stress is applied along the X, or electrical, axis the apex molecules are separated farther apart without changing the separation between the other molecules. This causes a displacement in the centres of the charges.

A shearing stress can cause a separation of the centres of the charges along the Y, or mechanical, axis. A simple shear stress is one in which forces act normal to the direction of space separation rather than along it, as shown in Figure 2 by the two arrows normal to the Y axis. Such a shear does not occur in nature, but rather a pure

Figure 2

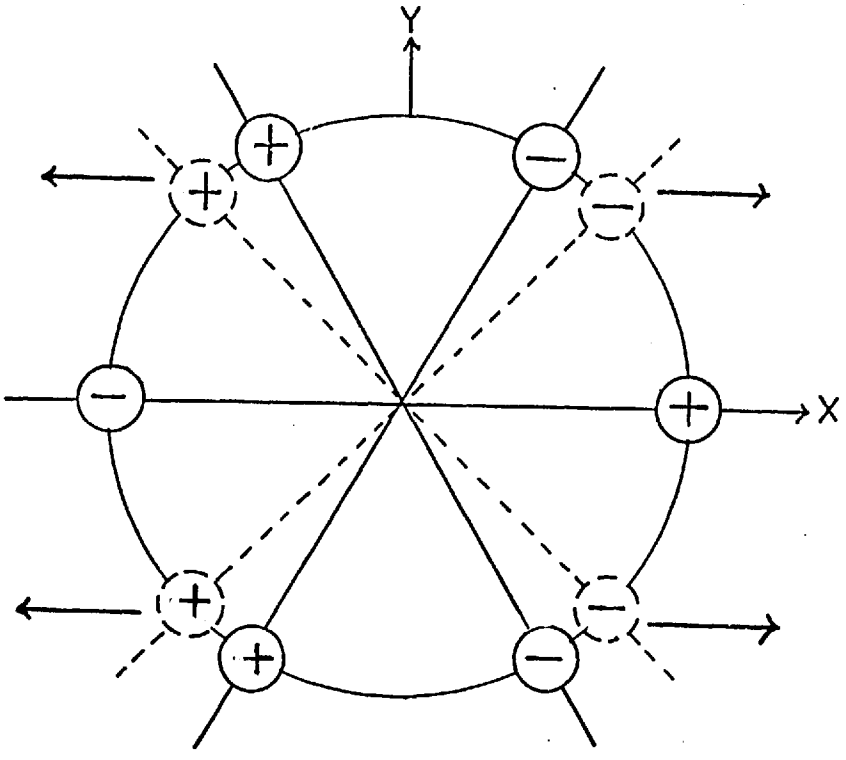

(A)

Longitudinal Strains Applied to a Quartz Molecule (42)

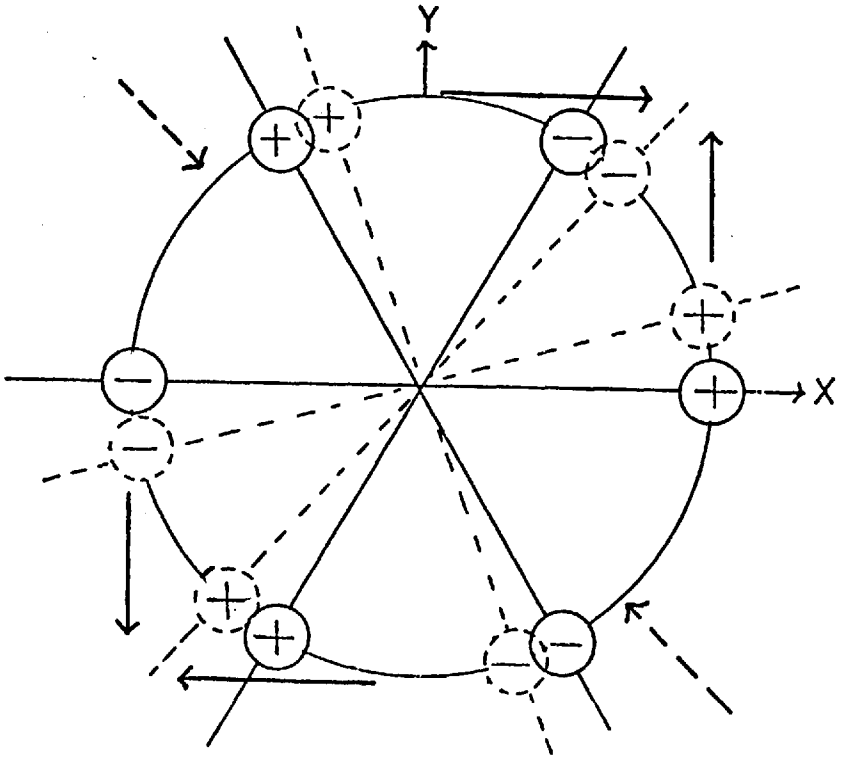

(B)

Shear Strains Applied to a Quartz Molecule

shear, which consists of two simple shears that can be resolved along directions 45° from the crystal axes; one an extensional stress and the other a compressional.(42)

There are three basic types of motion excited in quartz crystals - extensional, shear and flexural.

1.Extensional

In this mode particle motion takes place in essentially one direction so as to alternately stretch and compress the elastic medium.

2.Shear

Piezoelectric plates vibrating in shear are widely used for frequency control of oscillators, as for example, the AT quartz plate uses a fundamental thickness shear mode in which particle motion is principally at right angles to the thickness.

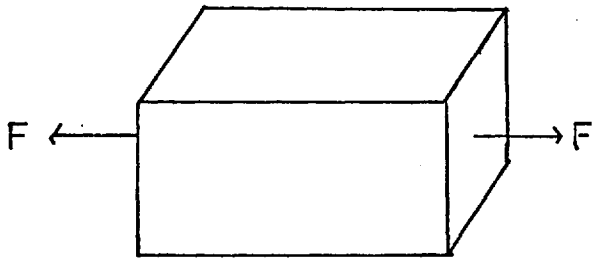

Bar under tensional strain

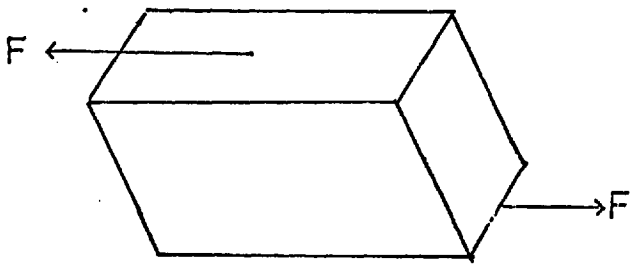

Bar under shearing stress

3.Flexural

This is movement of the plate about nodal points.

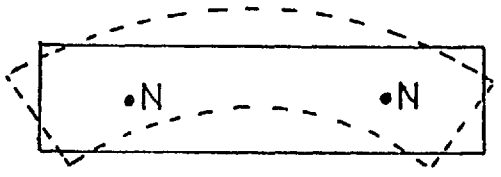

2.3 Crystal Cut

A misnomer occurs throughout the literature on piezoelectricity, strictly speaking, it is plates of quartz cut from a host crystal which are used as controlling crystals; however, these plates are also referred to as quartz crystals and this convention will be followed in this thesis.

The quartz crystals are cut from the main crystal at very specific angles, which ensure specific physical properties, the temperature coefficient of the crystal being the most important. The particular angle of cut is designated by two letters, such as AT, BT etc..

The first cut obtained was a longitudinal vibration along Y, or the mechanical, axis by a field applied along the X, or electrical, axis.(42) This mode gave a good resonance, free from other modes, but to obtain a reasonably high frequency the length had to be made too small to be practical.

Soon after, the thickness vibrating crystals were used, with the frequency being determined by the thickness. High frequencies were easy to obtain since the thickness could be made very small. The disadvantage with this type, is that harmonics and overtone modes of all the lower frequency types of motion, produce frequencies near the frequency of the thickness mode, and it is difficult to select the desired mode. This is especially true for the thickness vibrating X cut crystal and led to its abandonment in favour of Y cut crystals vibrating in shear. (42)These, however, had the disadvantage of a temperature coefficient of 86 ppm/°C.

Following this, investigations were carried out to determine the variation of the properties of the crystals with the orientation of the cut. All the cuts had one edge along the X axis making positive

and negative angles with the Y axis, and had a component of field along the Y axis producing a shearing motion, until the angles of cut approached 90° from the Y axis.The lower the angle, the more strongly will the shear mode be driven.The frequency constant varies with the angle of cut, having a minimum at + 31° and a maximum at - 59°;these two points correspond to angles for which the high frequency shear mode has zero coupling with troublesome low-frequency shear mode vibrations.Crystals cut at these angles will have a much cleaner frequency spectrum that Y cut crystals. The temperature coefficient of frequency also varies with the angle and theoretically becomes zero at angles of + 35° - 15' and - 49° , which are the AT and BT cuts respectively.The AT angle is nearer the Y axis and will be more strongly driven, but the BT has the advantage of having a higher frequency for the same thickness.

Advantages of AT Cut

1) Two cuts are normally used in detectors - the AT cut with a low temperature coefficient, and the AC cut with a high temperature coefficient. King, determined the coefficients for these cuts at various temperatures.(43) The AT cut had a zero coefficient at - 18°C and + 74°C, where the coefficient changes sign. The region in between these turnover points was not found to exceed 3.3 Hz/°C,or 0.3 ppm/°C and thus only simple temperature control is necessary. The AC has a smoothly increasing coefficient making it of use as a thermometer.

2) Strong couplings do exist to flexure modes of motion for the AT cut crystal,although none occur between the thickness shear and face shear modes.These can be minimised by controlling the dimensional ratios of the crystal.(41)

3) Smaller thicknesses lead to an improved mass sensitivity,which to

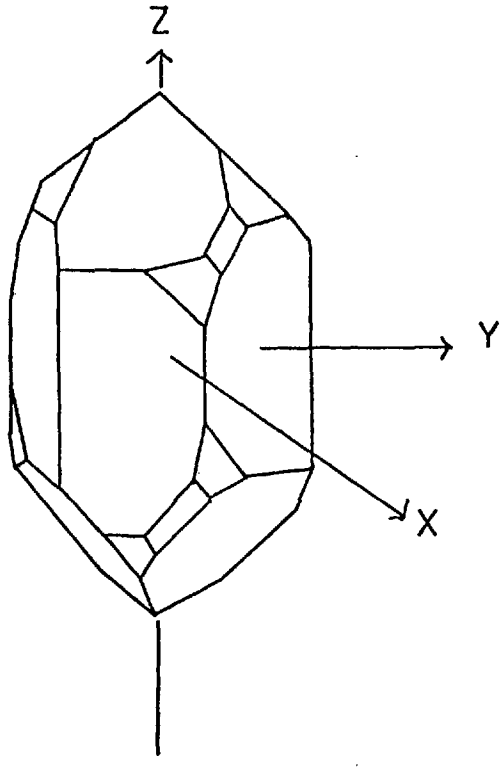

Figure 3 Right-handed Quartz

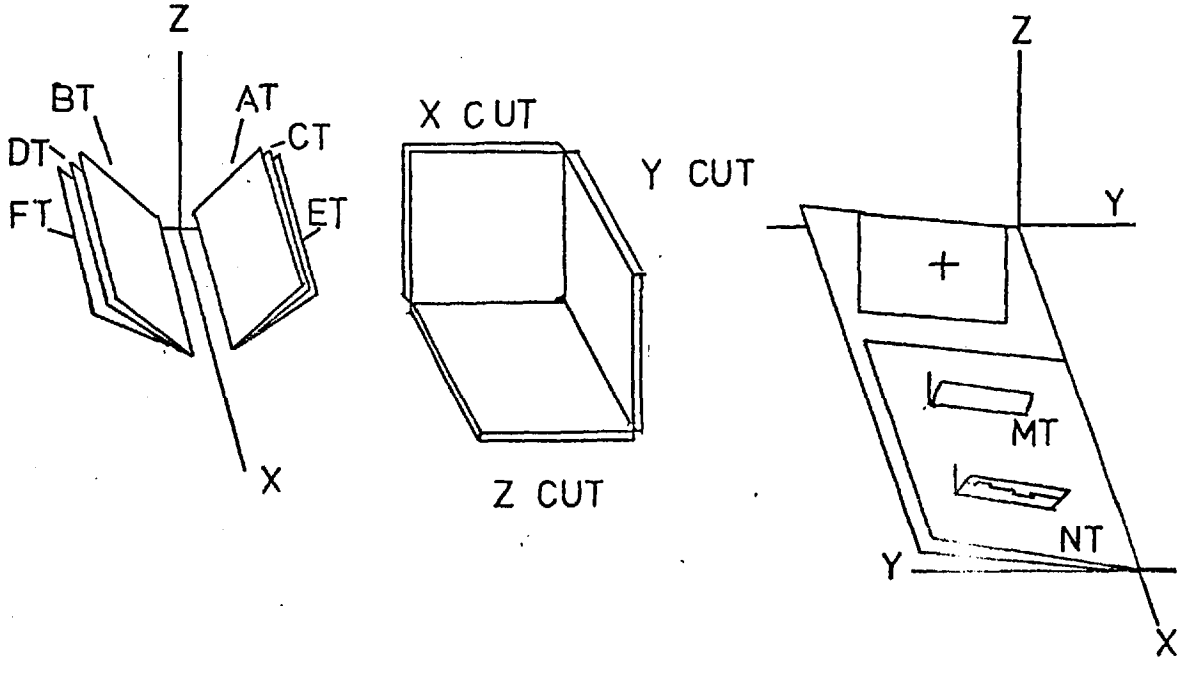

Figure 4 Principal Cuts of Quartz

a first approximation is inversely proportional to the thickness.

4) Higher capacitance ratio and low electromechanical coupling constant exist which reduces the dielectric constant correction.(44)

Summary

It can be seen from the above paragraphs why quartz piezoelectric crystals have been used.

1. They provide a coupling between the electrical circuit and the mechanical properties of the crystal.
2. The internal dissipation is very low,and the density and elastic constants are very low,so that a crystal cut always has the same frequency constant.
3. At specified orientations crystals have advantageous mechanical properties eg. low temperafure coefficient,freedom from secondary modes of motion.
4. The crystals are sturdy and mechanically stable.

2.4 Equations Relating Frequency of the Crystal to Added Mass

There have been several derivations of equations relating added mass to the frequency change of the crystal. The derivation most often referred to is that by Sauerbrey in 1959.

2.4.1 Sauerbrey's Equation (45,46)

This equation relates pressure changes produced by changes in the mass of thin metal films deposited on quartz,to the subsequent change in frequency. The assumption is made that a uniform metal film of any material deposited on the crystal will give the same frequency shift as an identical mass of quartz.

The movement of quartz in a thickness shear mode represents a standing transverse wave, the thickness of the plate being 1/2 wavelength. This is shown in Figure 5 a) and b).

The velocity, v, of a wave is given by

$$v = F\lambda$$

where F = Frequency
λ = Wavelength

For a quartz plate of thickness d, the velocity of the elastic transverse wave in the direction of the plate thickness, v_{tr}, is

$$v_{tr} = F.\ 2d \qquad (1)$$

More complex derivations of v_{tr} which ultimately reduce to the above can be found in the literature. (40,41,42)

Rearranging (1) gives

$$F = \frac{v_{tr}}{2d} = \frac{N}{d} \qquad (2)$$

where $v_{tr}/2 = N$, is the frequency constant and is a function of the crystal cut.

For AT cut crystals it is 1670 kHz-mm and for a BT cut crystal it is 2500 kHzmm. (45)

Differentiating (2) gives

$$dF = -\frac{N}{d^2}\, dd \qquad (3)$$

But the thickness d is related to the mass, M_q, of the plate, the density, ρ, and the area A.

$$d = \frac{M_q}{A.\rho} \qquad (4)$$

Therefore

$$dd = \frac{dM_q}{A.\rho} \qquad (5)$$

Substituting (2) and (5) into (3) gives,

$$dF = - \frac{F\, dM_q}{d.A.\rho} \qquad (6)$$

This reduces to $F = - 0.38 \times 10^6 \frac{F}{d.A.} M_q$ (7)

Another equation obtained is,

$$dF = - \frac{F^2\, d\, M_q}{N.A.\rho} \qquad (8)$$

Substituting values of 2.65 g cm^{-3} for ρ and 1670 kHz mm for N gives the following equation for the frequency change ΔF with added mass, ΔM.

$$\Delta F = - 2.3 \times 10^6 \frac{F^2 \Delta M}{A} \qquad (9)$$

This is termed the Sauerbrey Equation.

Thus it can be seen that the controlling parameters for the frequency change are added mass, area and thickness.

King developed the equation further by introducing a constant k. (47)

$$\Delta F = k \Delta M \qquad \text{where } k = 2.3 \times 10^6 \frac{F^2}{A} \qquad (10)$$

If ΔF_o = frequency change due to application of coating

ΔM_o = weight of coating

ΔF = frequency change due to sorption of vapour

ΔM = weight increase due to sorbate

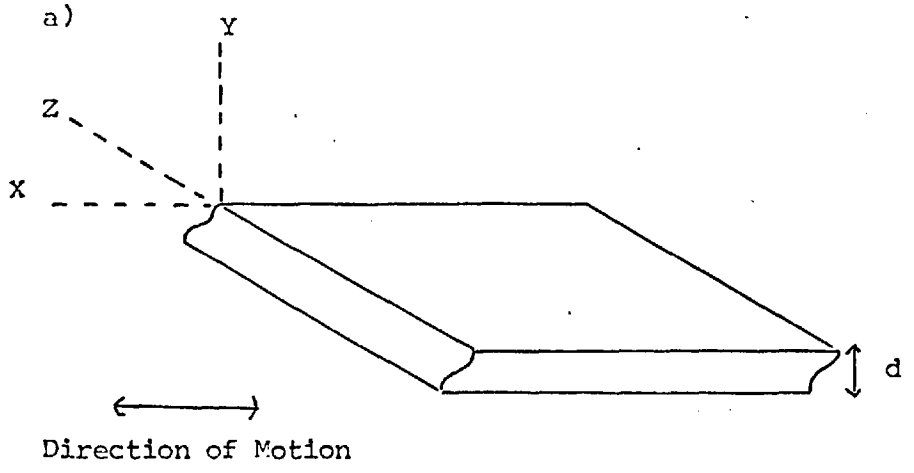

Figure 5 Thickness-shear Vibration in an AT Cut Crystal

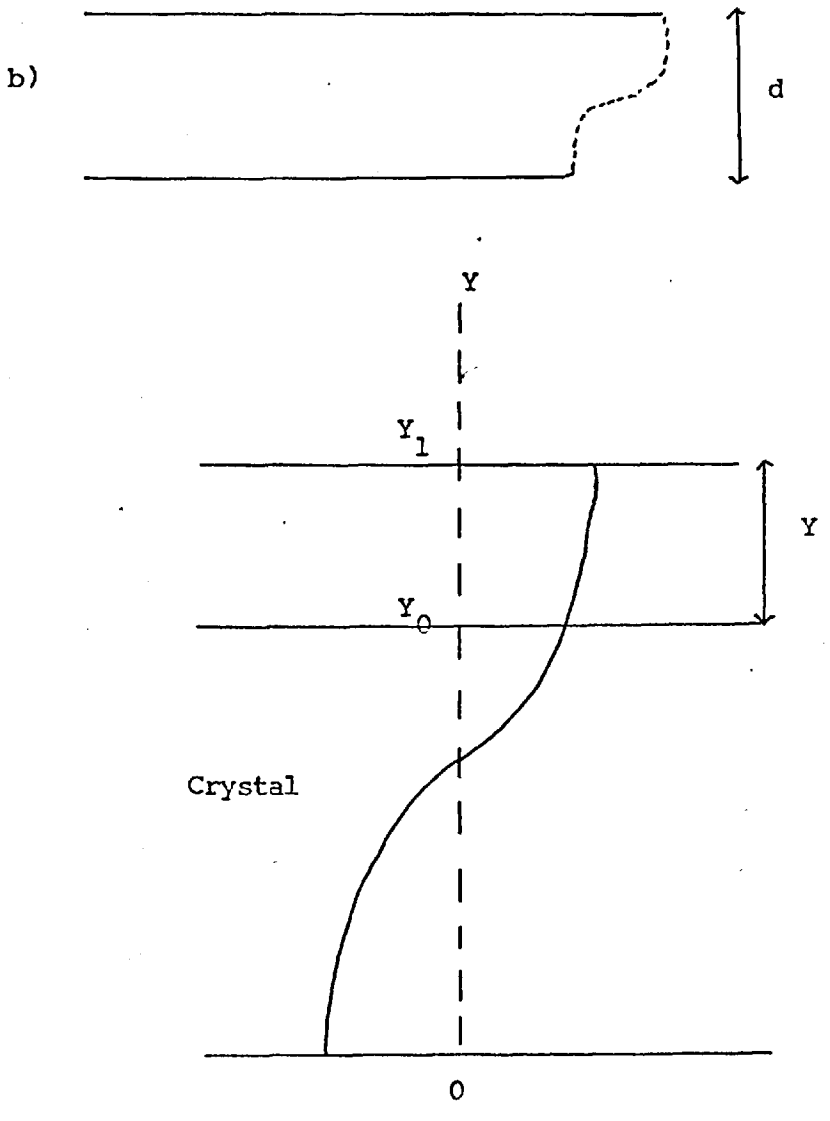

Figure 6 Representation of the Shear Motion of a Coated and Uncoated Quartz Plate. (101)

Substituting into the above equation

$$\Delta F_o = k\Delta M_o$$

and $$\Delta F = k\Delta M$$

Therefore $$\frac{\Delta F}{\Delta F_o} = \frac{\Delta M}{\Delta M_o} \qquad (11)$$

Rearranging gives $$\Delta F = \frac{\Delta F_o \Delta M}{\Delta M_o} \qquad (12)$$

Similar derivations have been made by other workers eg. Eschback and Kruidhof,(48) Janghorbani (49)

2.4.2 Lostis' Equation (51)

An earlier derivation of the equation relating frequency change to added mass was made by Lostis in 1958. His method involved a consideration of the displacements of coated and uncoated crystals.

The basic equation for the displacement (u_1) of any point in the wave path at a distance y from the origin O at time t' is given by,

$$u_1 = A_1 \cos \frac{o_1 y}{v_1}, \sin o_1 t' \qquad (13)$$

See Figure 6

where o_1 = angular velocity of an uncoated crystal

$v_1 = \sqrt{\frac{e}{d}}$ = velocity of a transverse wave through the quartz

A_1 = peak amplitude of the wave motion in the crystal

Similarly, the displacement at any point in the crystal coating at a distance y_1 from y at time t' is given by:

$$u_2 = A_2 \cos \frac{o_2(y_1 - y)}{v_2}, \sin o_2 t' \qquad (14)$$

where u_2 = displacement in the layer

A_2 = peak amplitude of the wave in the layer

$V_2 = \sqrt{\frac{e_2}{r_2}}$ = velocity of a transverse wave through the coating

e_2 = elastic coefficient of the coating

r_2 = density of the coating

o_2 = angular velocity of a particle in the coating

At the point y_0, the displacements are the same,

therefore,

$u_1 = u_2 = u$ and $o_1 = o_2 = o$. Let $\Delta y = (y_1 - y)$

Thus combining the equations 13 and 14 :-

$$A_1 \cos \frac{o y_o}{v_1} = A_2 \cos \frac{o \Delta y}{v_2} \qquad (15)$$

At y_0, the crystal plate, and coating at each instant are in equilibrium such that the following stress equality could be made.

$$e \frac{du_1}{dy} = e_2 \frac{du_2}{dy} \qquad (16)$$

Thus equation 15 may be rewritten in terms of equation 16

$$-\frac{o}{v_1} \cdot e A_1 \sin \frac{o y_o}{v_1} = -\frac{o}{v_2} \cdot e_2 A_2 \sin \frac{o \Delta y}{v_2} \qquad (17)$$

Dividing 17 by 15 :-

$$\frac{e}{v_1} \tan \frac{o y_o}{v_1} = \frac{e_2}{v_2} \tan \frac{o \Delta y}{v_2} \qquad (18)$$

Since $o = o_1 + \Delta o$

Then $$\frac{o y_o}{v_1} = \frac{o_1 y_o}{v_1} + \frac{\Delta o y_o}{v_1} = \pi + \frac{o y_o}{v_1} \qquad (19)$$

Therefore

$$\tan o \frac{y_o}{v_1} = \frac{y_o \Delta o}{v_1} \qquad (20)$$

Similarly it can be shown that

$$\tan \frac{o \Delta y}{v_2} = \frac{o_1 \Delta y}{v_2} \qquad (21)$$

Substituting 20 and 21 in 18

$$\frac{e_1}{v_1^2} \cdot y_o \Delta o = \frac{e_2}{v_2^2} \cdot o_1 \Delta y \qquad (22)$$

Now $v = \sqrt{\frac{e}{r}}$

Thus

$$\frac{\Delta y}{y_o} = \frac{r_1}{r_2} \frac{\Delta o}{o_1} \qquad (23)$$

Since $o = \pi 2 F$ where F = frequency of the wavemotion

$$\frac{\Delta F}{F_o} = \frac{r_2}{r_1} \frac{\Delta y}{y_o} \qquad (24)$$

Now if the area of the coating = A', and the mass of the coating applied to the face of the crystal plate $= \Delta m$,

Then:

$$\Delta m = \Delta y \cdot r_2 \cdot A'$$

and

$$\frac{\Delta F}{F_o} = \frac{\Delta m}{A'} \cdot \frac{1}{r_1 y_o} \qquad (25)$$

This is termed the Lostis equation. The derivation required no knowledge of the elastic constants of the mass added to the surface. However, very thin even layers are required on the surface of the resonating plate in order that the layer could be considered as an extension of the crystal plates' surface.

2.4.3 Stockbridge's Equation

A different derivation using Rayleigh perturbation analysis was carried out by Stockbridge (50)

Rayleigh showed that a small change in the inertia or elastic stiffness of a mechanically vibrating system perturbs the resonant frequency, F_n , of the system according to:

$$f_n^2 = \frac{c_n + \Delta c_{nn}}{a_n + \Delta a_{nn}} = F_n^2 \frac{1 + \Delta c_{nn} / c_n}{1 + \Delta a_{nn} / a_n} \qquad (26)$$

where c and a are the coefficients in quadratic expansion for the potential energy and kinetic energy of the system vibrating in mode, n, and f_n is the perturbed frequency of the system.

If a small perturbing mass is added at the antinode of vibration where it does not store potential energy, Stockbridge showed that $\Delta c_{nn} = 0$ and that

$$a_n = \frac{\rho}{2} \int_v U^2 \, dV \quad \text{and} \quad \Delta a_{nn} = \frac{1}{2} \int \sigma [U(h)]^2 \, dA \qquad (27)$$

where σ = mass added per unit area

h = half thickness of plate

U = velocity of plate at any point

v = volume of the plate in motion

A = area and ρ = density

Hence:

$$f_n^2 = F_n^2 \frac{1}{1 + \left[\int_A \sigma \left[U(h)\right]^2 dA\right] \Big/ \left(\rho \int_v U^2 dv\right)} \qquad (28)$$

In practice approximations must be made - a) the mass may not be added uniformly over the antinodal surface b) the area over which the mass is added may not coincide with A_1 the area of the antinodal surface in motion, and c) the variation of displacement across the area perpendicular to the thickness may itself vary as an unknown function of the thickness co-ordinate.

To overcome this, Stockbridge introduced the factors, K_1, K_2 and K_3.

$$\text{Thus } f_n^2 = F_n^2 \frac{1}{1 + K_1 \dfrac{m K_2 K_3}{A_a \rho h}} \qquad (29)$$

This reduces to

$$\frac{|\Delta F|}{F_n} = \frac{K_1 K_2 K_3 m}{2 A_a h \rho} \qquad (30)$$

where m = total mass added over area of addition A_a

Therefore

$$\frac{m}{A_a} = K_n \rho \frac{r|\Delta F|}{F_n} \qquad (31)$$

The Stockbridge Equation

where $K_n = 1/ K_{1,2,3}$ for the n th mode

K_1 is greater than unity for plates more sensitive to added mass at their face centres.

K_2 is less than unity when the mass added does not cover the are of quartz in motion.

K_3 will vary with surface curvature.

Summary

Sauerbrey Equation $$\Delta F = - 0.38 \times 10^6 \frac{F \Delta M}{dA}$$

Lostis Equation $$\Delta F = \frac{F_o \Delta M}{A r_1 y_o}$$

Stockbridge Equation $$|\Delta F| = \frac{F_n m}{K_n r A_a \rho}$$

As can be seen, all the equations are of the type

$F = k m$.

The Sauerbrey has a negative sign indicating a lowering of the frequency on adding mass to the plate. This has been verified in practice, although there have been some exceptions which will be discussed later. The Stockbridge equation has $|\Delta F|$ and therefore allows for positive and negative changes in the frequency.

2.5 Review of the Development of the Quartz Crystal as a Detector

Radio engineers have known for some time that marking a crystal with a pencil or ink will cause it to shift its resonating frequency.(52)

One of the earliest applications of this property was made by Van Dyke in 1951 in measuring the dew point of water. The principle was to determine the temperature at which water condensed onto one surface of a crystal. The opposite side of the crystal was subjected to an alternating cycle of cooling and heating, with the cooling cycle continuing until the dew point is reached. Monitoring the frequency of the crystal showed when this occurred.(53)

The first mathematical derivation of the relationship between the mass and the frequency was made by Lostis in 1958. (54) The following year he published a paper describing a system in which a quartz crystal was used as a reference for a film thickness monitor.(55) The same year Sauerbrey published an alternative derivation in a paper on the use of crystals for weighing thin layers.(45) He tested the equation experimentally and found that it was valid for a finite plate if the whole area vibrating was covered with the vacuum evaporated gold film. The third derivation by Stockbridge was not published until 1965, and used Rayleigh perturbation analysis.(50)He determined experimentally K, the constant of the equation, by evaporating gold onto a crystal and from the weight gain, he calculated the expected frequency change.The ratio of the calculated to the experimental frequency change gave K.

Several workers have utilised quartz crystals as film thickness monitors in various processes which have a vacuum deposition stage. Oberg and Lingensjo (56) reported that a 3.5 MHz crystal, acting as a deposition rate monitor, could measure upto 20,000 Å of a metal

before cleaning of the crystal was necessary. McKeown measured the sputtering rates of gold in an argon beam (57) and other workers have prepared thin metal films using a quartz monitor.(58,59,60,61) Eschback and Kruidhof developed a microbalance in which the crystal forms part of the receiving plate. It is suspended from a vacuum microbalance together with the oscillator circuit fed by a solar cell. When a small coil is placed in the vicinity of the oscillator, the frequency shifts can by monitored without contact, thus reducing a source of error.(48)

The quartz crystal microbalance has also been used to follow chemical reactions. Some examples of weight gain data for sulphuration and oxidation of vacuum deposited metal films are given by Shiojiri et al (62); oxygen sorption in submicron films of asphalt have been studied by King (63); oxidation stability of elastomers has been measured(64); corrosion rates were monitored by fixing the corrodible specimen to the crystal in a corrosive atmosphere.(65)

Various adsorption isotherms have been studied by Slutsky and Wade, and Khan. Approximate isotherms for hexane and water vapour on Y cut crystals are reported (66),and for hexane and argon (44,67), by using the crystal to weigh the partial monolayers adsorbed onto its surface. Stockbridge analysed the frequency changes which occurred on admitting gases to the microbalance at room temperature and atmospheric pressure. Partial monolayers of various gases adsorbed onto the crystal surface were determined and the relationship between frequency change and gas pressure derived.(68) The chemisorption of oxygen on evaporated aluminium films was found to be about 1/2 order using a quartz microbalance.(69) Florio used the microbalance to measure the chemical composition of alkali-antimonide films during photocathode formation. (70)The antimony film was evaporated onto the crystal at room

temperature and the subsequent reaction with alkali metal at elevated temperatures was monitored by the frequency change of the crystal.

The first application of the quartz crystal as a sorption detector with a view to pollution monitoring was made by King in 1964. (52,43) A crystal coated with di-n-butyl phthalate was found to respond more to alcoholic breath than to normal breath. Following this discovery it was shown that many kinds of detector were possible when a crystal was coated with a material which could interact with a vapour. Calibration curves have been obtained for water sorption on molecular sieves,polymers, silica gels, metal electrodes etc.(52) Hysteresis effects have been noticed to take place with the use of deliquescent salts,eg. lithium chloride, as moisture detectors.(52,71); the effect was a time lag occurring in the desorption of the absorbed species. Both lithium chloride and lithium bromide were found to exhibit hysteresis effects, but calcium chloride did not. King holds several patents for moisture detectors.(72-75) Other workers have also developed moisture detectors -one method was to switch the gas streams moving across the crystal from a wet stream to a dry stream every 30s. This gave the crystal, coated with a sulphonated polystyrene, a high selectivity and response, and extended the lifetime of the coating considerably (76,77). Gjessing et al (78) developed a radio-sonde humidity element consisting of a SiO_x evaporated film on a crystal. They reported that there was no hysteresis between 15 and 95% humidity. Instruments are now commercially available for moisture detection.One based on a hygroscopic polymer coated crystal, marketed in 1964, gave a detection of ppm levels in 30s.(52) A new analyser, developed by Du Pont, eliminates hysteresis effects by periodically heating the crystal instead of flow switching. A mass change of 4 ng is reported to give a 1 Hz change.(79)

A great deal of work has been carried out using coated crystals as sulphur dioxide detectors with a variety of coatings. Gas chromatography liquid phases have been found to be the most successful since the sorptions are reversible and the coating is easy to apply to the crystal. Guilbault and Lopez-Roman (80) reported the use of sodium tetrachloromercuriate and other compounds for sulphur dioxide detection. The coatings in order of sensitivtity were sodium tetrachloromercuriate, Silicone QF-1, Versamid 900, Apiezon N, Carbowax 20M and Silicone SE30. The sodium tetrachloromercuriate was found to absorb 4.01 µg sulphur dioxide in 15 minutes, compared with 0.40 µg for the Silicone QF-1. However, the same workers published a later paper describing a Carbowax 20M coated crystal being used in conjunction with a gas chromatograph. The range of sulphur dioxide determined was 1 - 100 ppm.(81) Frechette et al (82,83) screened a number of substrates and reported a detection limit of 5 ppm sulphur dioxide. They used a static system, ie. the sample gas was not flowing over the crystal, and found that the best coating was a 1:1 copolymer of styrene and dimethylaminopropylmaleiimide. Karmarkar and Guilbault used various amines, notably triethanolamine and quadrol, to detect sulphur dioxide at ppb levels.(84) A later paper describes the elimination of moisture interferences by using hydrophobic filters, which has the disadvantage of reducing the sensitivity to 0.1 ppm.(85) A systematic approach for the evaluation of triethanolamine as a sulphur dioxide sorption detector coating was made by Cheney and Homolya.(86) A parametric approach was used to evaluate the coating's sensitivity to changes in temperature and sulphur dioxide concentration, and information is published on areas largely neglected by other workers.

Quartz crystals have also been the subject of several Ph.D.

theses. Hartigan (87) used coated crystals for amine classification and sulphur dioxide detection. The crystals were coated with various amines which were classified in order of their basic strength towards the reference acid sulphur dioxide, as measured by the frequency change. This method also determined the potential of an amine as a coating for sulphur dioxide analysis; most coatings were found to be too volatile, but phenyldiethanolamine was found to be the most favourable with a detection limit of 1×10^{-8} moles sulphur dioxide, (0.025 ppm). Street (88) found that triethanolamine was a suitable coating and gave a sensitivity of 0.025 ppm sulphur dioxide, with a range upto 12 ppm. A method of improving amine coatings by modifying the chemical properties whilst retaining the favourable physical properties was carried out by Pribil.(89) Coatings were prepared from Aliquat (methyl tricaprylyl ammonium chloride) by extracting into it various anions eg. $Cr_2O_7^{2-}$, MnO_4^-, IO_4^-, VO_3^-, Mn^{III}-EDTA ,$Fe(CN)_5NO^{2-}$, $HgCl_4^{2-}$. The highest sensitivity was found for Aliquat containing $Cr_2O_7^{2-}$ and MnO_4^- anions, with an increase of 50 times that found for Aliquat sorption of sulphur dioxide.

The amount of sulphur dioxide in automobile exhausts and industrial stack gases has been measured using a quadrol coated crystal.The concentrations in the exhausts lie in the range 20 - 50 ppm and upto 300 ppm occurs in refinery stack gases. (90)

Ammonia and nitrogen dioxide have been detected at ppb levels using crystals coated with UCON coatings (polyalkene glycols) (91) Mercury in soils has been measured by amalgamating the mercury released from the soil onto the gold electrodes of the crystal. Detection limits of 5 ng/l for mercury in a continuous stream and 0.7 ng for the total mass of vapour in a gaseous sample as drawn up from the soil are given. (92) A similar method was used by Scheide and Taylor,(93,94) for

mercury in air. A commercially available 'film badge' worn on the lapel has been developed by the National Bureau of Standards.(95)By measuring the change in frequency, it is possible to calculate the concentration of mercury to which an individual is exposed.

Organic chemicals have been analysed using a crystal detector usually with prior separation on a gas chromatography column.With this method the coating does not have to be specific towards the compounds but only to have a reasonable sensitivity.

Karasek and Gibbins used a crystal coated with Carbowax 20M operating at room temperature to detect alcohols, ketones,hydrocarbons, etc. in the ppm range.(96)Compounds in the boiling range 40 - 200°C are separated on a column less than 20 inches in length, with short retention times and large responses. This has direct application to low temperature chromatography, so that compounds normally unstable above room temperature can be analysed. A later paper by Karasek and Tiernay (97) used the same partitioning coating on the crystal as in the column to determine the minimum detectable quantities for a range of compounds from sulphur dioxide to heavy hydrocarbons.

The gas phase reactions of mono-, di-, and trimethylamines with various metal salts have been studied using the crystal in a vacuum system.(98)Iron (III) chloride was found to be the most promising coating. Mercury (II) bromide has been used to detect organophosphorus compounds, notably diisopropylmethylphosphonate (DIMP) (99). An improvement was made using a complex of iron (III) chloride - DIMP as the coating ie. Fe $(DIMP)_x Cl_3$,which gave a detection limit below 10 ppm (10 $\mu g/m^3$).(100)

Edmonds (101) screened nine different coatings for seven vapours and developed detectors which could detect the compounds below their threshold limit values.

Earp compared the piezoelectric crystal detector to a thermal conductivity cell for quantitative analysis and found that it was as good or even better, and that it was possible to obtain results from mixtures which would not be expected to be analysed.(102) The coatings were liquids and the relationship between the response and the retention volume, and log response and the reciprocal of temperature for gas chromatography coatings was demonstrated experimentally. Janghorbani (49.) considered linking a partitioning liquid coated crystal detector to a digital computer for rapid data acquisition. Later, Janghorbani and Freund, developed equations for the detector performance as a function of the systems parameters, in particular, the solute-solvent parameters, and tested them experimentally.(105)

One area in which the crystals have been used, but has received little attention is in the field of aerosol mass concentration monitors. Olin, Sem and Christenson constructed and tested a piezoelectric - electrostatic aerosol mass concentration monitor which measured particle mass with an accuracy of 5% in about 10 s. (105,106) The monitor used a point-to-plane electrostatic precipitator to deposit particles onto a piezoelectric microbalance. The technique was applied to automobile exhausts, laboratory and office aerosols and cigarette smoke. Chuan (107) used a thin adhesive layer on the crystal to ensure efficient capture of the particles. The sensitivity was 10^{-11}g.

Another unique use of the piezoelectric crystals was for electrogravimetric trace analysis of metals.(108) Mieure used a gold electrode of a 3.0 MHz crystal as the cathode of a d.c. polarograph. The frequency of the crystal was measured before and after electrolysis to determine the mass of metal deposited on the electrode. The main metal analysed was cadmium (109), although nickel, zinc, indium and lead were also studied.(110) Cadmium was studied in the range 5.0×10^{-4} to

5.0×10^{-8} M. Selectivity could be achieved by using masking agents or by varying the applied voltage.

The current work which has been carried out is summarised in Table 6 and Table 7. It is difficult to compare the results since different workers use different coatings and conditions for analysis, and often a limit of detection is not stated. However, the tables do show the range of research and the sensitivities are given where they are quoted by the authors.

As can be seen from the tables, the detection limits are below the threshold limit values for all the common pollutants listed.

Only one method of analysis for CO_2 using the crystal detector has been reported, and that was to convert the CO_2 to water for subsequent analysis. Buck et al (112) reported that CO_2 could be converted to water using a borosilicate tube approximately 20 cm in length, 0.7 cm in diameter and charged with anhydrous lithium hydroxide. The tube was placed in an aluminium heat sink, 14 cm in length, and maintained at $210 \pm 10^{\circ}C$. King (52) reported that reasonable results for the detection of CO_2 could be obtained by combining Buck's converter with a piezoelectric water detector.

It was decided that since the analysis for CO_2 and CO using coated crystals had not been reported, this was a good area for investigating the potentiality of the piezoelectric detector system in conjunction with an array of suitable absorbents for both gases.

Table 6 Inorganic Compounds Analysed using the Crystal Detector

Sample	Coating	Detection Limit[1]	T.L.V.[2]	Ref.
H_2O	$LiCl, CaCl_2, LiBr$			52,72
	Sulphonated polystyrene	0.1 ppm		73,76
	Vinyl benzenes			74,75,77
	SiO_x	2×10^{-8} g		78
	MgF_2, BaF_2, NaF			78
	Molecular sieves			52,74
	P_2O_5, H_3PO_3			111
H_2	Convert to HCl			111
Hg	Gold electrode	7×10^{-10} g	1 mg/10m^3	92,93,94
H_2S	Lead acetate		20 ppm	74,47
	Ag, Cu			74,47
	Anthraquinone disulphonic acid			74,47
NO_2	MnO_2	0.004 ppm	9 mg/m^3	88
	UCON			91
N oxides	Convert to H_2O or NH_3			111
NH_3	UCON		35 mg/m^3	91
SO_2	$Na_2 HgCl_4$		13 mg/m^3	80,88
	quadrol	1 ppb/0.05 ppm		84,85,90
	Triethanolamine	1 ppb/0.05 ppm		86,84,88
	Other amines			82,87
	Styrene DMAPM	Below 5 ppm		82,83
	Carbowax			81,88,97
	Ag			62
	Phenyldiethanolamine	0.025 ppm		87

Table 6 Continued

Sample	Coating	Detection Limit	T.L.V.	Ref.
SO_2	Convert to SO_3			111
	Ni (II) OH			88
	PbO_2			88
CO_2	Convert to Water		9000 mg/m^3	52,112
Particulates				105,106,107
Metals in Solution				108,109,110

Note 1 The detection limits quoted are in the same units as used by the original authors.

Note 2 The Threshold Limit Values are quoted from the CRC Handbook of Chemistry and Physics. 1974-1975

Table 7 Organic Compounds Analysed using the Crystal Detector

Sample	Coating	Detection Limit[1]	T.L.V.[2]	Ref
n-Hexane	Carbowax	2×10^{-6}g	1800 mg/m^3	97
	Pluronic L64	826.1 mg/m^3		101
n-Heptane	Carbowax	7×10^{-7}g	2000 mg/m^3	97
n-Octane	"	4×10^{-7}g	1900 mg/m^3	97
n-Nonane	"	4×10^{-8}g	-	97
	Rubber Cement	4×10^{-9}g	-	97
n-Decane	Carbowax	3×10^{-8}g	-	97
	Rubber Cement	5×10^{-9}g	-	97
n-Undecane	Carbowax	2×10^{-8}g	-	97
	Rubber Cement	2×10^{-9}g	-	97
n-Dodecane	Carbowax	2×10^{-8}g	-	97
	Rubber Cement	4×10^{-9}g	-	97
Ethanol	Carbowax	8×10^{-6}g	-	97,96
Benzene	"	4×10^{-7}g	10 ppm	97
o- Xylene	"	2×10^{-7}g	435 mg/m^3	97
	Pluronic L64	31.3 mg/m^3		101
Cumene	Carbowax	3×10^{-7}g	245 mg/m^3	97
Mesitylene	"	9×10^{-8}g	-	97
p-Cymene	"	9×10^{-8}g	-	97
n-Hexyl Benzene	"	3×10^{-8}g	-	97
Acetone	"		2400 mg/m^3	96
	"	279.5 mg/m^3		101
2- Hexanone	"	2×10^{-7}g	410 mg/m^3	97
2-Heptanone	"	2×10^{-7}g	465 mg/m^3	97
2-Octanone	"	2×10^{-7}g	-	97
2-Nonanone	"	2×10^{-7}g	-	97
Cyclohexanone	"		200 mg/m^3	97
Ethyl acetate	"	4×10^{-7}g	1400 mg/m^3	97
Ethyl Propanoate	"	3×10^{-7}g	-	97
Ethyl Butanoate	"	2×10^{-7}g	-	97
Ethyl Pentanoate	"	2×10^{-7}g	-	97
Ethyl Hexanoate	"	4×10^{-8}g	-	97
Ethyl Benzene	Pluronic L64	33.7 mg/m^3	435 mg/m^3	101
Cyclohexane	Squalane	410.4 mg/m^3	1050 mg/m^3	101

Table 7 Continued

Sample	Coating	Detection Limit	T.L.V.	Ref
Chloroform	Carbowax	117.4 mg/m^3	240 mg/m^3	101
DIMP	$Fe(DIMP)_xCl_3$	10 ppm		100
	$Hg(II)Br_2$			99
Paraoxon	$Fe(DIMP)_xCl_3$	10 ppm		100
Monomethylamine	$FeCl_3$	5×10^{-9}g	12 mg/m^3	98
Dimethylamine	"	5×10^{-9}g	18 mg/m^3	98
Trimethylamine	"	5×10^{-9}g	-	98

General Coatings

Hydrocarbons	Squalane	74, 47
	Silicone Oil	74, 47
	Apiezon Grease	74, 47, 102
Aromatics	Sulpholane	74
	Polyethylene Glycol	74
	oxydipropionitrile	74
Deoxygenated Compound	Aldol-40	74
	Dinonylphthalate	74
	Tide	74

Note 1 The detection limits quoted are in the same units as used by the original workers.

Note 2 The Threshold Limit Values are quoted from the CRC Handbook of Chemistry and Physics. 1975-1975

Chapter 3 The Experimental System

The experimental system used in conjunction with the quartz crystal microbalance is basically very simple and can be divided into three sections, the electronics, the cell and the gas handling system. In brief it consists of the crystal housed in a suitable cell to facilitate sample presentation, and electronic oscillator to cause the crystal to vibrate at its natural frequency and a means of monitoring changes in the frequency.

3.1 The Crystal and the Electrical System

3.1.1. The Crystal

The crystals used were AT cut, resonating nominally at 9.0 MHz ($\pm$ 50 KHz) in their fundamental thickness shear mode. Each consisted of a 10 mm x 10 mm x 0.1mm plate of quartz, with vacuum deposited gold electrodes on each surface of the plate. The crystals were mounted in uncemented phosphor-bronze clips attached to a holder of the type HC6U. The outer metal can was not sealed to the holder. The crystals were supplied by the Quartz Crystal Co.,New Malden,Surrey.

3.1.2. The Oscillators

The crystals were driven at their fundamental frequency by oscillator circuits of the Pierce type. The circuits were constructed from kits supplied by the International Crystal Mfg. Co.,Oklahoma and were designed to give a broad tuned circuit providing oscillation over the frequency range 6.0 - 10.0 MHz. The output signal was 0.2V RMS across a 50Ωload, and the frequency was within 0.02% of the nominal. The circuit's power requirement was 4 to 9 V D.C. at 20 mA and a 1 V change in the supply caused a 0.001% change in the frequency.The

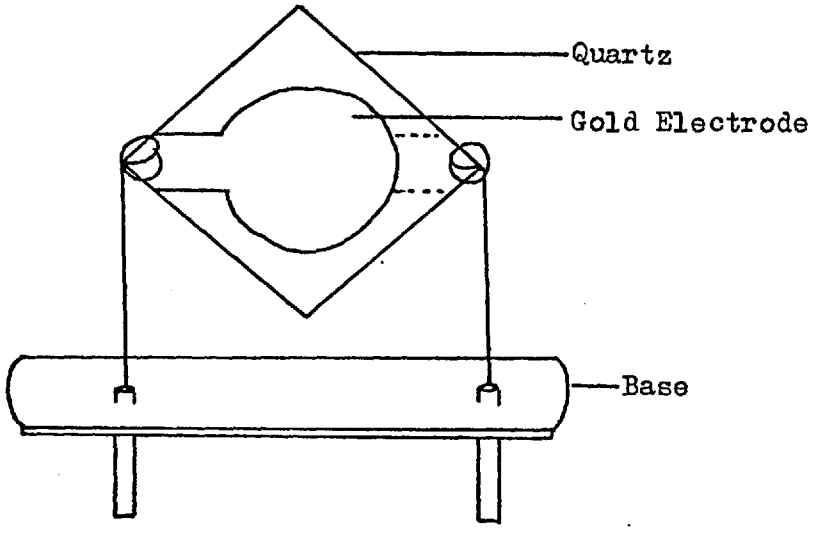

Figure 7 The Quartz Crystal

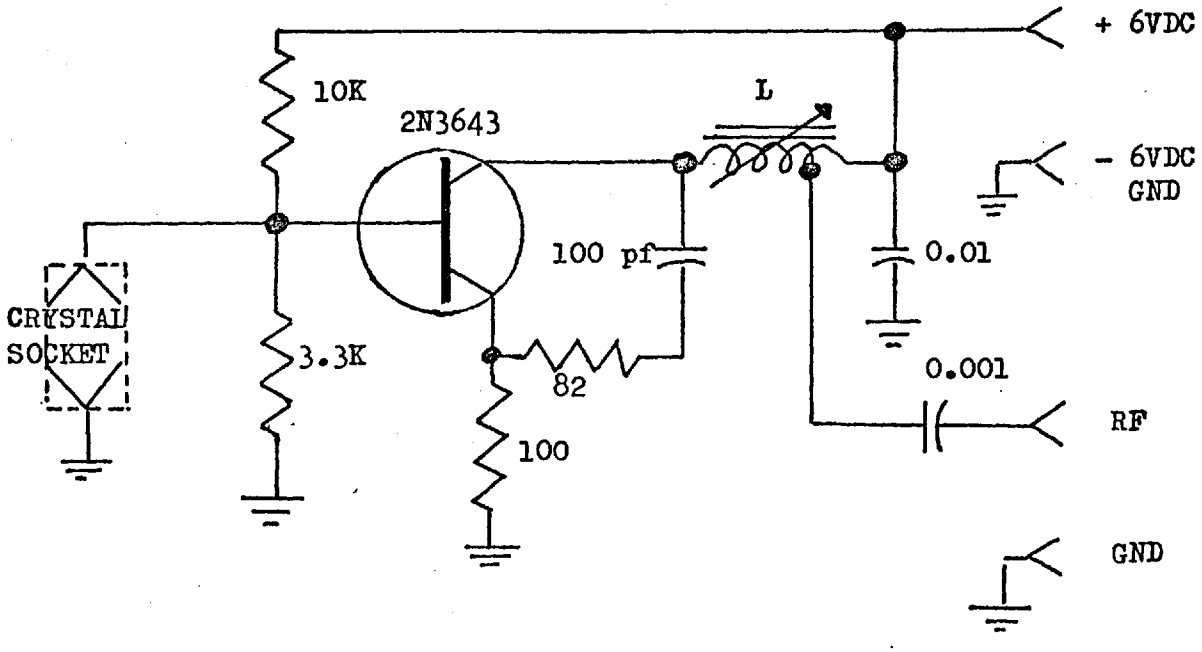

Figure 8 The Oscillator Circuit

operating temperature range is 0 - 50°C.

The circuit diagram is shown in Figure 8.

3.1.3 The Power Supply

The power supply used was the model LM50/30 from Coutant Electronics Ltd.,Reading. The power supply provided a continuously variable, highly stable output in both constant current and constant voltage modes and could deliver 0-30 V with a maximum current output of 0.5 A. It was used in the constant voltage mode at 9 V. A 10% change in the mains voltage altered the output voltage by 1 mV,which in turn would cause a frequency change of 0.1 Hz for a 9 MHz crystal. This is better than the sensitivity of the digital counter.

When two oscillators were used they were both powered from the same supply and were connected in parallel.

3.1.4 The Digital Counter

The Digital Counter was a model 7737 from A.M.F. Venner,New Malden,Surrey, fitted with Option Z so that a parallel 1-2-4-8 BCD output could be interfaced with a digital/analogue converter. The display consisted of seven digits. The frequency range of the counter when operating with a sinusoidal input was from 0 to 50 MHz. The gating time, ie. the period over which the instrument counts the number of incoming pulses, was variable in decade steps from 0.1 μs to 10s The gating time was controlled by a standard frequency reference source in the counter, a 10 MHz crystal controlled oscillator.The accuracy of a measured frequency is $\pm$ 1 count, ie. for a 9 MHz crystal the reading would be 9000000 $\pm$ 1 Hz for a 1s gating time.The significance of the gating time and accuracy can be demonstrated by considering the above example with a 1 μs gating time.The display

would read 9 with an accuracy of $\pm$ 1; for a 10s gating time the display would read (9)000000.0 $\pm$ 0.1 Hz (the first digit -9- would be carried off scale and therefore not seen). It was found that the 1s gating time was the most useful and was used throughout the study.

3.1.5 Digital/Analogue Converter and Chart Recorder

The converter used was a Hewlett-Packard Model 580A/003 coupled with a workshop built interface to the digital counter.The converter accepts parallel BCD inputs and provides analogue output for a strip-chart or X-Y recorder, in this case a Servoscribe 1s potentiometric flatbed recorder, model RE 540.50. A selector switch on the converter was set to convert the last two digits of the frequency so that each division on the chart recorder represented a 1 Hz change in frequency, for a 100 mV full scale deflection. A chart speed of 10 $mm.min^{-1}$ was found to be adequate to follow the frequency change caused by sample introduction.

3.1.6 The Water Bath

For thermostatting purposes a Grant water bath from Grant Instruments,Cambridge, was used, which operated in the range 0- 100°C. A motor driven paddle was incorporated to ensure good mixing.

A flow chart for the electrical system is given in Figure 9.

3.2 The Cell Design and the Carrier Gas System

3.2.1 The Carrier Gas System

The cells were designed to isolate the crystal from the outside atmosphere and to provide a means for sample presentation. A flow chart of the cell and carrier gas system is given in Figure 10.

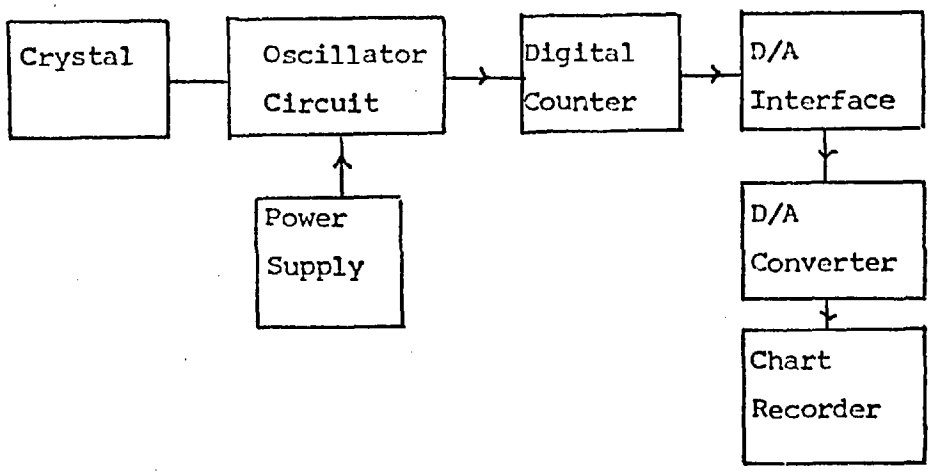

Figure 9 Flow Chart for the Electrical System

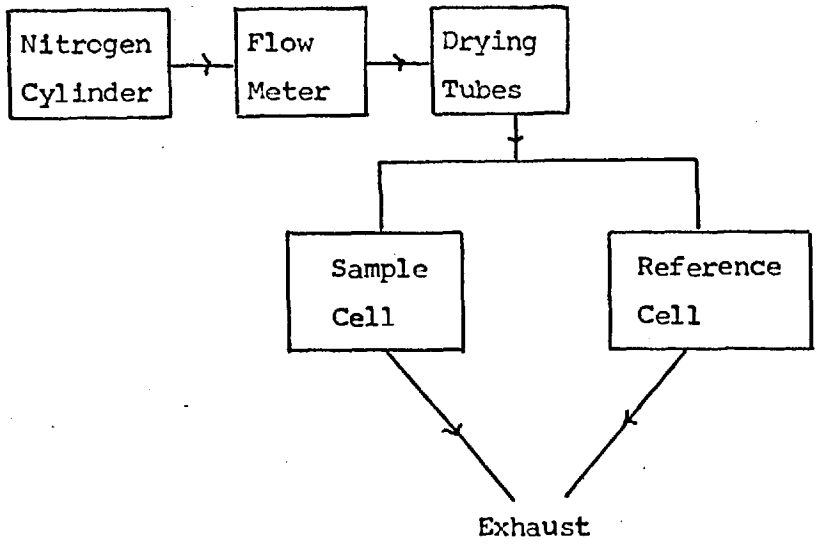

Figure 10 Flow Chart for the Carrier Gas Line

The carrier gas used was oxygen-free nitrogen which was dried either by passing it through a magnesium perchlorate drying tube, or if higher flow rates were needed, and the magnesium perchlorate was found to interfere by causing a pressure build-up owing to the fine particle size, then two drying tubes of silica gel and calcium chloride were used. A fresh drying tube of calcium chloride was found to be satisfactory for drying the nitrogen, but it was saturated after a time and was responsible for spurious signals.

The nitrogen was delivered at a pressure of 1.4×10^4 N/m^2 through nylon tubing (O.D. $\frac{1}{4}$ ") connected with brass couplings throughout. The flow rate was controlled with a fine regulating valve with a p.t.f.e. diaphragm, and a calibrated tapered tube and float flow meter within the range 20 - 500 cm^3/mn. For lower flow rates the flow was measured on a laboratory constructed meter using a glass U tube part-filled with water, which acted as a manometer to measure the pressure drop across a short length of capillary tube through which the carrier gas flowed. The dimensions of the capillary tube were calculated using Poiseuille's equation and the flow meter was calibrated against a bubble flow meter.(101)

Since the different carrier gas drying systems and the two flow meters are used extensively throughout the study, the following shorthand system will be used to avoid confusion.

Drying System	Code	Flow Meter System	Code
1) $Mg(ClO_4)_2$	X	1) Bubble Flow Meter	R
2) Silica gel/$CaCl_2$	Y	2) Capillary Flow Meter	S
3) $CaCl_2$	Z		

3.2.2 The Cell Design

Several different cell designs were used throughout the study and these will be coded to provide easy identification. There are two basic cell types - static and dynamic. The static cell provides a stable atmosphere of nitrogen for the crystal, into which the sample can be added, and the overall change in frequency can be monitored over a long time interval. The dynamic cell provides a moving carrier gas across the crystal, into which, the sample can either be presented as a solitary pulse of gas, or as a dilute sample over a longer period.

3.2.2.1 Static Cell - Cell A

A glass cell was constructed for the static system studies,(88) and it is illustrated in Figure 11.

The cell was mounted on a perspex base fitted with phosphor-bronze spring clips. A crystal holder connected to an oscillator with coaxial cable was sealed into the base. The cell could be flushed with nitrogen and then isolated from the gas stream by turning the two taps. The sample was introduced into the cell through a silicone rubber septum using a gas tight syringe. The volume of the cell was 27 cm^3 and thus the final concentration of the sample could be calculated.

For temperature studies a heater was constructed by wrapping asbestos paper around the cell. On top of this was wound nichrome wire and then a final layer of asbestos paper. The heater was driven from a separate power supply.

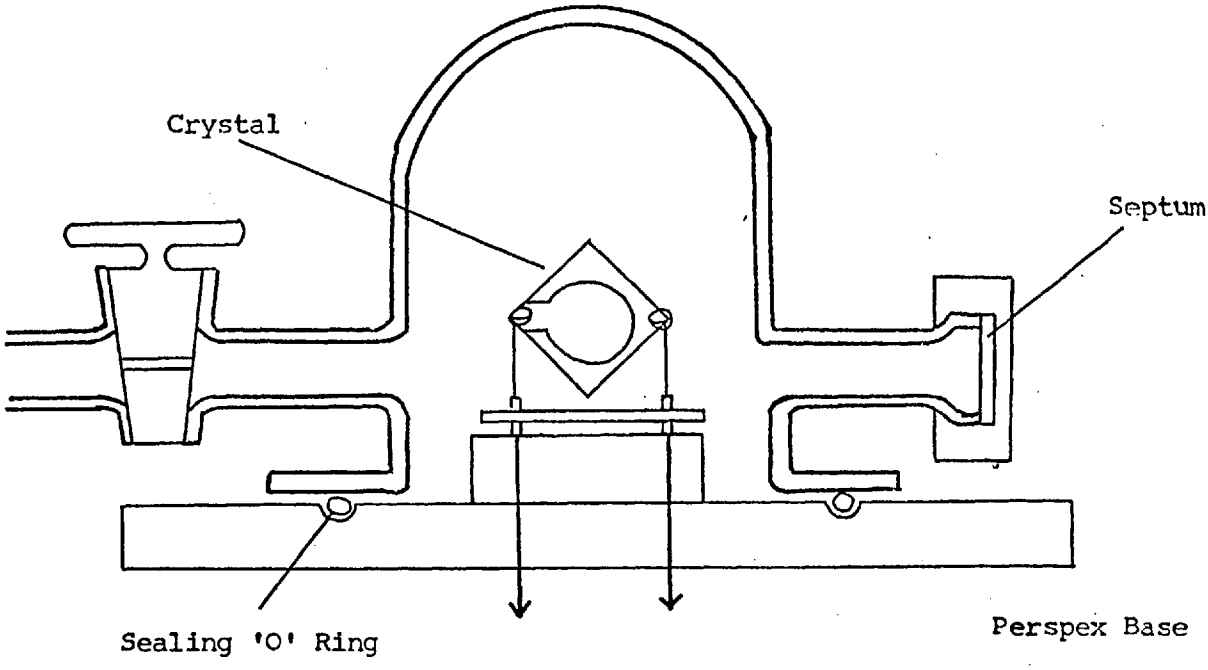

Sectional Elevation

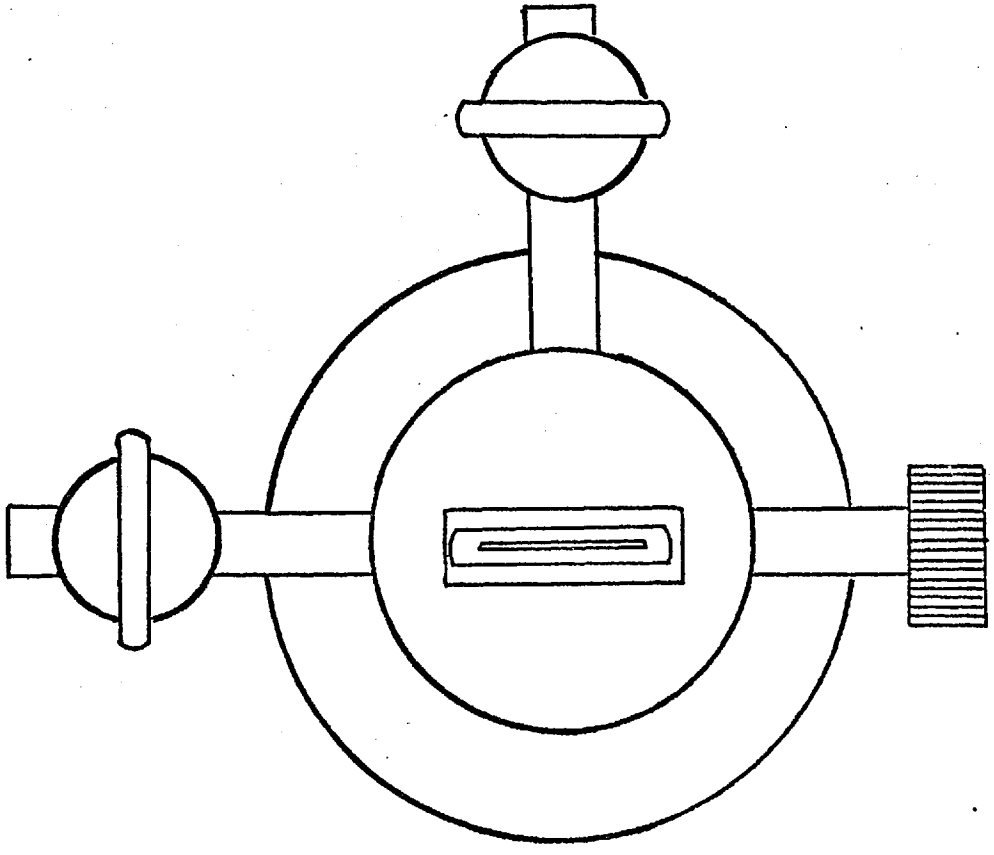

Plan

Figure 11 Glass Cell - Cell A (88)

3.2.2.2 Dynamic Cells

In a dynamic system the cell design is far more important and the main considerations are as follows.

1) The cell volume must be as low as possible to ensure rapid detector response.

2) The cell volume must not affect the sensitivity of the detector to equilibrium attaining samples.

3) The cell must be designed to ensure that the coating of the crystal is exposed to the maximum amount of the sample.

4) The cell must be gas and water tight in order to prevent sample loss and leakage on immersion in a water bath.

5) The removal and replacement of the crystals should be simple and reproducible.

6) The cell should be easily flushed with nitrogen after a sample presentation to avoid cross contamination of samples.

7) The cell should be robust and solid so that it is able to withstand external shocks, eg. an object being dropped on the bench in the vicinity of the cell.

Impinger Design Cell

A design which satisfies many of these requirements was used by Bristow in his mercury vapour cell.(92) The detector was constructed from the metal cap,which usually seals the crystal,and two holes, 0.0028" in diameter were drilled in the opposite faces of the cap normal to the centre of the gold electrodes of the crystal. The carrier gas divided into two and passed through these holes to the crystal, impinging directly onto the crystal surface. The exit for the gas was a third hole drilled in the top of the cap.

Bristow found that the collection efficiency was high for

this cell. A similar design was used by Karmarkar and Guilbault.(84,85, 90)

Spoiler Design Cell

This design was used by King (74,75), Cheney and Homolya(86), and Hartigan (87). The carrier gas stream impinges on one edge of the crystal which acts as a spoiler, splitting the gas stream. The gas passes either side of the crystal to an exit.

A third type of cell is a combination of both the spoiler cell and the impinger cell. The carrier gas impinges on the crystal face and is split into two moving around the crystal to an exit on the other side of the cell. This type of cell was used by Karasek and Gibbins.(96)

These cells are depicted in Figure 12 . The third type of cell mentioned would be expected to give consistent results for a crystal coated on one side only, but for a crystal coated on both sides anomalous results would occur since the gas is not impinging equally on both coatings. The spoiler design has the disadvantage in that it requires accurate machining in order to maintain reproducible splitting of the gas stream. This can be readily appreciated from Figure 13 .Incorrect machining of the holes or poor alignment of the crystal in the cell will cause inaccuracies in sample presentation to the crystal which will be more noticeable for a crystal coated on both sides. For the impinger cell accurate machining is needed to align the holes with the electrode surfaces although a greater degree of tolerance can be allowed than for the spoiler design. Thus it can be seen that the impinger cell is the more practical of the three.

Impinger Cell

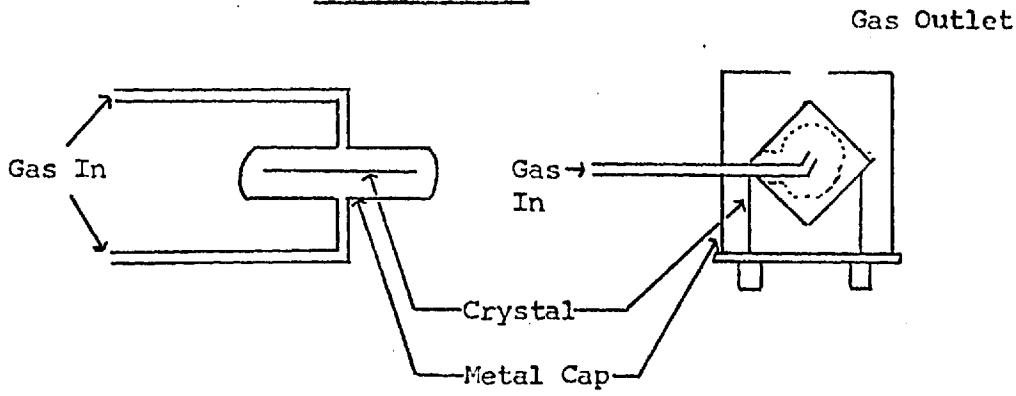

Spoiler Cell

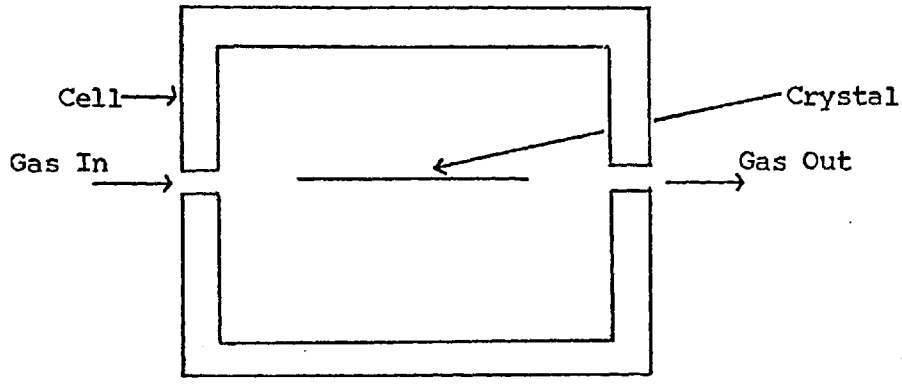

Combination Cell

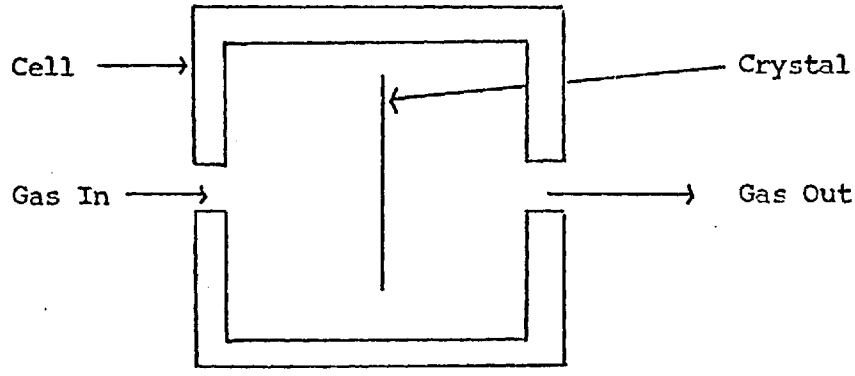

Figure 12 Types of Dynamic Cells

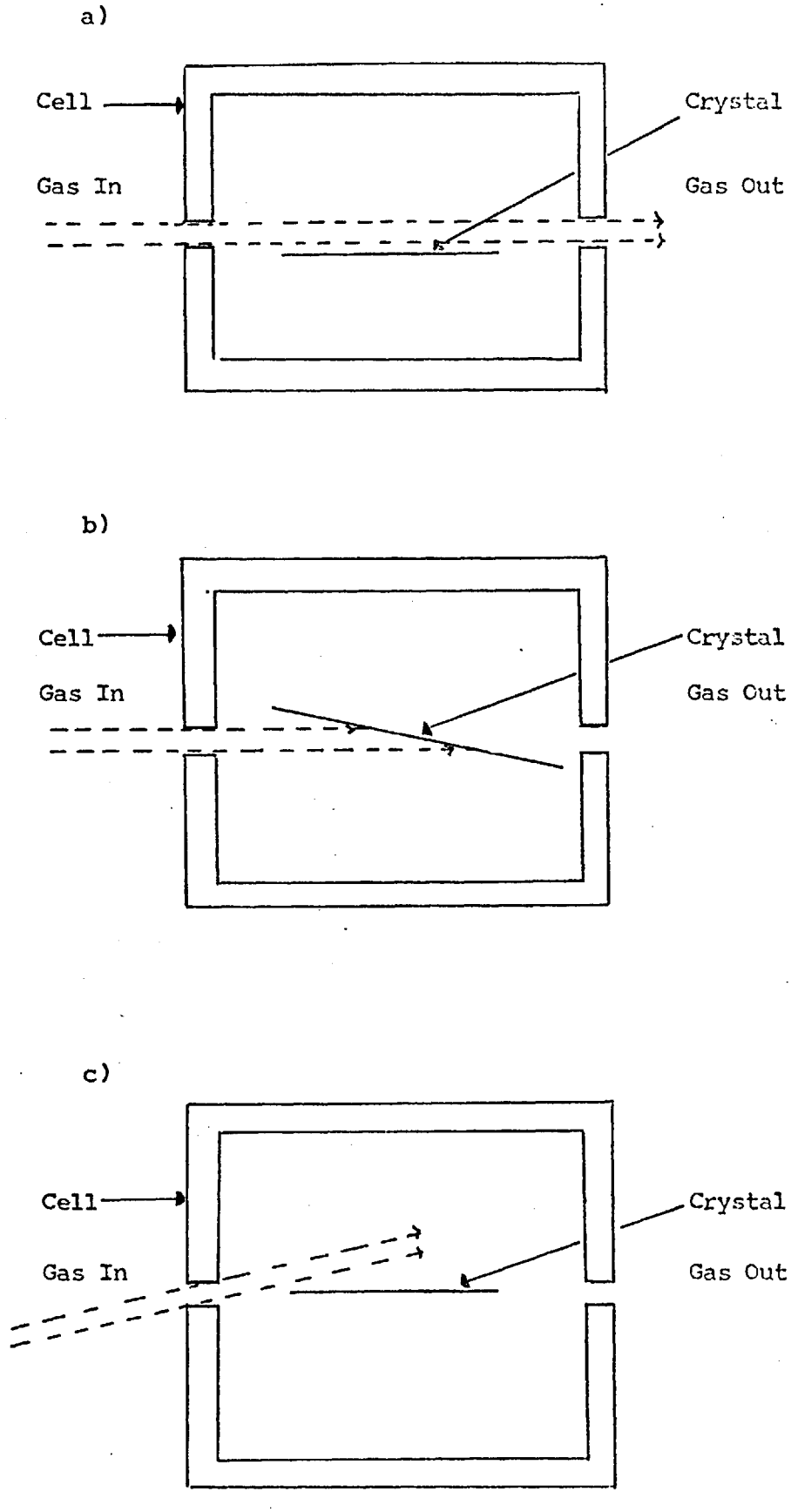

Figure 13 The Spoiler Cell

3.2.2.2.1 Cell B

This cell was based on the design by Bristow (92) and is shown in Figure14. The carrier gas is directed through two holes in the can (0.61 mm in diameter) onto the centre of the crystal's electrodes. The exit is a $\frac{1}{4}$" diameter hole in the side of the can.

The cell was used for the work on iodine pentoxide and for this had to be maintained at a temperature of 150 -160°C. The cell was encased in a 4" square box with a small heater down each side. The heater consisted of nichrome wire (18-67Ω/m) wound on a former of pyrex tubing supported by a copper wire through the centre of the tubing. The power applied to the heater was 16V d.c. at 0.6 A,ie 9.6 W. The rest of the box was filled with insulating fibre glass wrapped in tin foil to reflect the heat back to the cell. The oscillator circuit was fixed to the top of the box using spacers and was connected to the crystal using an adaptor made from a crystal socket and crystal base. The cell and heater box are shown in Figure 14b).

The temperature in the cell was measured using a chromel-alumel thermocouple, of which, one junction could be placed inside the exit tube of the cell via a brass 'T' piece, and the other junction was immersed in an ice/water bath.

3.2.2.2.2 Cell C

This cell was designed to overcome the difficulties in replacing the crystals in the phosphor-bronze clips of the holders after they had been removed for weighing purposes. This was a problem only experienced with one batch of crystals where the clips were so tight that it was easy to snap the edges of the crystals.

As can be seen from Figure 15 the design was based on the spoiler system. It was felt that for liquid coatings this would be

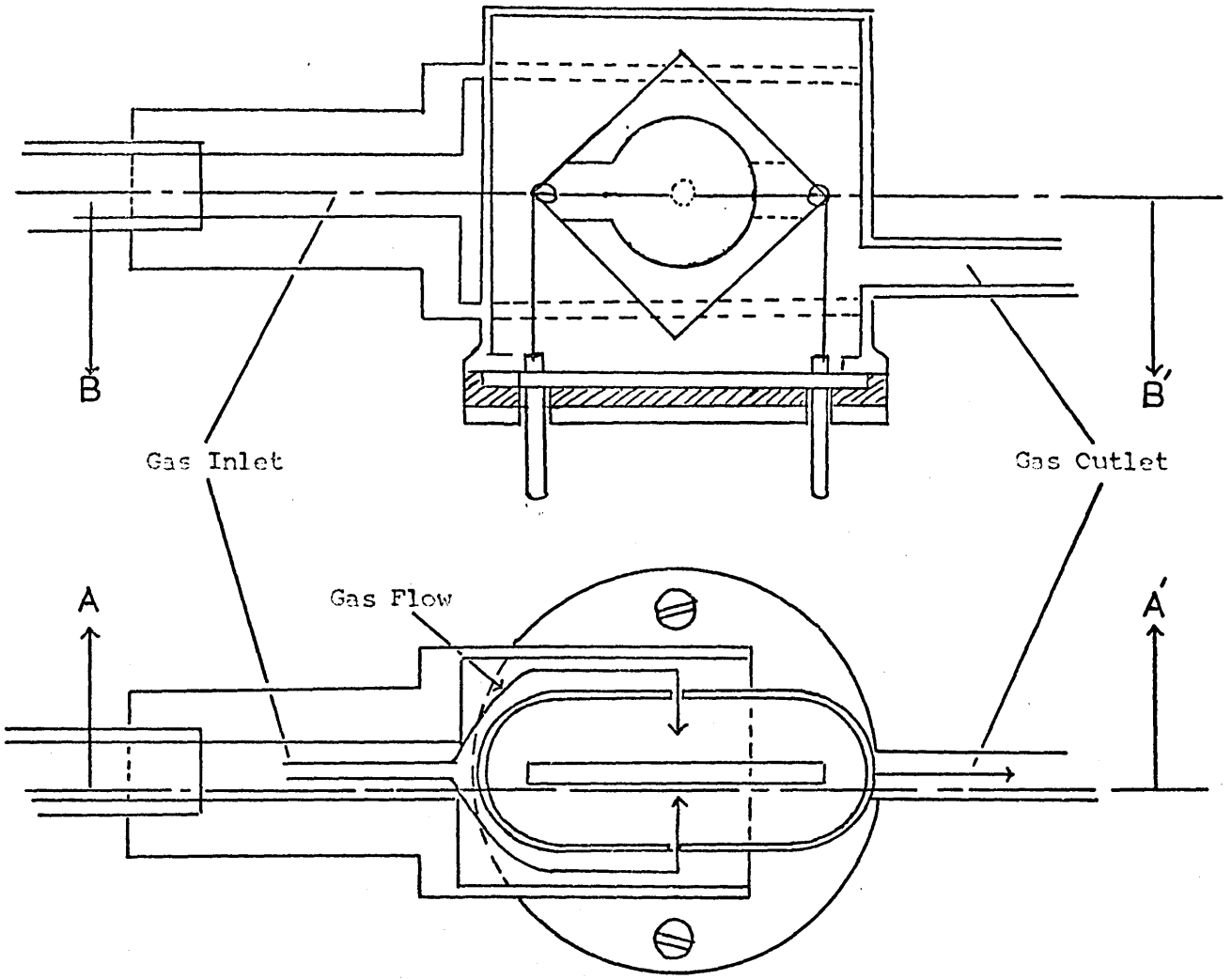

Figure 14(a)

Sectional Elevation, AA' and Sectional Plan BB' of Impinger Cell B (SS)

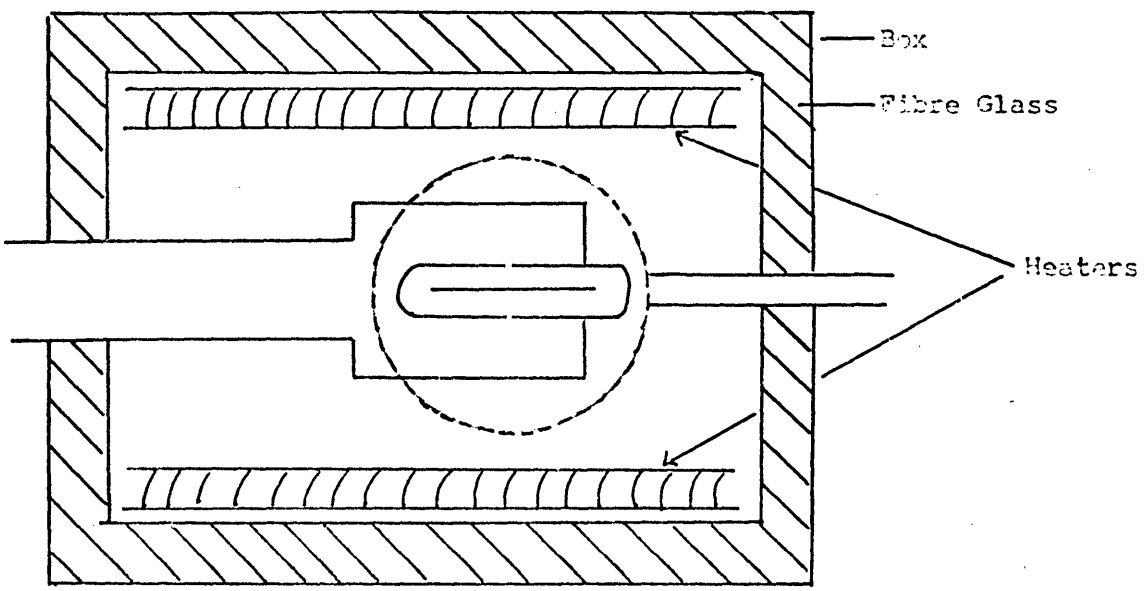

Figure 14(b)

Cell B in the Heater Box

more advantageous than the impinger design since a greater surface area of the coating would be presented to the sample and thus improve the attainment of equilibrium. The cell was constructed from two $1\frac{1}{2}$" squares of perspex. Perspex was chosen for two reasons, it is an inert material with respect to the gases used in this study, and it is clear allowing any coating change taking place to be observed. The bottom half of the cell had a 1 cm square well cut into it, with a narrow ledge down two opposite sides on which the crystal was placed. Level with this ledge, such that the crystal splits the gas stream in half, were drilled the gas entrance and exit holes. The carrier gas flowing through $\frac{1}{4}$" nylon tubing was forced into 2 mm copper tubing in order to enter the cell, flows across the crystal and out of the cell *via* a second copper tube. The top of the cell was a flat perspex plate which was screwed down onto the base sandwiching a tin foil and vacuum grease gasket to prevent gas leaks. Let into the top and bottom of the cell, diagonally opposite each other, were two screws, which could be screwed down to touch the corners of the crystal electrodes. The power was supplied to the crystal from the oscillator circuit *via* these two screws.

This cell was eventually abandonned because it could not be made water tight, and therefore, could not be conveniently thermostatted. Another disadvantage was that great care was needed in tightening the screws down onto the crystal in order to avoid snapping the corners.

3.2.2.2.3 Cell D

This cell was designed and used by Street (88) and is shown in Figures 16,17. The gas was split by the crystal and flowed diagonally across the cell to the exit;efficient flushing of the cell was also ensured by this design.

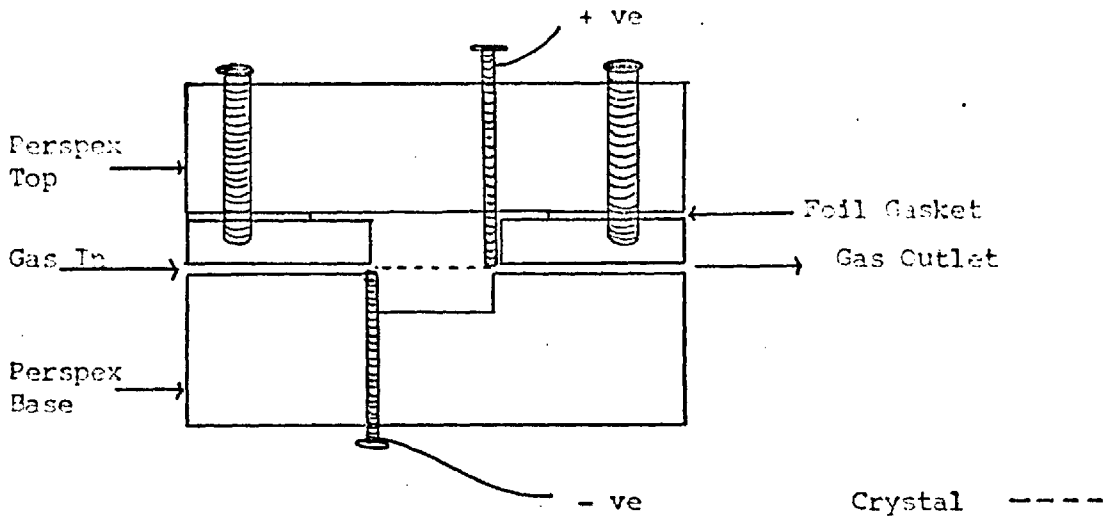

Figure 15 Vertical Section Through Cell C

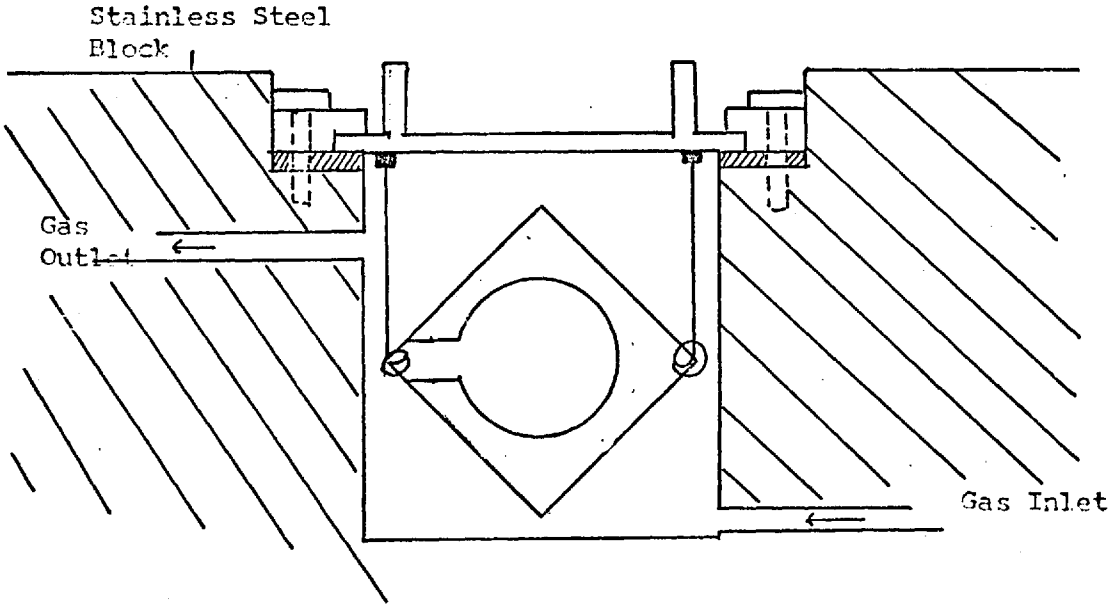

Figure 16 Section Through Cell D (88)

Figure 17 Section Through Stainless Steel Cell, D (88)

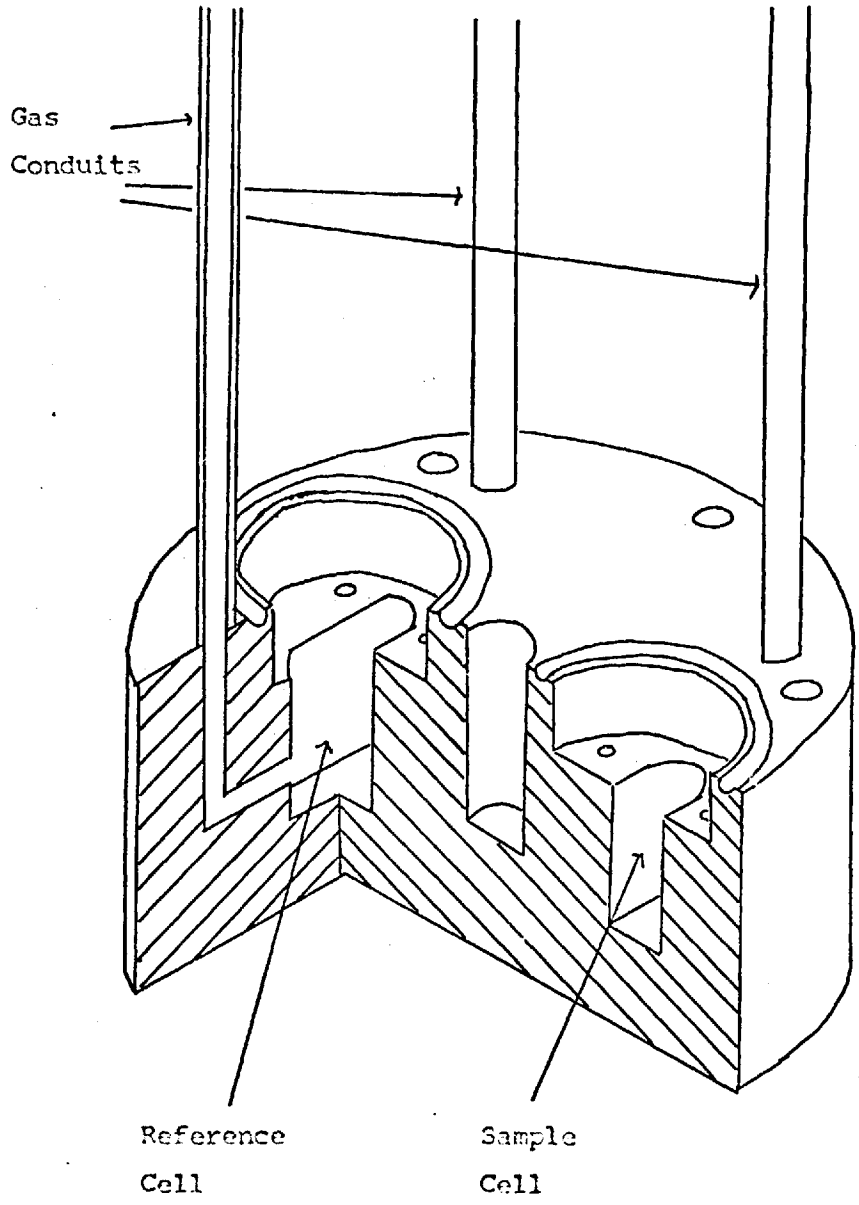

Two cells of this design were constructed in such a manner that both completed cells were in the same block of stainless steel. The two cells, one for the reference and one for the sample crystal, were isolated from small, rapid temperature changes in the environment by virtue of the large thermal capacity of the cell block. The cells were water tight, but it was found necessary to seal the top of each cell with Plasticene to prevent gas leaks.

3.2.2.2.4 Cell E

This cell was of a similar design to cell D, except that the two cells were not combined. The gas entered the cell impinging on the crystal electrodes and left by a small exit hole above the entrance holes. The cell is shown in Figure 18 .

The cell was designed and used by a co-worker (89) and was used by the author only for the work on mercuric oxide, in conjunction with cell D.

It is advantageous to describe the system for the mercury oxide work at this point and a flow chart of the equipment is given in Figure 19 .

Cell D was used to monitor any CO_2 being evolved and Cell E monitored the liberated mercury. The reaction furnace was based on two pyrex tubes - an inner and an outer. The inner tube of I.D. 4 mm and length 18 mm was filled with pelletised red mercuric oxide. The pellets were formed using powered mercuric oxide in a Perkin-Elmer pellet press. They were held in place in the tube by plugging the ends of the tube with glass wool. The outer tube, 15 mm long and of I.D. 7mm, was slotted through a 4" square metal box and was used as a former for a heater of nichrome wire ($16.2\Omega/yd^2$) . The box was filled with glass wool which acted as a very effective insulating material for the system.

Figure 18 Cell E

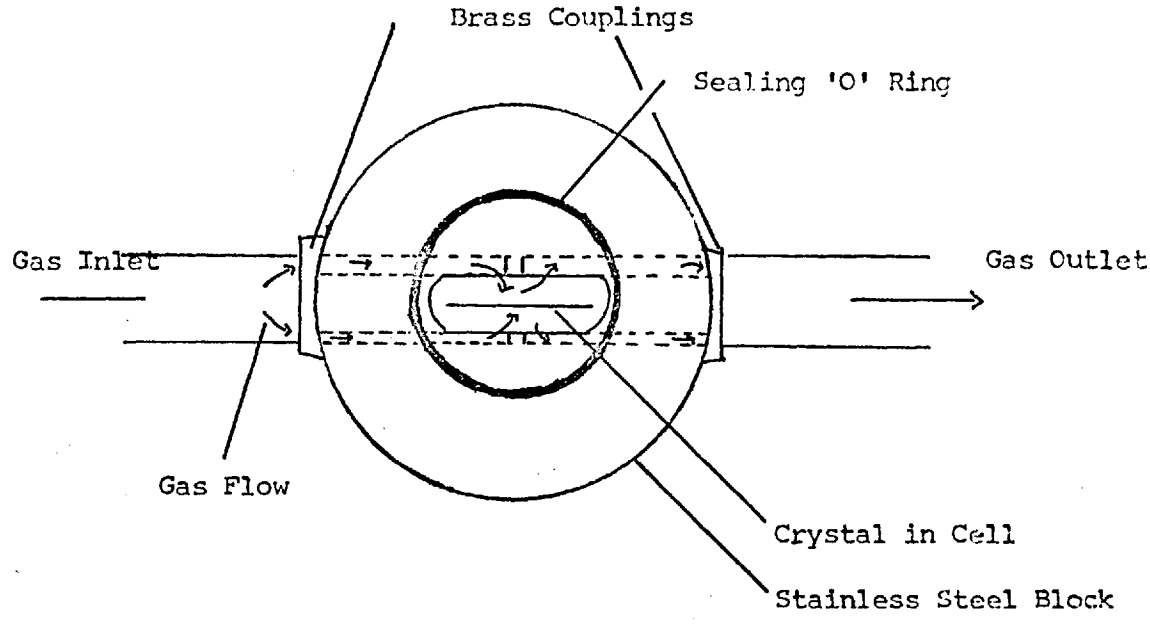

Sectional Elevation of Cell

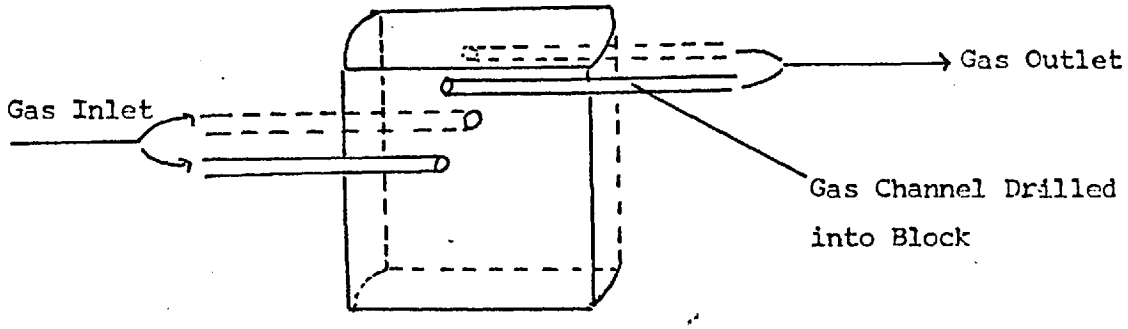

Diagram of Cell -(the Stainless Steel Block is not shown)

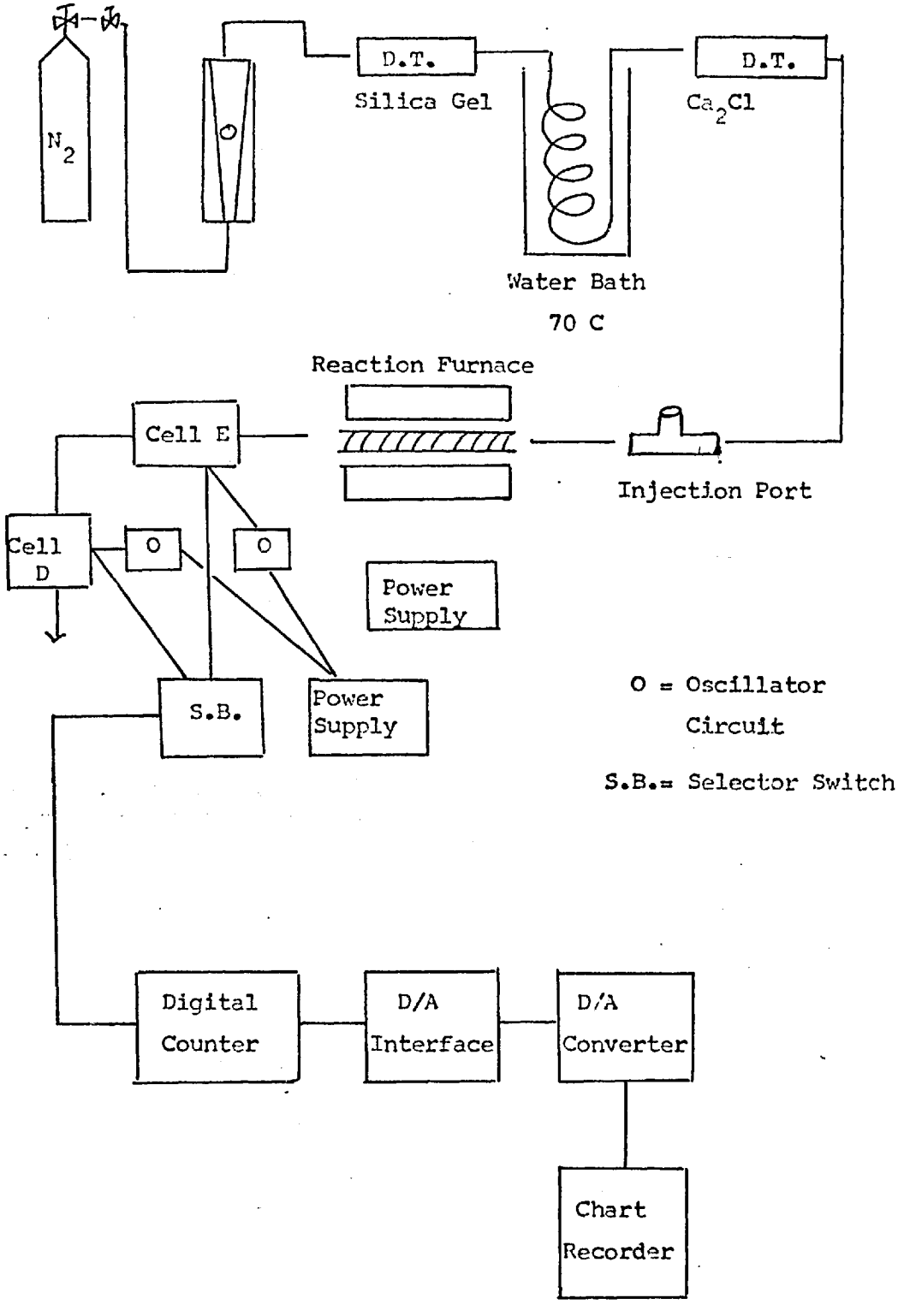

Figure 19 Flow Chart for Mercuric Oxide System

Other design features of the cells will be discussed as they arise in the text.

3.3 Sample Gas Handling System

The sample gases used in this study were CO and CO_2, obtained in small lecture cylinders from Air Products Ltd.. The sample gas was allowed to expand from the cylinders into a 100 cm^3 evacuated glass reservoir. The reservoir was filled to a pressure approximately 10 torr greater than atmospheric. Aliquots of the gas could be withdrawn by a syringe through the rubber septum and injected into the cell. The reservoir is shown in Figure 20 .

Two types of injection port were used in the cells; a brass 'T' piece coupling was inserted into the carrier gas line and the third connection used to hold a rubber septum.The second method was via a glass Y piece,incorporated with a holder for a septum, and fitted into the gas line prior to cell D. These injection ports are shown in Figure 21 .

The above gas reservoir held only pure gas and another reservoir fitted with Teflon taps, to avoid contamination from the stopcock grease, was constructed for dilute samples. A previous worker (88) had established that during the preparation of dilute samples of sulphur dioxide, serious contamination had been caused by the grease absorbing and releasing sulphur dioxide.The reservoir also incorporated a mercury pressure levelling device, so that on withdrawal of a 5 - 10 cm^3 sample, the pressure of the reservoir could be equilibrated to atmospheric pressure before removing the syringe needle. This minimised sample error caused by pressure fluctuations and also prevented contamination by air seeping through the septum.The presence

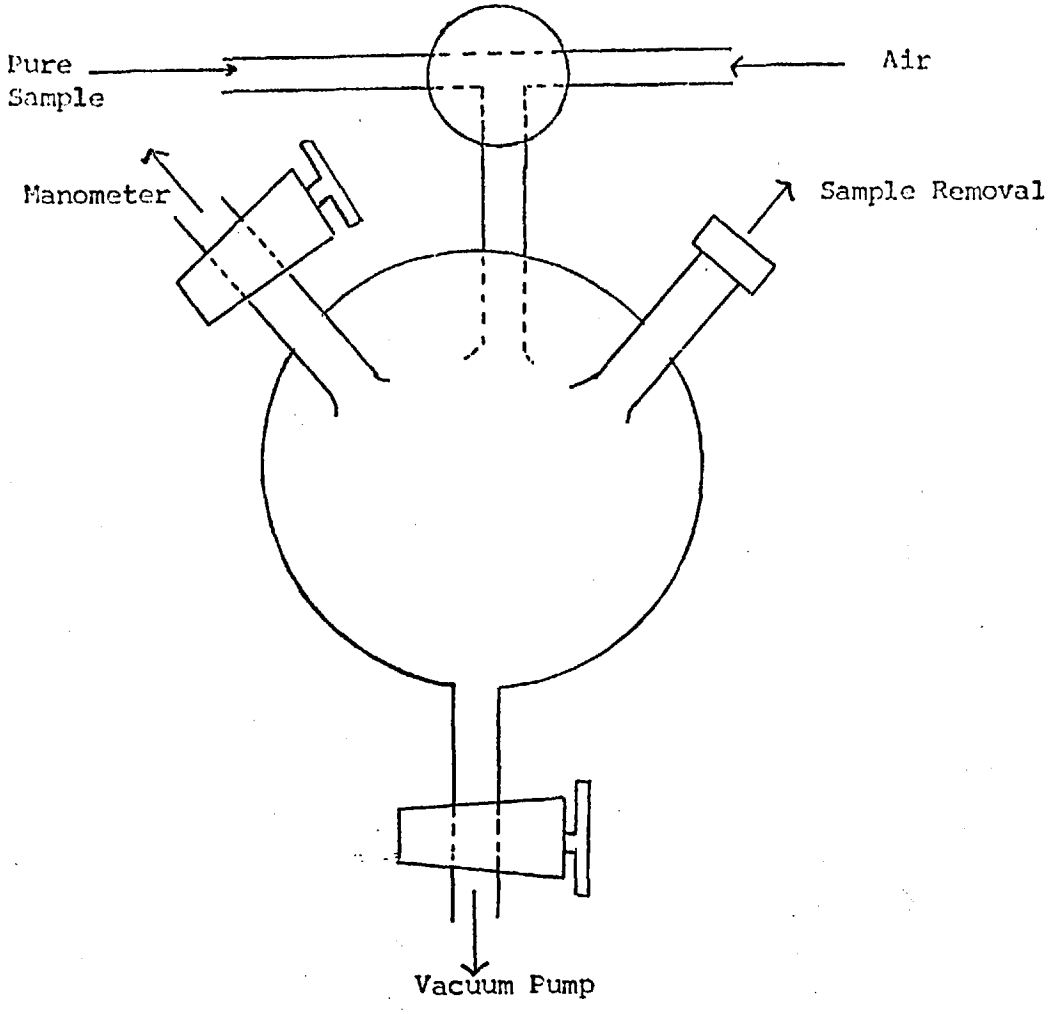

Figure 20 Gas Reservoir

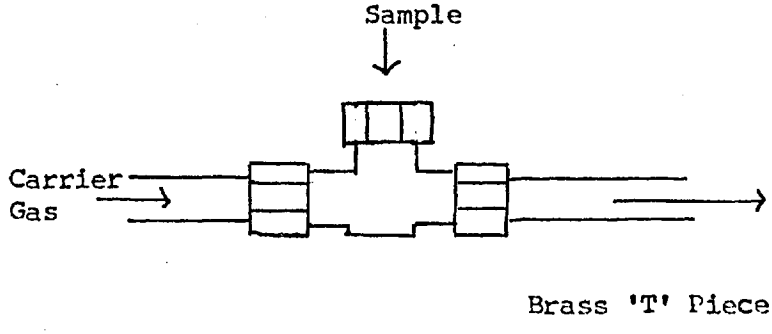

Brass 'T' Piece

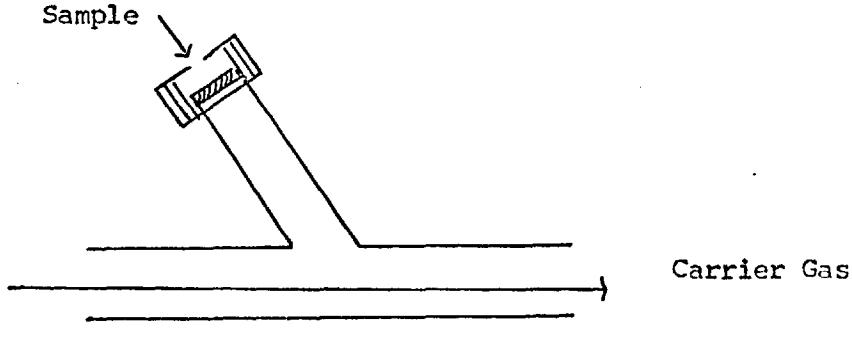

Glass 'Y' Piece

Figure 21 Injection Ports

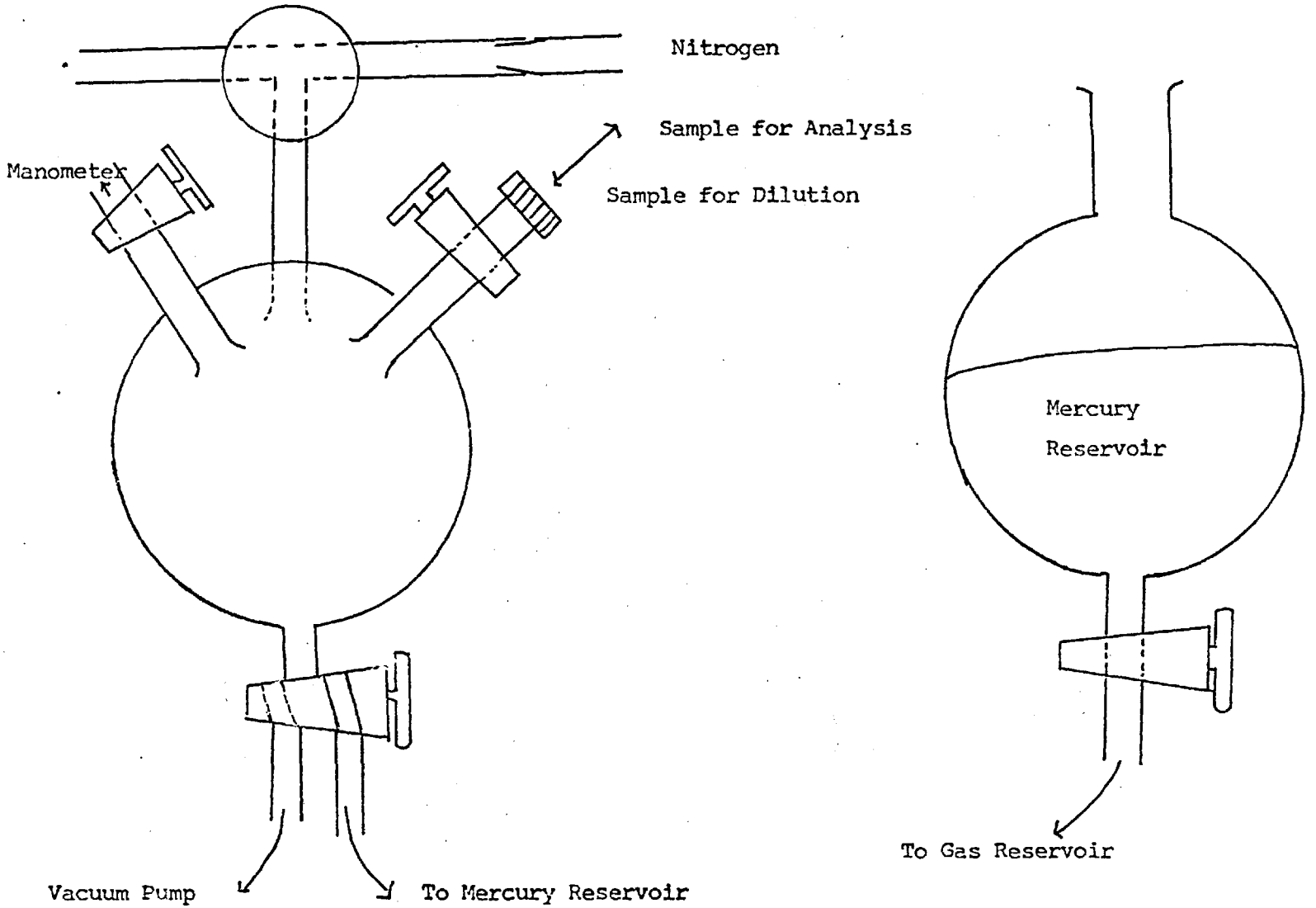

Figure 22 Gas Reservoir and Mercury Levelling System

of the mercury in the reservoir may be responsible for anomalous results obtained with dilute solutions of CO_2 and this will be explained later. The reservoir is shown in Figure 22.

The gas solutions were prepared by injecting a known amount of sample gas into the evacuated reservoir and then diluting it with dried nitrogen to atmospheric pressure.

Methods of Injection

Small aliquots of gas were injected into the cell using gas tight microsyringes from Scientific Glass Engineering Ltd.,(S.G.E.) Australia. Two sizes of microsyringe were used, a 10 µl capacity subdivided into 2 µl aliquots, and a 100 µl subdivided into 10 µl aliquots. The samples were injected rapidly into the carrier gas as pulses.

In later work it was necessary to present samples over a longer period (5- 15 min) in order to monitor the equilibrium effects. Two methods were used, the first being a complex method that had many associated problems, and the second was a workshop built syringe pump.

The first was based on an asbestos plug flowmeter as used by Saltzman and Wartburg (114,115) to prepare standard low concentrations of nitrogen dioxide. The system used was a modification of this, built by a co-worker (89) and is shown in Figure 23 . It consisted of three separate parts -a) carrier gas and vacuum line, b) the sample delivery system, and c) the pressure and flow measuring panel. The system supplied dried nitrogen to the cell and to the aspirator bottle, via taps 2 and 3.

The principle was that the aspirator bottle and the plastic bag were evacuated via taps 2 and 3. A sample of gas was injected through the septum into the aspirator bottle and diluted with nitrogen

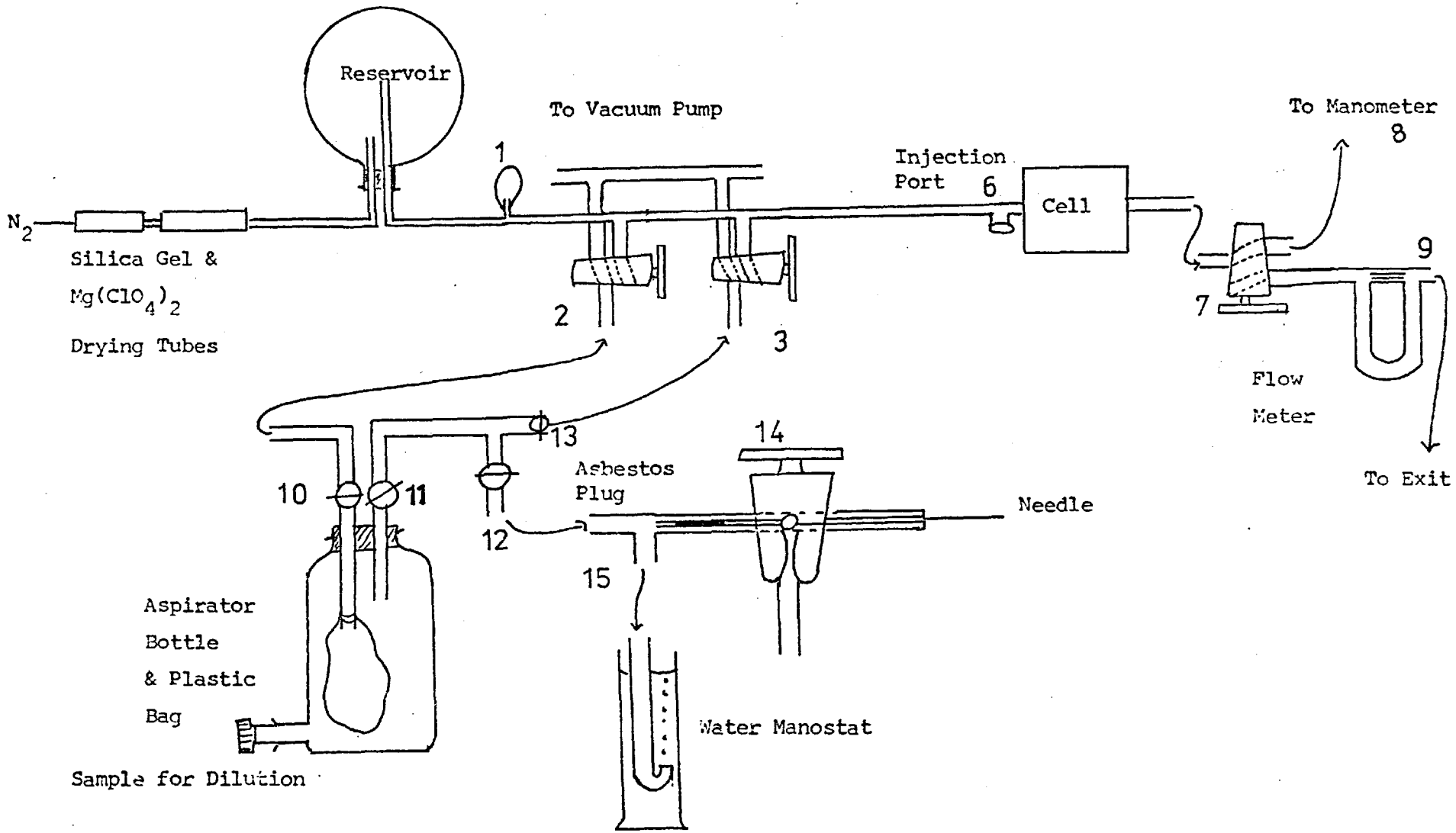

Figure 23 Asbestos Plug Flowmeter System (not to scale)

via tap 3. The rubber teat (1) indicated a lower pressure than atmospheric in the line by collapsing and could be used as a visual indicator, in conjunction with a manometer to show when the pressure in the aspirator bottle had reached atmospheric pressure. The pressure inside the bottle was raised to about 10 torr above atmospheric pressure in order to maintain a gas flow from the bottle. With tap 13 closed and taps 10, 11 and 12 open, nitrogen could be passed into the plastic bag which slowly inflated to expel the dilute sample gas through taps 11 and 12.

The asbestos plug flowmeter is shown in the diagram. Outlet 15 was connected to a water manostat and the gas was bubbled through a sinter in order to minimise any pressure build-up. The head of water determined how much gas was vented through 15, which in turn determined the gas passing through the asbestos plug in the capillary tube of the tap. A needle was incorporated to facilitate sample presentation to the cell. The flow rate through this needle was measured by inserting the needle into a capillary flowmeter.

The second method for long sample presentation was to use a workshop built syringe pump. This consisted of a motor driven piston which pushed on the syringe piston gradually emptying the syringe. The pump had only one speed and emptied a 5 cm^3 syringe in 7.5 min. The syringes used were 5 and 10 cm^3 ground glass, Chance Interchangeable syringes, fitted with a Teflon needle, 30.5 cm in length. The syringes were found to be sufficiently gas tight under the operating conditions used. Since the flow rate of the carrier gas and sample gas was known, the dilution factor, and hence the final concentration in the cell of the sample could be calculated.

3.4 Experimental Investigation of Instrumental Parameters

3.4.1 The Quartz Crystal

The quartz crystal has two parameters which can be varied - the cut and the frequency. The reasons for choosing the AT cut have already been examined in the preceding chapter.

The most widely available commercial crystals have fundamental frequencies of 5, 9, 15 and 22 MHz. The overriding factors in the choice of frequency is the increasing mass sensitivity with increasing frequency,(110), and the increasing temperature sensitivity with frequency.(116)

5 MHz crystals have a low temperature coefficient, but also a low mass sensitivity.They were used by Olin et al (105) and Warner and Stockbridge (117).

15 MHz crystals have a high mass sensitivity (2600 Hz/μg) (52), but also have high temperature coefficients and are very thin and fragile. These crystals were used by Guilbault (98,99) and Bristow(92).

Most workers have used 9 MHz crystals which have a reasonable mass sensitivity (400 Hz/μg) (100), and temperature coefficient (- 1.1 Hz/°C),and offer a compromise between high mass sensitivity and high temperature coefficient.

The crystal must be firmly clamped. Berndt and Love (118) reported variations in the frequency of the crystal if subjected to slight mechanical shock.

3.4.2 Temperature

Since the crystals are temperature sensitive, this is a parameter that needs some consideration.

Quartz crystals have been used as accurate thermometers.

Smith and Spencer used a 5 MHz crystal with a temperature- frequency ccefficient of about 80 ppm/°C (119) and Wade and Slutsky (120) reported a temperature resolution of a few 10 - 1000s of a degree over the range 77 - 435 K. King and Camilli supported thin film thermocouples on quartz for differential thermal analysis over the range - 125 to 500°C, and obtained calorimetric data based on indium which agreed with literature values.(121)A paper by Warner and Stockbridge (117) discusses the effect of temperature variations on the resonant frequency of the crystal. They found that quartz plates,in particular the thicker ones, exhibited for a period of time much larger frequency changes than are predicted by their equilibrium temperature coefficient, whenever the ambient temperature was changed. This effect was deduced to be partly due to the temperature change, but due more to the effect of temperature gradients within the quartz plate. This can be minimised by controlling the thermal environment of the crystal and by using thin plates.

For the investigation of temperature effect on a single uncoated crystal, cell B in the heating box was used. The temperature at the crystal was measured using the thermocouple. The frequency change was measured using the internal standard of the digital counter. No carrier gas was flowing. The results are given in Figure 24 . As the crystal is heated the frequency falls and reaches a fairly constant level as the temperature stabilises.The heater was switched off after one hour, and as the temperature of the cell falls, there is a corresponding increase in the frequency.

The temperature coefficient for the system between 20°C and 67°C is 3.5 Hz/°C which is approaching the zero temperature coefficient of a perfectly aligned AT cut crystal.

The effect of temperature changes on a coated crystal will

Figure 24 The Effect of Temperature on an Uncoated Crystal

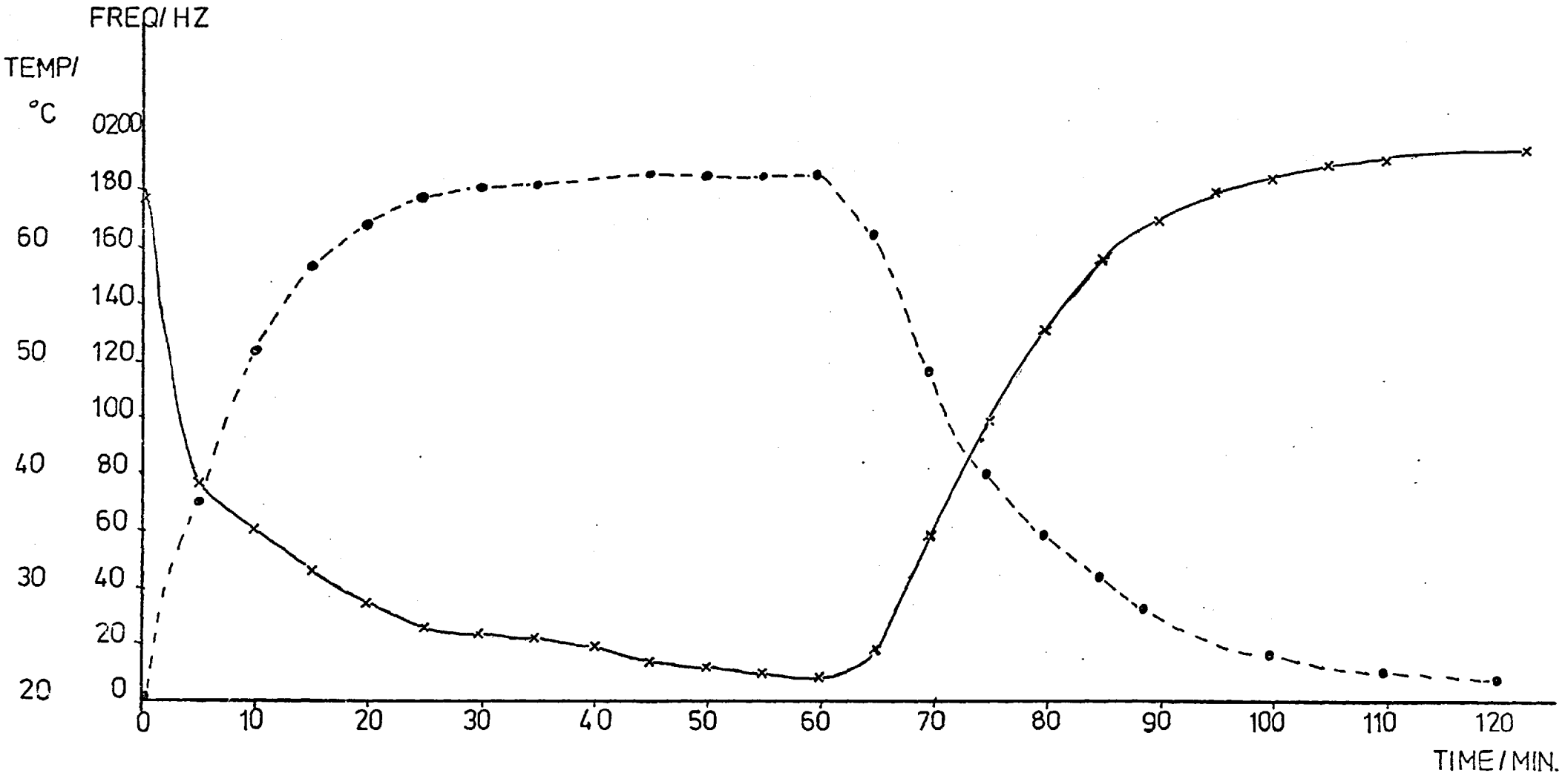

be discussed later in the text.

The crystal can be thermostatted in several ways.The easiest method is to immerse the cell into a water bath,which is held at a controlled temperature. Another simple method is to use integral crystal heaters. These are special crystals with an integral heating element combined with the electrode; on one electrode surface, are combined an electrode to accept the electric current, and one to act as a thin thermocouple. King (43) found that these crystals were ideal for use as a reactive gas detector with the reaction occurring on the crystal, whilst the environment remained at ambient.

3.4.3 Single Sided versus Double Sided System

It is pertinent to discuss here, the relative merits of the single versus the double sided system, since many workers believe that the use of a double sided system minimises the effects caused by temperature, pressure, flow rate changes and coating bleed. However, the author has found that it was not always advantageous to use the double sided system, since it tended to confuse the results.

1) Single Sided System

This is the system where a single cell is used to monitor the interaction of sample and coating. A clean uncoated crystal, under ideal conditions, will have a constant frequency with little,or no, drift. For a coated crystal, in a flowing gas stream and subject to temperature fluctuations, there will be a drift in the frequency which can be either positive or negative in sign. Initially, on placing a coated crystal in a cell there will be erratic frequency drift, often with large frequency changes. This is caused by temperature effects caused by the gas flow and by instability of the coating as a

constant vapour pressure is established in the cell. The coating will evaporate,or 'bleed' from the crystal into the carrier gas causing loss of mass and,therefore, an increase in the frequency.

Thus for a single sided system, the crystal will be subject to frequency changes caused by:-

1) Effect of temperature
2) Coating changes
3) Coating interaction with the carrier gas or dust and moisture in the system.
4) Gas pressure and flow rate fluctuations.

As will be shown later, these factors all contribute to the loss of sensitivity for the coating.

2) Double Sided System

This system is designed to give some measure of correction by instrumental means for the above factors influencing the frequency. The system involves the use of an additional crystal and cell, to act as as a reference. The frequency of both the crystals are compared so that, in the ideal case,only the interaction between sample and coating will be displayed in the results.

There are two methods of achieving this - by using a mixer circuit,or by using the frequency ratio facility of the digital counter.

Mixer Circuit

Consider the sample crystal frequency f_s and the reference crystal frequency f_r, both being altered by an amount,x, due to a temperature fluctuation, and giving rise to a displayed frequency of f_s' for the sample and f_r' for the reference.

Therefore:-

$$f_s' = f_s + x$$

$$f_r' = f_r + x \qquad (32)$$

From the mixer circuit is obtained, $f_s' - f_r'$ which in this case will equal $f_s - f_r$, and means that the error caused by the temperature fluctuation will have been directly compensated if the response of the two crystals is identical.

Any change in the sample crystal, y, caused by addition of sample to the coating can be followed directly.

If $$f_s'' = f_s + x + y$$
$$f_r' = f_r + x \qquad (33)$$

Then from the mixer is obtained $f_s'' - f_r' = f_s + y - f_r \qquad (34)$

Thus, the mixer output follows the change in frequency of the sample crystal.

However, should the cause of the frequency change be a function of the frequency itself, then the mixer circuit cannot compensate for this.

Consider:-

$$f_s' = f_s + (f_s x) \quad = f_s (1 + x)$$

$$f_r' = f_r + (f_r x) \quad = f_r (1 + x) \qquad (35)$$

From the mixer is obtained:-

$$f_s' - f_r' = (f_s - f_r) + x(f_s - f_r) \qquad (36)$$

Another problem of mixer circuits is the possibility of 'lock-on', where if the frequencies of the two crystals are similar,

one of the oscillators appears to control, or 'pull', the other. This effect can usually be overcome by placing each oscillator in a Faraday cage.

The other method of comparing the frequencies, is to use the ratio facility of the digital counter. The two frequencies are fed into the counter and the displayed count is the ratio f_s / f_r . This ratio is obtained by substituting the frequency of the reference crystal for that of the internal standard. A switch at the back of the counter allows, either this ratio to be displayed, or f_s, which is the same as is obtained from a single sided system.

It is possible to calculate f_r from a knowledge of the ratio f_s / f_r and f_s.

ie Displayed count = $f_s / f_r = D$

Therefore $f_r = f_s / D$ (37)

This method can compensate for errors which are a function of the frequency.

From equation 35

$$f_s' = f_s (1 + x)$$

$$f_r' = f_r (1 + x)$$

Therefore

$$\frac{f_s'}{f_r'} = \frac{f_s}{f_r} \qquad (38)$$

However, the other type of error cannot be compensated for using the ratio facility.

From equation 32

$$f_s' = f_s + x$$

$$f_r' = f_r + x$$

Ratioing these gives :-

$$\frac{f_s'}{f_r'} = \frac{f_s + x}{f_r + x} \qquad (39)$$

Thus it can be seen that neither the mixer cicuit nor the frequency ratio method can compensate for all errors. In practice, where a double sided system is used, the digital counter was used to process the results. In general, it was felt that a single sided system offered the advantage that the frequency was a true representation of what was happening to the crystal.The response to sample presentation was usually rapid (< 30s) and was little affected by the drift.

3.4.4. Coating Bleed

This, as has been mentioned previously,is the main contributor to the drift in frequency of the crystal. An investigation was carried out to ascertain whether the loss of coating was a function of temperature.

Cell D was used, with flow meter S and drying tubes X and Z. The drift was monitored for a crystal coated on the whole of both sides with triethanolamine, which is used as a liquid gas chromatography stationary phase. The carrier gas flow was kept constant at 10 cm^3/min. Figure 25 shows the drift of a clean, uncoated crystal with temperature variation. The temperature was controlled by immersing the cell,as far as possible, into the water bath and allowing the temperature of the stainless steel to equilibrate before any measurements were made. As can be seen from the graph, the drift remains almost constant,although the frequency did shift to lower values as the temperature was raised. Figure 26 shows the drift for a coated crystal as a function of

Figure 25 Drift of the Frequency of an Uncoated Crystal with Temperature

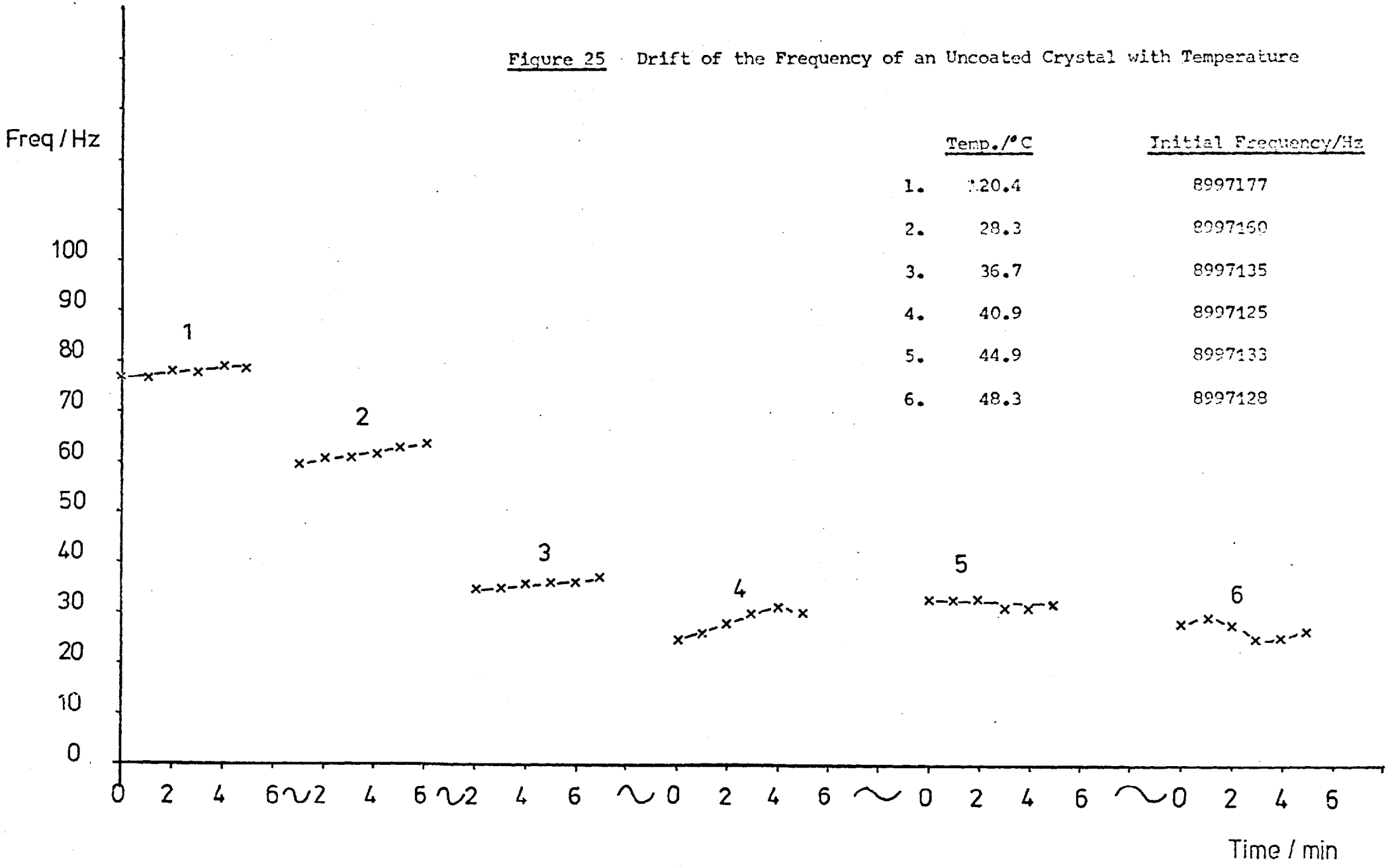

	Temp./°C	Initial Frequency/Hz
1.	20.4	8997177
2.	28.3	8997160
3.	36.7	8997135
4.	40.9	8997125
5.	44.9	8997133
6.	48.3	8997128

Figure 26 Drift of a Coated Crystal as a Function of Temperature

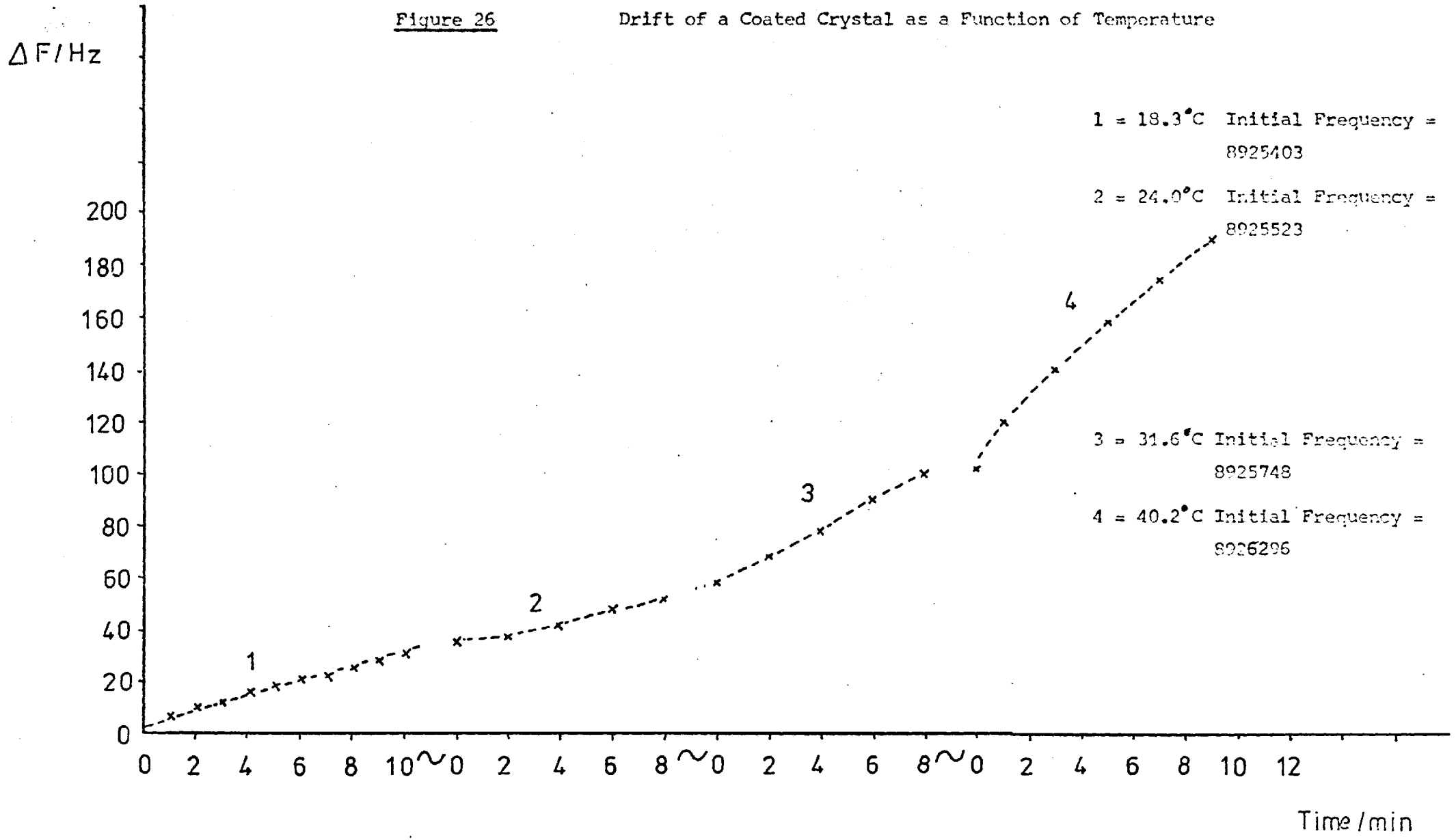

temperature. The plots are drawn on the same graph to allow comparison of the gradients, but the frequency scale on the ordinate is not an absolute scale, since for T = 18.3°C the crystal frequency starts at 8925403 Hz and for T = 24°C the frequency starts at 8925523.
The gradients of the lines are as follows:-

Temperature (°C)	Gradient
18.3	0.55
24.0	0.60
31.6	1.05
40.4	1.70

Thus it can be seen, that as the temperature increases the drift, owing to loss of coating, becomes more pronounced. This is as to be expected since the vapour pressure of liquids increases with increased temperature.

To ascertain whether an external reference crystal could compensate for the drift, the above experiment was repeated, monitoring both the coated sample srystal and an uncoated crystal in the adjoining cell. The results are tabulated below.

Table 8 The Effect of Temperature on Coated and Uncoated Crystals

Temperature (°C)	Gradient for Sample Crystal	Gradient for Reference Crystal
16.6	0.64	0.65
26.5	0.40	0.53
37.0	0.35	0.34
42.2	0.21	0.21

The drift of the crystal is virtually the same, whether using

the internal or external reference, showing that the temperature cannot be compensated for using the frequency ratio method.The fact that the drift is decreasing as the temperature increases, serves to illustrate the problems arising in the study of coated crystals. During this particular experiment the gas was undried and it is possible that the drift effect was caused by interference from the moisture.

The effect of temperature on crystals coated with triethanolamine will be examined in greater depth in a subsequent section. It is sufficient to state here, that the temperature does have an effect on the coating bleed, although it is not predictable and cannot be compensated for by using an external reference crystal.

The coating bleed could, in theory, be compensated for, by using a coated reference crystal. In practice, it is virtually impossible to obtain two crystals with coatings matched closely enough to give an accurate compensation and so no experimental verification of this theory has been made.

3.4.5 Carrier Gas Flow Rate and Pressure

Earp (102) investigated the effect of increasing the flow rate of sample gas, on the response of the detector. He found that the response decreased with increasing flow rate. King (75) passed inert gas over a crystal at differing flow rates to attempt to measure any possible background frequency changes due to a varying flow rate. He concluded that there was little effect on the fundamental frequency of the crystal.

The flow rate would be expected to affect the coating bleed rate, the loss of coating being more rapid at faster flow rates. The response on presenting short duration samples would be expected to

decrease, since the time for equilibrium to occur is reduced.

Figure65shows calibration curves for rapid injections of CO_2 into the carrier gas passing over a crystal coated on one electrode only with diethanolamine. The flow rate of the carrier gas was varied from 5 to 37 cm^3/min. The response decreased with increased flow rate, except for a flow rate of 5 $cm^3$3min, which gave a lower response than that of 12 cm^3/min. This is probably due to sample dilution occurring prior to the crystal which is minimised by the use of a faster flow rate.

Stockbridge (122,123,124) immersed AT cut crystals in a variety of gases and discovered that the frequency of oscillation was a reproducible function of the gas pressure and the molecular weight of the gas. Some gases (eg. H_2 and He) caused the frequency to rise with pressure, whilst others (eg. Kr and Xe) gave a frequency drop followed by a rise. The frequency changes were reproducible although non-linear and were caused, not by sorption onto the electrodes, but were a predictable consequence of the mechanical properties of the gas, considering it as a hydrodynamic fluid. The resonance frequency of the crystal can be predicted as a function of the gas pressure by taking into account;1) the effect of hydrostatic pressure on the elastic moduli of quartz, and 2) the reaction of the vibrating crystal to the complex shear impedance of the gas.

Since the pressure was found to have a complex and significant effect upon the frequency of the crystal, the carrier gas pressure was kept as close to atmospheric, as possible, whilst maintaining a sufficient pressure to move the carrier gas. The working pressure was chosen to be 1.4×10^4 N/m^2.

3.5 Coating Application Techniques

The quartz crystal detector is a specific mass detector, the specificity being obtained by the choice of coating. The coating is some material which will adhere to the surface of the crystal and by its chemical or physical properties will interact, preferably with a high degree of specificity, with the component of interest. It is the coating which determines the accuracy and precision of the crystal detector and this section will deal with the parameters which influence the sensitivity of the coating.

Any compound that is considered to be a possible coating material should satisfy the following requirements.

1) It should be possible to apply the compound to the crystal in a reproducible manner.
2) If the coating is a volatile material, it should have a reasonable 'lifetime' on the crystal to enable measurements to be made.
3) The crystal must still be able to oscillate with a reasonable amount of the coating present.
4) It should operate at, or near, room temperature to avoid temperature control problems.
5) For a pollution detector the coating should be selective,although as a gas chromatography detector it should interact with a wide range of component gases.
6) To avoid exhaustion of the coating it should undergo reversible sorption with the sample gas.
7) It should be able to operate on the micro scale.

Many types of materials can be used as coatings, workers have used solid coatings, metals and liquids. Of particular interest are the gas chromatography stationary phases which range from viscous liquids

to solids. King (113) reported that they show a linear relationship between the concentration of solute vapour and the fractional weight pickup. They also have the advantage of giving reversible sorptions but are not, in general, selective.

Before considering the methods of coating the crystals, there are three important parameters of a coating which should be mentioned. These are:-

1) The mass of the coating

2) The area of the coating

3) The position of the coating on the crystal surface.

Recapping on the basic crystal detector equation, that of Sauerbrey,

$$\Delta F = 2.3 \times 10^6 \times F^2 \times \frac{\Delta M}{A}$$

The change in frequency, ΔF, is proportional to the change in mass, ΔM, and inversely proportional to the area over which the coating extends. Obviously, the greater the mass of the coating the more sample is likely to react and it is necessary to optimise the mass and minimise the area of the coating.

1) Mass of Coating

Although it would appear that the mass could increase without restriction, this is not, in fact, the case. For a crystal there is a definite mass loading beyond which it is almost impossible for the crystal to oscillate.

Behrndt and Love (118) state that in thickness shear oscillations, an anti-node is formed at the surface of the plate and material deposited at this antinode will only influence the frequency by its weight, ie the elastic constants of the material do not contribute to the frequency shift, provided the material is applied as a thin film.

This was also an assumption made by Sauerbrey in deriving his equation. (45)

King (52) reported that metals deposited on the crystal to adjust the frequency, and many other solids, do not greatly affect the crystal's ability to vibrate. When liquids are deposited on the quartz surface, the ability to vibrate is often impaired, because the vibrating crystal surface is dissipating energy in the liquid.

The relationship between the frequency change and increasing mass has been tested experimentally by several workers and a linear relationship verified. The variation in response with the mass of coating was examined using a crystal coated over the whole of one side with triethanolamine. The crystal was placed in cell B, with a carrier gas flow rate of 20 cm^3/min. Rapid injections of 40 µl CO_2 were used as standards. Figure 27 shows the frequency response plotted against the frequency change on coating, ΔF_c. The results are given in Table 9.

Table 9 The Frequency Response for 40 µl Injections of CO_2 as a Function of the Frequency Change on Coating

Frequency Change on Coating (Hz)	Response to Injection (Hz)
4938	-4
8103	-15
11295	-16
13854	-24
16267	-33
20379	-42
20676	-54
21484	-45

An interesting example of a frequency change, which is an increase, versus the mass will be discussed in a later section.

Figure 27 The Variation in Response versus the Frequency Change on Coating

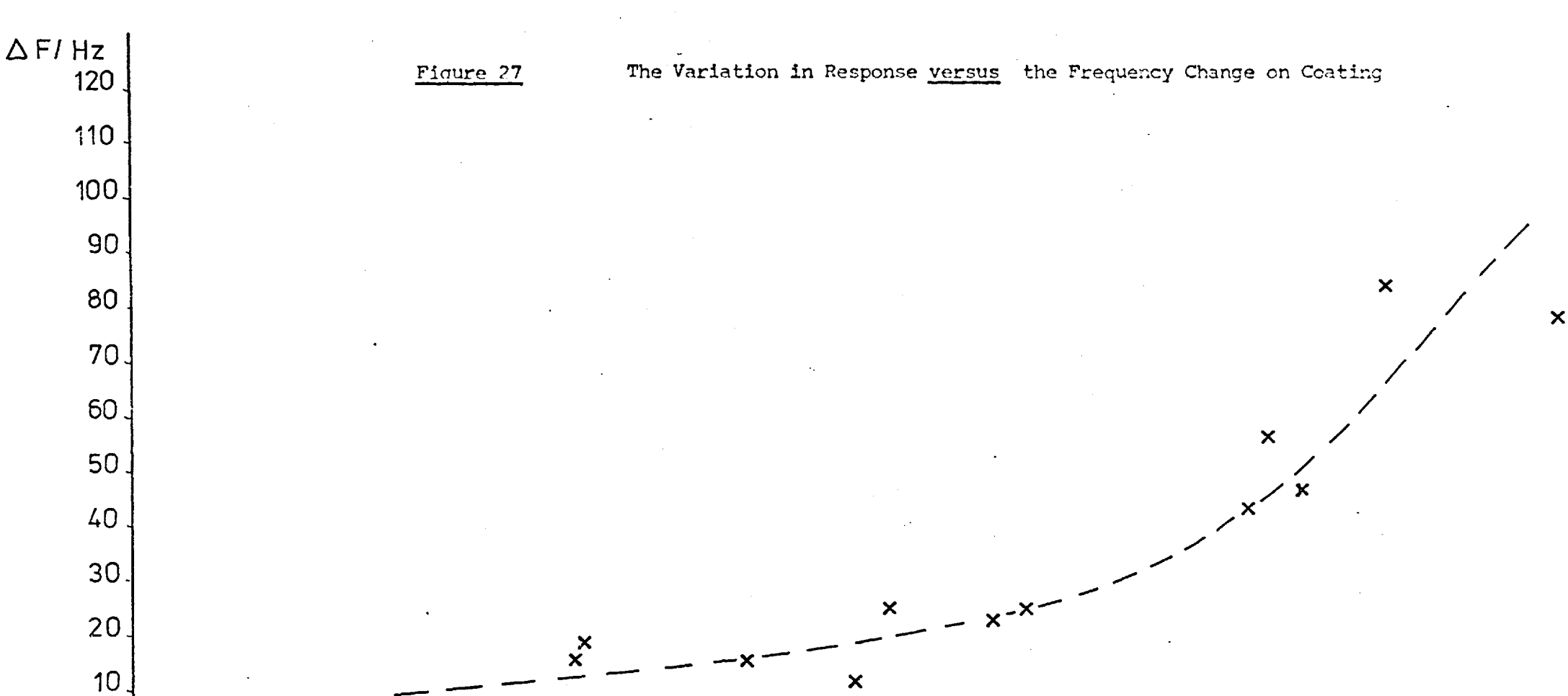

2) Area of Coating and Position

From the Sauerbrey equation, it follows that, as the area of the coated electrode is decreased, the sensitivity of the crystal for weighing purposes increases.

Sauerbrey (46) studied the vibrational patterns of thin vibrating quartz plates using the modulation of a beam of light incident to the surface of the crystal. The amplitude distributions of the vibrations within the surface of the crystal were determined and were found to vary considerably, reaching a maximum at the centre of the crystal. This is shown in Figure 28 . This means that for the maximum effect, coatings should be placed at the centre of vibration. The maximum area of vibration is that covered by the electrodes.

Earp (102) investigated this and found that, in practice, as the area of the coating decreased, the sensitivity increased to a maximum. As the coating area became even smaller the response decreased owing to less surface area of the coating being available for sorption.

King (73) found that more sensitive readings could be obtained by placing a small amount of coating at the centre of the crystal, than by placing a large amount on the edges. Edmonds (101) found that a deposit of Apiezon grease when placed in three positions on the crystal electrode, gave greater frequency changes for coating when placed in the area above the centre of the electrode.

The crystals used in this study, were coated on the electrodes only, except for one particular coating, triethanolamine. This coating, on different occasions, was applied to one, or both, of the electrodes, or, to one, or both, faces of the crystal. Usually, either both faces or both electrodes were coated which rendered it difficult to weigh the crystal and consequently, no mass versus frequency change studies were made.

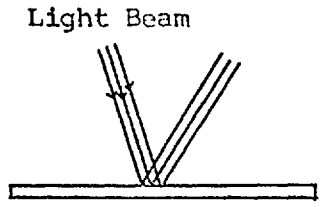

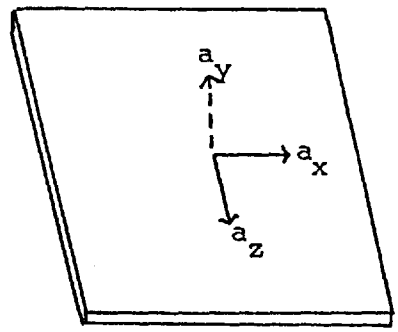

Vibration Components of a Thin Quartz Plate on the Surface

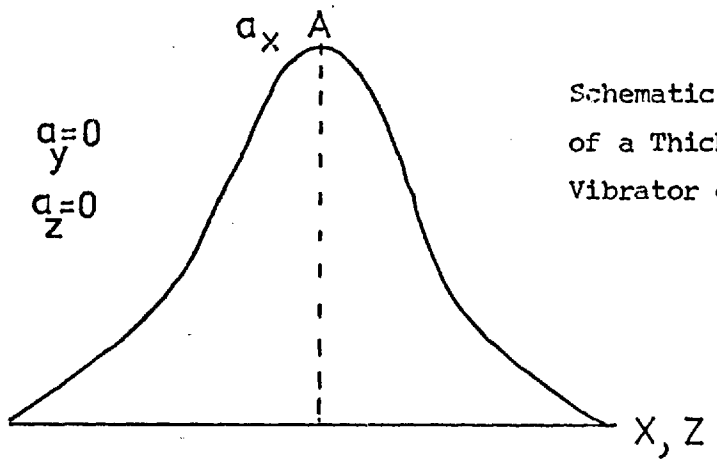

Schematic Amplitudes of a Thickness Shear Vibrator on the Surface

Figure 28 Sauerbrey's Work in Studying the Amplitude Distributions in Vibrating Quartz Plates.

3.6 Coating Techniques in the Literature

There are several techniques in use and these will be briefly reviewed.

1) Dissolution in a Solvent

The material to be applied to the crystal is dissolved in a volatile solvent. An aliquot is placed on the crystal using a micro-litre syringe and as the solvent evaporates the coating material remains fixed to the crystal. Problems do arise with this method, as surface tension effects within the liquid droplet, or poor wetting ability, combine to give an uneven coating as the solvent evaporates. If the coating is too irregular the crystal will not oscillate.

Guilbault and co-workers applied quadrol to the crystal using chloroform as the solvent. The solution was brushed over the crystal with a tiny brush in order to obtain reproducible coatings.(84,85,90)

Janghorbani (104) used a syringe to deposit the solution,but followed this,with heating the crystal,in an oven for several hours, to ensure that the coating spread uniformly. Karasek and Gibbins also advocated allowing the coating to spread to a uniform layer.(96) Edmonds(101) discovered that supercooled Carbowax gave considerably greater responses to chloroform than the waxy solid form of Carbowax. The supercooled coating was formed by heating the coating to allow uniform spreading and then cooling the crystal very slowly. Clean and dust-free conditions were essential for the process.

Guilbault *et al* reported that smooth coatings were difficult to produce either by dipping the crystal into a solution of the coating material, or by depositing material with a syringe. The most reliable method was to spray the solution onto the crystal with a commercially available spray kit. The crystal was masked so that only the electrode was coated. (98,100)

Hartigan (87) investigated the effects of spraying a coating onto the crystal and found that increasing the mass of coating by spraying multiple layers was inefficient.This became worse as the distance between the spray source and the crystal was reduced. He concluded that the lower layers were being disturbed by successive layers causing the error.

King (113) reported that solid substrates could be applied with glue, or cement, and fine powders could be deposited from either solutions or suspensions. A loose powder deposited on the surface of the crystal does not adhere and will not cause a frequency change, and it is for this reason that powders must be either bonded to the crystal with a glue, or deposited from solution.

If the coating material is a metal or metal oxide, it is possible to make the plated electrodes from the desired metal, or to convert the electrode material to the oxide form.(113)

King (72) coated a crystal with deliquescent salts, such as lithium chloride, by vacuum evaporation. Masks were used to denote the area of deposition and the mass of deposit was monitored by the frequency change of the crystal.

3.7 Coatings Used for Carbon Dioxide and Carbon Monoxide Analysis

The coatings were chosen initially by a consideration of the chemical properties of the two gases. This presented several problems, because, although many compounds will give reactions with CO or CO_2, the conditions required for the rection are prohibitive for the crystal detector; for example, the gold electrodes will lift off the quartz surface above 350-400°C ,and many reactions of CO_2 take place in an aqueous medium.

Another factor to be considered, is that although many compounds are reactive on the macroscale they are not on the microscale, when applied to the crystal, probably owing to the reaction time being longer than the time for which the sample is in contact with the coating.

The coatings used were both solids and liquids and are tabulated below.

Table 10 Coating Materials Used for CO and CO_2 Analysis

Gas	Solid Coatings	Liquid Coatings
CO	Iodine Pentoxide	
	Nickel	
	Miscellaneous solids	
CO_2	Sodium Hydroxide	Triethanolamine
	Calcium Hydroxide	Diethanolamine
	Miscellaneous solids	Miscellaneous amines

3.7.1 Liquid Coatings

The work in this study was mainly concentrated on the two amine coatings, triethanolamine and diethanolamine. The use of triethanolamine was investigated for two reasons, despite reports by other workers that CO_2 did not react, and that CO only reacted in concentrations above 10,000 ppm.

a) The bleed rate of the coating was of an acceptable level - a few hZ/min.

b) It could, possibly, be used as a carrier medium for other materials.

There were two methods of applying the triethanolamine to the crystal. A drop of the liquid was placed on the crystal using the plastic tip of an Eppendorf Pipette and smoothed over the entire face of the crystal using a piece of 'non-fluffy' tissue.The coating was

polished with small circular movements until the crystal started to oscillate. Occasionally the crystal would start to oscillate, and stop on being placed in the cell. This was probably due to a capacitative effect of the gas in the cell and was overcome by polishing the crystal further.

The other method was to use a paper cloth hole reinforcement, clipped to the crystal, which acted as a mask for the electrode. A drop of the liquid was placed on the centre of the electrode and the coating was polished over the electrode surface. The main problem encountered with this method of coating the crystal was that the triethanolamine tended to creep outwards and down the crystal with a net drop in sensitivity.

Drift of a Crystal Coated with Triethanolamine

When a freshly coated crystal was placed in a cell, the frequency drift was very rapid, but after 1-2 hours, it had stabilised to a constant rate. The drift of a coated crystal was usually very stable, 10 Hz/min and positive in direction, ie the frequency was increasing.Occasionally for short periods of time, the drift became very erratic.During the course of half an hour the drift,as monitored on the chart recorder, changed direction twice with a period of erratic drift in between. This is shown in Figure 29 .The positive drift pattern is that expected, but there is no obvious explanation for the negative drift.Since there was no sample presentation during this time, the only possible materials which could be being absorbed were moisture or some other contaminant in the gas stream. It was noticed that the calcium chloride drying tubes had become saturated and that it was probable that moisture was being released unevenly. The drying tube was replaced for two of magnesium perchlorate and fresh calcium chloride.

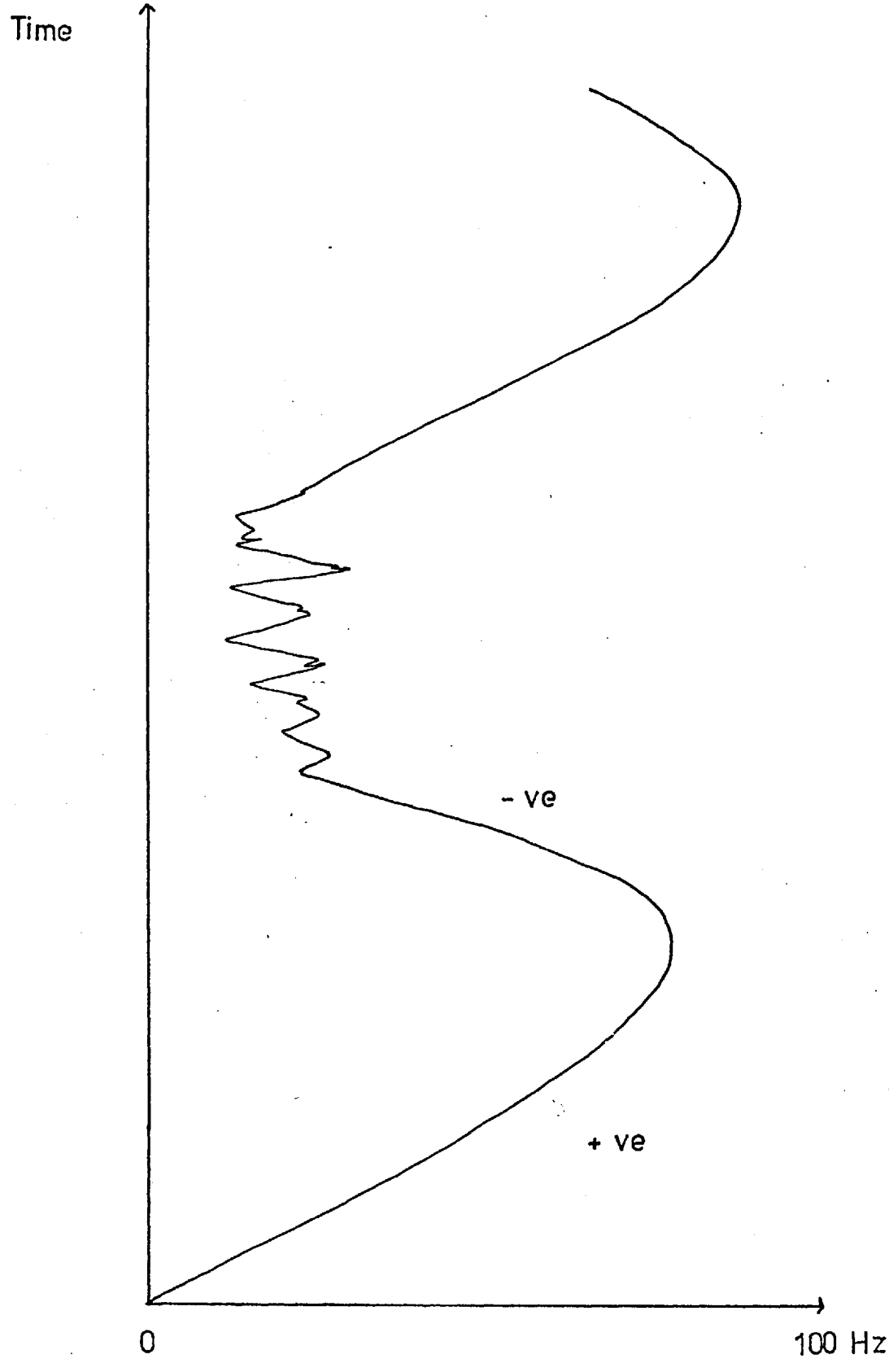

Figure 29 Drift of a Coated Crystal with Time

As the drying tube was removed the frequency dropped rapidly and then increased as the tubes were replaced.This change was probably due to air contamination, either of moisture or of CO_2. Injecting a small amount of moist air into the cell caused a large frequency drop,thus supporting the theory that the negative drift pattern obtained was the result of moisture release from the calcium chloride.

The effect of temperature on the drift was investigated. The drift was monitored for a coated crystal at different temperatures, by immersing the cell in the water bath and allowing it to reach equilibrium before making any measurements. The data obtained has already been mentioned in the section on coating bleed (3.4.4) and was seen to be of a steadily increasing linear pattern. In repeating this experiment, the drift was found to be directional as shown in Figure 30. It was noticed that the drift was due to loss of coating. The frequency of the crystal used for Figure 30 was 8953635 Hz and on coating the new frequency was 8925403 (ΔF_c = - 28232).The following day the frequency had risen to 8934445 (ΔF_c = - 19190) indicating a loss of coating material.

The drift, for a coated crystal, at various temperatures, was monitored over one hour, since all measurements for a calibration of the crystal should be able to made in that time.The drying tubes were removed. The plots obtained at temperatures of 37°C,26.5°C and 42.2°C were straight lines. The plot obtained at 16.6°C, which was the unthermostatted room temperature, (varying from 16.6-16.9°C), was a gentle curve, with a straight portion between 15 and 45 minutes after the start of the experiment.Consequently, the gradients of the lines were measured in this region. The experiment was repeated with the drying tubes in place and very shallow linear plots were obtained.

Figure 30 Drift of Coated Crystal with Variation in Temperature

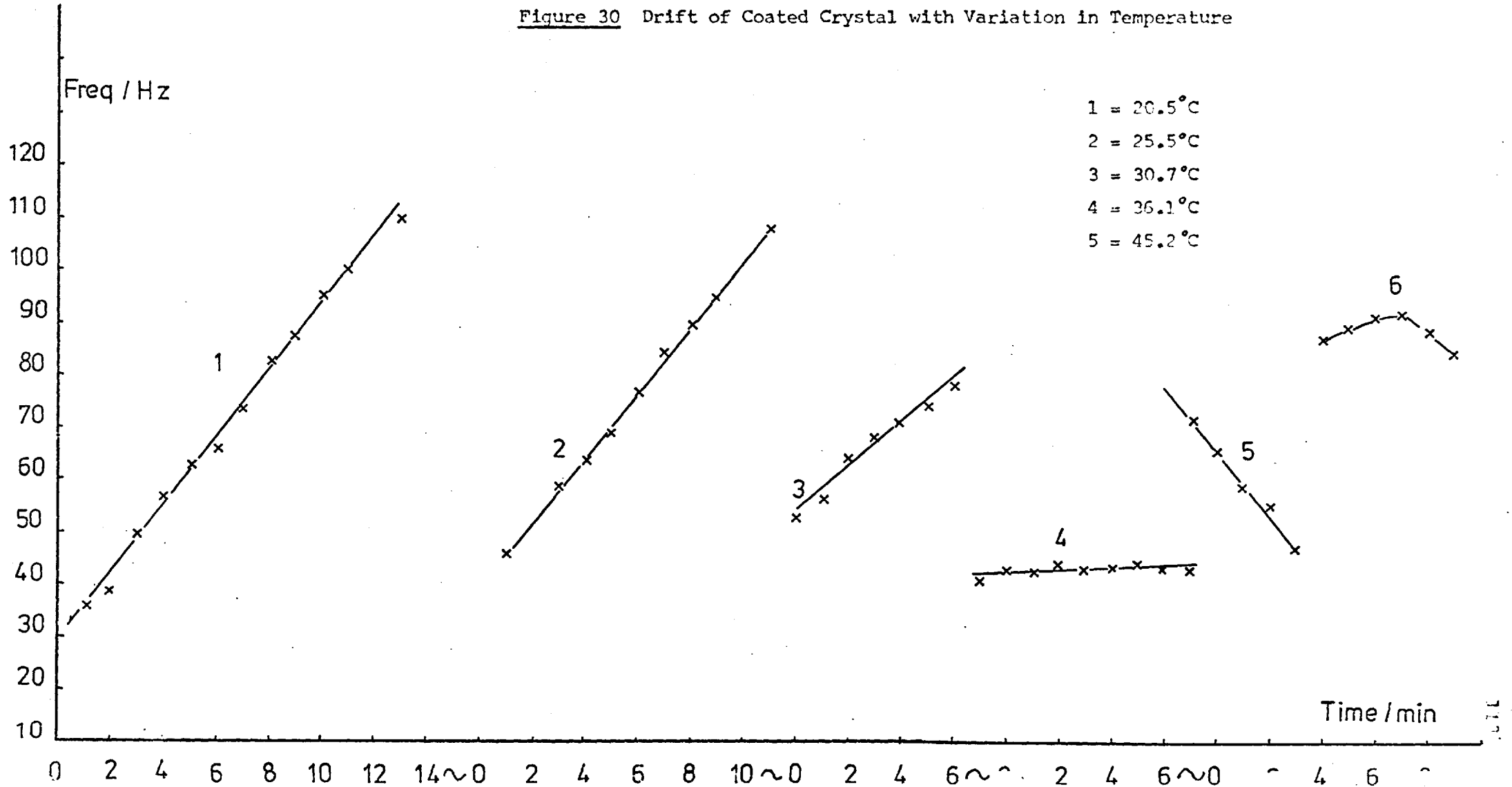

The gradients were measured and are quoted in Table 11.

Table 11 The Effect of Dried Carrier Gas on the Drift of a Coated Crystal at Various Temperatures

Dried Gas		Undried Gas	
Temperature (°C)	Gradient	Temperature (°C)	Gradient
20.4	0	16.6	0.6
31.9	0.06	26.5	0.4
41.6	0.05	37.0	0.3
		42.2	0.3

It would appear that the drying tubes do control the drift to a certain extent, which indicates that the moisture present in the carrier gas is interacting with the coating to some extent. The main problem encountered with the drying tubes was that they did cause pressure build-up of the carrier gas owing to restriction of the flow by the particles.

In conclusion it was found to be necessary to monitor the drift for some time prior to sample presentation and to discard any crystal showing anomalous behavior.

Diethanolamine

The diethanolamine was a solid at room temperature and was dissolved in water to enable it to be deposited on the electrode by a syringe. A solution was prepared containing 29.96 µg/µl. 0.4 µl of the solution was deposited on the electrode and smeared over the gold surface using the syringe needle. The protective cap was placed over the crystal and the unit placed on top of the power supply, which was warm, in order to facilitate evaporation of the solvent. The coating formed as a 'damp' looking circular deposit. With a few exceptions the

crystal would not oscillate if more than 0.4 µl was placed on each electrode, ie. 11.98 µg. The crystals were either coated on one or both electrodes.

Table 12 shows the frequency change on coating obtained for different crystals with deposits of either 0.6 µl or 0.4 µl of diethanolamine solution.

Table 12 Frequency Change on Coating with Diethanolamine Solution

µl Solution	Electrodes Coated	Clean Frequency/Hz	Coated Frequency/Hz	ΔF_c/Hz
0.6	2	8998757	8961624	- 37133
0.6	2	8998801	9075530	+ 76729
0.6	2	8998706	8968904	- 29802
0.6	2	8998727	a)8980946	- 17781
			b)8970726	- 28001
0.4	2	8998087	8975803	- 22284
0.4	2	8962287	8943862	- 18425
0.4	2	8962247	8943064	- 18528
0.4	2	8962918	8947583	- 15335
0.4	1	8962519	8950711	- 11808
0.4	1	8933899	8937841	- 3942
0.4	1	8962317	8957643	- 4674
0.4	1	8971796	8956936	- 14860
0.4	1	8963148	8951204	- 11944
0.4	1	8950926	8941858	- 9068

The two frequencies a) and b) are the frequency changes obtained as each electrode was coated. One crystal gave a high frequency on coating and this will be discussed in a later chapter.

The method of coating is not reproducible and the variation in response is caused by fluctuations in the thickness of the coating, and of its area.

The diethanolamine gave stable drift patterns of 10-15 Hz/min..

Several other amines were screened as potential coatings, but the drift was found to be unacceptable. The amines are listed below.

Table 13 Amines Screened as Potential Coatings

Amine	Volatility	Reaction to CO_2
Triethanolamine	Low	Very good
Diethanolamine	Low	Very good
Trimethylamine	Fairly rapid	None
Triethylamine	Rapid	-
n-Butylamine	Rapid	-
Monononylamine	Fairly rapid	Very slight
Ethylenediamine	Fairly rapid	Very slight
Benzylamine	White deposit	None

No quantitative study of the volatility of these amines was made, since they were unacceptable as coatings.

3.7.2 Solid Coatings

There were several different methods of applying the solid coatings and these will be dealt with separately.

Dissolution in a Solvent

The coatings iodine pentoxide and sodium hydroxide were dissolved in water and applied using a microlitre syringe.

The coatings of iodine pentoxide were all uneven ring structures and gave a frequency increase on coating. These coatings will be discussed in more detail in the section on the high frequency effect.

The solution of sodium hydroxide contained 30 μg/μl and 0.4 μl was applied to the electrode. The crystal was placed in the cell with a flowing gas stream, in order to evaporate the water quickly. The crystal was dried by this method to minimise contamination of the

coating by atmospheric CO_2. The coating formed a 'damp' circular deposit, which once the crystal had stabilised in the cell, gave a smooth and increasing drift pattern. The main problem encountered with this coating was that during the course of the experiment, the crystal might suddenly stop oscillating or jump several 100s Hz. A possibly related effect that was noticed during the course of drying the crystal, was that the crystal would stop oscillating and then restart. The liquid drop was placed on the crystal and the frequency would increase as the water evaporated.The crystal would then stop oscillating, and as the solid form of sodium hydroxide was formed, it would restart. The cause of this is that during the transition phase from liquid to solid, the coating dissipates the energy from the crystal and prevents the oscillation.

No drying tubes were used with the sodium hydroxide coating and a moisture cell, as shown in Figure 31 , was incorporated in the system. The moisture cell consisted of a sample jar with a plastic top. Into this top was inserted a brass coupling so that it could be fitted into the carrier gas line with a brass 'T' piece.

The coatings were not uniform and the frequency change on coating was unpredictable.

Table 14 Frequency Change on Coating with Sodium Hydroxide

Ul Solution	Electrodes Coated	Clean Freq. Hz	Coated Freq. Hz	ΔF_c/Hz
0.4	1	8939886	8971969	+ 32226
0.4	1	8940108	8938578	- 1530
0.4	1	8939240	8923924	- 15316
0.4	1	8940144	8931343	- 8801
0.4	1	8938683	8932001	- 6682
0.6	1	54540	42159	- 12381
0.6	1	49534	42688	- 6846

Figure 31 Moisture Cell

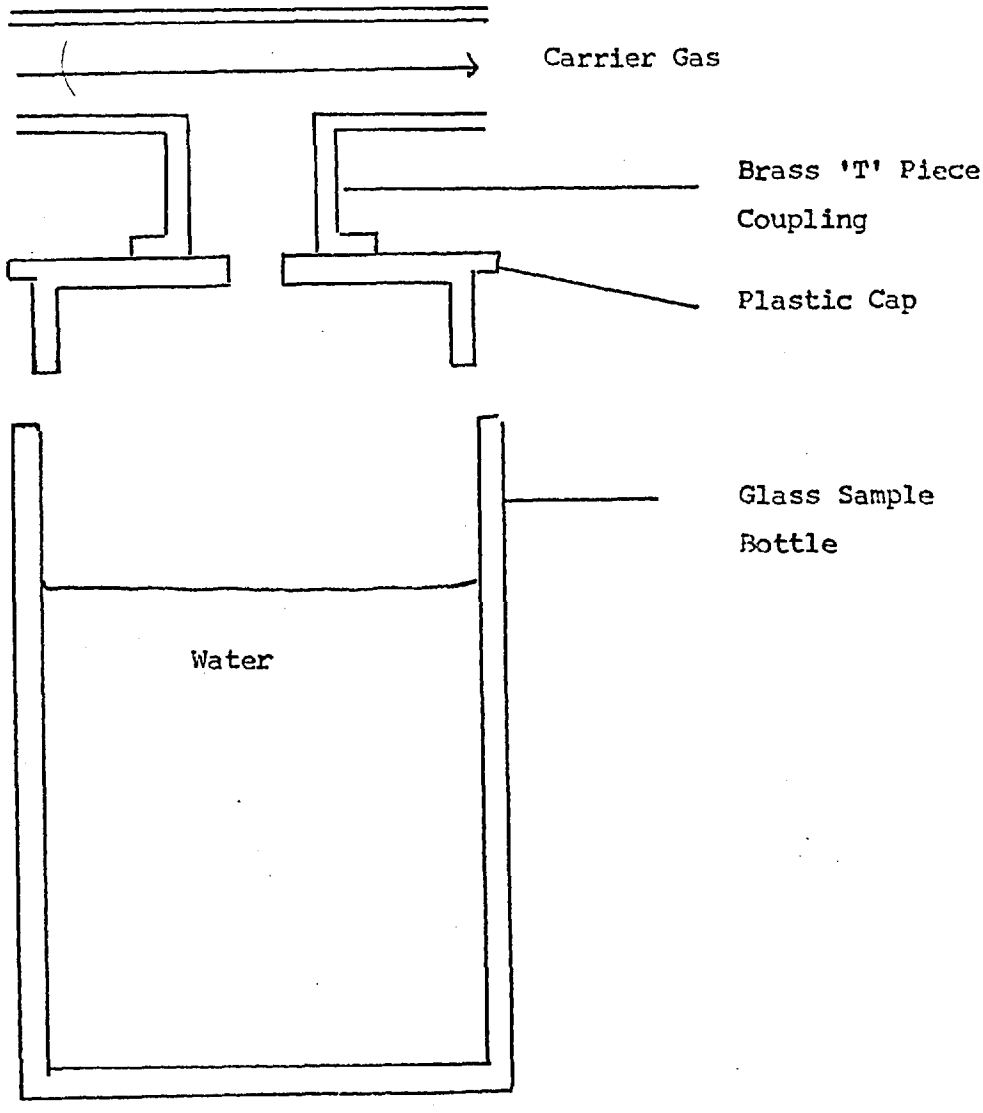

The results obtained with presentation of CO_2 were surprising, there were some crystals which gave the usual decreasing response, and some which an initial small decrease followed by a high frequency increase. This variation in response will be discussed in the section on the high frequency effect.

Solids in a Triethanolamine Mull

Some of the solids were mixed with a little triethanolamine using a mortar and pastle. The mixture was then placed on the crystal in the same manner as triethanolamine. The reason for doing this, was to take advantage of the favourable coating and drift properties of triethanolamine, whilst attempting to use the absorption properties of the solids.

Latex Bonded Solids

This method used latex to glue the solid onto the crystal. The latex was applied to the crystal as a dispersion in water. As the latex dried it left a sticky surface on the electrode. A small amount of the solid was placed on the latex deposit and compressed with a small piece of computer card. The excess material was then brushed away. During the coating technique, the crystal was removed from its holder.

The latex used was an acrylate polymer, Acronal 4D, manufactured by B.A.S.F., Ludwigshaven, W. Germany. It was shown that a dispersion of 10 g/l Acronal 4D in water containg approximately 0.1% by volume of Dispex N40, a wetting agent, was adequate for providing deposits in the range 1.40 to 3.94 mm diameter. Generally, 0.4 µl of the dispersion were used. (88)

Even with the excess loose solid removed from the crystal, the crystal would not always oscillate, and the coating had to be brushed

firmly with a small brush until the crystal started to oscillate.

The latex itself formed a stable deposit and was resistant to the effect of heating upto 90°C. A deposit of powdered nickel on the latex ceased to oscillate at 30°C and restarted on cooling. This was presumably due to the latex not bonding the nickel strongly enough so that damping of the vibrations occurred.This meant that the latex bonded deposits were of little use above room temperature.

The frequency changes for some crystals coated with latex are given in Table 15.

Table 15 The Frequency Change on Coating a Crystal with Latex and Nickel

µl Latex	Freq. Change with Latex /Hz	Freq. Change with Nickel/Hz
0.4	- 1865	- 13361
0.4	- 2726	- 14098
0.4	- 2103	- 4829

The result for the last coating is possibly due to an error in coating.

Several solids were bonded to crystals using latex, eg. nickel powder, sodium hydroxide,lithium hydroxide,calcium chloride,manganese dioxide, activated charcoal,molecular sieves,and copper oxides. None of these coatings gave a favourable response with either of the two gases.

Electroplating

Nickel was electroplated onto the crystal as a possible coating for CO using the formation of nickel carbonyl.

ie $Ni + 4\ CO \xrightarrow{50\ C} Ni(CO)_4$

An electroplating solution of 0.4g $NiSO_4$,9.0g $(NH_4)_2SO_4$ and 70 cm^3 NH_3 (0.88) in 150 cm^3 water was used.This solution was diluted with

an equal volume of water. The crystal electrode was wired as one electrode and the other was a platinum wire. 3.5V at 35 mA was passed for 2 min..A fine deposit of grey nickel was obtained,which was washed with water and dried.A frequency change of - 30076 Hz was obtained for 138 μg nickel, which indicates a mass sensitivity of 218 Hz/μg.

The crystal was placed in cell B in the heater box and heated to 86°C.The carrier gas flow rate was 10 cm^3/min. There was no reaction obtained for either short injections of CO, or continuous presentation of pure CO from an aerosol can. The crystal was placed in the static cell with the heater, and maintained at a temperature of 55°C.Again no response could be obtained for samples of CO. It would seem that the surface of the nickel was too smooth for the reaction to occur. The form in which the nickel is presented to the CO is an important factor in this reaction. The work on nickel was not continued.

Chapter 4 The Solid Coatings

The solid coatings used showed deviation from the frequency changes as predicted by the Sauerbrey equation. Instead of the frequency decreasing on coating or on sample presentation, it sometimes increased. This is termed the 'high frequency effect'. The effect has not been reported in the literature by other workers in the field of crystal detectors, although it has been noticed by co-workers of the author. The author has not studied the effect in detail, as this was being undertaken by Street.(88), but the results obtained, with relevant observations will be presented in this chapter.

4.1 Iodine Pentoxide

Large amounts of CO are usually estimated by absorption in an ammoniacal solution of cuprous chloride. Small amounts are best estimated by using the redox reaction with iodine pentoxide (I_2O_5)

$$I_2O_5 + 5CO \xrightarrow{150^\circ C} I_2 + 5CO_2$$

Air containing the gas is thoroughly dried by passing it through a tower containing potassium hydroxide sticks and calcium chloride, and then through phosphorus pentoxide. It then passes through a tube of I_2O_5 maintained at 160°C. The iodine liberated is absorbed in aqueous potassium iodide solution and is titrated with standard thiosulphate.

This reaction was adapted for use with the crystal detector. I_2O_5 was dissolved in water and applied to the crystal electrode in 1 µl aliquots using a microlitre syringe. The water was evaporated by placing the crystal in an oven at 200°C for 10 minutes.

Instead of the expected decrease in the frequency an increase

was observed. The results obtained in coating several crystals are given in Table 16.

Table 16 The Frequency Change Observed for I_2O_5 Coatings

Crystal No.	µl I_2O_5 Soln.	Clean Freq./Hz	Coated Freq./Hz	ΔF_c/Hz
1	0.5	8951784	8978750	+26966
1	0.5	8951784	8980094	+28310
2	0.5	8953618	8987688	+34070
3	1.0	8954436	9020458	+66022

From this can be deduced the fact, that the effect is not restricted to one particular crystal.

An accurate I_2O_5 solution was prepared to check whether some form of contamination had occurred and whether it was an isolated effect. The solution contained 25.26 µg/µl I_2O_5 and for most of the crystals the solution was diluted with an equal volume of water. The crystals were weighed before the deposition and after the heating stage using an Oertling Microbalance. From this the weight of the deposit was calculated. The area of the deposit was measured using a travelling microscope. The deposit invariably formed as a broken ring and the area had to be estimated. This was done by assuming the coating formed a circle with an inner circle missing.

Several crystals were used in this study, and the frequency change, the weight change and the area were measured and are recorded in Table 17. The crystals were only coated on one electrode and the deposit was, in theory, 12.63 µg/µl.

From the Sauerbrey equation the frequency change is proportional to the change in mass over the area, ie $\Delta F \propto \frac{\Delta M}{A}$

Table 17 The Frequency Change on Coating for Deposits of I_2O_5

Crystal A
Weight 504.0 µg
Clean Frequency 8949987 Hz

Crystal B
Weight 585.5 µg
Clean Frequency 8951052 Hz

Crystal	µl I_2O_5	ΔM/µg	ΔF/Hz	Area/mm^2	ΔM /Area /µg/mm^2
A	1	10.5	- 16698	1.77	5.9
A	1	24.5	+ 46853	0.81	30.2
A	1	41.4	+ 40555	2.31	17.9
A	1	54.0	+ 39671	2.06	26.2
A	0.5	57.5	+ 34326	2.60	22.1
A	0.5	54.9	high & low	2.54	23.6
A	0.5	77.3	+ 33162	2.34	33.0
A	0.5	79.6	+ 34476	2.66	29.9
A	0.5	99.4	+ 33625	7.55	13.2
A	0.5	109.4	+ 27449	2.49	43.9
A	0.5	117.2	+ 30564	3.02	38.8
A	1	121.7	+ 31667	2.96	41.1
A	1	144.4	+ 30103	3.02	47.8
A	1	183.5	+ 31673	3.20	57.3
A	2	323.8	+ 32803	3.02	107.2
A	2	-	no oscillation		
B	1	41.2	+ 47157	4.60	9.0
B	2	36.6	- 25559	5.64	5.8
B	1	53.6	- 61380	4.53	11.8
B	1	54.9	- 46220	5.40	10.2

The aliquots of I_2O_5 were added successively without cleaning the crystal.

For a weight change of 54.9 µg crystal A was unstable and was oscillating at high and low frequencies.

In an attempt to ascertain whether there was a critical loading factor, the frequency change on coating was plotted against the mass/area for the coating. The graph obtained is shown in Figure 32 .Most of the data lies scattered about a line of negative gradient in the top half of the graph. The data in the bottom half, the negative frequency changes, falls between 0 and 12 $\mu g/mm^2$. This would suggest a link between the frequency change being high and the mass per unit area of the coating.

For crystal A only one low frequency response was obtained, and for B only one high response. This indicates that it is not a function of the crystal, since both crystals experienced high and low frequency changes.

The high effect is not a function of the mass of the coating alone, since crystal B gave a high frequency at 41.2 μg and low frequencies at 32.6 and 53.6 μg. Crystal A over this range was giving high frequencies.

Similarly it is not a function of the area alone, since the area for the low coating frequency of B was 4.6 mm^2 and for the high 4.53 mm^2.

A similar plot was obtained by Street (88) for collodion deposits. The turnover point was 7 - 8 μg which is in the same region as for I_2O_5. Street attempted to reproduce this plot with Apiezon but no correlation was obtained, which could be owing to the fact that the coating was not a flat, even film, but hummock shaped, which affected the mass/area calculated.

To determine whether the high frequency effect was a function of the central portion of the electrode region, small deposits were made around the electrode surface as shown in the diagram.

Figure 32 Frequency Change on Coating versus Mass/Area for Deposits of I_2C_5

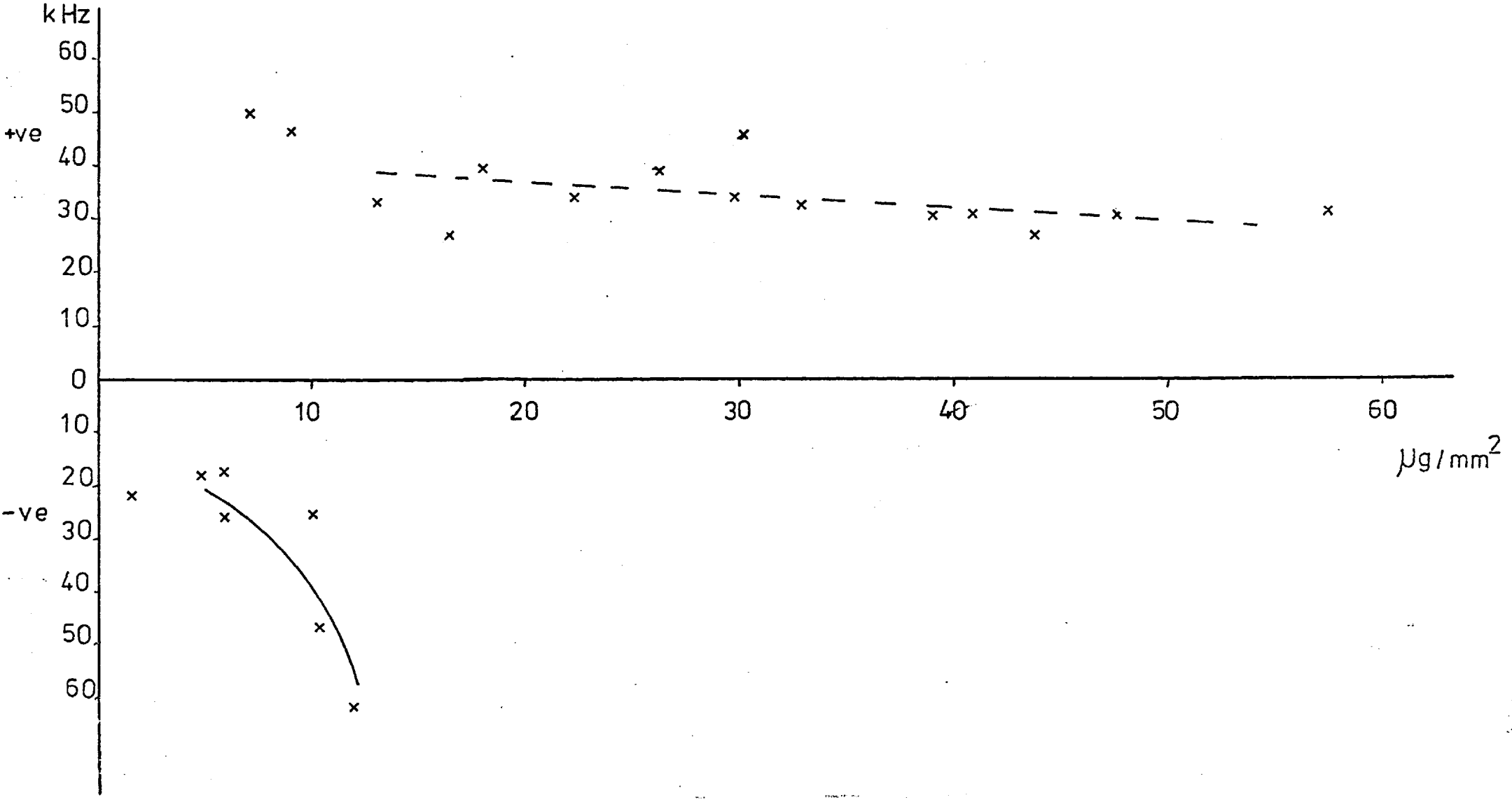

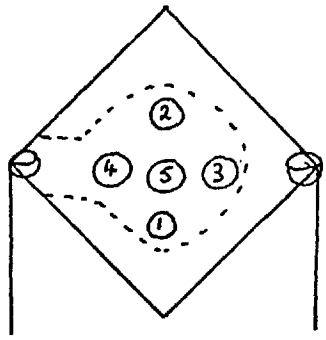

Each deposit was formed from a 0.5 μl drop and were all circular rings with a thin central coating. The deposits were made successively without removing any of the others. The results are given in Table 18.

Table 18 Frequency Change on Coating for Different Regions of the Electrode

Position	$\Delta F_{overall}$ Hz	$\Delta F_{coating}$ Hz	$\Delta M_{overall}$ μg	$\Delta M_{coating}$ μg	Area mm^2	$\Delta M/A$ $\mu g/mm^2$
1	- 15382	- 15382	17.5	17.5	1.50	11.7
2	- 12758	+ 2624	23.8	6.3	0.66	9.5
3	- 15487	- 2729	35.6	11.8	1.62	7.3
4	- 30253	- 14766	59.9	24.3	1.67	14.6
5	- 40501	- 10248	70.6	10.7	1.77	6.0

A consideration of the total weight over the total area versus the frequency change gives the data in Table 19.

Table 19

Position	ΔM_{total}	$Area_{total}$	ΔF_c	$\Delta M/Area$
1	17.5	1.50	- 15382	11.69
1 + 2	23.8	2.16	- 12758	11.05
1 + 2 + 3	35.6	3.78	- 15487	8.04
1 + 2 + 3 + 4	59.9	5.45	- 30253	9.83
1+2+3+4 + 5	70.6	7.22	- 40501	8.99

The results are inconclusive. Position 2 deposit gave an overall frequency decrease, although it was an increased frequency response for the coating. The mass/area value gives no indication as to the cause of the effect.

The actual coating of I_2O_5 was highly irregular and formed incomplete rings which were very nonreproducible. A typical coating is shown in the diagram below.

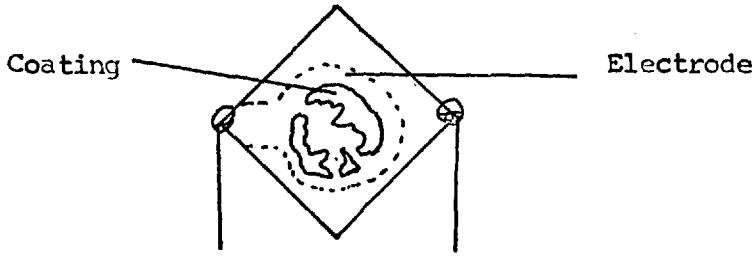

The high frequency effect could be a function of the irregularity of the coating.

I_2O_5 was the only coating used that had to be operated at fairly high temperatures and it proved to be unstable. The system used for this study was cell B in the heater box, with a carrier gas flow rate of 10 cm^3/min through the cell.

The drift of a crystal coated with 1 µl I_2O_5 at a temperature of 140 - 143°C was found to be about 30 Hz/min. The temperature was increasing slowly since the heater was not thermostatted; however, over a 3°C range the frequency change would be expected to be fairly low.

An attempt was made to obtain a response with injections of CO with little success. The results are in Table 20, and are very poor. The response expected would be a slight frequency drop as the CO is sorbed onto the coating, followed by a frequency rise as CO_2 and I_2 are evolved. The peak profiles are shown in Figure 33 . Only the profile for injection (c) shows the expected frequency rise, and this

Figure 33 Response Profiles for CO on I_2O_5

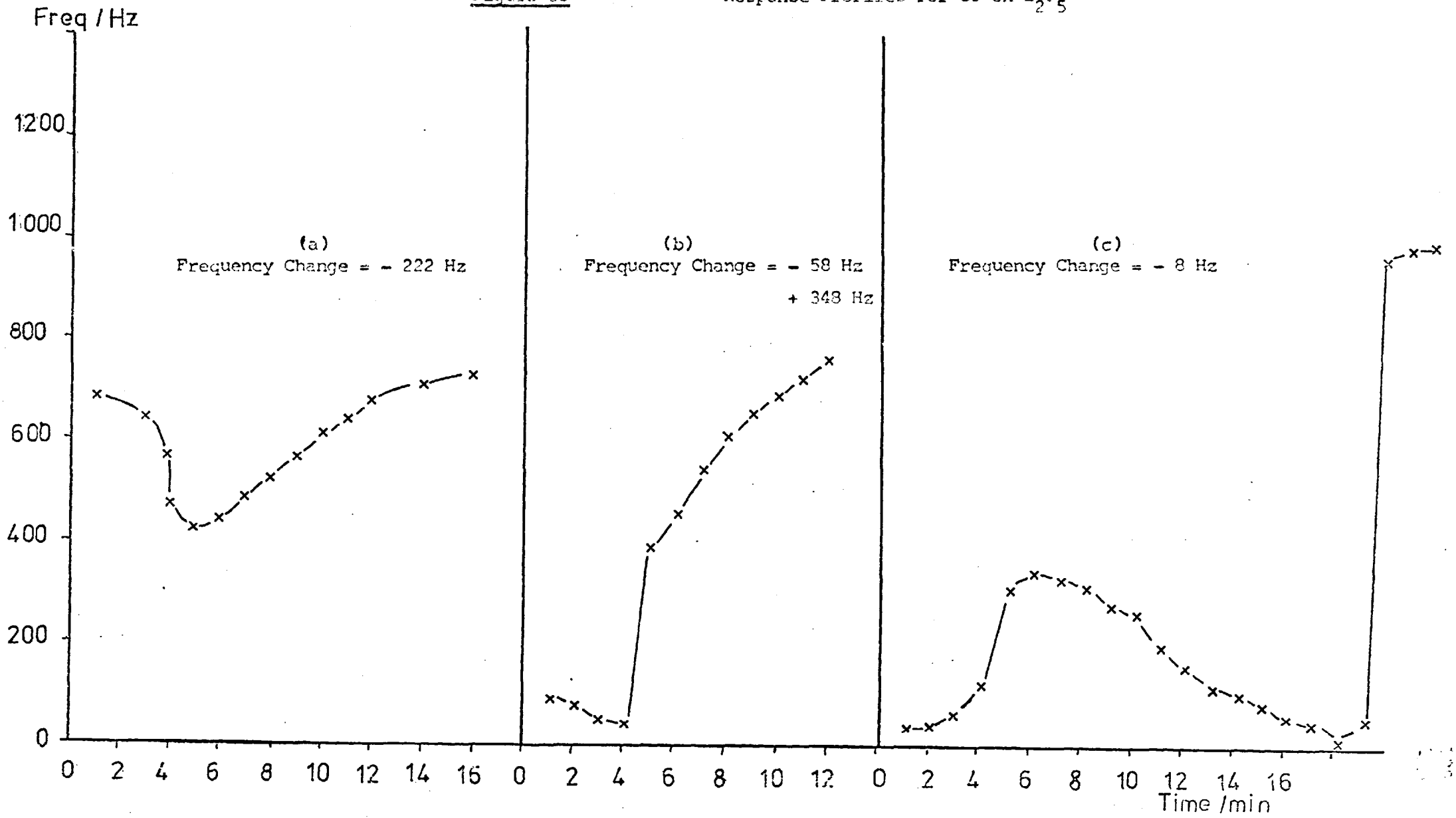

Table 20 The Response for CO on I_2O_5

ΔF_c = + 36308

Crystal	Injection Size/Ul	Response/Hz
1	a) 25	- 222
	b) 25	- 52
2	c) 10	- 25 + 348
	d) 10	- 8

could be a coating effect, as the frequency tended to jump even when there was no sample presentation.

The use of I_2O_5 as a suitable coating was not considered for the following reasons:-

1) The frequency on coating was unpredictable in that it went high and low.
2) The coated crystals tended to be unstable.
3) A constant operating temperature of 140°C was difficult to maintain.
4) The coating was very sensitive to moisture.
5) The sensitivity of the coating decreased rapidly with successive injections.
6) The minimum detection limit based on the best response of 222 Hz was calculated to be 113 ppm.
7) The I_2O_5 caused damage to the electrodes, channelling into the gold, and on washing, the gold was removed with the coating.

One effect which was noticed with the I_2O_5 system and also with other coatings, was that the frequency change as the solvent evaporated went through zero. The frequency started to fall as the solvent evaporated, became erratic and then the crystal stopped

oscillating. When the oscillations recommenced the crystal was exhibiting the high frequency effect.

4.2 Sodium Hydroxide

The study of the use of sodium hydroxide for CO_2 detection gave further information on the high frequency effect.

A sodium hydroxide solution was prepared by dissolving several pellets of sodium hydroxide in water. 0.4 µl was placed on the electrode and left to evaporate in an oven for 2 minutes at 120°C.

The reaction utilised was as follows:-

$$NaOH + CO_2 \longrightarrow Na_2CO_3 + H_2O \xrightarrow{CO_2} 2NaHCO_3$$

The initial results were disappointing with 250 µl CO_2 giving a response of - 33 Hz.

Since the reaction is usually carried out in solution the calcium chloride drying tubes were removed from the gas line. The crystal was coated with 0.4 µl solution and left at room temperature to enable the solvent to evaporate slowly.There was a marked difference in the coatings obtained, those from the oven being a white powder, and those left at room temperature a 'damp' clear looking deposit.

The coating was not very stable with a drift of about 20 Hz/min. On presentation of a sample of CO_2 there was a frequency increase, although the coating frequency change had been the normal decrease.

Table 21 The Response for CO_2 on NaOH

Injection Size/µl	Response/Hz	ΔF_c = - 7671
25	+ 140	
25	+ 175	
25	+ 230	

The responses obtained were unexpected in that they were high frequency changes and owing to the improvement in the response with successive injections.

Repeating the experiment with a freshly coated crystal gave similar high responses - 10 µl gave + 253 and + 204 for a coating frequency change, ΔF_c , of - 5397 Hz. The reaction time, the time for the maximum frequency change to occur, was 30s. The peak shapes for this crystal were different from the ones for the first crystal. The first was acting in an integrating mode, in that the CO_2 was sorbing onto the coating and not desorbing, which is to be expected with the carbonate formation. The peak profiles and the accompanying drift pattern are shown in Figures 34 & 35. For the second crystal the drift was slowly increasing. The injections caused a sudden rise in frequency, which was followed by a slower decrease. (See Figure 35). The profile is analagous to sorption and desorption except the frequency change is opposite in sign.

It was decided that the frequency increase on sample presentation might be due to the sample sorbing onto the coating and causing a critical mass/area. In order to study this, an accurate solution of NaOH was prepared containing 32 µg/µl. The crystal was coated with 0.4 µl on one electrode. The carrier gas flow rate was 10 cm^3/min. The results obtained for rapid injections of CO_2 are given in Table 22.

Table 22 Response for CO_2 on NaOH.

Crystal	Injection Size/µl	Response/Hz	ΔF_c/Hz
B	10	+ 51	- 15077
A	10	+ 14	- 8586
A	50	+ 10	- 9055

Figure 34 Response for CO_2 on NaOH

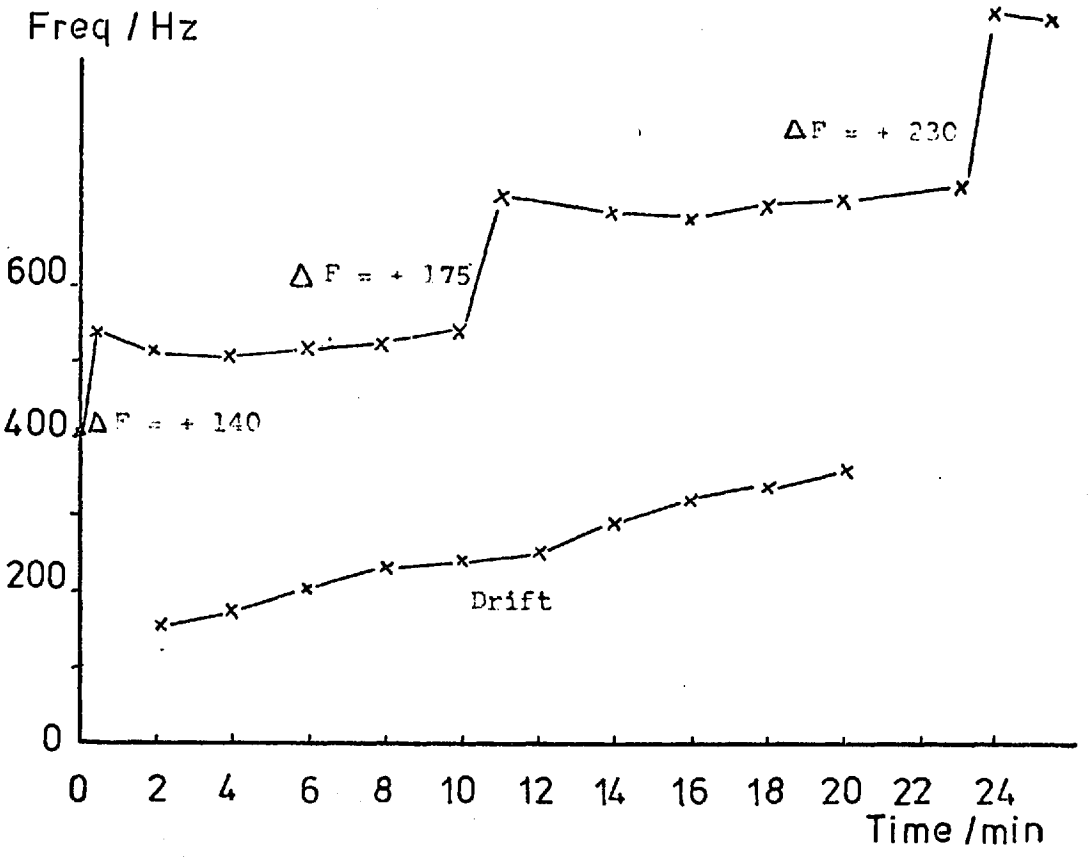

Figure 35 Response for CO_2 on NaOH

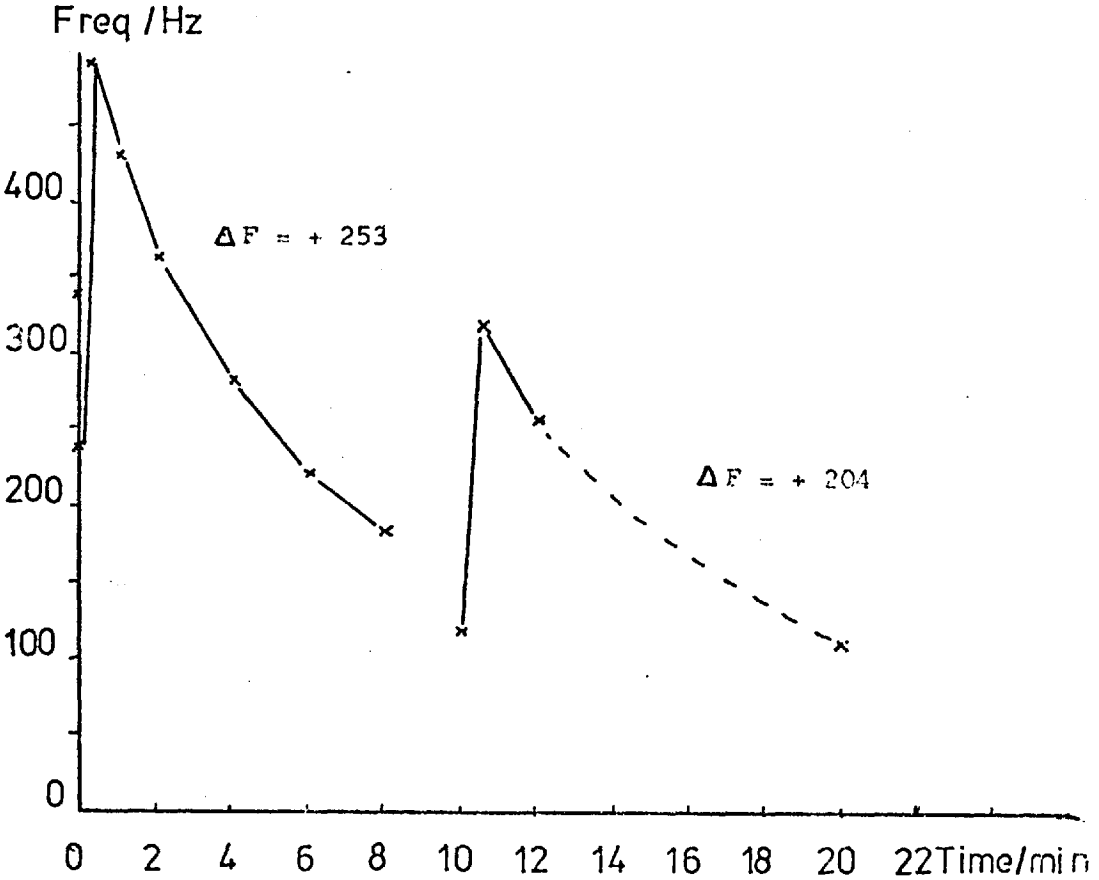

The results were lower than those obtained previously, indicating that the different solution might be having an effect. The experiment was repeated using the approximate NaOH solution which had been used before. As can be seen from Table 23, the responses were much higher.

Table 23 Response for CO_2 on NaOH

Crystal	Injection Size/µl	Response/Hz	ΔF_c = - 11800 Hz
B	10	+ 298	
B	10	+ 240	
B	10	+ 72	
B	10	+ 34	
B	25	+ 25	

A third solution containing 30 µg/µl NaOH was prepared and a crystal coated with 0.4 µl as before. A moisture cell was placed in the gas line to give a controlled humidity. The responses obtained were of a different type, the frequency first dropped and then rose to give a high frequency change. The results are given in Table 24, and the responses are measured from the frequency at the time of injection.

The results are becoming increasingly complex. From crystal 3, it seems that the crystal is behaving normally, ie frequency decrease, and then changes over to the high frequency response. Since there is carbonate formation, it is possible that the critical mass/area is reached. The profile plot for the third injection of Table 24 is given in Figure 36 .

The coating solution was diluted with an equal volume of water in an attempt to reduce the mass of the deposit, and a larger volume (0.6µl) was applied to the crystal to obtain a larger area for the

Table 24 Response for CO_2 on NaOH

Crystal	Injection Size/µl	Response(-ve) Hz	Response(+ve) Hz	ΔF_c /Hz
1	10	- 5	+ 116	+ 32226
	10	- 38	+ 96	
	10	- 37	+ 126	
	10	- 98	+ 972	
	10	- 3	+ 161	
	10	- 1	+ 28	
2	10		+ 43	- 15316
3	10	- 73		- 8801
	10	- 12		
	10	- 63		
	10		+ 47	
	10	no response		
3	10	- 396		- 6682
	10	-1010		
	10		+ 59	
4	10		+ 96	- 8018
	10		+ 190	

Figure 26 Profile of Response of CO_2 on NaCH

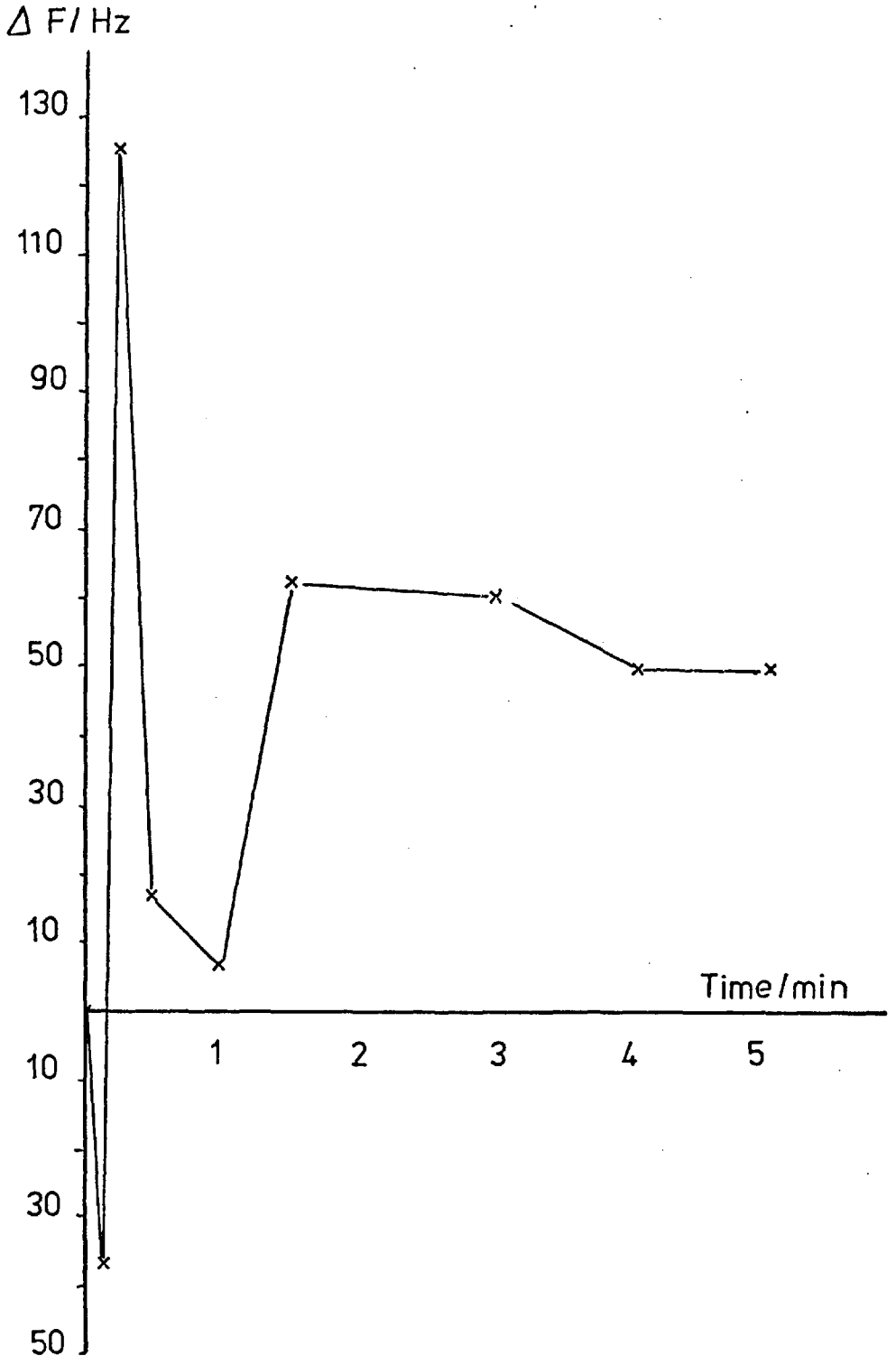

Figure 37 Response for CO_2 on NaOH

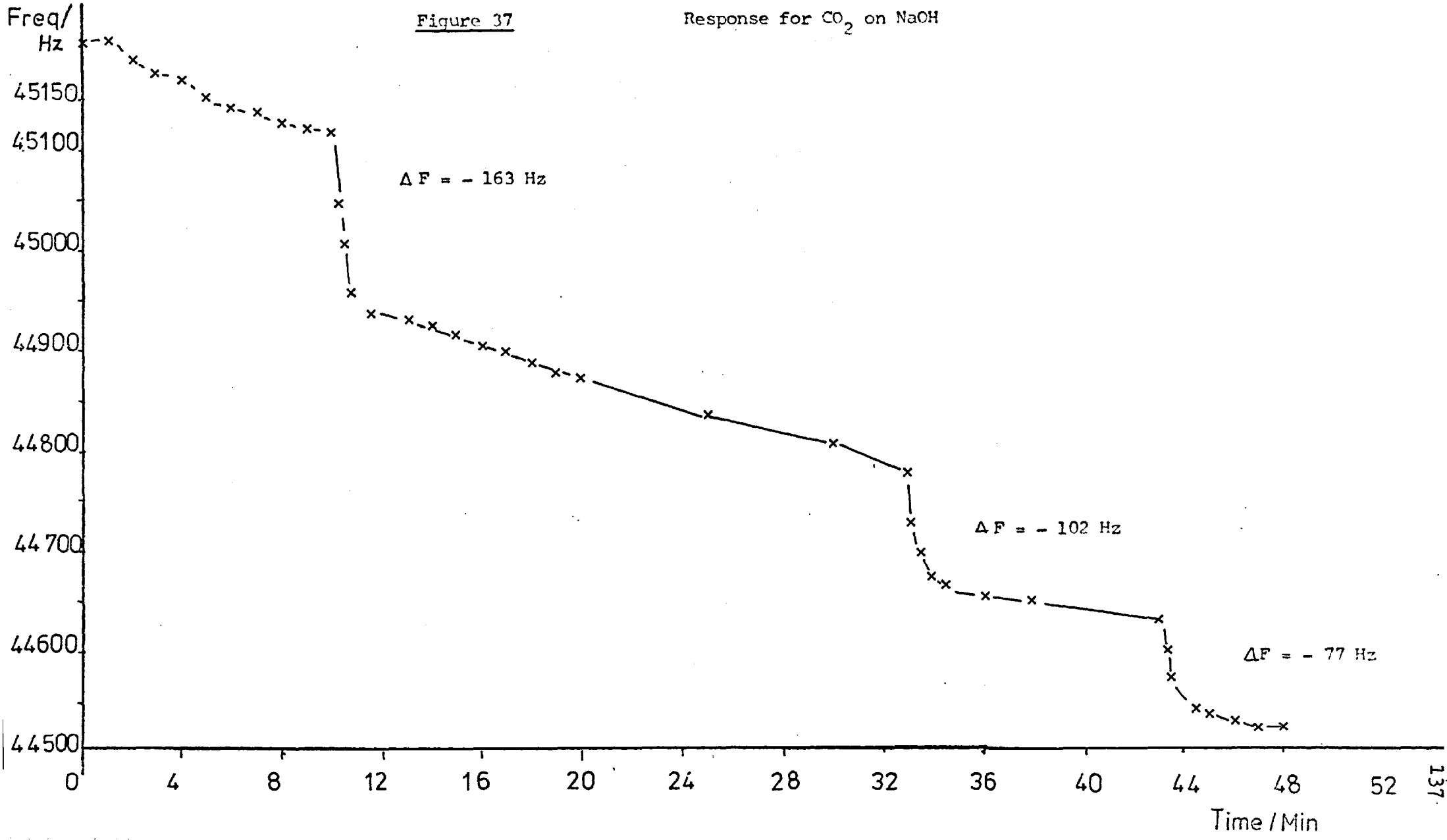

coating. The results obtained were of the normal pattern with the frequency change being a decrease. The crystal, as is shown in Figure 37, was acting in an integrating mode with the CO_2 being permanently absorbed into the coating. The frequency change on coating was - 8830 Hz, and the responses for 10 µl injections were - 163, - 102, and - 77 Hz. The response is decreasing as the coating becomes exhausted by carbonate formation.

The more dilute solution did not solve the problem. An investigation was made into the lifetime of the coating using this solution and the responses obtained were of the high effect. The lifetime of the coating is shown in Figure 38 from the data of Table 25.

Table 25 The Lifetime of the Coating with Successive 10µl injections

Injection No.	Response/Hz	ΔF_c = - 9090
1	+ 108	
2	+ 88	
3	+ 79	
4	+ 67	
5	+ 74	
6	+ 63	
7	+ 57	
8	+ 47	
9	+ 42	
10	+ 39	
11	+ 43	
12	+ 31	
13	+ 36	
14	+ 42	
15	+ 31	
16	+ 35	
17	+ 30	

Figure 38 Lifetime of NaOH Coating

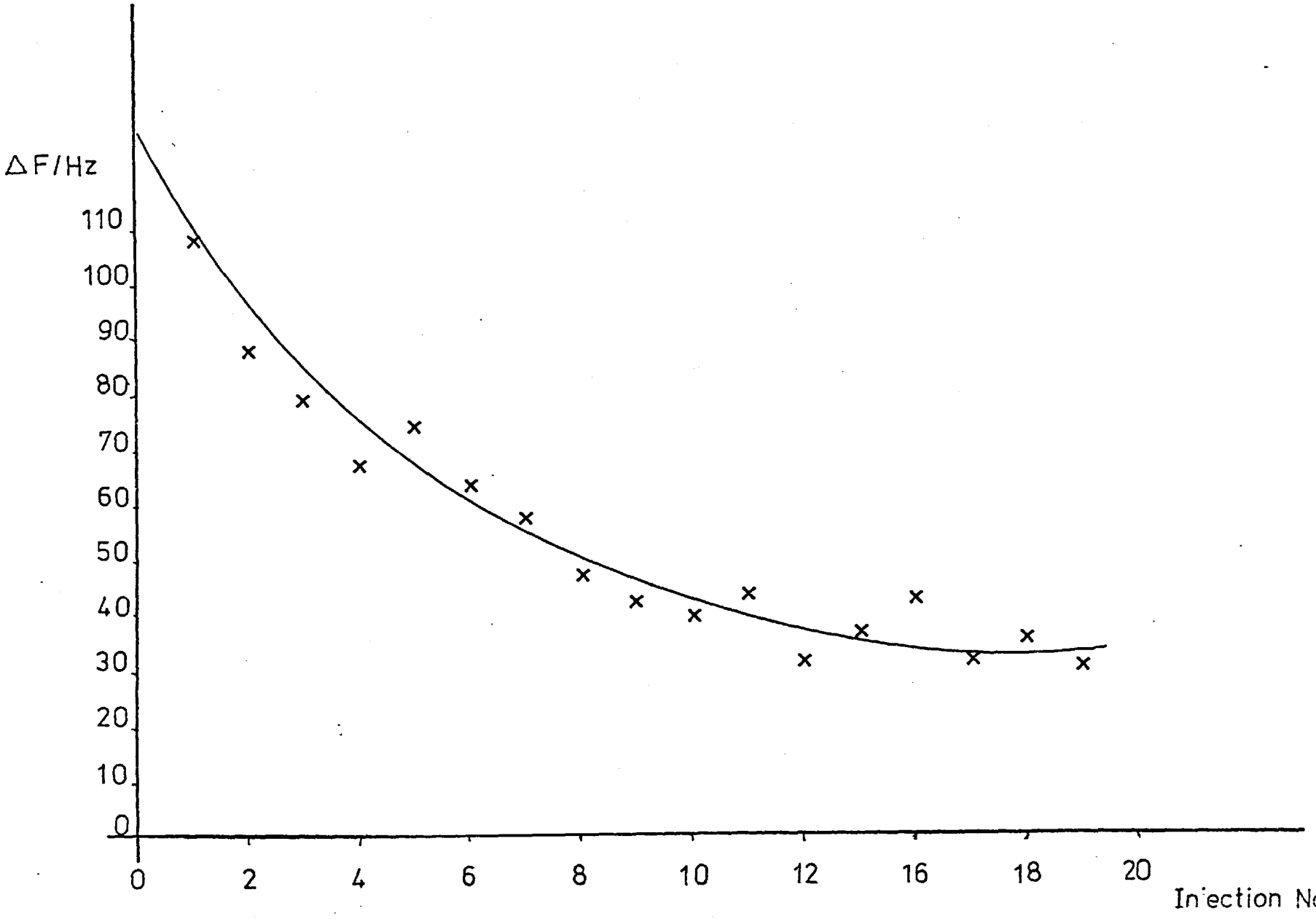

The response falls off with successive injections as the coating becomes saturated with CO_2. The plot of the frequency change for injection number shows a curve approximately hyperbolic in shape.

With this coating, the magnitude of the initial responses for the 10 µl injections, was similar to that obtained for a coating giving low frequency changes (cf Table 24). This suggested that the magnitude of the response was the same for similar injections and coatings although the sign was not.

An even more dilute solution, containing 11 µg/µl NaOH was prepared and the crystal coated with 0.4 µl on one electrode. The frequency change on coating was low and the responses for sample presentation were low. Table 26 shows successive 10 µl injections - all the responses obtained were of a low frequency change and decreased with successive injections.

Table 26 Response for CO_2 on NaOH

Injection No.	Response/Hz	ΔF_c = - 4019 Hz
1	- 87	
2	- 86	
3	- 157	
4	- 148	
5	- 138	
6	- 129	
7	- 119	
8	- 114	
9	- 80	
10	- 66	
11	- 35	
12	- 47	
13	- 49	
14	- 47	
15	- 31	
16	- 23	
17	- 19	

The maximum mass of NaOH deposited from 0.4 µl solution is 4.4 µg

The mass of CO_2 in a 10 µl injection is 19.64 µg

The overall reaction is that 1 mole of CO_2 reacts with 2 moles NaOH.

Therefore 4.4 µg of NaOH should react with 2.42 µg CO_2

Thus, even in one injection of CO_2, there is more than enough CO_2 presented to saturate the coating. It is the residence time of the sample in the cell which prevents total saturation occurring on the first injection.

The $NaOH/CO_2$ system was eventually abandonned for the following reasons:-

1) The frequency on coating generally went low, but the response went low, high, and low and high, which was too unpredictable for an analytical system.
2) The response fell rapidly with successive injections.
3) The crystal tended to be unstable when coated and would stop oscillating unpredictably.

The system did yield some results of interest in the study of the high frequency effect.

4.3 The Relationship between the High and Low Frequency Responses

The magnitudes of the high and low frequency responses were similar, and it would follow that if the only difference was the direction of change, then there might be some relationship between the high and low responses of a crystal which gives a rapid direction change.

A coated crystal was placed in cell C, with a carrier gas flow rate of 10 cm^3/min and the moisture cell incorporated.As the coating dried the crystal stopped oscillating and then restarted, which was probably caused by the change from liquid to solid. The area

of the deposit was 6.1 mm^2. The results obtained are given in Table 27, and the frequency changes are measured from the frequency on injection.

Table 27 Response for CO_2 with successive 10 µl Injections

Injection No.	Response (-ve) Hz	Response(+ve) Hz	$\Delta F_c = -11225$
1	88	100	
2	93	160	
3	68	70	
4	50	53	
5	46	41	
6	22	58	
7	30	36	
8	28	58	
9	10	29	
10	19	48	
11	16	42	
12	17	39	
13	13	34	
14	11	27	
15	7	23	
16	6	28	
17	8	27	
18	7	31	

The responses were all of the following form

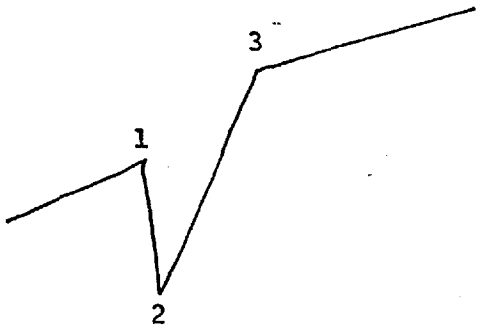

1 - 2 is -ve response

1 - 3 is +ve response

There is a general trend for both the positive and negative responses to decrease with successive injections. Little information can be

gained from a consideration of the separate positive and negative responses, and in the following table (28) the overall response (ie (1 - 2) + (3 - 2)) is calculated.

Table 28

-ve Response Hz (1-2)	+ve Response Hz (3-1)	Overall +ve Response/Hz (3-2)	Overall Δ F (3-2)+ (1-2)
88	100	188	276
93	160	253	346
68	70	138	206
50	53	103	153
46	41	87	133
22	58	80	102
30	36	66	96
28	58	86	114
10	29	39	49
19	48	67	86
16	42	58	74
17	39	56	83
13	34	47	60
11	27	38	49
7	23	30	37
6	28	34	40
8	27	35	43
7	31	38	45

There is a general trend in the overall response of a frequency decrease.

The data is plotted in Figure 39 as frequency response versus injection number. The lower curve represents the initial frequency decrease, the middle curve the subsequent frequency increase, and the upper curve the total frequency change. The three curves are very similar to each other and to that in Figure 38 . This could indicate that the high and low frequency changes are, in fact, part of

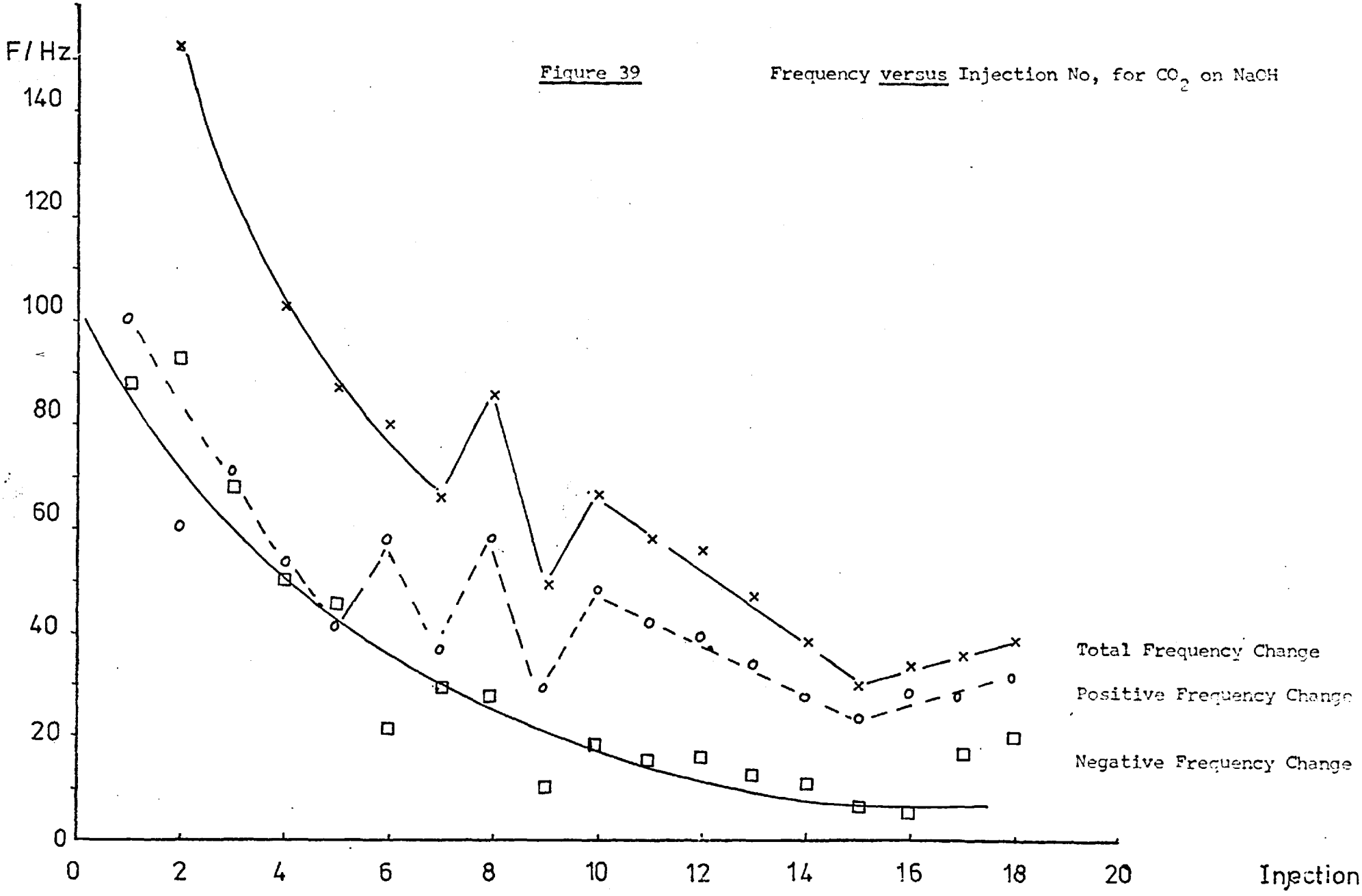

Figure 39 Frequency versus Injection No, for CO_2 on NaCH

an overall frequency change, the sign of which changes as a critical mass/area is reached. The other possibility is that the increase is due to loss of CO_2 or H_2O vapour from the coating. If it was due to a CO_2 loss, the positive response would be expected to be similar to the negative response, ie the same amount or less CO_2 must be desorbed than is absorbed. If it was due to loss of H_2O the frequency increase should be less than the frequency decrease for the following reason:- 1 mole CO_2 produces 1 mole H_2O, and since the frequency change is caused by a change in the mass of the coating, CO_2 must produce a greater change than H_2O owing to its larger molecular weight. Neither of these possibilities can explain the observed frequency changes.

An attempt was made to calculate the mass of CO_2 being absorbed on the coating from the frequency change.

The Sauerbrey equation is:-

$$\Delta F = 2.3 \times 10^6 F^2 \frac{\Delta M}{A}$$

ie $$\Delta F = k \frac{\Delta M}{A}$$

For this particular crystal k was calculated to be 1.829×10^8.

The mass of CO_2 absorbed was calculated from the Sauerbrey equation by substituting the frequency change, the area and k. The frequency changes used were a) the overall negative frequency drop, b) the overall positive frequency rise, and c) the overall frequency change. The masses calculated are given in Table 29.

The mass of NaOH on the crystal is 4.4 μg which produces a frequency change of - 11225 Hz, which is a change of 2551 Hz/μg. On this basis, 2.9×10^{-2} μg would be expected to give a frequency change of 74 Hz. The experimental frequency change was 88 Hz, showing that the

Table 29 Masses Calculated from the Data of Table 28

Injection No.	Mass Calculated From		
	Overall - ve Freq./μg x 10^2	Overall +ve Freq./μg x 10^2	Overall Freq. Change/μg x 10^2
1	2.9	6.2	9.1
2	3.1	8.3	11.4
3	2.2	4.6	6.8
4	1.7	3.4	5.1
5	1.5	2.9	4.4
6	0.7	2.6	3.3
7	1.0	2.2	3.2
8	0.9	2.8	3.7
9	0.3	1.3	1.6
10	0.6	2.2	2.8
11	0.5	1.9	2.4
12	0.6	1.8	2.4
13	0.4	1.6	2.0
14	0.4	1.3	1.7
15	0.2	1.0	1.2
16	0.2	1.1	1.3
17	0.3	1.2	1.5
18	0.2	1.3	1.5

coating is behaving according to the Sauerbrey equation.

A graph is plotted for the initial frequency drop,mass change versus the injection number, and for the overall frequency change, mass change versus the injection number, in Figure 40.

The mass change from the frequency decrease, falls with each injection which is as expected considering the saturation of the coating.The mass change from the overall frequency change, also falls with each injection, although less smoothly.

Although no quantitative conclusion can be reached, it would appear that there is some relationship between the low, high and overall responses, and that all are a measure of the total response.

4.4 The High Effect as a Function of the Circuit Employed

The fact that other workers have not reported the high frequency effect could be dependent on which oscillator circuit was being used. Several different circuits were available to the author- the International Crystal Co. circuit used throughout this work and by Street,(88), a workshop built copy of this using English equivalent components, and a circuit constructed by the Ministry of Defence,Porton Down. A crystal which was coated with NaOH and was oscillating in a high frequency state was plugged into each of the above circuits. Only the International circuit gave a frequency for the crystal, the other two would give no oscillations.

4.5 The High Effect as a Function of the Coating

Two crystals were coated with 0.4 µl NaOH solution (11 µg/µl) in an identical manner, and the area and the properties of the coatings were compared.

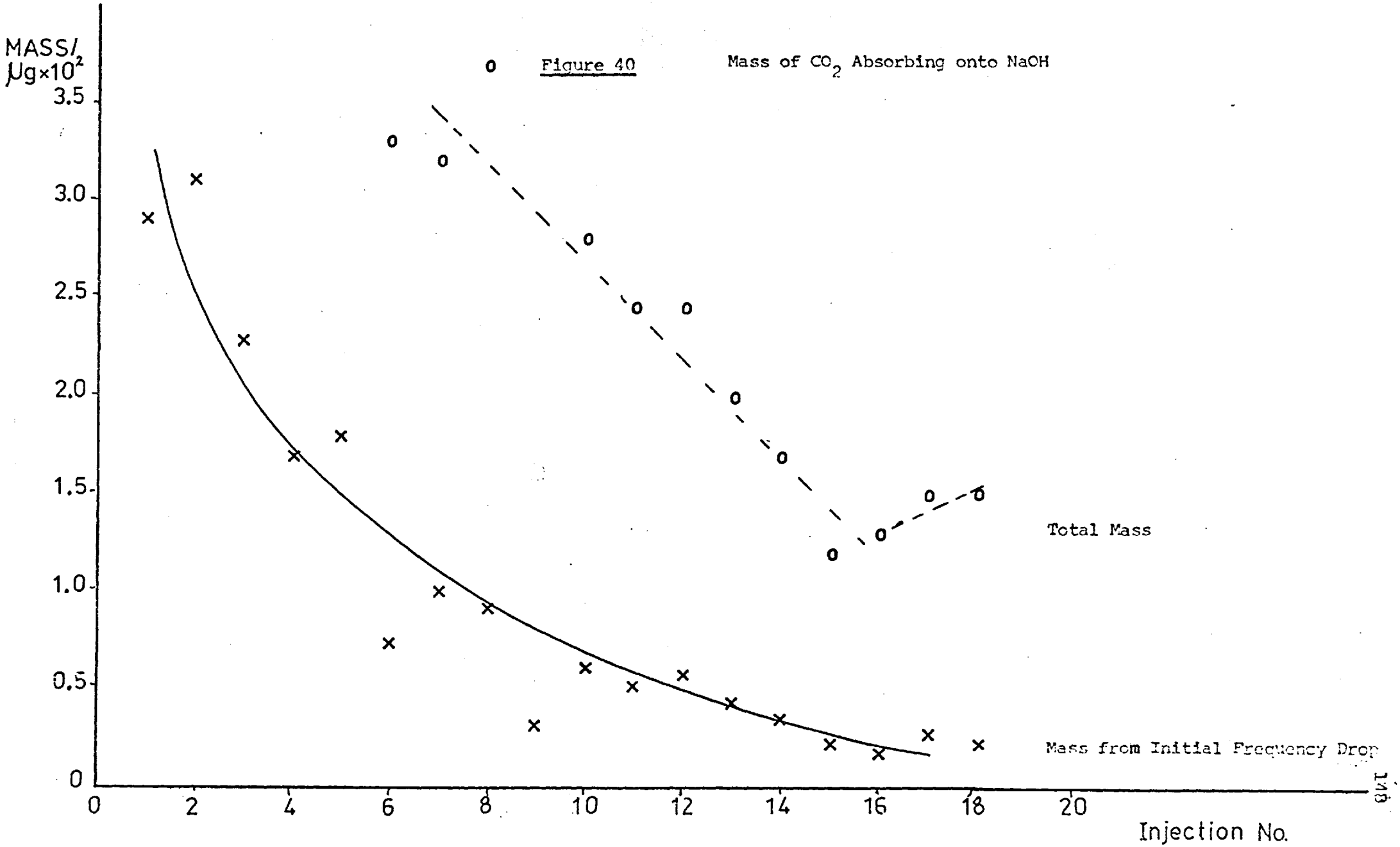

Figure 40 Mass of CO_2 Absorbing onto NaOH

Crystal A

ΔF_c = - 11150 Hz

Area of Coating = 0.028 cm^2

Shape of Deposit = circular with a crystalline centre

Response to 10 µl Injections = 1) + 41 Hz

2) + 9 Hz

3) No change

Crystal B

ΔF_c = - 6530

Area of Coating = 0.022 cm^2

Shape of Deposit = circular but not crystalline

Response to 10 µl Injections = 1) Very fast decrease by about 435000 Hz

2) Very fast decrease by about 680000 Hz
After 35s the frequency alternated between high and low.

3) Fast decrease by about 560000 Hz, and again behaving as above (2)

On placing crystal B in the cell, the crystal stopped oscillating, and when it restarted the crystal was oscillating high by + 46666 Hz.

It would appear that the form of the coating is a contributory factor to the high frequency effect.

4.6 Potassium Hydroxide

This coating gave high frequencies on coating and sample presentation which were similar to those for NaOH.

4.7 Calcium Hydroxide

Again the performance of this coating was the same as NaOH.

4.8 Lithium Hydroxide

The LiOH gave virtually no response with CO_2 and had probably become saturated with atmospheric CO_2 during the preparation stage. No attempt was made to control this, as the behaviour of the coating would be expected to be similar to NaOH.

4.9 Latex Coated Crystals

No latex coated crystal gave a high frequency effect.

4.10 Gas Chromatography Stationary Phases

The only stationary phase which gave a high frequency effect was diethanolamine, which at room temperature is on the borderline between solid and liquid.

0.6 µl of a solution containing 27.9 µg/µl, was placed on both electrodes of a crystal. The frequency change on coating was + 76729 Hz. The crystal on coating with the liquid drop was oscillating low, it then stopped, and restarted high which would indicate formation of the solid diethanolamine.

The frequency responses for 1.0 µl injections were - 206, - 211, - 198, and - 209, which is the normal response.

The following day the frequency had fallen below the clean frequency of the crystal and on examination the coating could be seen to have spread across the electrode approximately doubling its area. This supports the mass/area theory as a cause of the high frequency effect.

Another crystal coated with 0.6 µl of a solution containing 42 µg/µl diethanolamine, could be made to oscillate high or low by tuning the oscillator coil with the powdered iron slug.

4.11 Summary of the High Frequency Effect

Although most of the evidence is inconclusive, the following conclusions can be made about the high frequency effect.

1) It is not related to one specific crystal.
2) The same crystal is capable of oscillating high or low on coating and sample presentation.
3) It is mainly noticed with solids.
4) It is not a function of only the mass or area of the coating, but is related to the mass/area of the deposit.
5) The form of the deposit is related to the effect, in that it is more likely to occur with irregular deposits.
6) Some crystals can be made to oscillate high or low by tuning the coil.A similar effect is noticed on placing a coated crystal in a cell or in its protective cap, when occasionally it will stop oscillating owing to a change in its environment.
7) It occurs with crystals coated on one or both sides.
8) A crystal on coating can either oscillate high or low, and then on sample presentation it can give a positive or a negative response.

ie

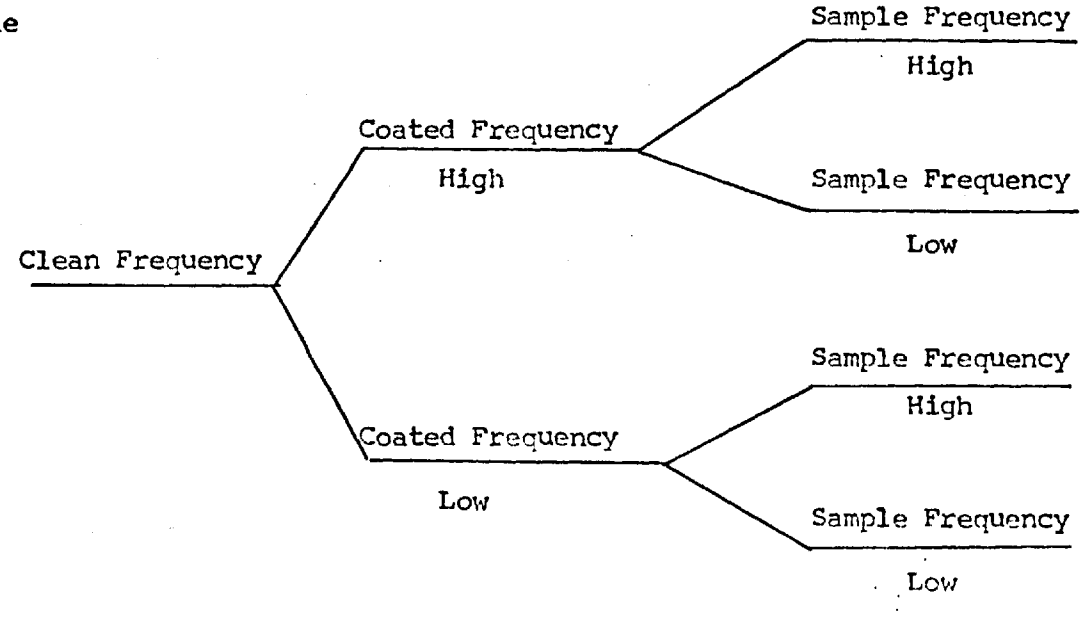

The only combination not encountered by the author was the response high for both coating and sample presentation, although this has been observed by a co-worker.(88)

The only report on the high frequency effect which could be found in the literature, was by Heising in 1946. In discussing the need for cleanliness in the manufacturing process of quartz plates, he reported that foreign matter on the plate will usually lower the frequency but that there are instances when the added matter tends to stiffen the plate and increase its frequency.This was observed when a thin film of rosin was deposited on the surface of the plate. Rosin is an amorphous resin.

This stiffening of the plate can be shown by a simple mathematical consideration.

The fundamental equation for the velocity of a wave through the crystal as given by Cady is:-

$$v = \sqrt{\frac{q}{\rho}}$$

where

v = velocity

q = stiffness factor

ρ = density

If the stiffness factor, q, is increased, there will be an accompanying increase in the velocity.

The frequency has been given by:-

$$F = \frac{v}{\lambda}$$

λ = wavelength = $\frac{1}{2}$ plate thickness,d

$$F = \frac{v}{2d} \qquad (2)$$

Thus increasing the velocity will give an increased frequency.

The alteration of the frequency by added mass, is a mechanical effect, whereas tuning the coil to effect a frequency change is an electrical effect.

The quartz crystal is an electromechanical transducer, coupling an electrical system with a mechanical system. An electromechanical transducer has the ability to convert electrical energy into mechanical energy and vice versa. Street (88) investigated the high frequency effect and proposed the idea that the effect was due to a change in the mechanical loading of the crystal.

With reference to Figure 41 , two equations will describe the behaviour of the system; one is written in terms of the electrical variables and must include the electrical effects arising from motion in the mechanical system; and the other, is in terms of the mechanical variables and includes all the mechanical effects arising from currents or voltages in the electrical system. (130)

These are;-

$$E = Z_e I + T_{em} v$$

$$F = T_{me} I + z_m v$$

where T_{em} and T_{me} are transduction coefficients describing the electromechanical coupling, the direction being denoted by the subscripts. Important properties of the electromechanical interaction can be shown by studying the driving-point impedance of the system at either its electrical or mechanical terminals. The electric driving-point impedance at a terminal pair is defined as the complex ratio of the voltage across the terminal pair to the current entering and leaving the terminal pair, when all other electromotive forces and current sources are suppressed. Setting F = 0 in the above equation, and solving for I in terms of E

gives:-

$$Z_{ee} = \left(\frac{E}{I}\right)_{F = 0} = Z_e + \frac{-T_{em}T_{me}}{z_m}$$

Similarly the mechanical driving-point impedance z_{mm} is:-

$$Z_{mm} = \left(\frac{F}{v}\right)_{E = 0} = z_m + \frac{-T_{em}T_{me}}{z_e}$$

The additive term represents the modification of the impedance caused by a change in the coupled circuit.

The motional impedance, z_{mot}, is defined as $\frac{-T_{em}T_{me}}{z_m}$

and therefore, rewriting the equation gives:-

$$Z_{ee} = z_e + z_{mot}$$

The motional impedance was first discovered by Pierce and Kennelly, when they were studying the variation of impedance with frequency for a telephone receiver, and found that the electrical impedance could be influenced by the motion of the coupled mechanical system. They discovered that a discrepancy in their measurements was caused by one setting the receiver on its side and the other on its face, thus altering the acoustic loading on the diaphragm.

A similar effect was noticed separately by Street and the author, that a coated crystal would oscillate outside of its can or a cell, but not always when placed inside. The environment of the can or cell was affecting the mechanical loading of the crystal.

An electrical effect was produced by turning the slug in the coil and bringing about a frequency change.

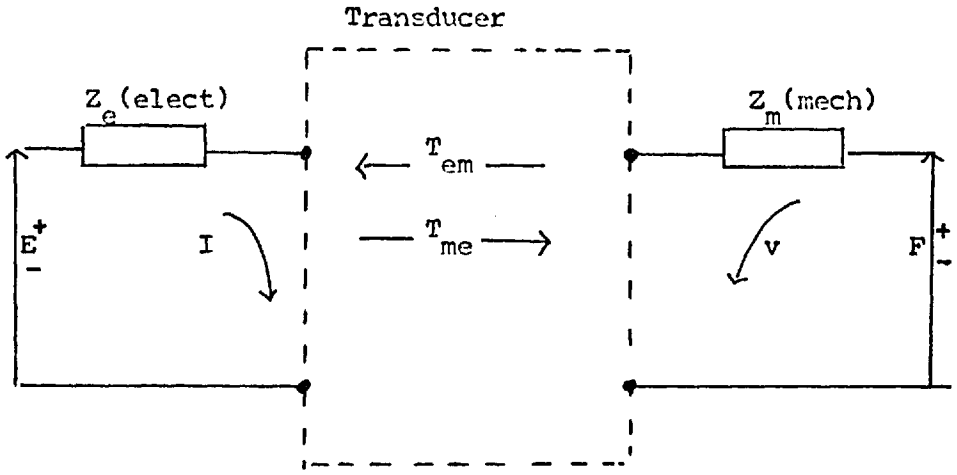

Figure 41 Schematic Representation of an Electromechanical Transducer. (130)

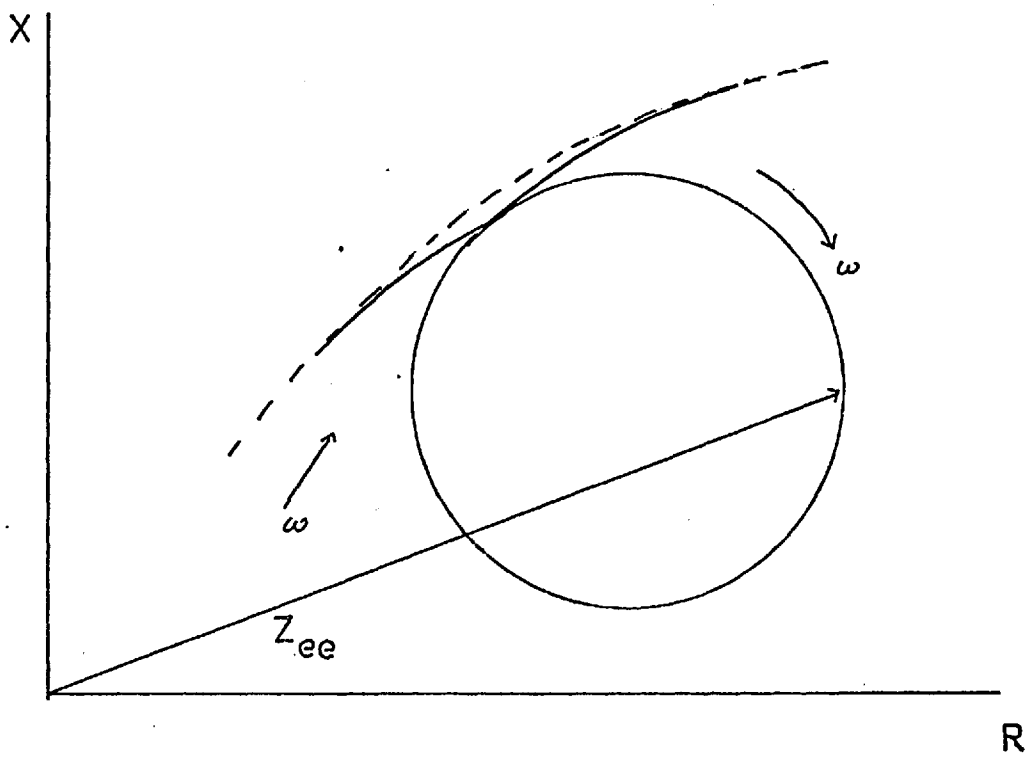

Figure 42 The Vector-impedance Locus. (130)

The variation of the mechanical impedance z_m with the frequency can be represented as a vector drawn from the origin in the real-imaginary plane. This is derived by Hunt (130). As the frequency changes, both the magnitude and the phase angle of the vector change and the tip of the vector will trace out a curve, called the impedance locus.

At low frequencies, the phase angle of z_m is very nearly $-\pi/2$ corresponding to 'stiffness control' of the mechanical system, whilst at very high frequencies the phase angle approaches $+\pi/2$ as is characteristic for 'mass control'. This was obtained by varying the frequency, but similarly the same effect should be produced by varying the mass-stiffness control of the mechanical system. It may be this which is causing the high frequency effect.

Further study is needed on the high frequency effect and no conclusion as to the cause has been made by the author, only to suggest that it is probably the coating affecting the stiffness of the crystal.

Chapter 5 Triethanolamine

5.1 Introduction

Several amines have been extensively investigated as suitable coatings for the crystal detector, in the study of sulphur dioxide.

Karmarkar and Guilbault (84) found that triethanolamine and quadrol gave linear responses to sulphur dioxide in the concentration range 10 - 30 ppb. Hartigan carried out a systematic study of various amines and their response to sulphur dioxide.(87) Amongst several, he found that diethanolamine,triethanolamine and phenyldiethanolamine had acceptable bleed rate from the crystal and gave reasonable responses to sulphur dioxide. Cheney and Homolya (86) carried out a systematic approach for the evaluation of triethanolamine as a possible coating for sulphur dioxide detection, and studied various parameters to determine methods of improving the sensitivity.

According to the work of Karmarkar and Guilbault, (84), CO_2 was not found to interfere with triethanolamine and CO had to be present in concentrations greater than 10,000 ppm to interfere. This is completely opposite to results obtained by the author as the following work will show.

Triethanolamine was originally investigated as a possible coating because a co-worker (88) had shown it to have a good response to sulphur dioxide, and,more important, a bleed rate which was within acceptable limits to enable measurements to be made.

The triethanolamine used was obtained from Phase Separations Ltd.,Deeside. The crystal was coated by placing a drop of triethanolamine on the crystal and smoothing it over the desired area with a tissue. Throughout the study, different areas were coated, either, one or both electrodes, or, one or both faces. The triethanolamine, being a viscous

liquid, tended to creep across the crystal surface, particularly if only the electrode was coated. The method used to overcome this, to some extent, was to coat the crystal over the entire face, although even then, with the crystal held vertically, the coating slowly crept down to the bottom of the crystal. The net effect was to remove coating from the sensitive electrode region of the crystal, and thus, reduce the sensitivity of the detector.

Two different dynamic system cells were used in this study. Cell C was employed to hold the crystal horizontally, with the upper surface coated, in order to minimise the coating creep. Cell D was used with the crystal held vertically.

Calibration graphs were obtained for both of these cells to enable a comparison to be made.

Cell C

The crystal was coated over one side. The carrier gas was undried with a flow rate of 10 cm^3/min.. Injections of CO_2 in the range 10 -100 µl were made, with the coating being allowed to recover before the next injection.A minimum of three injections were made for each volume and averaged. The sample was presented as a pulse in the carrier gas. It was reasonable to assume that there was little,or no, sample dilution, since the injection was made in 1-2s into a gas stream flowing at 0.6 cm^3/s. By assuming that there was no dilution taking place, the maximum concentration in the cell was calculated, and it was from this value that the minimum detection limit was calculated. Consequently, the detection limits are probably lower than stated. The volume of cell C was 1 cm^3 which is half that of the other cells.

The calibration graph for this cell is plotted in Figure 43A from the data given in Table 30.

Figure 43 Calibration Graph for CO_2 on Triethanolamine in Cell C

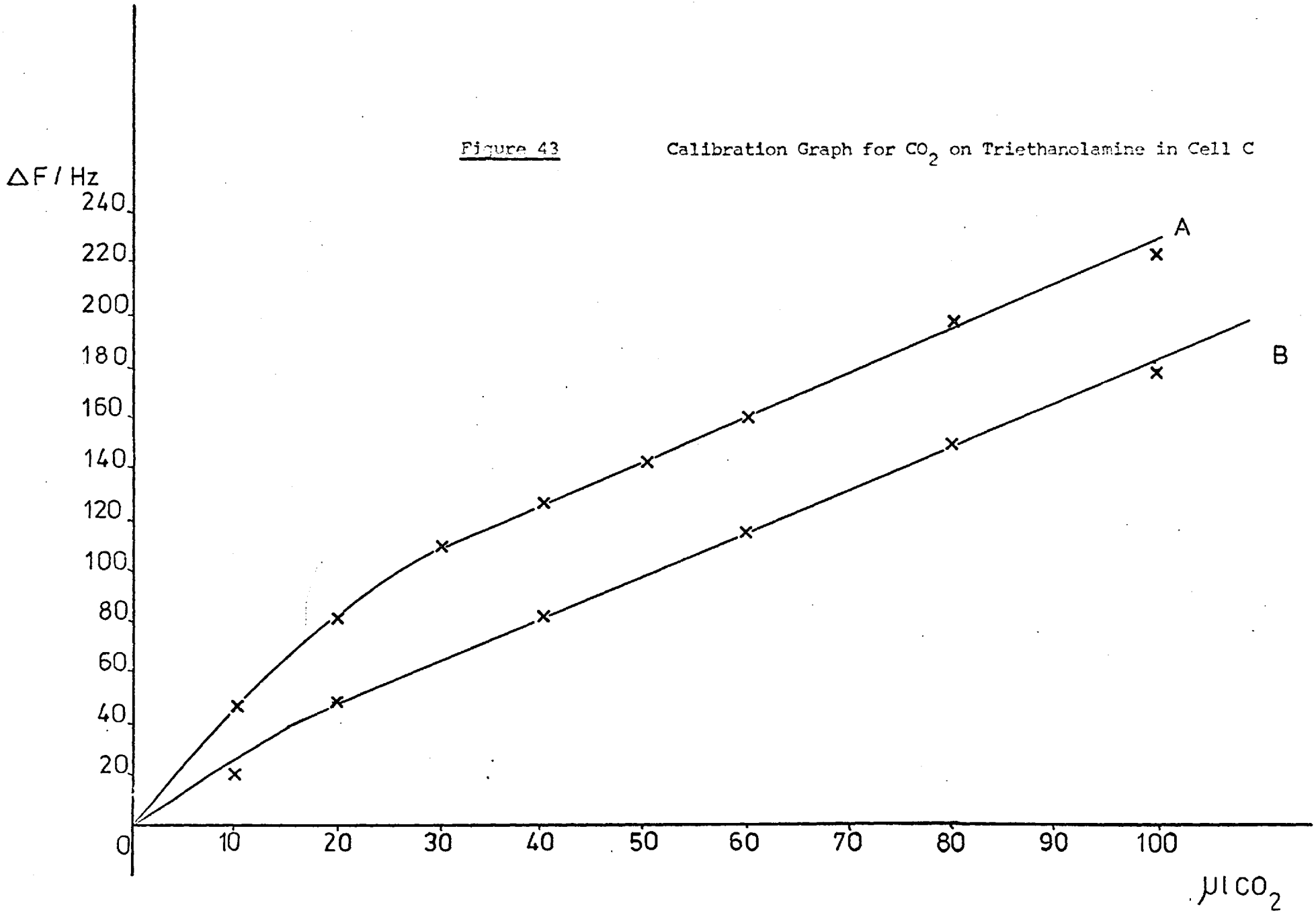

Table 30 The Response Obtained for CO_2 on Triethanolamine in Cell C

Frequency clean crystal = 8994293	Weight clean crystal = 458 µg
Frequency coated crystal= 8974473	Weight coated crystal= 598 µg
Frequency change ΔF_c = - 19820	Weight of coating = 140 µg

Injection of CO_2 (µl)	Response(Hz)
10	49.5
20	80.7
30	110.0
40	129.0
50	142.0
60	154.5
80	197.5
100	222.5

As a check on whether the response was decreasing during the course of the experiment, owing to exhaustion of the coating, a 10 µl injection was made after the 100 µl injections, and gave a response of - 44Hz. This was within the acceptable range.

The graph obtained shows a curved calibration for CO_2 on triethanolamine. The minimum detection limit based on a frequency change of twice the least count, ie 2Hz, is 404 ppm , which although this is below the threshold value, is still very high to be of use analytically. The concentration is given as ppm (v/v).

An injection of 10 µl sulphur dioxide was made under the same conditions and gave a response of - 1621 Hz, indicating a detection limit of 1.2 ppm. This also illustrates difference in the sensitivity of the coating towards CO_2 and SO_2.

The previous calibration graph was the best obtained for this particular cell, and the majority followed the pattern of that given in Figure 43B, where the response has decreased although the frequency change

on coating has increased. The data is given in Table 31. The comparison of the two graphs serves to illustrate the problems which can be encountered with the crystal detector. It might appear that it is simply a case of coat the crystal, present the sample and monitor the response. In practice, this is far from the truth, in that, all the parameters of both the crystal and the coating need to be considered, and each crystal must be separately calibrated.

Table 31 Response for CO_2 on Triethanolamine in Cell C

Injection Size (µl)	Response (Hz)	ΔF_c = - 22949 Hz
10	- 20	
20	- 49	
40	- 82	
60	-131	
80	-150	
100	-176	

Cell D

The same method was used to obtain a calibration graph for CO_2. Unfortunately, the crystal was coated with less triethanolamine than for the previous studies, but the same curved calibration graph is obtained. The graph is plotted in Figure 44 from the data in Table 32.

Table 32 Response for CO_2 on Triethanolamine in Cell D

Injection Size (µl)	Response (Hz)	ΔF_c = - 15378 Hz
10	- 19	
20	- 31.5	
30	- 44.5	
40	- 54	
60	- 54	
80	- 84	
100	- 92	

Figure 44 Calibration Graph for CO_2 on Triethanolamine in Cell D

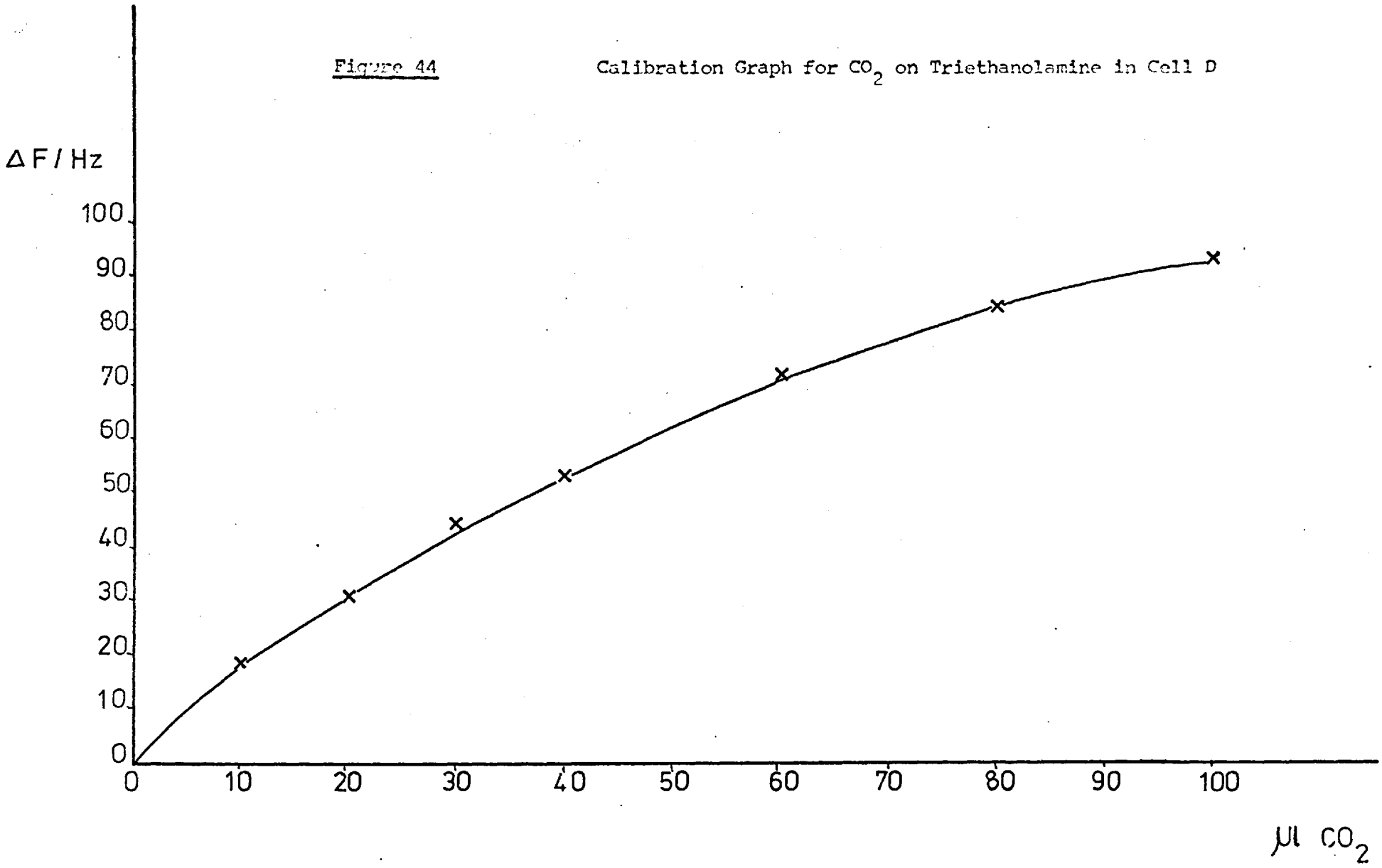

The volume of the cell is 2 cm^3 which means that a 10 µl injection is equivalent to a cell concentration maximum of 5000 ppm(v/v) which is half that found in cell C. A comparison of a 10 µl injection into cell C and a 20 µl injection into cell D should show some correlation.

Table 33 Comparison of Injections for Cells C and D

Cell C		Cell D	
Injection (µl)	Response (Hz)	Injection (µl)	Response(Hz)
10	20	20	31.5
20	49	40	54.0
40	82	80	84
50	98	100	92

The coating mass is less for cell D than for cell C , and this would indicate that cell D is the more efficient. Other problems associated with cell C, such as gas leaks, eventually led to its abandonment.

Static Cell

A brief study was made using a crystal coated on one electrode in the static cell. The frequency change on coating was - 18120 Hz. A 100 µl injection gave a response of - 46 Hz, and a repeat after flushing the cell with nitrogen gave - 45 Hz. The crystal was responding to a concentration of 3704 ppm, giving a minimum detection limit of 161 ppm.

5.2 Calibration Graphs

The method of coating the crystal which was most used,was to apply the triethanolamine over the entire crystal surface. It proved difficult to tailor the frequency drop by an exact amount each time and thus a method for comparing the response for different masses

of triethanolamine proved necessary.

A crystal was coated with successive increments of triethanolamine, which was smoothed over the crystal to provide as near a uniform surface as possible. The injection size chosen to act as a standard was 40 µl, since this gave reasonable responses. A graph of frequency change on sample presentation versus frequency change on coating, is plotted in Figure 45 . As can be seen, the graph curves upwards at higher values of the coating frequency indicating higher responses for the injections.

Referring back to equation 9, the Sauerbrey equation.

$$\text{ie} \qquad \Delta F = -2.3 \times 10^{6} \frac{F^{2} \Delta M}{A}$$

This can be expressed as $\Delta F = \frac{K \Delta M}{A}$

where K is a constant.

For this experiment, the mass of CO_2 injected is kept constant, and the area is kept constant by coating the entire crystal surface. This means that the frequency change on sample presentation should be proportional to the mass of tricthanolamine on the crystal. It has been shown that the most sensitive region of the crystal is the electrodes, and therefore, any triethanolamine placed outside this area may not be weighed so accurately. It may be for this reason that the graph obtained, curves. The other possibility, is that the graph consists of two straight lines meeting at a ΔF_c of about 16000 Hz. Since the frequency response will depend on the surface area and the mass of the coating, with a constant surface area, there may be a critical mass below which the coating becomes saturated before

Figure 45

Response for 40 µl Injections CO_2 versus Frequency Change on Coating with Triethanolamine.

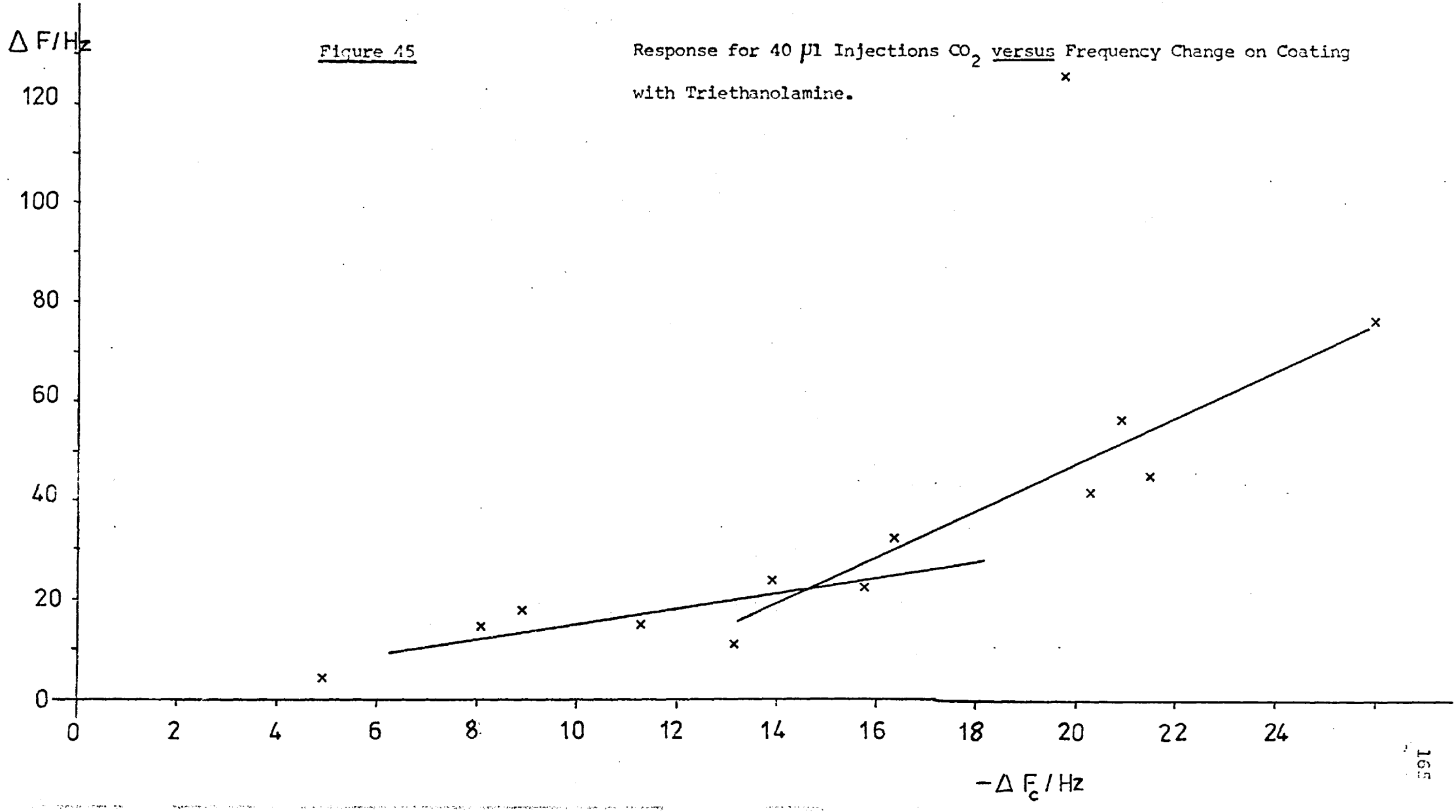

equilibrium occurs.

An investigation was carried out to determine whether the curving of the calibration graph was a coating effect, or an instrumental one, such as the injection technique. Although the injections were made rapidly there would be a slight difference in time for a 10 µl and a 100 µl injection, owing to the extra distance the syringe plunger has to travel. To test this possibility, the syringe was filled with 0- 100 µl of CO_2 and then diluted to 100 µl with nitrogen. The gas solution was allowed to equilibrate prior to injection. The syringe plunger was depressed slowly over a set time period (8s). The responses obtained are given in Table 34.

Table 34 Response for CO_2 with Constant Sample Size over 8 s.

µl CO_2 in 100 µl Injection	Response (Hz) ΔF_c = - 15378
10	- 11
20	- 18
40	- 24
60	- 35
100	- 44

The responses were lower than expected, (compare Table 32, the same crystal), but the injections are taking at least twice as long, and dilution must be occurring prior to the cell.

The experiment was repeated with an injection time of 18 s. Again, the responses are lower owing to dilution. The data is given in Table 35, and both graphs are plotted in Figure 46 .

Although the plot for the 18s injection time is poorly defined, a straight line can be drawn through the points. The shorter injection time gives a curved graph, and since the injection volume was kept constant, the curving must be owing to a concentration effect.

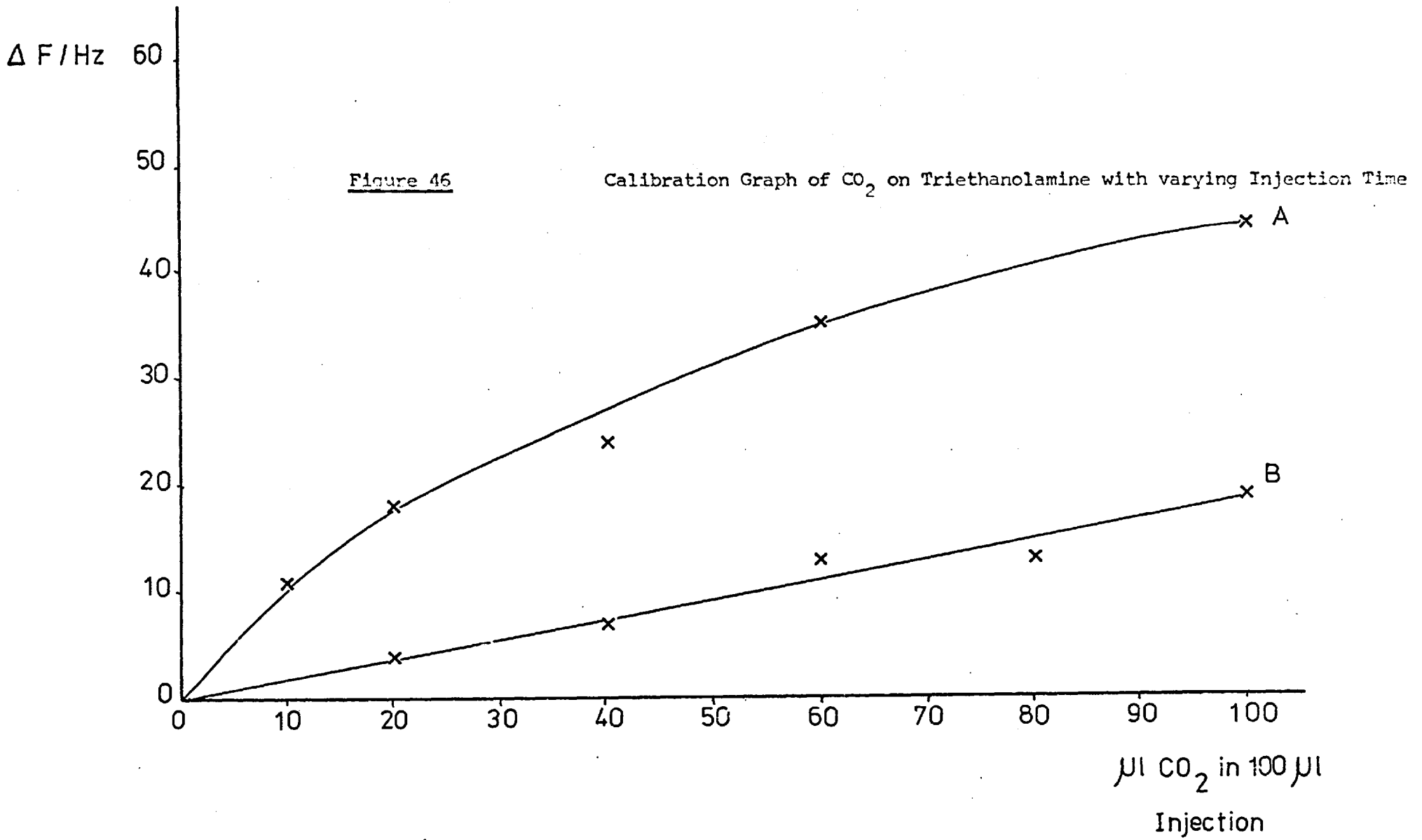

Figure 46 Calibration Graph of CO_2 on Triethanolamine with varying Injection Time

The results for the longer injection time support this theory, since a linear plot was obtained for more dilute gas solutions.

Table 35 Response for CO_2 with Constant Sample Size over 18s

µl CO_2 in 100 µl Injection	Response (Hz)
20	- 4
40	- 7
60	-13
80	-14
100	-19

The calibration curves obtained were consistently curved, although they were reproducible. Since the explanation lies with a concentration effect, it is probably caused by saturation of the surface of the coating at larger concentrations, or to insufficient residence time in the cell for equilibration to occur.

5.3 Variation in Response with the Method of Injection

The calibration curves obtained above were all plotted from data for short,rapid injections of 0 - 100 µl. The main problem with rapid injections, is that there is insufficient residence time of the sample in the cell for equilibration of the sample and coating to occur. The presentation of sample gas over a longer period of time should overcome this.

The first method of producing long gas samples, which was tried, was the asbestos plug flowmeter arrangement. The problems encountered with this were numerous.The flow rate through the asbestos plug was irregular and a back pressure across the needle would stop the gas flow from the aspirator bottle.The results obtained were erratic and totally unreproducible, with no correlation between samples of

the same concentration, or between samples of different concentrations.

A selection of the results obtained are given in Table 36.

Table 36 Responses obtained using the Asbestos Plug Flowmeter

ΔF_c /Hz	Concentration CO_2 in cell/ppm	Response /Hz
33600	48	- 167
	48	- 56
	160	- 25
	160	- 31
28600	480	- 16
	800	- 88
	800	- 31
43200	9600	- 72
	9600	- 54
	500	- 55
	124	- 99
	124	- 44
	158	- 42
	96	- 39

To test whether a complex of the form Triethanolamine -CO_2 was being formed and contaminating the coating, a crystal was heated to 40°C after receiving a sample. It has been reported that the complex Triethanolamine- CO_2 is stable at 0°C and unstable at 100°C, and therefore, the effect of heating should decompose any complex formed. On cooling and repeating the sample injection, a response much lower than the first, was obtained, which suggests that the cause of the decreasing response of the coating is not complex formation.

The cause, from subsequent investigations, would appear to be oneof the following:-

1) A build up of back pressure across the needle may be occurring and restricting the flow of sample gas.

2) The asbestos plug may not be allowing a uniform flow rate of gas to pass.

3) It is not a function of the coating. A crystal which was giving poor results for long sample presentation, was calibrated using rapid injections. The graph obtained was as expected.

4) It is possibly a contamination effect, although successive runs with the same sample would be expected to give similar results.

Calibration curves were obtained for two isolated crystals in this study. The graphs are given in Figure47 and the data is in Table 37. The frequency response is plotted against the final concentration in the cell.

Table 37 Calibration Curve using the Asbestos Plug Flowmeter

System:- Cell D, drying tube Z, flow meter R.

Gas Flow 10 cm^3/min

ΔF_c = - 33583 Hz -both electrodes coated.

Concentration in Cell/ ppm	Response /Hz	
12	- 28	
16	- 28	Fig. 47 (b)
38	- 34	
57.6	- 64	(Fig. 47 (a) data
91.2	- 70	for Day 1)
ΔF_c = - 34243 - both electrodes coated		
9	- 29	
19	- 43	Fig. 47 (c)
48	- 76	
115	-153	
96	- 84	

The second graph cannot be used as a calibration graph, since one point falls a long way off the line, but it does illustrate that

Figure 47 Calibration Graphs using Long Sample Presentation

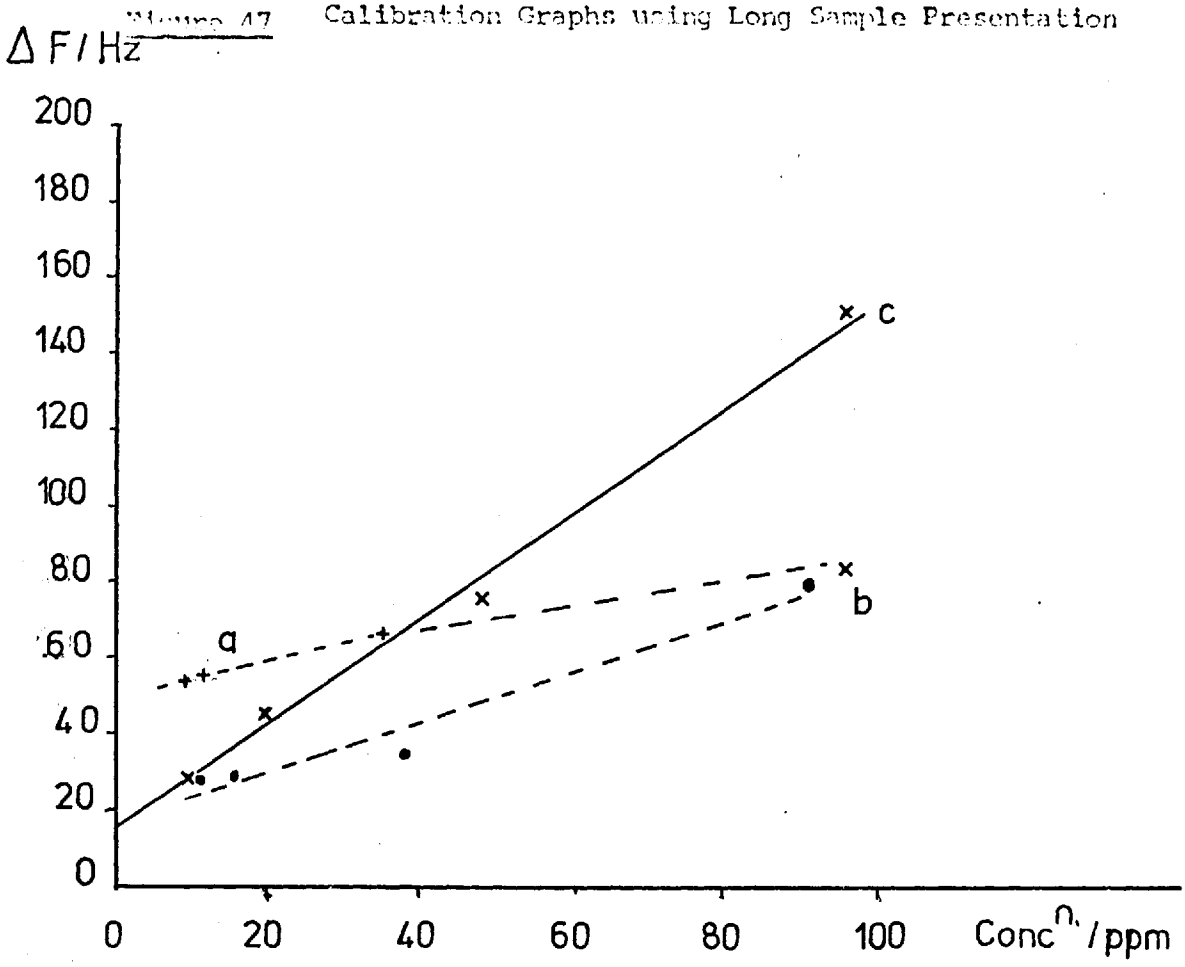

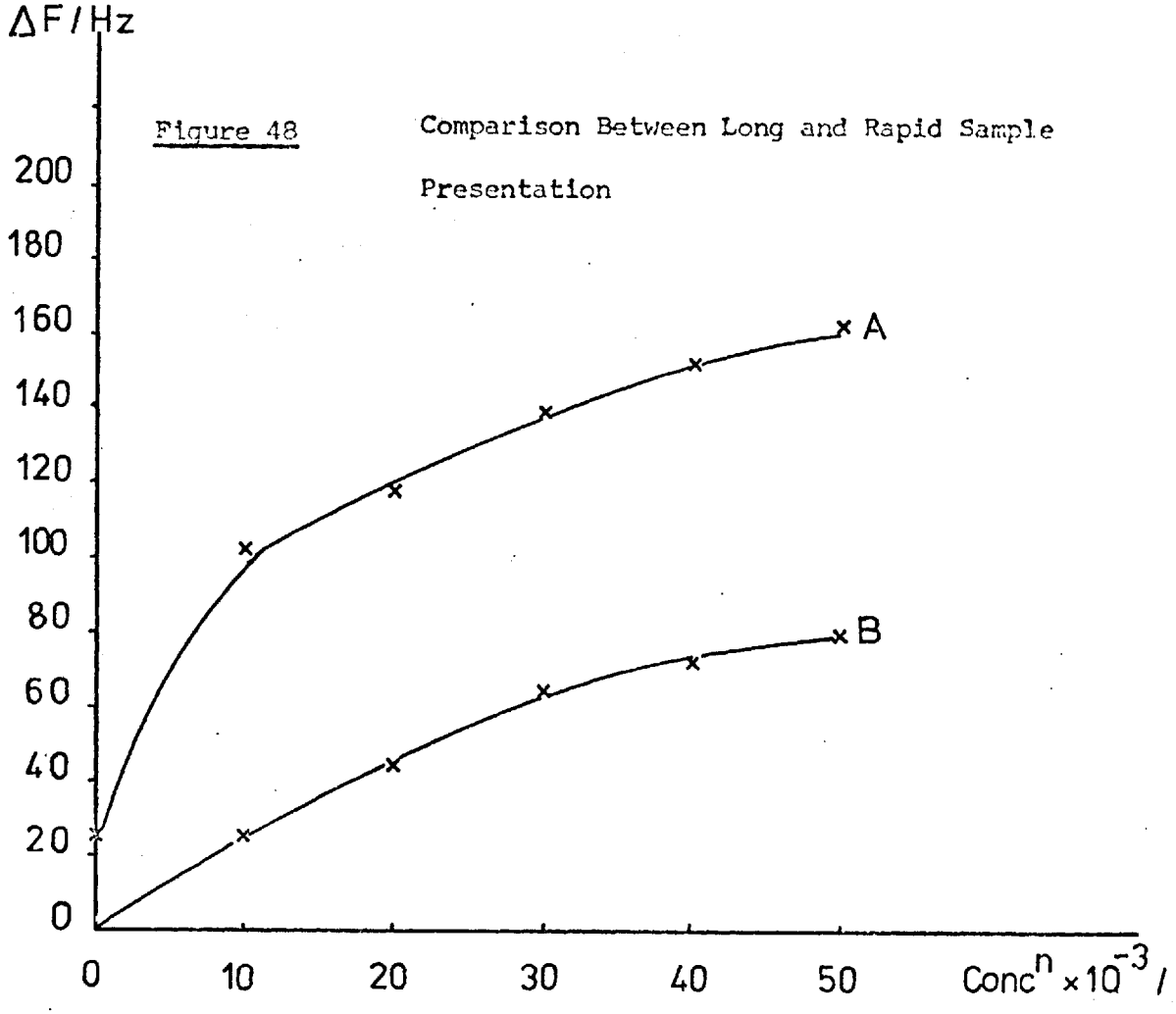

Figure 48 Comparison Between Long and Rapid Sample Presentation

a linear relationship between response and concentration could be obtained. Both the graphs cut the ordinate at 15 - 17 Hz indicating that a background correction is necessary. A long presentation of nitrogen gave a response of - 16 Hz which would suggest that the background is owing to the actual injection.

Since long sample presentation improved the sensitivity of the crystal considerably, a syringe pump was built to overcome the errors involved with the asbestos plug flowmeter.

As before, erratic results were obtained when dilute gas samples were injected into the carrier gas. The syringe used was 5 cm^3 and the dilute gas solutions were prepared in the mercury levelling gas handling system.The results are listed in Table 38.

Table 38 Response obtained for dilute gas samples

System:- Cell D, drying tube Y, flow meter R.

ΔF_c = - 34000 Hz, both electrodes coated.

Flow Rate of Carrier Gas = 12.5 cm^3/min.

Concentration in Syringe ppm	Concentration in Cell ppm	Response Hz
air		- 41
nitrogen		- 7
8000 CO_2	426	- 76
8000 CO_2	426	- 76
4000 CO_2	214	- 53
4000 CO_2	214	- 66
4000 CO_2	214	- 45
12000 CO_2	640	- 56
12000 CO_2	640	- 59

Both of the methods for preparing the gas solutions, the asbestos plug flowmeter system and the syringe pump had one thing in common.The nitrogen used in prepaing the dilute solutions was a

separate system from the main carrier gas supply and was dried in the asbestos plug flowmeter system.This nitrogen diluted the CO_2 in the aspirator bottle and the mercury levelling system. It is feasible that contamination was occurring at some point in this gas line, such as at the drying columns, or from the rubber connections.Another possibility of contamination in the mercury levelling system, is from the mercury itself. Any mercury present in the sample gas would amalgamate to any gold of the electrodes remaining uncoated, or possibly it might be sorbed by the coating. A third explanation is that the concentration of sample being presented is too low and the crystal is responding to the mechanical shock of the injection.

An attempt was made to test for this, by preparing the gas solutions in the syringe. A quantity of CO_2(0 - 5 cm^3) was withdrawn from the main reservoir,and made upto 5 cm^3 by withdrawing nitrogen from the carrier gas line. A rubber septum was placed on the end of the needle to prevent atmospheric contamination whilst the solution equilibrated. The results obtained proved to be more consistent and a calibration graph could be plotted.See Figure 48A and Table 39.

Table 39 Calibration curve for CO_2 using 5 cm^3 syringe

cm^3 CO_2 in syringe	Concentration in cell ppm	Response Hz
0		- 29
0		- 22
1	10667	-103
1	10667	-102
2	21334	-120
2	21334	-116
3	32001	-139
3	32001	-139
4	42668	-155
4	42668	-151
5	53333	-174

ΔF_c = - 17719 Hz - both electrodes coated

The graph is curved and cuts the ordinate at 25 Hz.

A direct comparison of this graph was made with one obtained from using rapid injections. The concentration in the cell for a 20 µl injection is 10,000 ppm, and this response should compare with the third injection in the above table. The same crystal and coating were used for the study. Table 40 gives the responses obtained.

Table 40 Calibration curve for CO_2 using rapid injections

Injection Size /µl	Response/Hz
20	- 29
20	- 26
40	- 48
40	- 44
60	- 65
60	- 66
80	- 73
80	- 73
100	- 83
100	- 79
50 N_2	- 5

From a consideration of Figure 45 , the crystal is behaving as expected for a ΔF_c of 17719 Hz. The data is plotted on Figure 48B.

A comparison of the results from Tables 39 and 40 gives the following:-

Table 41 Comparison of Responses for Long and Rapid Sample Presentation

Concentration (ppm)	Response, long /Hz		Response, rapid /Hz	
10700	a) - 102	b) - 75	a) -27	b) - 22
21300	- 118	- 91	- 46	- 41
32000	- 139	-112	- 65	- 60
42700	- 153	-126	- 73	- 68
53300	- 174	-147	- 81	- 76

The responses labelled (a) are the uncorrected values, and those labelled (b) are those corrected for the background.

The evidence shows that the long sample presentation has improved the sensitivity of the coating by, approximately, a factor of 2, as compared to the sensitivity obtained for the rapid injections. This is, as anticipated, since the coating reaches equilibrium with the CO_2 during the period over which the sample is presented.

The sensitivity for the system, based on results obtained for a concentration of 10700 ppm, is 208 ppm for the long injections, and 909 ppm for the rapid injections.

The detection limit is poor in terms of an analytical use, but it is well below the threshold value of 5000 ppm, and just below the atmospheric level of 315 ppm.

5.4 Peak Shapes

The peak shape is defined as the plot of the frequency decrease on sample presentation with subsequent increase, with time.

a) Long Sample Presentation

The peak shapes for the samples listed in Table 25 are plotted in Figure 49.

All the profiles are of the same basic shape - a deep 'U' shaped trough.

ie

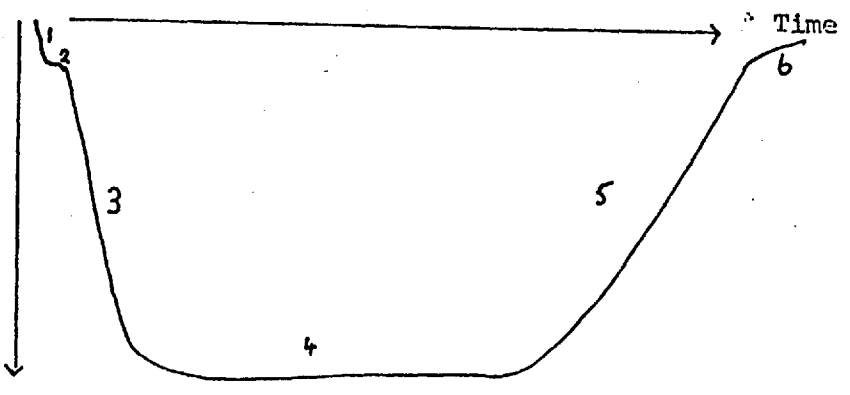

Figure 42

Peak Profiles for Long Sample Presentation of CO_2 on Triethanolamine

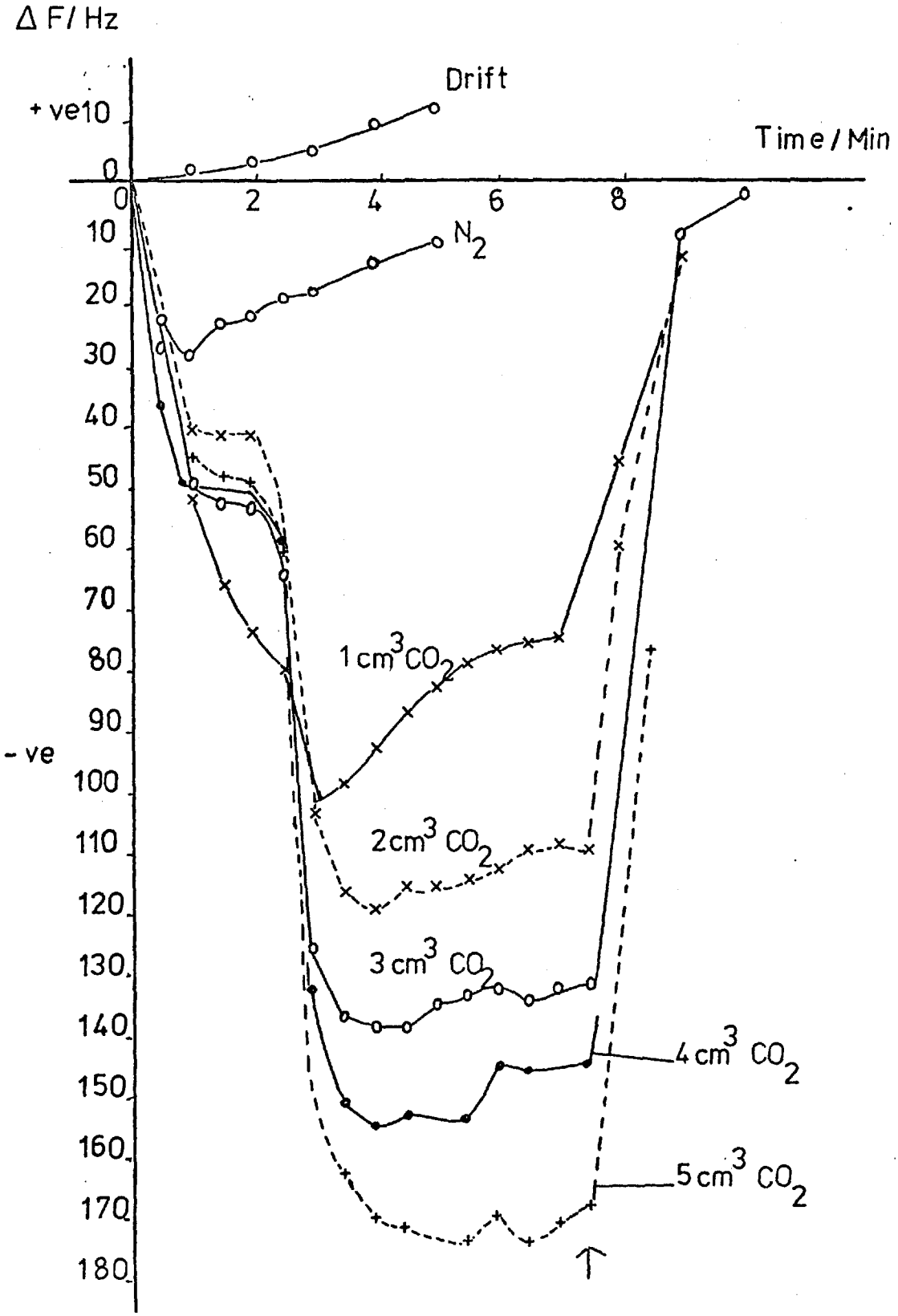

Region 1 This region denotes the initial sorption onto the coating

Region 2 This is an inflexion point which appears for all the samples injected, although it is less noticeable for the 10700 ppm injection.

Region 3 This is the rapid sorption of CO_2 onto the coating.

Region 4 Equilibrium between the CO_2 and the coating is established.

Region 5 Sample presentation is stopped after 7.5 minutes, and the CO_2 is rapidly desorbed from the coating.

Region 6 The normal drift pattern is re-established.

For the 10700 ppm sample, equilibrium is rapidly reached and the natural drift of the crystal is re- established. Once the sample presentation is stopped the CO_2 is rapidly desorbed.

That the response is owing to CO_2 sorption is shown by a consideration of the nitrogen peak shape. There is an initial response caused by the injection, which is possibly owing to the slight change in the carrier gas flow rate; this is followed by the drift pattern being re-exerted.

The peak profiles obtained from the system using the syringe pump were compared to those obtained from the asbestos plug flowmeter syatem.The different types of peak shape are shown in Figure 50.

1) The peak shape is a low shallow trough, which reaches equilibrium and then rises rapidly even before the sample presentation is stopped.
2) This is the extreme case of plot (1).
3) This is similar to (1) except the equilibrium takes longer to occur and the trough is not so wide.

The rapid rise of the plots after what would appear to be the equilibrium position is far greater than the drift of the coating. In

Figure 50 Peak Profiles for CO_2 using Asbestos Plug Flowmeter

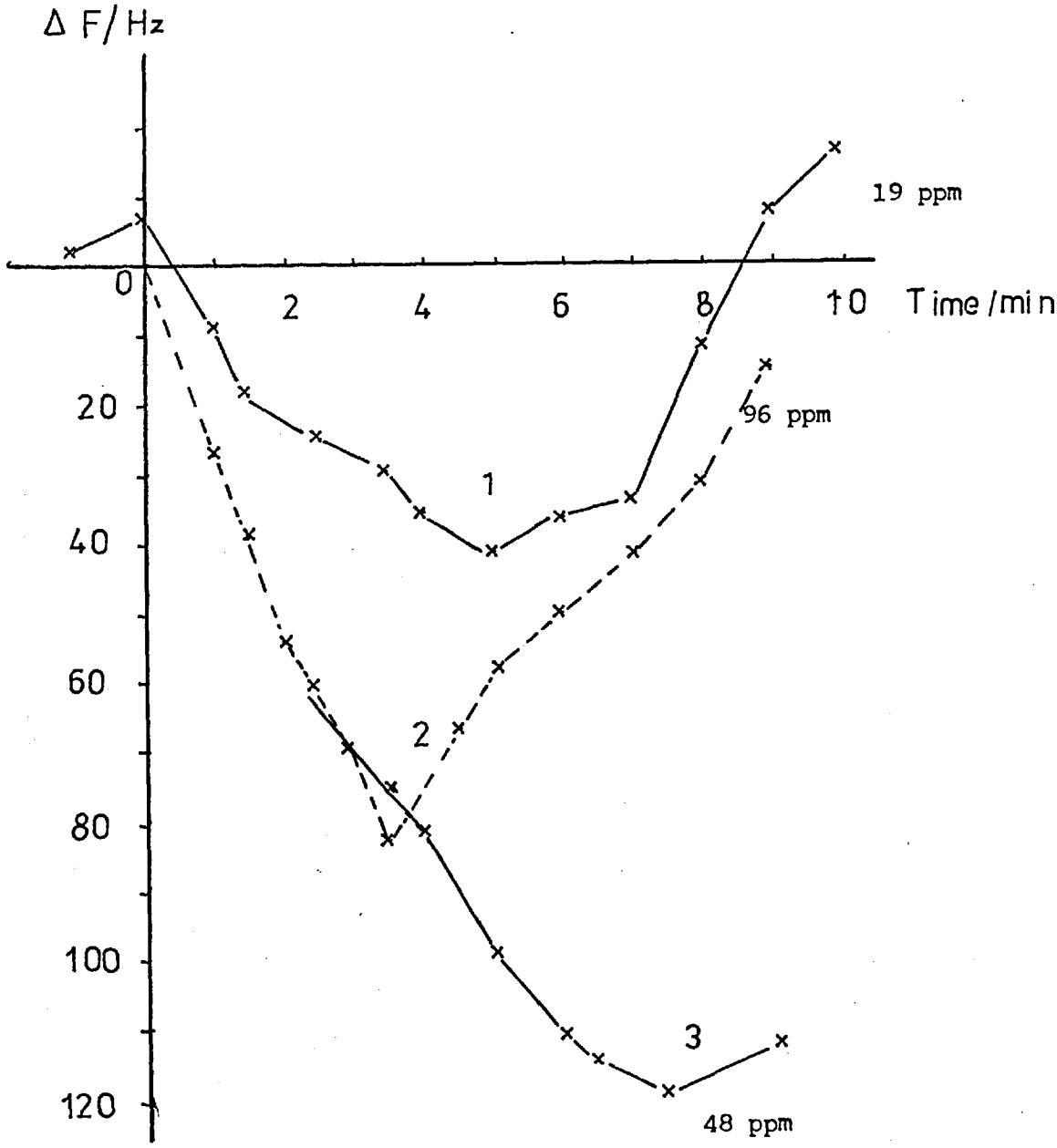

(2), in particular, it would seem that the CO_2 is being rapidly desorbed after 3.5 minutes. If this increase was due to drift alone, once the sample presentation was stopped, the increase should be even greater. In most cases this was not observed and lends support to the theory that the sample is being prevented from passing through the asbestos plug.

The most important point to notice from the plots , is that the inflexion point is not present, except possibly in plot (1). The probable explanation is that the inflexion point is owing to the beginning of the sample front reaching the cell and becoming diluted. The crystal responds to this concentration and as more sample reaches the cell, the concentration reaches that in the carrier gas and the frequency falls again. This inflexion is not seen for the other system, since the flow rate is faster and the sample front is less pronounced. The flow rate of the sample into the carrier gas for the asbestos plug is 1.2 cm^3/min, compared with 0.7 cm^3/min for the syringe pump.

b) Rapid Sample Presentation

The peak profiles are characterised by a rapid decrease in frequency which reaches a minimum within 30s, and is followed by a rapid rise which is back to the starting frequency within 1 min.

Figure 51 shows the peak profiles. As the concentration is increased the peak width at half the height remains constant and the degree of tailing becomes more pronounced. The peaks are very similar to those obtained in gas chromatography.

5.5 Recovery of the Coating

From Figure 51 it is apparent that the desorption of CO_2 is very rapid and the coating has recovered within 2 min. Thus, for

Figure 51 Peak Profiles for Rapid Injections of CO_2

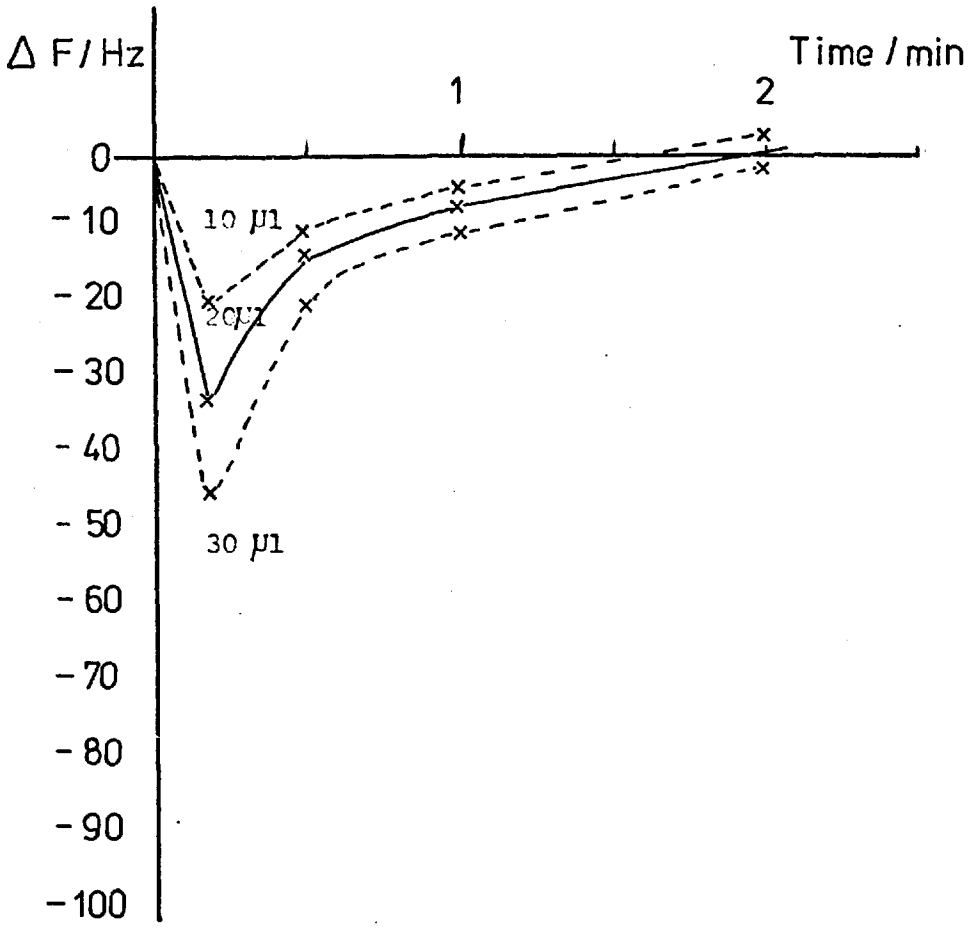

single injections a sample can be presented every 2 min..

With the long sample presentation, the coating again recovers very quickly on cessation of the injection. This can be seen by referring back to Figure 49 ,the sample presentation is stopped after 7.5 min at which point a rapid frequency increase occurs, denoting CO_2 desorption, and within 2 min the coating has returned to its starting frequency. For long sample presentation it was found to be advisable to wait a further 5 min to ensure complete CO_2 desorption, and to allow the drift pattern to be re-established.

It is worth noting that the recovery time is dependent on the bonding strength of the triethanolamine - CO_2 complex formed. For the triethanolamine - SO_2 complex, the recovery time is considerably longer, being 5 min reported for a concentration of SO_2 in the cell of 0.077 ppm, and over 1 hr with concentrated gas solutions.(88)

5.6 The Effect of Temperature on the Response of a Coated Crystal

CO_2 is reported to form a complex with triethanolamine which is stable at 0°C and unstable at 100°C.(131) The mechanism is uncertain but may be an acid-base reaction.

A clean crystal was coated on both sides with triethanolamine and placed in cell D, with a carrier gas flow rate of 10 cm^3/min. The cell was immersed in a water bath and allowed to reach equilibrium before any measurements were made. The frequency change on coating was - 12860 Hz, and as a check on the performance of the crystal, 40µl were injected. The response expected from Figure 45 was about 20 Hz, had the crystal only been coated on one side, and therefore, for this crystal a change of about 40 Hz was expected.The frequency response obtained was - 38 Hz, denoting that the crystal is behaving in a

Table 42 The Effect of Temperature on the Response of a Coated Crystal

Day No.	Temp./°C	Response to Injection/Hz 10 µl	40 µl	ΔF_c/Hz	Plot
1	21.4	13, 13	38, 38	- 12232	1
	30	6, 6	20, 21		
	42	2, 2	12, 11		
2	20	10, 8	42, 30		2
	30	1	9, 12		
	41.7		8, 8		
	53.5		3, 3		
1	4	39, 39	100, 107, 108	- 23084	3
	22.8	23, 22	70, 66, 69		
2	19.5	14, 14	53, 50	- 19336	4
	27.7	8, 8	29, 31		
	32.6	7, 5	26, 24		
	37.2	5, 6	22, 23		
	41		16, 16		
	45.5		9, 9		
	49.1		6, 6		
1	2.4		93	- 24099	5
	3.7		81, 82		
	16.5		71, 72		
	24		54, 54		
	28.8		47, 34		
	37		34, 32		
	44.2		26, 25		

normal manner. Measurements for 10 µl and 40 µl injections were made at room temperature (21.4°C), 30°C, and 42.2°C, and the results are given in Table 42. The experiment was repeated with other crystals, over a wider temperature range and for several days. The data is included in Table 42.

The data for the 40 µl injections is plotted on Figure 52 with the frequency response versus temperature. All the plots are similar and with the exception of number 3, are in order of decreasing masses of coating, as measured by the frequency change on coating. The plots for the same crystal on successive days are different owing to the loss of coating caused through heating the crystal.

A similar graph for response versus temperature was obtained for cyclohexane by Earp.(102)

King (113) predicted that the performance of the sorption detector could be predicted from a knowledge of the gas chromatography data on the particular coating. Earp (102), derived the relationship between the response and the temperature.

A well known equation in gas chromatography is,

$$\log V_g = \frac{-\Delta H}{2.3\ RT} + c \quad \propto \quad k \log \text{response}$$

where V_g is the specific retention volume

ΔH is the heat of solution of a gas in a liquid substrate

R is the ideal gas constant

T is the absolute temperature

c is a constant (102)

The solution process is usually exothermic and hence a plot of log V_g versus 1/T over short temperature ranges will give a straight line of positive slope. Since retention volumes generally decrease with increasing temperature, the absolute response of the sorption detector

Figure 52 The Effect of Temperature on the Response of a Coated Crystal.

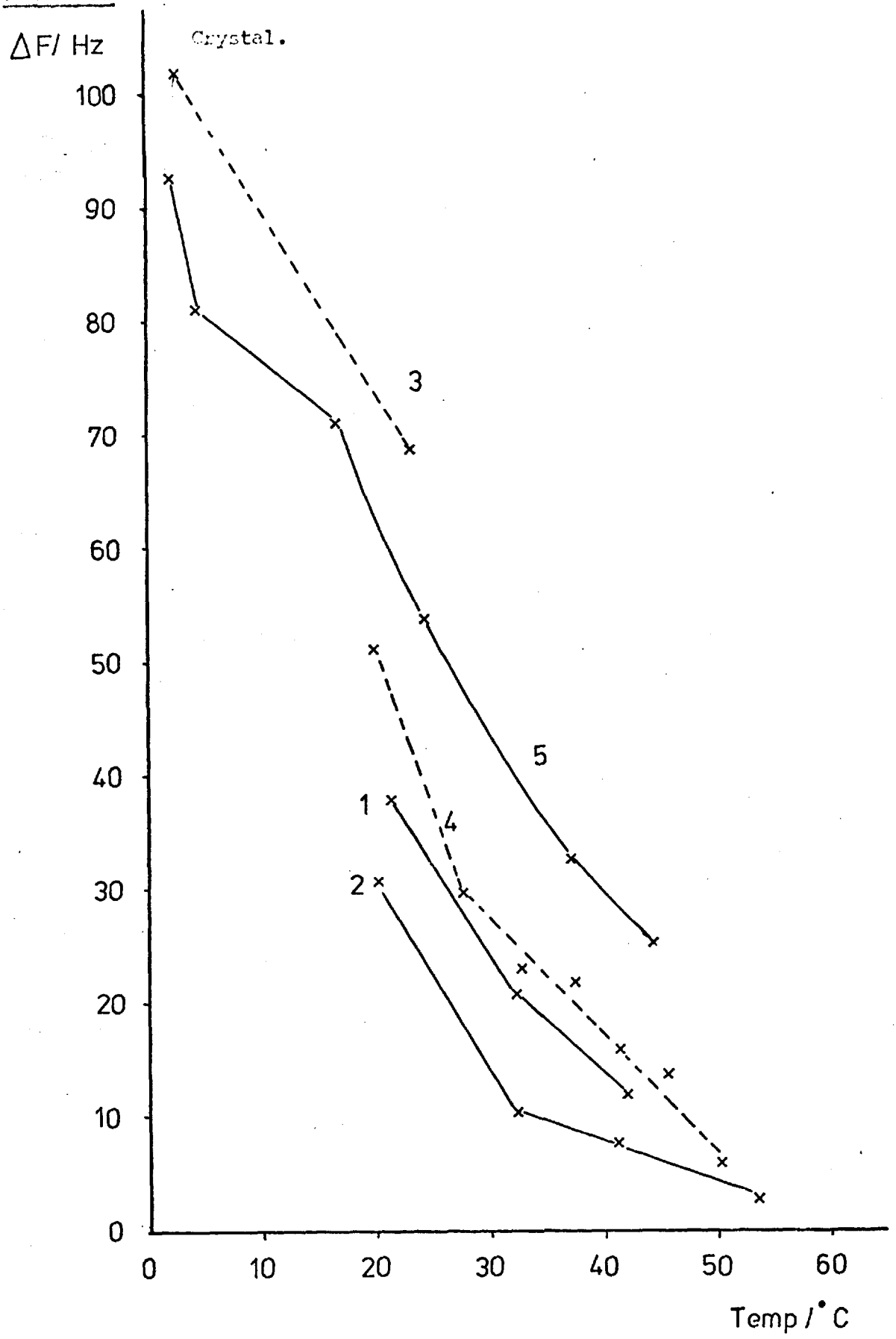

should likewise decrease. In addition, the log of the response should be linearly related to the log of the retention volume, and a log response versus 1/T should be linear.

This relationship can also be reached by considering the equilibrium constant K_{eq}.

Assuming the reaction is

$$CO_2 + (C_2H_4OH)_3N \longrightarrow \text{complex}\left[TEA - CO_2\right]$$

$$\text{Therefore } K_{eq} = \frac{[CO_2]\,[TEA]}{[\text{Product}]} \tag{40}$$

But $[CO_2]$ and $[TEA]$ are constant for the experiment and, therefore,

$$K_{eq} \propto \frac{1}{[\text{Product}]} \tag{41}$$

$$\text{But} \quad \ln K_{eq} = \frac{-\Delta H}{RT}$$

and therefore,

$$\ln K_{eq} \propto \frac{1}{T} \tag{42}$$

Taking logarithms of (40)

$$\ln K_{eq} = \ln [CO_2] + \ln [TEA] - \ln [\text{Product}] \tag{43}$$

But $[CO_2]$ and $[TEA]$ are constant

Therefore,

$$\ln K_{eq} = \ln [\text{Constant}] - \ln [\text{Product}] \tag{44}$$

Substituting (42) in (44) gives

$$\frac{-\Delta H}{RT} = \ln [\text{Constant}] - \ln [\text{Product}]$$

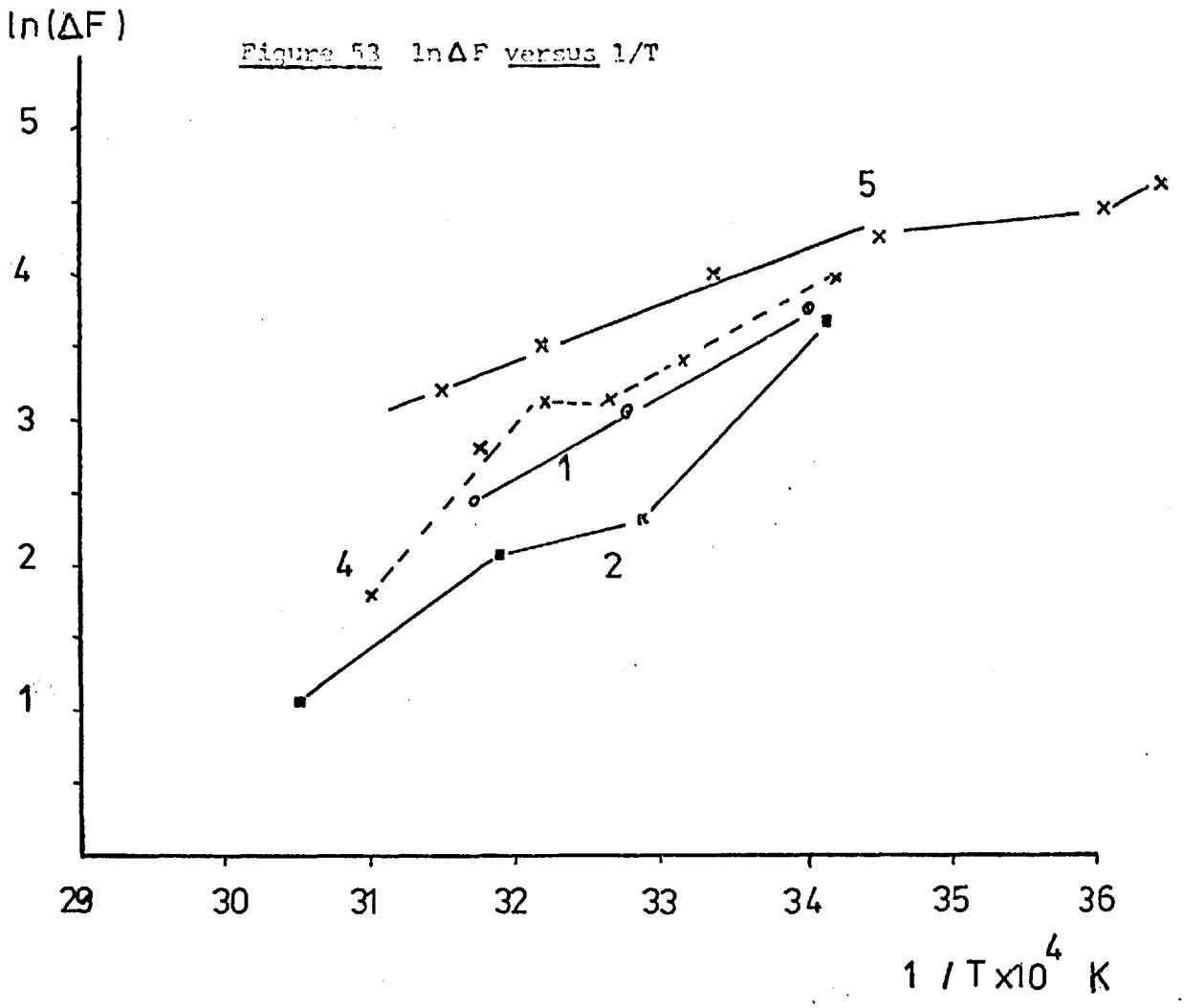

Figure 53 ln ΔF versus 1/T

Rearranging gives,

$$\ln[\text{Product}] = \ln[\text{Constant}] + \frac{\Delta H}{RT} \qquad (45)$$

Plotting $\ln[\text{Product}]$ *versus* $1/T$ gives a straight line.

But the $[\text{Product}]$ is proportional to the frequency change since $\Delta F = k\Delta M$. Therefore, plotting $\ln[\text{Response}]$ *versus* $1/T$ should give a straight line.

The $\ln \Delta F$ *versus* $1/T$ graphs are drawn for plots 1, 2, 4 and 5 from Figure 52 on Figure 53 The plots give straight lines with positive gradients with two exceptions. Both plot 2 and 4 show inflexion points at a temperature of 32°C. The cause is unapparent although it could be owing to an error in the frequency change. This is suggested by a repeat of the experiment over the temperature range which gave no inflexion point.

From these studies, it can be seen that there is a linear response of $\ln \Delta F$ with $1/T$, and that the optimum temperature for the response is as low as possible. In practice, the working temperature was chosen as room temperature, since it was difficult to keep the cell at a constant temperature of 0°C. The ice did not pack easily around the cell and the temperature of the cell varied as the amount of ice in contact with it varied. At a temperature of 34°C the coating took 30s to completely desorb the CO_2 , as compared to 1 min at room temperature, showing that the complex was more stable at the lower temperatures.

5.7 The Precision of the Coating

The precision of the system is very good for rapid injections. Figure 54 shows a plot of successive 40 µl injections on a crystal at 6°C. There is an initial drop in the response after which it stabilises.

Figure 54 Precision of Triethanolamine Coating for 40 µl Injections

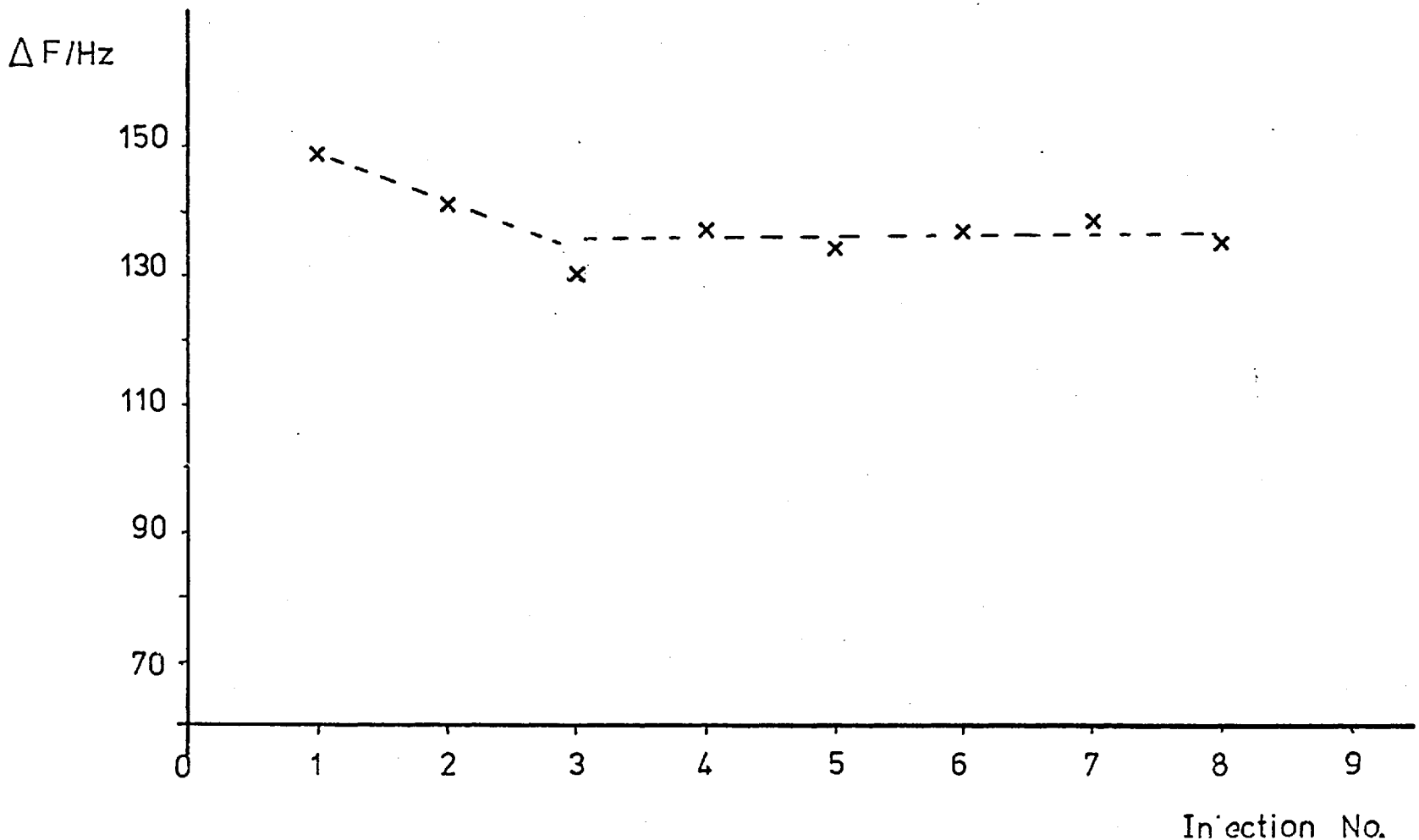

Table 43 Precision of Coating - Response for Successive 40 µl Samples

Injection No.	Response/Hz	ΔF_c = - 19600
1	- 149	
2	- 141	
3	- 130	
4	- 137	
5	- 134	
6	- 137	
7	- 138	
8	- 135	

For a coating change of 19600 Hz the response would be expected to be 45 - 50Hz, so the improvement of working at lower temperatures is immediately apparent.

Ignoring injection number 1, the mean is 136 with a standard deviation of $\pm$ 3.2 (2%)

5.8 Effect of Adding Different Compounds to Triethanolamine

A brief investigation was carried out to ascertain the effect of adding solids to triethanolamine. Various solids were mixed with a little triethanolamine using a pestle and mortar, and a small amount of this mixture was placed on the crystal. Solids were chosen which had been reported to interact with CO_2 and should give an enhancement of the response.

The results are tabulated in Table 44.

The application of powdered NaOH to triethanolamine improved the sensitivity considerably, - 183Hz for a 10 µl injection. Unfortunately the NaOH reacted with the CO_2 and the precision became worse.

Table 44 The Effect of Additives to Triethanolamine on the Response

Additive	ΔF_c/Hz	Expected response to 40 µl CO_2	Sample Size µl	Response/Hz
Molecular Sieve	- 22635	55 - 60	40	69, 71, 62
NaOH solution	- 10639	20	40	46, 48
NaOH powder	- 24187	65	10	183,155
LiOH	- 17576	35	10	144, 97
NaCl	- 25123	70	10	23
$MgSO_4$	-		10	18
$MnCl_2$	- 29180	90	10	15, 7
Activated charcoal	- 23000	60	40	80, 80
As_2O_3	- 32038	100	10	92, 95, 91, 55,41, 36

Table 45 Precision of Triethanolamine/CO_2 System

Injection No.	Response/Hz
1	- 183
2	- 155
3	- 164
4	- 174
5	- 201
6	- 176
7	- 150
8	- 155

The mean is 169.8 and the standard deviation is $\pm$ 16.2 (10%)

The use of powdered NaOH and LiOH improved the sensitivity, but gave an erratic response which decreased within a few injections. As_2O_3 again improved the response, although it too, decreased with time.

Activated charcoal gave a slight improvement to the response, about 20Hz for a 40 µl injection. The results were consistent, the responses being -

10 µl 32, 24, 28, 27, 27

20 µl 48, 49

40 µl 80, 80

The disadvantage was that the recovery time was extended to 10 minutes, indicating that the activated charcoal was adsorbing the CO_2.

5.9 Sensitivity

The sensitivity of the detection system depends on several parameters, the mass of the coating, the area of the coating and the

temperature.

Calculating the minimum detection limit from the data in Table 43 for a response of 136 Hz for 40 µl CO_2 at 6°C, gives 294 ppm (v/v).

The detection limit for a 10 µl injection at 4°C giving a response of 39Hz, is 256 ppm.The difference arises because the calibration graph is curved at the higher concentrations.

As was shown, the detection limit for long sample presentation was 208 ppm at room temperature, and studies at lower temperatures would be expected to improve this.

Chapter 6 Diethanolamine

6.1 Introduction

Diethanolamine was studied as a potential coating for CO_2 analysis as a comparison with triethanolamine. It was subsequently discovered that diethanolamine is a recognised absorbing material for CO_2 in manufacturing processes. (125, 126)

In solution, molecular ammonia and CO_2 react readily to form carbamic acid, which ionises immediately. A second molecule of ammonia neutralises the acid, giving ammonium and carbamate ions as the effective products. Primary and secondary amines, including the appropriate ethanolamines, and glycine and other amino-acids seem to react analagously to ammonia.

When CO_2 is absorbed in amine solutions, the chemical reaction which determines the rate of absorption, is that between CO_2 and amine. The reactions between CO_2 and OH^-, and CO_2 and H_2O are slow in comparison.

ie.

$$CO_2 + H_2O \longrightarrow HCO_3^- + H^+ \qquad (1)$$

Reaction 1 may be catalysed and the rate of absorption and the capacity of the amine thus increased. One catalyst used is potassium arsenite.

The reaction sequence for the absorption of CO_2 by diethanolamine is as follows:-

$$CO_2 + (C_2H_4OH)_2NH \underset{}{\overset{k_2}{\rightleftharpoons}} H^+ + (C_2H_4OH)_2NCOO^- \qquad (2)$$

where k_2 is the second order forward rate constant.

The carbamic acid will be almost totally ionised at the pH of the solution.

The hydrogen ion is neutralised by a second molecule of amine

in an instantaneous reaction.

$$(C_2H_4OH)_2NH + H^+ \longrightarrow (C_2H_4OH)_2NH_2^+ \qquad (3)$$

The overall reaction is therefore:-

$$2\,(C_2H_4OH)_2NH + CO_2 \longrightarrow (C_2H_4OH)_2NCOO^- + (C_2H_4OH)_2NH_2^+ \qquad (4)$$

Thus 2 moles amine react with 1 mole CO_2.

Other reactions also take place.

$$CO_2 + H_2O \longrightarrow HCO_3^- + H^+ \qquad (1)$$

$$CO_2 + OH^- \longrightarrow HCO_3^- \rightarrow CO_3^{2-} + H^+ \qquad (5)$$

The removal of the CO_2 by reaction processes 1 and 5 leads to partial reversal of reaction 2 , leading to hydrolysis of carbamate to amine and bicarbonate.

ie $H^+ + (C_2H_4OH)_2NCOO^- \longrightarrow (C_2H_4OH)_2NH + CO_2$

$CO_2 + H_2O \longrightarrow HCO_3^- + H^+$

The overall reaction is

$$(C_2H_4OH)_2NCOO^- + H_2O \longrightarrow (C_2H_4OH)_2NH + HCO_3^-$$

Similarly for the reaction between CO_2 and OH^-.

The absorption of CO_2 by solutions of amines is complicated by a phenomenon, apparently due to convection effects. (127) At short exposure times of amine to CO_2 , it would be expected that the concentration of free amine in the solution would be relatively unperturbed by the absorption process, and the reaction would be pseudo-first order. At longer exposure times the free amine near the surface

would become depleted, at even longer exposure times, the rate of absorption should be controlled by the diffusion of CO_2 and amine at the reaction zone. However, it is found that the reaction remains a pseudo-first order, regardless of the exposure time. It would seem that surface tension changes brought about by the reaction, produce an instability which gives rise to convection currents bringing fresh amine solution from the bulk to the surface. The enhancement caused by this effect is most noticeable with large concentrations of amine and high pressures of CO_2.

The diagram below represents this effect. (125)

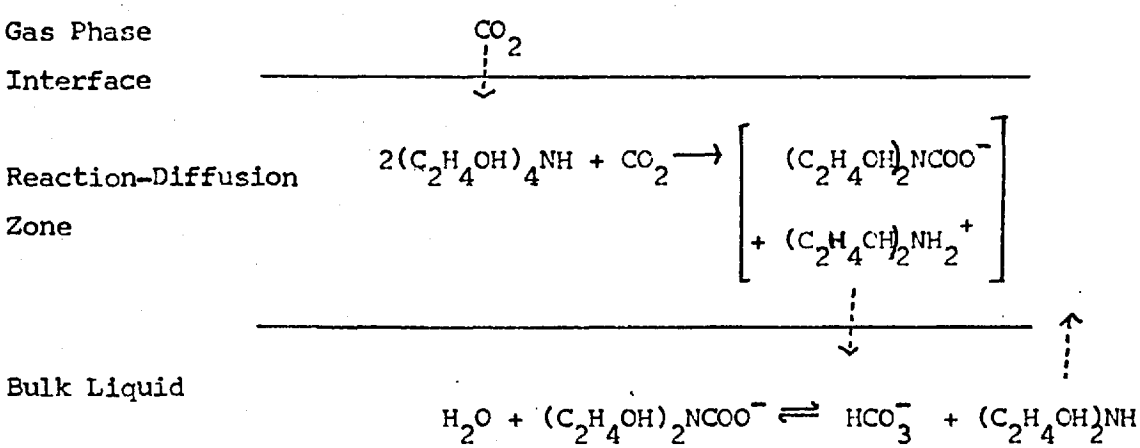

The amount of amine on a crystal is small, but the effect should favour long sample presentation to some extent.

6.2 Coating of the Crystal

The crystal is coated with 0.6 µl of a solution containing 28 µg/µl diethanolamine, or 0.4 µl of a solution with 42 µg/µl. The liquid drop is spread over the electrode area with the syringe needle, and allowed to evaporate in a warm place (eg. on top of the power pack.)

The coating formed a circular 'damp' looking deposit. Since the reaction occurs in solution the carrier gas was undried in order to provide trace quantities of moisture.

The coating formed a stable deposit, of which, the sensitivity was found to decrease rapidly over a few days.The crystals were either coated on one, or both electrodes, and the method was not found to be reproducible as was shown in chapter 3.

All the diethanolamine work was carried out using cell D.

6.3 Response of Diethanolamine to CO_2

The first results obtained for diethanolamine were very encouraging, although the response decreased with each injection.

a) Rapid Injections

A coated crystal was placed in the cell with a carrier gas flow rate of 12.5 cm^3/min, and allowed to stabilise. Successive 10 µl injections were made and the response was found to decrease. The crystal was left overnight with the carrier gas flowing, in order to further stabilise the coating. The following day the freqency change for the coating had decreased showing that some of the diethanolamine had evaporated.The crystal drift was more stable and a calibration graph was obtained. The results are given in Table 46 and the graph is given in Figure 55.

The response had decreased by a factor of 2 overnight. The response for the 10 µl injection falls off the line and this is probably owing to the use of a different syringe for this injection.

The crystal was again left overnight and the response checked the following day.

Table 46 The Response of Diethanolamine to Rapid Injections of CO_2

Day No.	Injection Size/µl	Response/Hz	ΔF_c/Hz
1	10	- 904	- 31626
	10	- 857	
	10	- 835	
	10	- 835	
	10	- 807	
2	10	- 414	- 14987
	10	- 457	
	10	- 446	
	10	- 456	
	5	- 230	
	5	- 218	
	5	- 226	
	3	- 137	
	3	- 128	
	3	- 131	
	8	- 315	
	8	- 293	
	8	- 307	
	8	- 297	
	6	- 219	
	6	- 230	
	6	- 218	
	6	- 219	
	9	- 308	
	9	- 295	
	1	- 56	
	1	- 37	
	1	- 42	
3	10	- 92	- 4079
	10	- 88	
	5	- 49	
	5	- 42	

The data in Table 46 is presented as it was obtained. The injections were not made in the order of their volumes for the following reason. By obtaining the responses for 10µl, 5µl and 3µl injections first, a better idea of the linearity of the calibration graph can be acquired. Starting with the lowest volumes, tends to produce a curved calibration graph owing to contamination of the coating.

Summarising the data, shows that the decrease in response is approximately proportional to the change in the frequency for the coating.

Table 47 Response versus the Frequency Change of Coating/Day

Frequency change on coating Hz	Day No.	Injection Size/µl	Response Hz
- 31626	1	10	- 835
- 14987	2	10	- 450
- 4079	3	10	- 90

The ratios of ΔF_c are 32 : 15 : 4 ,which is approximately 8 : 4 : 1
The ratios of the responses are 835 : 450 : 90 , which is approximately 9 : 5 : 1 .
The two sets of ratios show good agreement.

The experiment was repeated, with a crystal coated on both sides with 0.6 µl of the solution ie 16.8 µg/side.Again, on the first day of coating the response was found to fluctuate, and there was insufficient data for the second day of coating to plot a calibration graph. The coating frequency change between the two days was - 19837 Hz as compared with - 16639 Hz for the first crystal. A calibration graph for a third crystal, coated in the same way as the other two, was

obtained. This graph was similar to that for the first crystal and is shown in Figure 55B. The data for crystals 2 and 3 is given in Table 48.

Table 48 Response versus Frequency Change of Coating/Day

Crystal No.	Day No.	Injection Size/µl	Response/Hz	ΔF_c/Hz
2	1	10	- 807	- 37133
		10	-1036	
		10	- 935	
		10	- 852	
		10	- 859	
	2	5	- 240	- 17296
		5	- 232	
3	2	10	- 484	- 31607
		10	- 475	
		10	- 502	
		5	- 254	
		5	- 253	
		3	- 122	
		3	- 115	
		8	- 421	
		8	- 404	
		8	- 402	

The graph for crystal 3 is a straight line of gradient 0.7.

To determine the effect of coating the crystal on one side, a clean crystal was coated with 0.4 µl on one electrode. The responses obtained are given in Table 49. The room temperature was higher than usual (31.5°C) as it was in the middle of a heatwave. (The average room temperature was about 21°C.)

Figure 55 Calibration Graphs for CO_2 on Diethanolamine

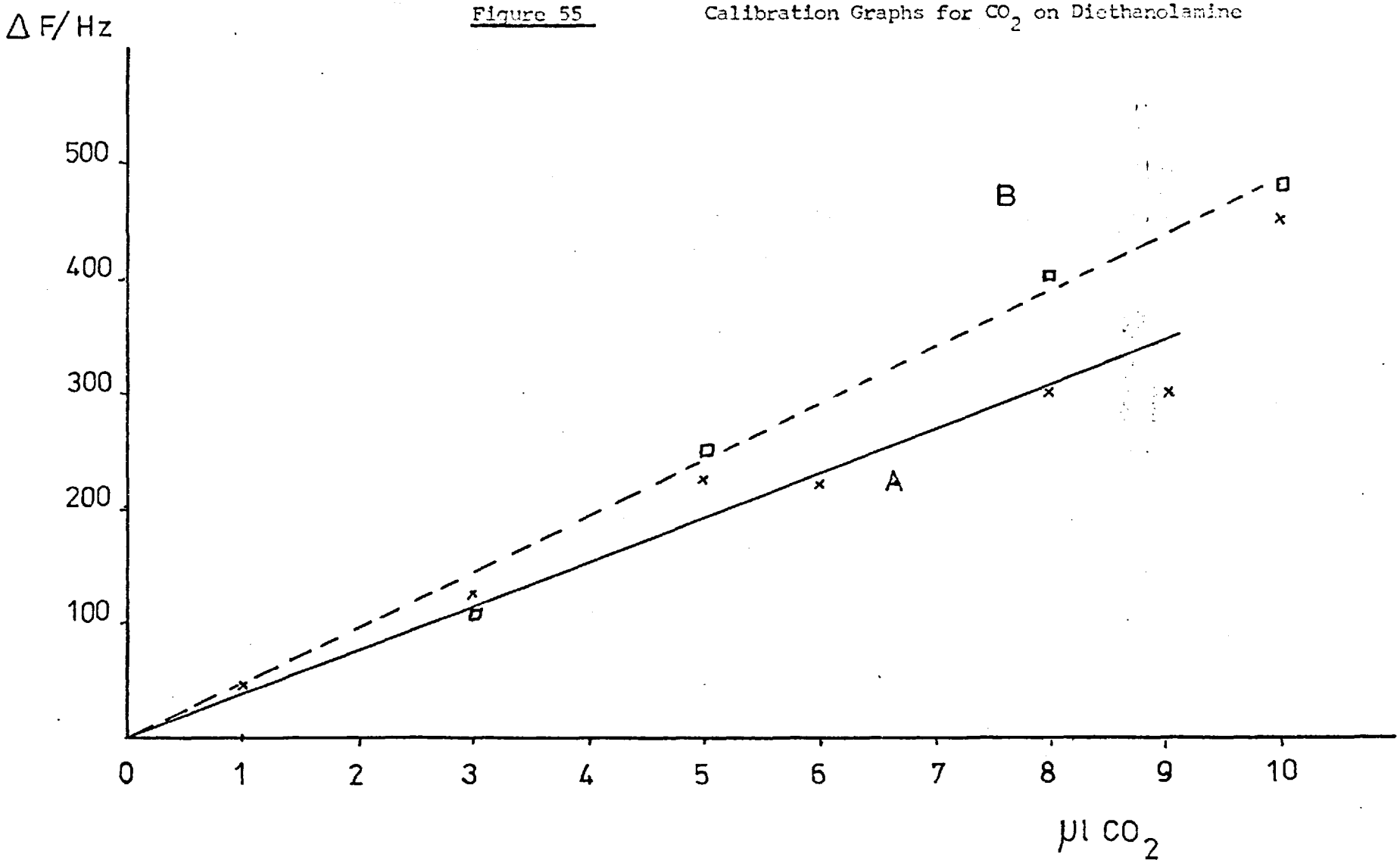

Table 49 The Response for a Crystal Coated on One Electrode

Injection Size /µl	Response/Hz	
10	- 221	ΔF_c = - 11808
10	- 300	Day 1 of coating
10	- 298	
20	- 544	
20	- 559	
30	- 720	
30	- 711	
50	- 937	
50	- 800	
50	- 923	
5	- 153	
5	- 165	

This graph is shown in Figure 56..

By comparing the response for 5 µl injections, it can be seen that, the crystal coated on one electrode on day 1, gave a lower response, than a crystal coated on both electrodes on day 2. Comparing the frequency change due to the coating, the crystal coated on both sides gave a response of - 225 Hz for a ΔF_c of 15000 Hz, and the crystal above gave a response of - 160 Hz for a ΔF_c of 11800 Hz. Allowing for the different masses of diethanolamine, it would seem reasonable that coating the crystal on both sides, approximately doubles its response, compared to that of a crystal coated on one side.

The detection limit calculated from the 10 µl response, for a mass of 16.8 µg diethanolamine on one electrode, is 33 ppm (v/v). For the crystal coated on both electrodes using the data for day 1, the detection limit is 12 ppm. This is a considerable improvement over the triethanolamine coated crystals.

Figure 56

Calibration Graph for Crystal Coated on One Electrode.

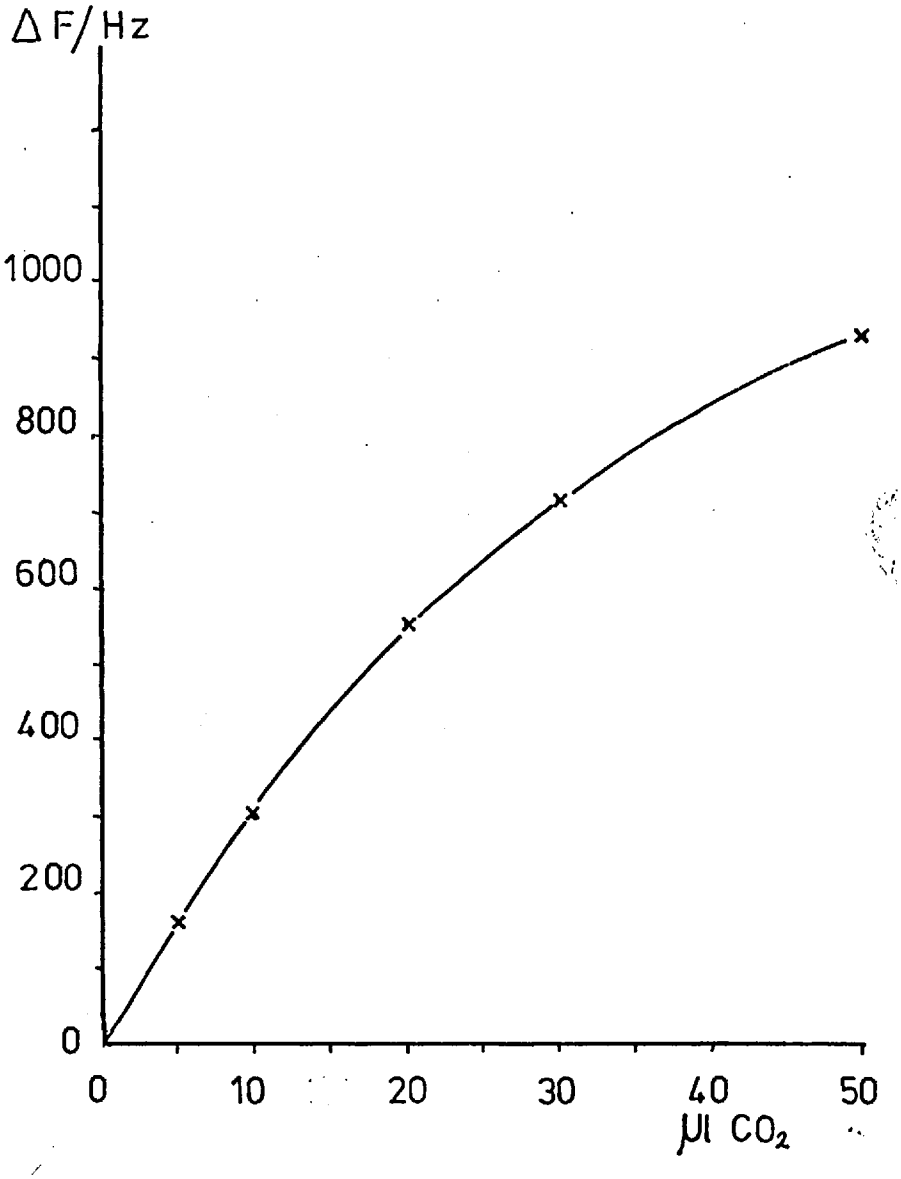

b) Long Sample Presentation

1) The Asbestos Plug Flowmeter

Similar problems were encountered with the asbestos plug flowmeter for diethanolamine as have been described for triethanolamine.

A crystal coated on both electrodes was subjected to a long sample presentation of a dilute gas solution. The solution was prepared in the aspirator bottle with 5 cm^3 CO_2 in 10 l nitrogen, and was passed into the carrier gas stream at a flow rate of 1.6 cm^3/min. This gave a concentration of CO_2 in the cell of 80 ppm. The overall response obtained was - 62 Hz.

The coating, as with the triethanolamine, began to recover before the sample presentation was stopped, and attempts to produce calibration graphs for the system were unsuccessful.

2) The Syringe Pump

A gas solution was prepared using the mercury levelling system. Between 1 and 4 cm^3 was diluted with 250 cm^3 nitrogen. 5 cm^3 aliquots were withdrawn using a syringe and injected into the carrier gas stream (12.5 cm^3/min). A straight line calibration graph was obtained which cut the ordinate at about 100 Hz. The graph is plotted in Figure 57A , from the data in the Table below.

Table 50 The Response of a Coated Crystal to CO_2 using Long Sample Presentation

cm^3 CO_2 in 250 cm^3 N_2	Concentration in cell/ppm	ΔF_c = - 18046 Response/Hz
1	213	- 221, - 173
2	426	- 242, - 154, - 288
3	639	- 374, - 325
4	852	- 480, - 416

Figure 57

Calibration Curves for CO_2 on Diethanolamine using Syringe Pump.

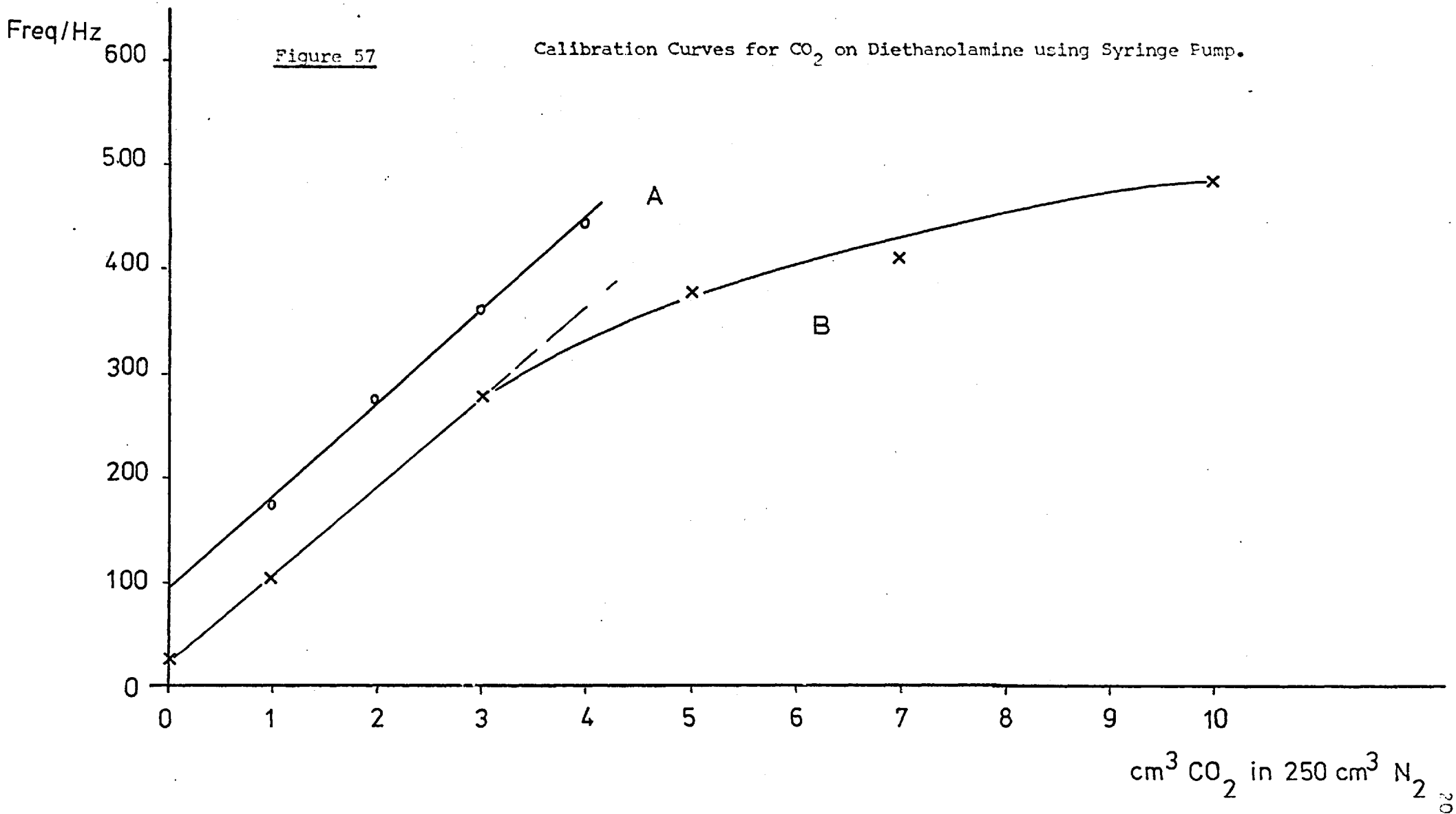

5 cm^3 nitrogen gave a response of - 79 Hz, and 5 cm^3 air gave - 80 Hz.

The responses were not very reproducible and decreased, which suggested that all of the CO_2 was not being desorbed. The low value of 154 Hz for the 2 cm^3 sample was probably due to an error.

The background level from the graph is 100 Hz which is very close to the values obtained for air and nitrogen. It is unlikely that the coating is responding to nitrogen, and thus the background must be due to either the mechanical shock of the injection to the system or to contamination occurring in the gas handling system. The air sample was withdrawn from the atmosphere and was undiluted. It is interesting to note that the response obtained was lower than that predicted from the calibration graph. Assuming the CO_2 concentration in the air is 315 ppm, the final concentration in the cell would be 17 ppm, and from the graph a response of 110 Hz would be expected. This would indicate that contamination was occurring, and is probably from the mercury vapour. This effect was noticed for triethanolamine where a background level corresponding to a frequency change of 17 Hz occurred. That the effect is more pronounced, is owing to the fact that not all of the gold electrodes were coated with diethanolamine, whereas they were with triethanolamine.

A repeat of the experiment gave the curved calibration graph shown in Figure 57B . The response has decreased since there is less diethanolamine on the crystal.

The detection limit, based on a corrected response of 54 Hz for a concentration of 213 ppm is 8 ppm. For the previous crystal with a corrected response of 100 Hz the detection limit is 4 ppm. Consequently it can be readily appreciated that each crystal needs to be calibrated prior to use as a detector.

Figure 58

Peak Profile for CO_2 on Diethanolamine using Asbestos Plug Flowmeter

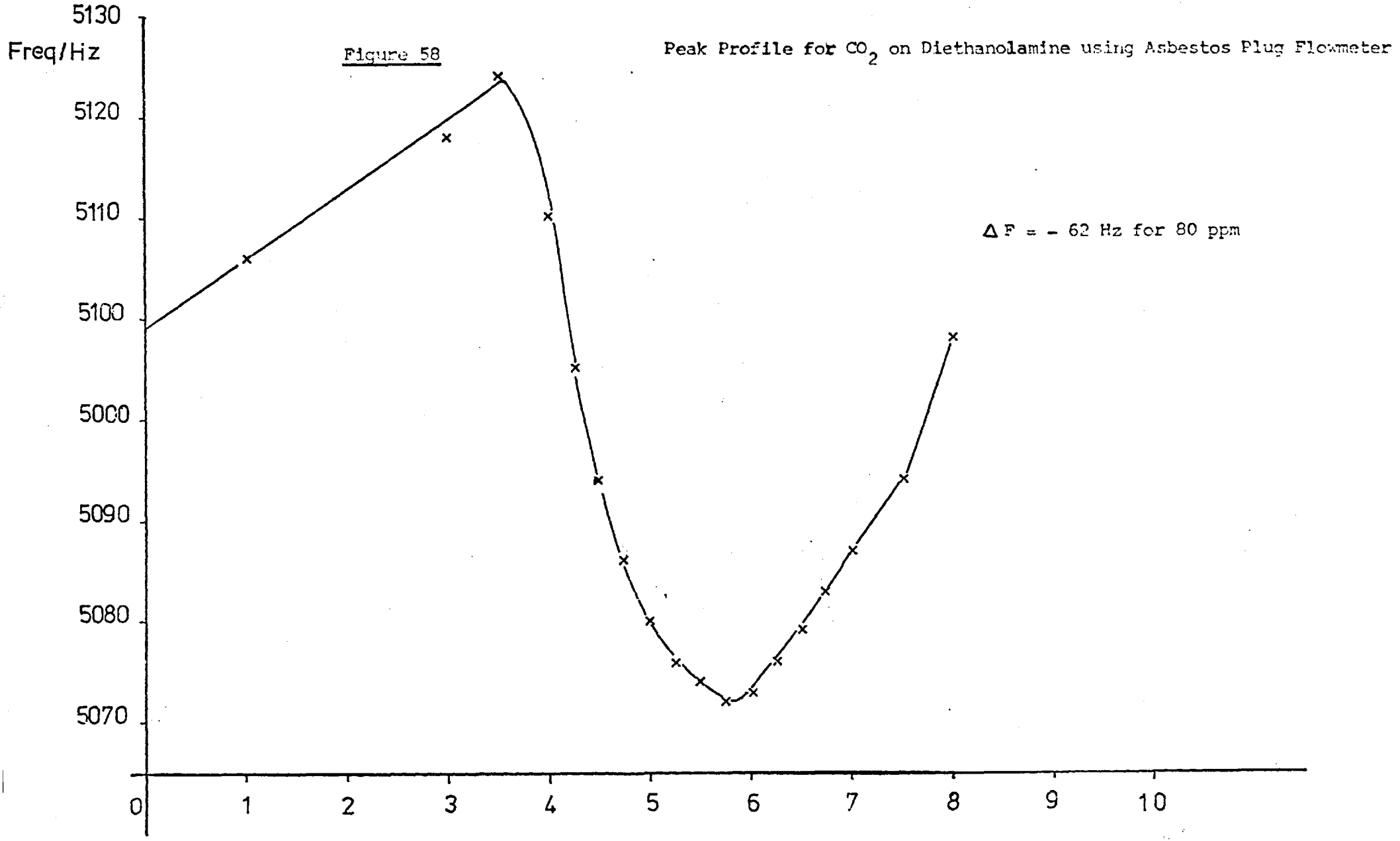

Table 51 Response of a Coated Crystal to CO_2 using Long Sample Presentation.

cm^3 CO_2 in 250 cm^3 N_2	Response/Hz	ΔF_c = - 10588 Hz
0	- 50, - 25	
1	-102, -106	
2	-281, -266	
3	-284, -272	
5	-379, -353	
7	-429, -388	
10	-483	

6.4 The Peak Profiles

a) Asbestos Plug Flowmeter

The response obtained for a long sample presentation of 80 ppm is shown in Figure 58 . The plot is characterised by a smooth frequency drop, which reaches the equilibrium and is then subject to a re-assertion of the drift pattern.Prior to cessation of the sample presentation,the frequency rises at a rate far greater than predicted by a consideration of the drift pattern,and would indicate that the CO_2 is being desorbed.The rate of desorption increases as the presentation is stopped.

b) Syringe Pump

The peak profiles for the data of Table 50 are plotted in Figure 59 , and are as expected. They consist of a 'U' shaped trough, showing sample absorption, equilibrium being reached , followed by CO_2 desorption. The nitrogen peak shows the effect due to the injection followed by re-establishment of the drift.

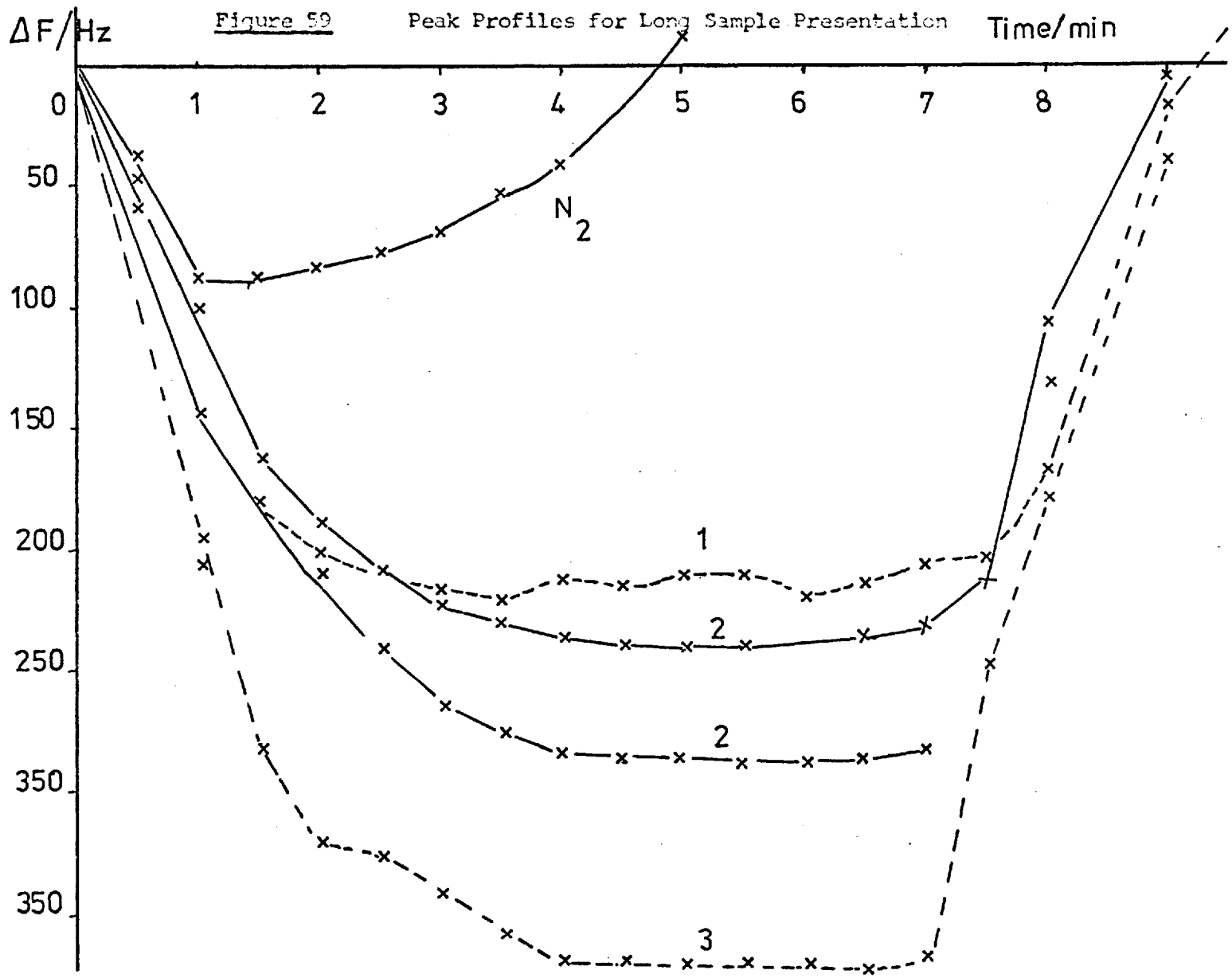

Figure 59 Peak Profiles for Long Sample Presentation

The inflexion peaks which were noticed in the triethanolamine study are missing, and this is probably due to the fact that more dilute gas samples were used for diethanolamine. It was previously suggested that the sample front was becoming diluted in the cell and that the coating was equilibrating with that concentration; as more sample reached the cell, the concentration would become constant and the main equilibration would occur. If a dilute sample is presented, the initial sample front may produce a concentration in the cell which is below the detection limit.

c) Rapid Injections

The profiles are very similar to those obtained for triethanolamine, with a rapid decrease followed by an increase as the CO_2 is desorbed. The degree of tailing is more pronounced, with the recovery time taking about 5 minutes. This would indicate that the diethanolamine-CO_2 reaction is more favourable than the corresponding triethanolamine-CO_2 reaction, which is to be expected considering the chemical reaction which occurs.

The peak profiles for the data of Table 46 are shown in Figure 60.

6.5 The Lifetime of the Coating

Although the diethanolamine gave greatly improved sensitivity towards CO_2 as compared with triethanolamine, there was one main disadvantage. The coating evaporated from the crystal within a few days and the sensitivity decreased daily. With some crystals, this effect was so pronounced that it was impossible to obtain a calibration graph.

An investigation was carried out to determine the lifetime of a diethanolamine coated crystal. Calibration graphs were plotted on

Figure 60 Peak Profiles for Rapid Injections of CO_2

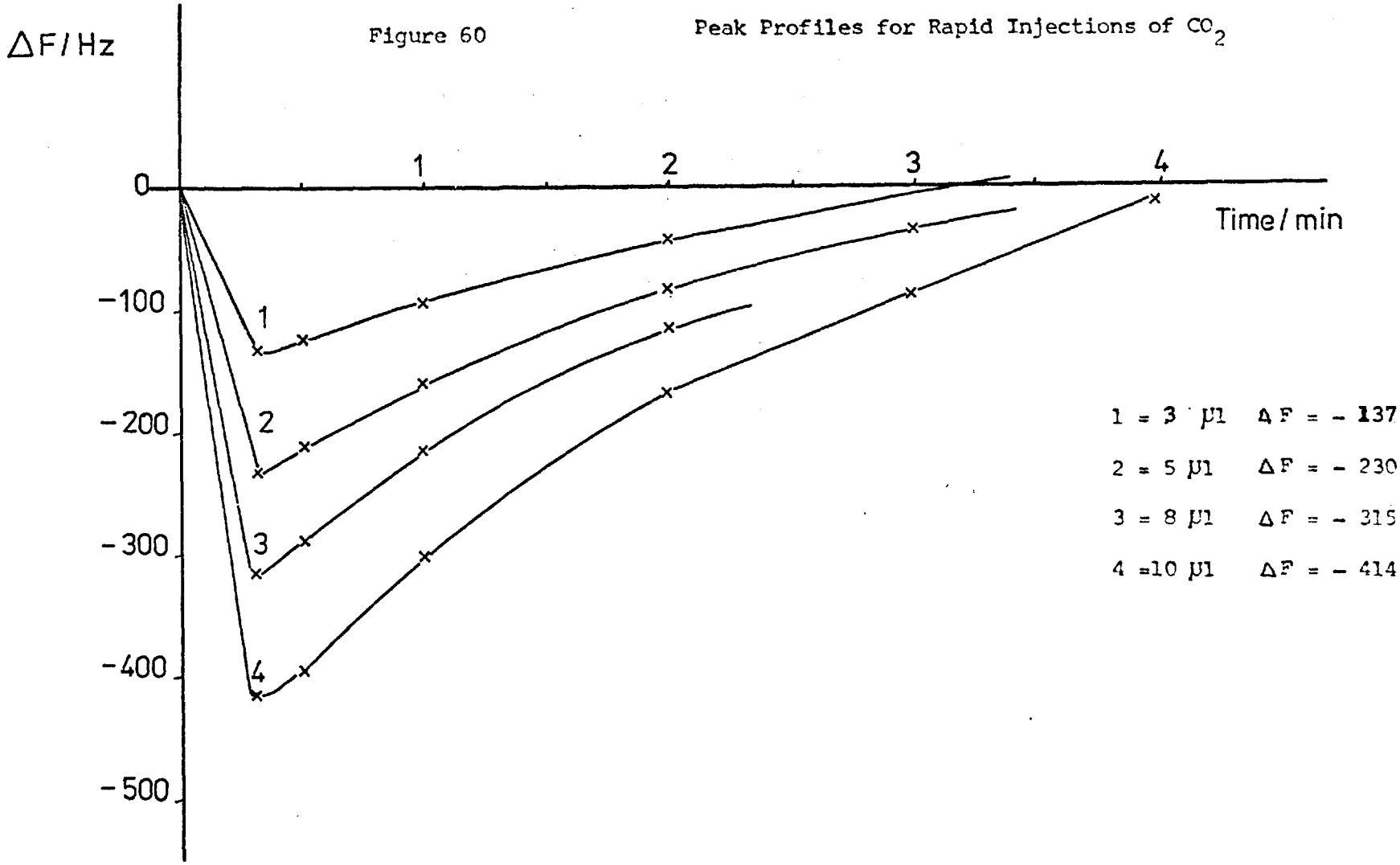

successive days for a crystal coated on both electrodes.

The responses are shown in Table 52.

Table 52

Lifetime of Crystal No. of days coated	Injection Size/Ul	Response/Hz	ΔF_c/Hz
1	10	- 646	- 38254
	10	- 594	
	10	- 594	
	10	- 544	
2	10	- 484	- 31607
	10	- 475	
	10	- 502	
	5	- 254	
	5	- 253	
	3	- 122	
	3	- 115	
	8	- 404	
	8	- 402	
3	10	- 381	- 22433
	10	- 392	
	10	- 405	
	5	- 232	
	5	- 199	
	5	- 199	
	5	- 181	
	3	- 130	
	3	- 128	
	8	- 315	
	8	- 315	
	1	- 56	
	1	- 53	
	10 N_2	- 2	
4	5	- 151	- 15220
	5	- 160	
	5	- 146	
	3	- 95	
	3	- 87	

Table 52 Continued

Day	Injection Size µl	Response/Hz
4	8	- 236
	8	- 230
	8	- 218
	10	- 271
	10	- 267
	10	- 262
	1	- 32
	1	- 29
	1	- 28

These graphs are given in Figure 61 . The calibration graphs for days 3 and 4 are straight lines. The plot for day 2 is a straight line for the 5, 8, and 10 µl injections, but the 3 µl injection response is off the line.

The fall in sensitivity is shown in Figure 62 , where the response is plotted against the lifetime of the crystal.The responses for each sample size are plotted separately and they fall on straight lines, which is as expected since the mass of the coating is decreasing from day to day, the amount being,about 7000 Hz/day. The lines cut the abcissa after 6 days.

6.6 The Precision of the Coating

The precision of the coating tends to vary from one coating to another, some being very good, and others giving a wide range of responses.

The responses for a series of replicate 10 µl injections are given in Table 53. Injections 1 - 10 were made with a 0 - 100µl syringe,

Figure 61 Calibration Graphs for CO_2 on Successive Days

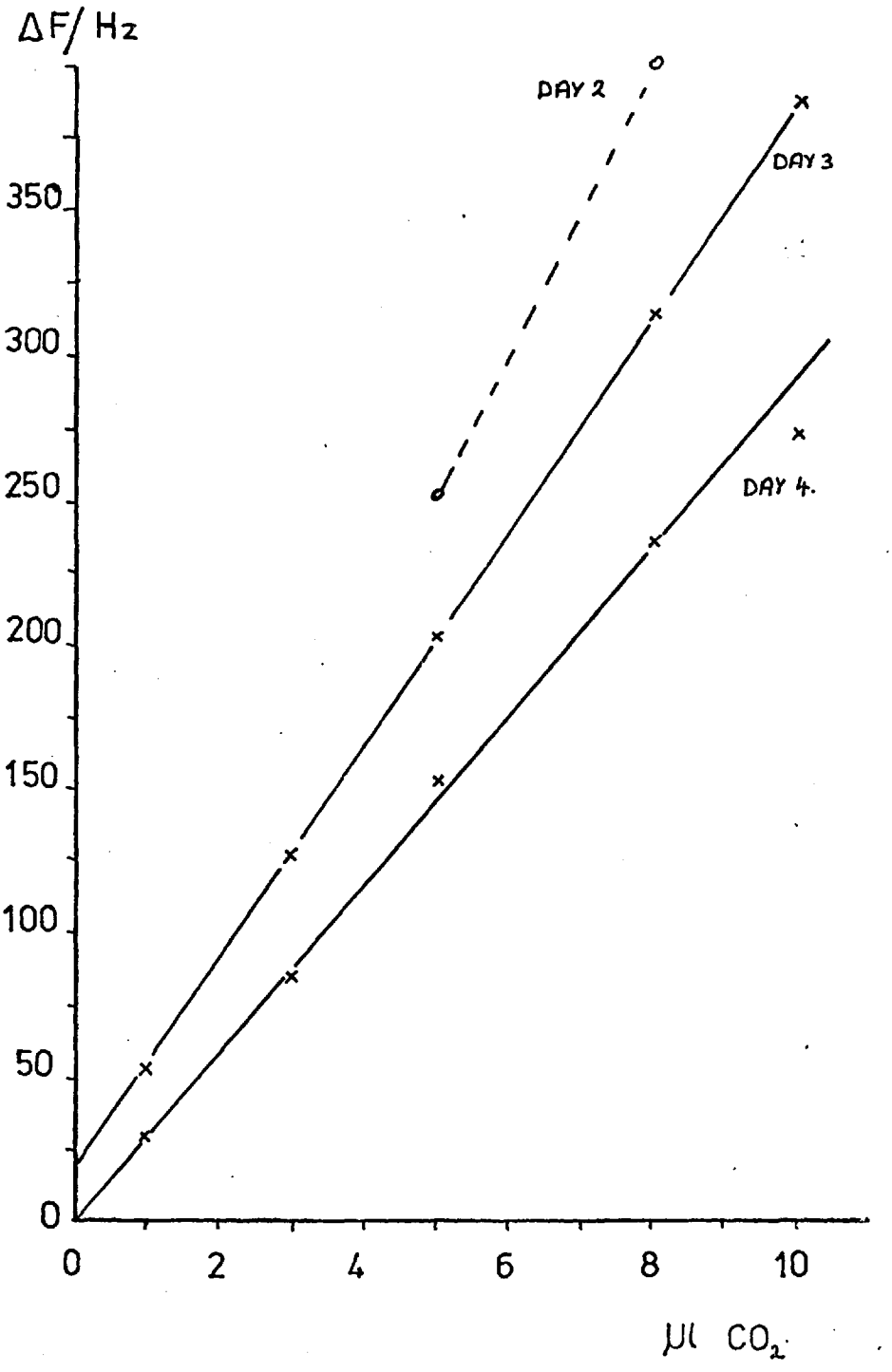

and injections 11 - 16 with a 0 - 30 µl syringe. The error between the two syringes accounts for the 10 µl value falling off the line in Figure 55 . The two syringes were not used in the same calibration graphs, the 0 - 100 µl syringe being used for that range, and the 0 - 30 µl syringe for the 0 - 10 µl range.

Table 53 Precision of the Coating for Successive 10 µl Injections

Injection No.	Response/Hz	ΔF_c = - 31607 Hz
1	- 262	
2	- 620	
3	- 634	
4	- 635	
5	- 535	
6	- 665	
7	- 644	
8	- 663	
9	- 647	
10	- 612	
11	- 381	
12	- 484	
13	- 275	
14	- 371	
15	- 475	
16	- 502	

It was noticed that injection 1 for a particular day was always lower than the rest, and it would appear that the coating needs 'priming' before a calibration is made.

The average value for injections 2 - 10 is 640 $\pm$ 34.8 Hz and for 11 - 16 it is 414 $\pm$ 80.2 Hz. It is, therefore, apparent that the 0 - 100 µl syringe could be filled more reproducibly than the 0 - 30 µl syringe and could be injected in a more reproducible manner, since the plunger had less distance to travel. This is an additional

Figure 62

Fall in Sensitivity of Diethanolamine Coating with Time

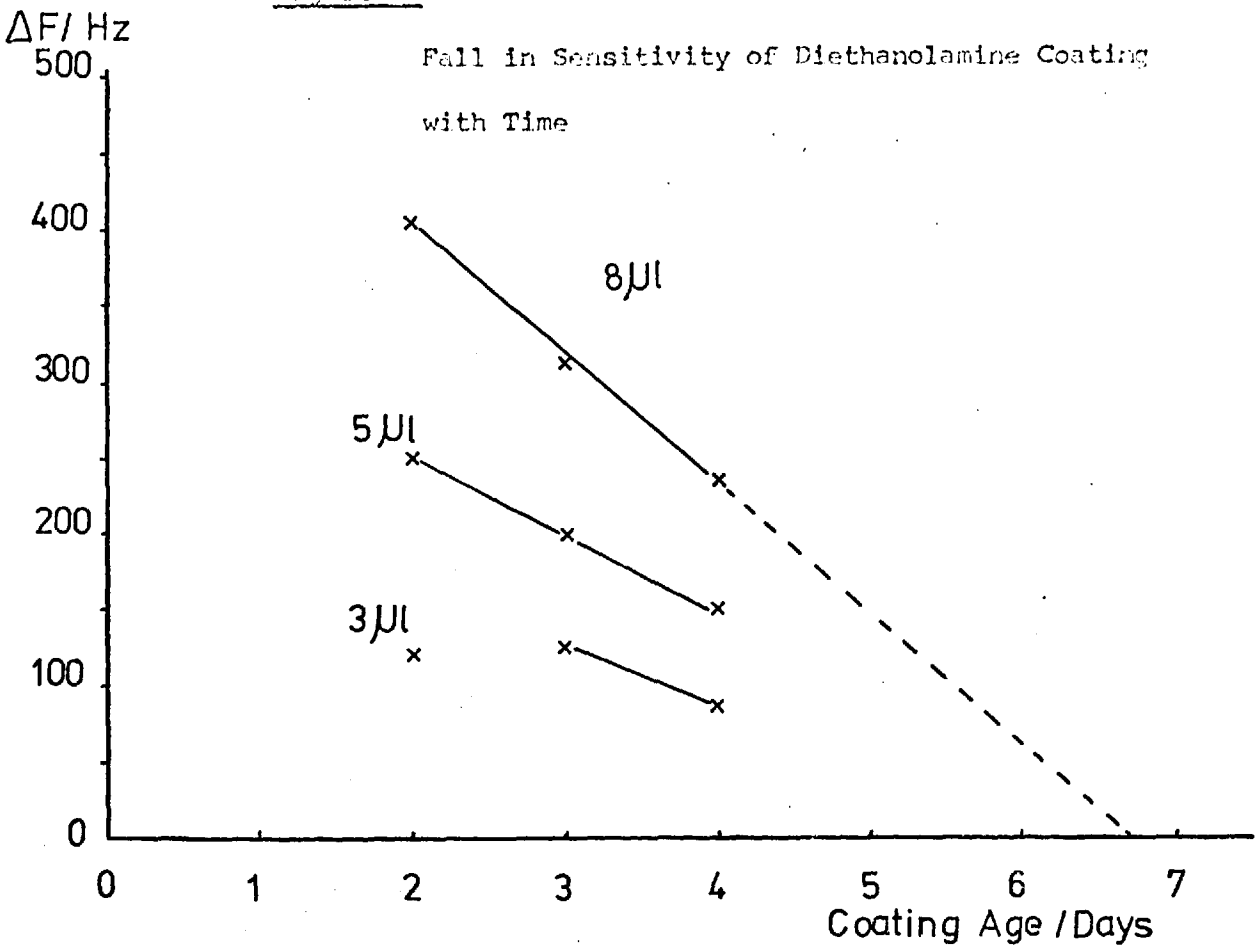

Figure 63

Response for 10 µl Injections versus Frequency Change on Coating

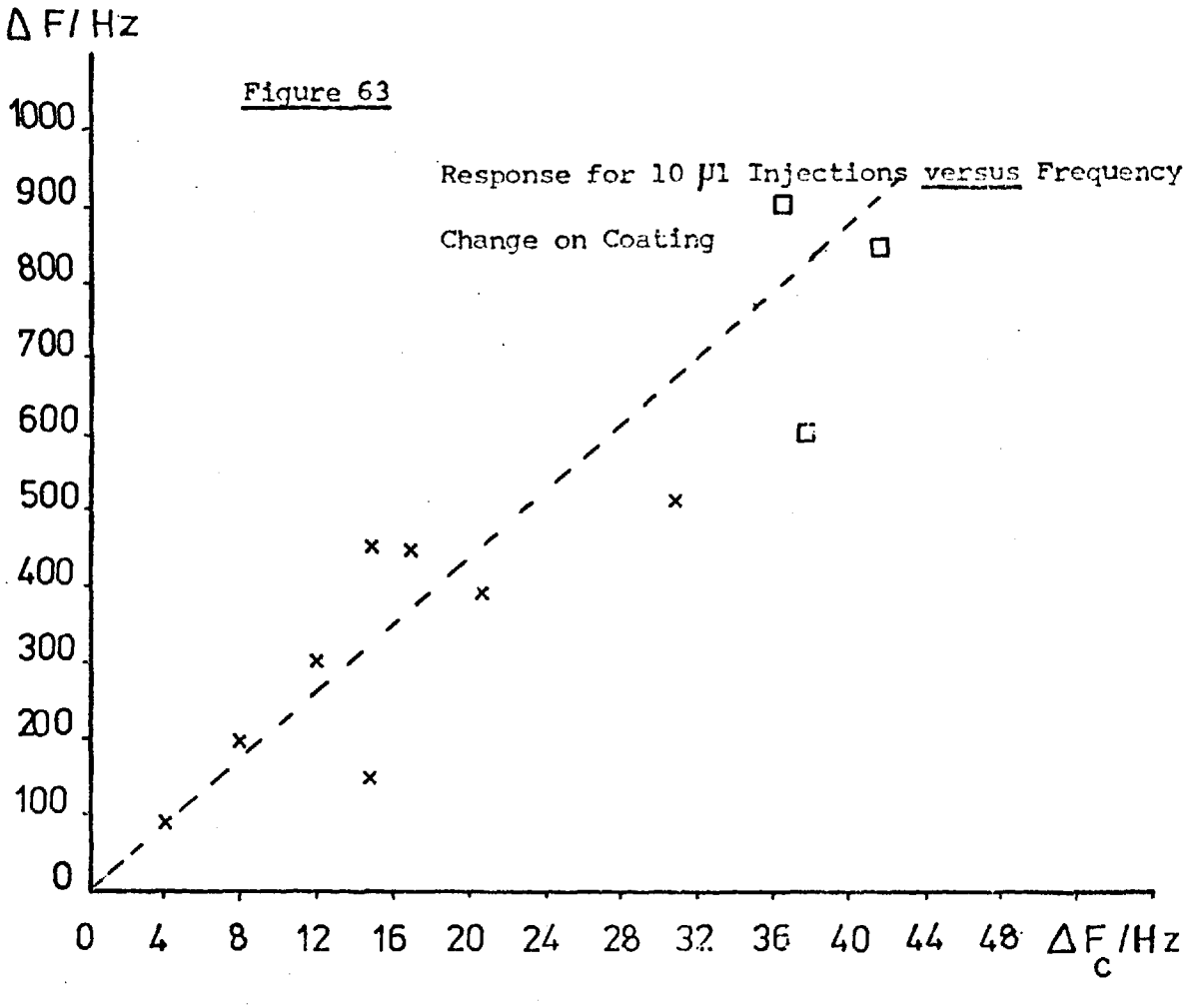

source of error.

6.7 The Relationship between the Response and the Frequency Change on Coating

A plot for the response of 10 µl injections of CO_2 against the frequency change on coating is shown in Figure 63.

The response for an injection on the first day of coating is represented as a square (□), and for subsequent days as a cross (×). The graph obtained is a straight line, and was constructed from results for several different crystals coated on both electrodes. The points are dispersed around the line because the area of the coating could not be kept constant. It can be seen that there is a linear relationship between the response and the amount of diethanolamine, as represented by the frequency change on coating.

6.8 The Relationship between the Response and the Temperature

Calibration curves for a crystal coated on one electrode, at temperatures of 31.5°C (room temperature) and 2.2°C (ice bath), were plotted for injections of 0 - 50 µl CO_2

The responses obtained were opposite to those found for triethanolamine. The triethanolamine - CO_2 complex was more stable at 0°C than at room temperature, whereas for diethanolamine the reverse was true.

The data for the calibration graphs of Figure 64 are given in Table 54.

There are several points to be mentioned which relate to these graphs.

1) The first injection for the temperature of 31.5°C is lower than subsequent responses. This is an effect which has been mentioned

Table 54 Relationship between Response and Temperature

Injection Size/µl	Response/Hz	Temp./°C	ΔF_c = - 11808 Hz
10	- 97	31.5	
10	- 221		
10	- 300		
10	- 298		
20	- 544		
20	- 559		
30	- 720		
30	- 711		
50	- 937		
50	- 923		
5	- 153		
5	- 165		
10	- 274	2.3	
10	- 245		
10	- 244		
20	- 393		
30	- 426		
50	- 505		
5	- 35		

Figure 64

Effect of Temperature on the Response

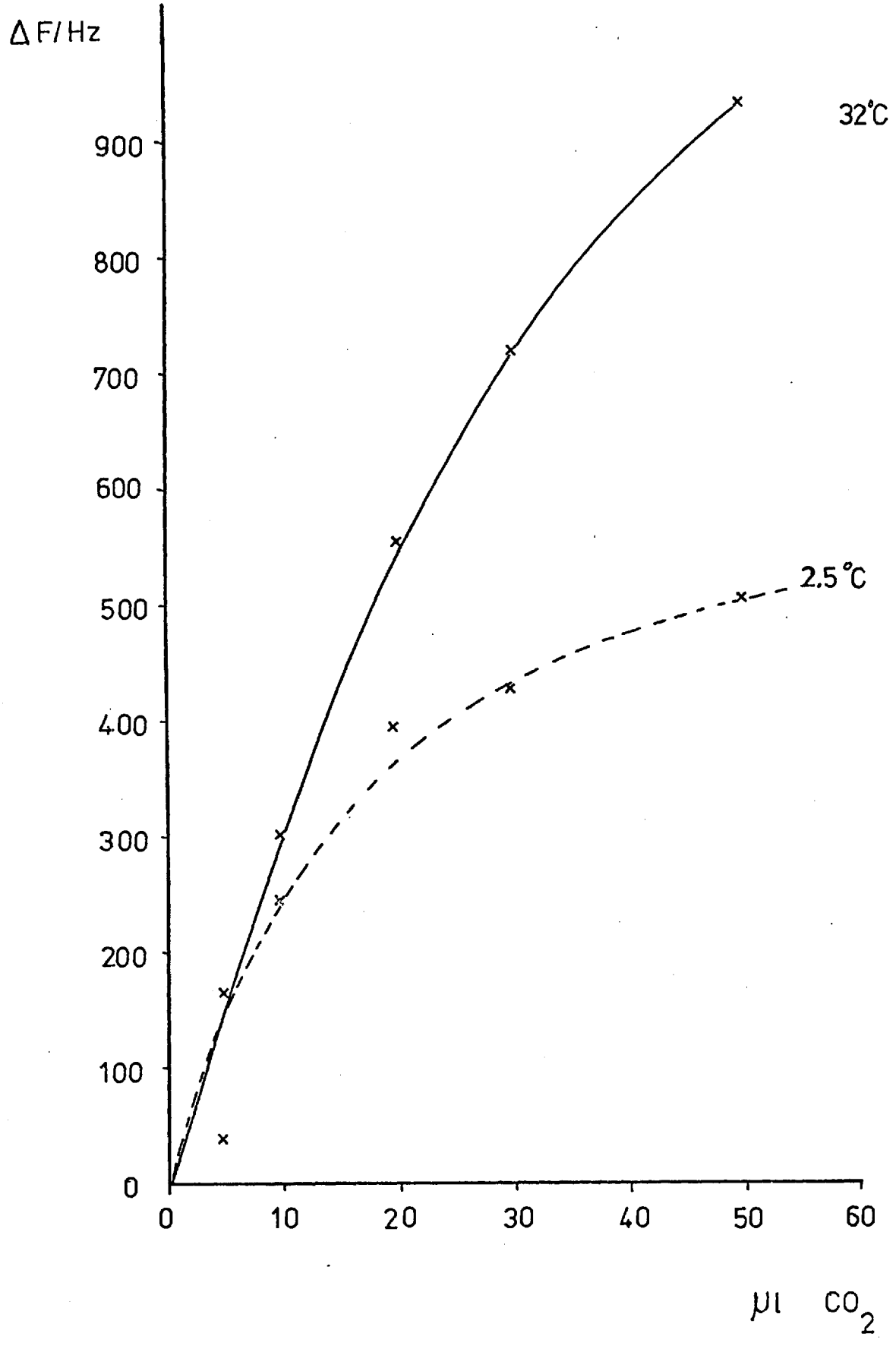

before.

2) The time to attain the maximum frequency change from the start of the injection was 20s at a temperature of 31.5°C, and 30s at 2.3°C.

3) The recovery time at 31.5°C was 3 min for a 10 µl injection and 5 min for a 20 µl injection. At 2.3°C the recovery time for a 10 µl injection was 30 min and it was for this reason that only one measurement was taken for each sample size.

4) The calibration graph at the lower temperature is more curved, possibly owing to contamination from CO_2 remaining on the coating.

From this it can be concluded that at lower temperatures, the forward reaction is slower, ie CO_2 reacting with diethanolamine,and that the backward reaction, the desorption of CO_2, is considerably slower. This would indicate a more stable reaction product.There is a competing effect which enhances the reaction at higher temperatures. The melting point of diethanolamine is 28°C, so that at 31°C it is a liquid and a solid at 2°C. As a liquid, the dissolution of CO_2 will be favoured.

6.9 Effect of Flow Rate on the Response

A crystal, coated on one electrode, was calibrated at different flow rates using rapid injections.

The data is given in Table 55 and plotted in Figure 65. The expected result is that the response should decrease with increased flow rate, owing to the decreased residence time of the sample in the cell. This is found for flow rates of 25, 50, and 75 cm^3/min. The 10 cm^3/min flow rate gives a lower response, probably because of dilution of the sample occurring in the carrier gas before the cell. The flow rate through the cell (D) is half the above rates, because the carrier gas is split into two, for the reference and sample cells.

Table 55 The Effect of Flow Rate on the Response

ΔF_c = - 12000 Hz

Flow Rate cm^3/min	Injection Size µl	Response Hz
25	10	- 453, - 442
	5	- 226, - 214
	20	- 726, - 696
	30	- 933, - 933
	50	-1137, -1130
10	5	- 205
	10	- 467, - 440
	20	- 706, - 681
	30	- 838, - 830
	50	-1014, - 996
50	5	- 124
	10	- 254, - 278
	20	- 455, - 437
	30	- 582, - 566
	50	- 745, - 754
75	5	- 101
	10	- 212, - 196
	20	- 342, - 341
	30	- 435, - 427
	50	- 602, - 610

Figure 65 Effect of Flow Rate on the Response

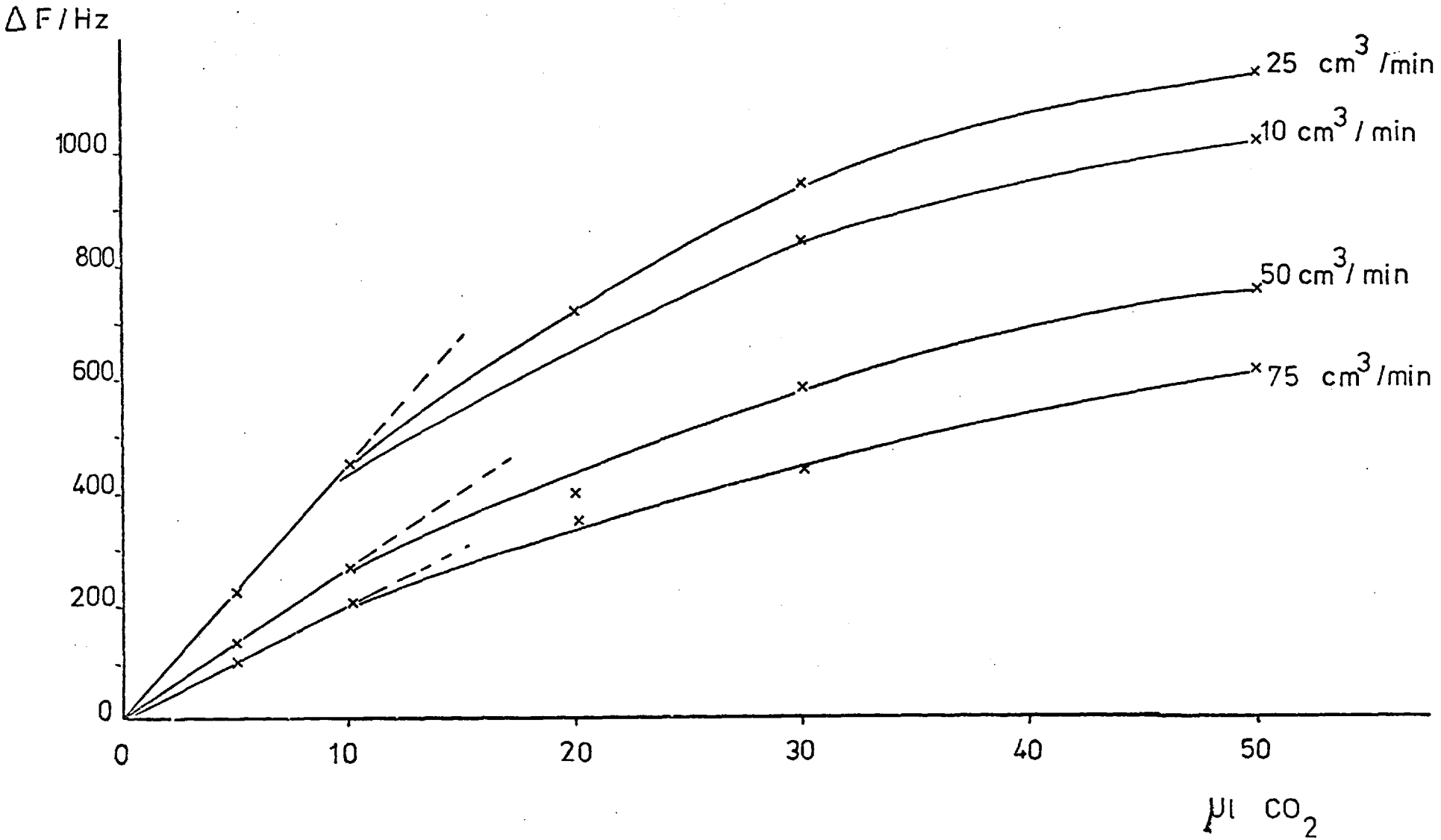

The optimum flow rate through the cell is 10 - 12 cm^3/min.

6.10 Sensitivity

As has been shown, the sensitivity of a crystal coated with diethanolamine depends on the mass and the area of the coating, the flow rate of the sample and the temperature.

A detection limit below 10 ppm was obtained for long sample presentation using the syringe pump, and for rapid injections the limit was 12 ppm. If all the conditions are optimised it should be possible to reduce this by a factor of 10.

Chapter 7 Mercuric Oxide

7.1 Introduction

In view of the results obtained for the reaction of CO with iodine pentoxide and the lack of any suitable coating material for the direct analysis of CO, an attempt was made to detect the gas by its conversion to CO_2.

The reaction used was that between CO and hot mercuric oxide.

$$CO + HgO \longrightarrow Hg + CO_2$$

The principle of mercury replacement has been used in several ways to provide a sensitive means of detecting CO in air. McCullough et al analysed the reaction extensively in an attempt to find a more accurate and less tedious method than the iodine pentoxide reaction.(128) The analysis was made, in one case, by measuring the weight change of a tube filled with mercuric oxide (HgO) as CO was passed through it, and the other caused the air carrying the liberated mercury to impinge directly on a selenium sulphide paper - the intensity of the blackening as measured by photometry, of the exposed paper being proportional to the mercury concentration. Seiler and Junge (.4) analysed the liberated mercury vapour by absorption at the 2537 Å line in an optical cell. Emission at this wavelength has also been used.(16). Palanos utilised flameless atomic absorption at 2573 Å for measuring the mercury vapour. He reported a sensitivity of less than 0.5 ppm and a range of upto 20 ppm (17).

The reduction of HgO to metallic mercury can be performed through a number of heterogeneous reactions. Gaseous reductants include CO, hydrogen and hydrocarbons.

The possible reaction pathways are:-

$$CO + HgO \longrightarrow CO_2 + Hg$$

$$H_2 + HgO \longrightarrow H_2O + Hg$$

$$CH_4 + 4\,HgO \longrightarrow CO_2 + 4Hg + 2\,H_2O$$

$$C_2H_4 + 6\,HgO \longrightarrow 2CO_2 + 6Hg + 2\,H_2O$$

$$C_2H_2 + 5\,HgO \longrightarrow 2CO_2 + 5Hg + H_2O$$

Although hydrocarbons usually occur at combined levels well below that of CO in the atmosphere, interferences can occur to give higher values of CO. However, the main interferent is hydrogen. Hydrocarbons can be removed from the sample by selective filters.

The other main reaction occurring, is the thermal decomposition of HgO to give a background level of mercury.

ie $2\,HgO \longrightarrow 2Hg + O_2$

McCullough et al (129) showed that the reaction of HgO with CO is favourable thermodynamically, and quoted the following free-energy equations.

$$HgO + CO \longrightarrow Hg + CO_2 \qquad \Delta H_{298} = -47.5 \text{ kcal.}$$

$$\Delta H_{473} = -50.0 \text{ kcal.}$$

Yellow HgO is active towards CO, but is unstable and without definite physical properties eg. the dissociation pressure is higher than the red form and decreases with time. The red form has a definite dissociation pressure-temperature relationship.

Workers have found that there are several conditions to be observed to ensure accuracy for the reaction.

1) Although moisture does not interfere with the reaction, it is adsorbed by HgO, even at 200°C, and will cause slight errors. Drying tubes of calcium chloride and magnesium perchlorate were found to be satisfactory.(129)
2) The reactor temperature should be regulated to control the background mercury level.(17) It should also be kept as low as possible.
3) A non-porous pellet of HgO should be used.(17)The pellet should be large enough to minimise the rate of change of surface area with consumption.

The experimental system for the HgO reduction has already been described and consisted of the reaction furnace, a crystal in cell E to detect the liberated mercury, and a crystal in cell D to detect the released CO_2.

The first attempt was made with powdered red HgO held in the reaction tube with glass wool, but the powder blocked the tube causing a pressure build-up. Pellets of HgO (B.D.H.,Poole) were formed and placed in the tube. The pellets were fractionally smaller than the diameter of the tube so that the carrier gas was forced around them. The pellets were approximately 6 mm in length, and the total weight of HgO was 1.7g. The temperature in the reaction furnace was 200°C.

The crystal in cell E, was a clean crystal with gold electrodes. The mercury in the gas stream amalgamated with the gold, giving rise to a frequency change. The crystal in cell D was coated, initially, on both electrodes with 0.4 µl diethanolamine solution. In later work only one of the electrodes was coated.

The main problem encountered, was one of severe drift for

the crystal in cell E, caused by irregularities in the mercury background levels. This was caused by mercury condensing in the tubing immediately after the reaction furnace, which was overcome by reducing the length of the tubing between the reaction tube and the cell to a minimum.Another cause of the drift was the temperature of the carrier gas which slowly heated the cell. Consequently limited studies were made using the mercury vapour analysing crystal, and the majority of the work was concentrated on analysing for CO_2. Cell D was placed 40 cm away from the reaction furnace to ensure that most of the mercury had condensed out of the vapour prior to the cell.

7.2 Calibration of the System

A calibration curve was obtained for the mercury vapour concentration due to CO.

The gas flow through the system was 250 cm^3/min at a pressure of 4.2×10^4 N/m^2. The gas was dried through silica gel and calcium chloride. The frequency of the crystal was drifting in a positive direction, caused by the temperature effect of the carrier gas overcoming the frequency drop due to mercury deposition. The crystal was stable with the drift at + 2Hz/min.

The CO was presented as discrete samples by injecting it through a rubber septum immediately before the furnace.

The results are given in Table 56. The responses were initially reproducible, but throughout the course of the experiment, the response was increasing. This could be caused by a 'priming' action of the HgO by the first samples, or to a sample 'hold-up' somewhere in the furnace. The system was left to stabilise for 2 hours and the experiment repeated.This data is included in Table 56.

Table 56 Response of Crystal to Mercury Vapour

Injection Size µl CO	Response/Hz
10	-41, -41, -44
20	-66, -66, -73
30	-93, -93, -95
50	-267, -360, -267, -291
40	-301
20	-105
After 2 hr	
10	-30, -25, -28
20	-48, -65, -56, -60
30	-77, -76
50	-135, -156, -125, -150, -156
20	-57, -63

The response obtained for the second series of injections are more consistent and reproducible as shown by the last two injections of 20 µl, agreeing with those previously made.

A calibration graph is plotted in Figure 66. A straight line of gradient 1.4 is obtained. The sensitivity is 357 ppm if the total concentration of CO which is possible in the cell is considered. Dilution of the sample must occur throughout the reaction furnace and in the carrier gas line prior to the cell, and therefore, although this is the overall sensitivity, that of the crystal is lower.

The response of the crystal became erratic after some time, owing to the mercury amalgam occupying a greater area than the available gold.

The experiment was repeated with a clean crystal and successive

Figure 66 Calibration Graph for CO over HgO

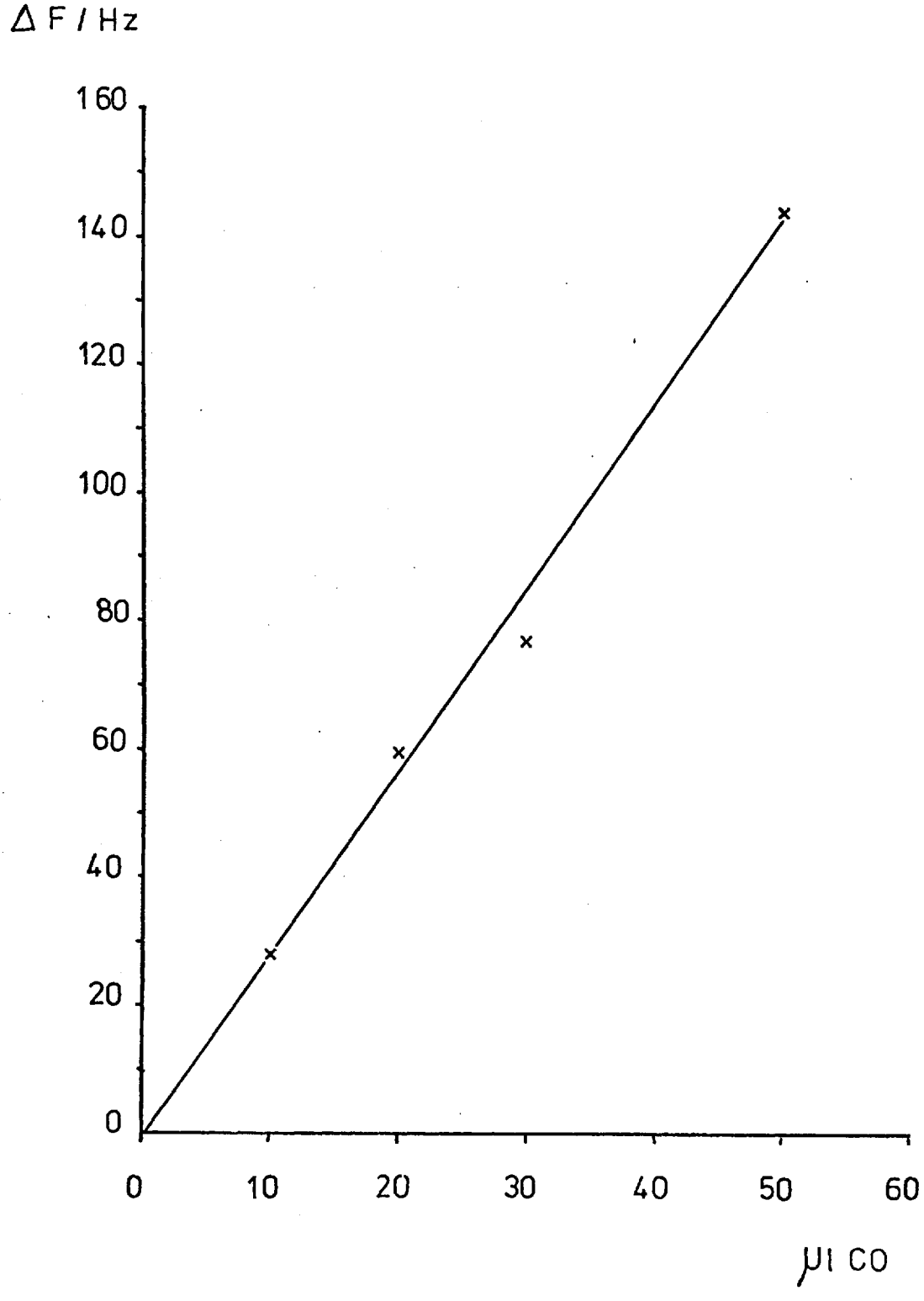

injections were made to determine the precision of the response.

Table 57 Precision of the Response for Mercury Vapour

Injection No.	Injection Size/µl	Response/Hz
1	20	- 214
2	20	- 255
3	20	- 261
4	20	- 273
5	20	- 228
6	20	- 236
7	20	- 162
8	20	- 135
9	20	- 199
10	20	- 151
11	10	- 34
12	10	- 36
13	10	- 29
14	30	- 202
15	30	- 209
16	40	- 345
17	40	- 443
18	40	- 478
19	40	- 499
20	10	- 65
21	10	- 30
22	10	- 35

As can be seen, the response for a few samples are reproducible, eg. injections 1 - 6, and 7 - 10. The responses for the 10 µl injections

are reproducible during the course of the experiment, but for the 40 µl injections there is an increase in the response. This suggests that the reaction is most favourable at lower concentrations and it could be a surface area effect of the HgO.

In order to overcome the problems associated with the mercury vapour detection, a calibration graph based on the detection of CO_2 with a diethanolamine coated crystal was constructed.

The flow rate was reduced to 25 cm^3/min and the pressure to 1.4×10^4 N/m^2. The furnace temperature was 183°C. The drift of the coated crystal was acceptable under these conditions.The results for the injections of CO are given in Table 58.

Table 58 Response of Coated Crystal to Liberated CO_2

Injection Size µl CO	Response/Hz	ΔF_c = - 9370 Hz One electrode coated
10	- 102, - 129, - 134	
20	- 190, - 188	
30	- 221, - 220	
50	- 259, - 258	
5	- 84, - 92	

The graph is given in Figure 67B.

A comparison of these results with those obtained for the mercury vapour analysing crystal shows a marked improvement. For 10 µl CO a response of - 130 Hz is obtained as compared with - 17 Hz previously.

The sensitivity based on the maximum concentration in the cell is 77 ppm, for a 10 µl injection, and 56 ppm for a 5 µl injection.

Figure 67 Calibration Graph of CO

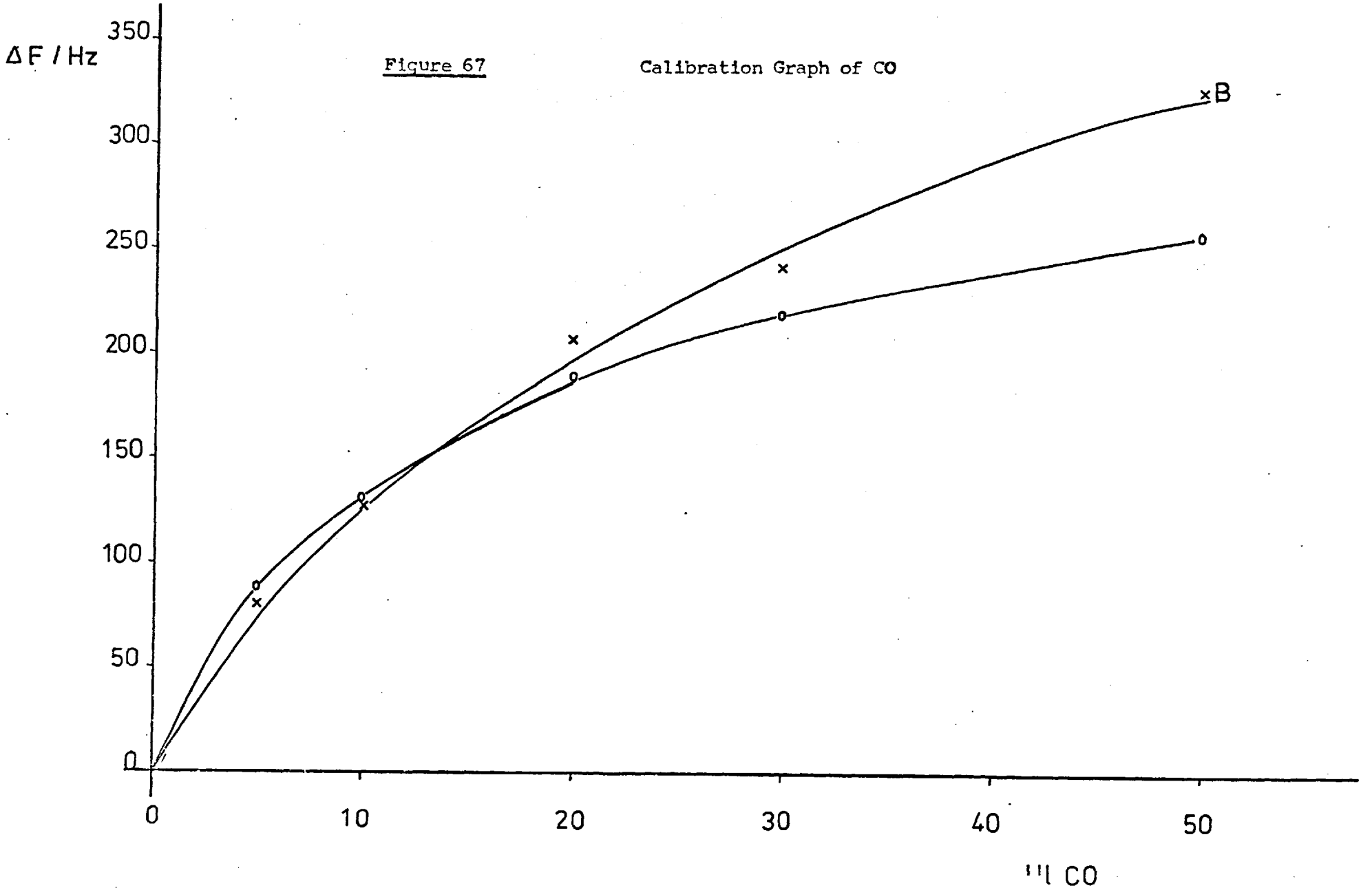

The difference in sensitivity arises because of the curving of the calibration graph.

7.3 Peak Profiles

7.3.1 Mercury Peak

The peaks for the data in Table 56 are plotted in Figures 68 and 69.

Figure 68 shows successive injections and responses. The baseline drift is worsening during the experiment as is shown by the gradient becoming steeper. The crystal is acting in an integrating mode, since the gold - mercury amalgam is not reversible.

Figure 69 shows the peak profiles in relation to each other. There is a rapid decrease in frequency, followed by a re-establishment of the drift. This is best shown in the plot for the 10 µl injection.

7.3.2 CO_2 Peak

The peak profiles for the CO_2 absorption are similar to those obtained previously for diethanolamine and are shown in Figure 70. The drift is in a negative direction and is re-established after about 2 minutes. At higher concentrationssthe peak width becomes narrower.

7.4 The Effect of Flow Rate on the Response

The effect of changing the flow rate was determined for a crystal coated on one electrode. The carrier gas flow rates used were 25 cm^3/min, and 10 cm^3/ min as measured at the flow meter, but owing to stream splitting through the cell D, at the crystal the flow rates were 12.5 and 5 cm^3/min. A flow rate of 50 cm^3/min produced too great a drift for any measurements to be made.

Figure 68 Successive Injections for CO

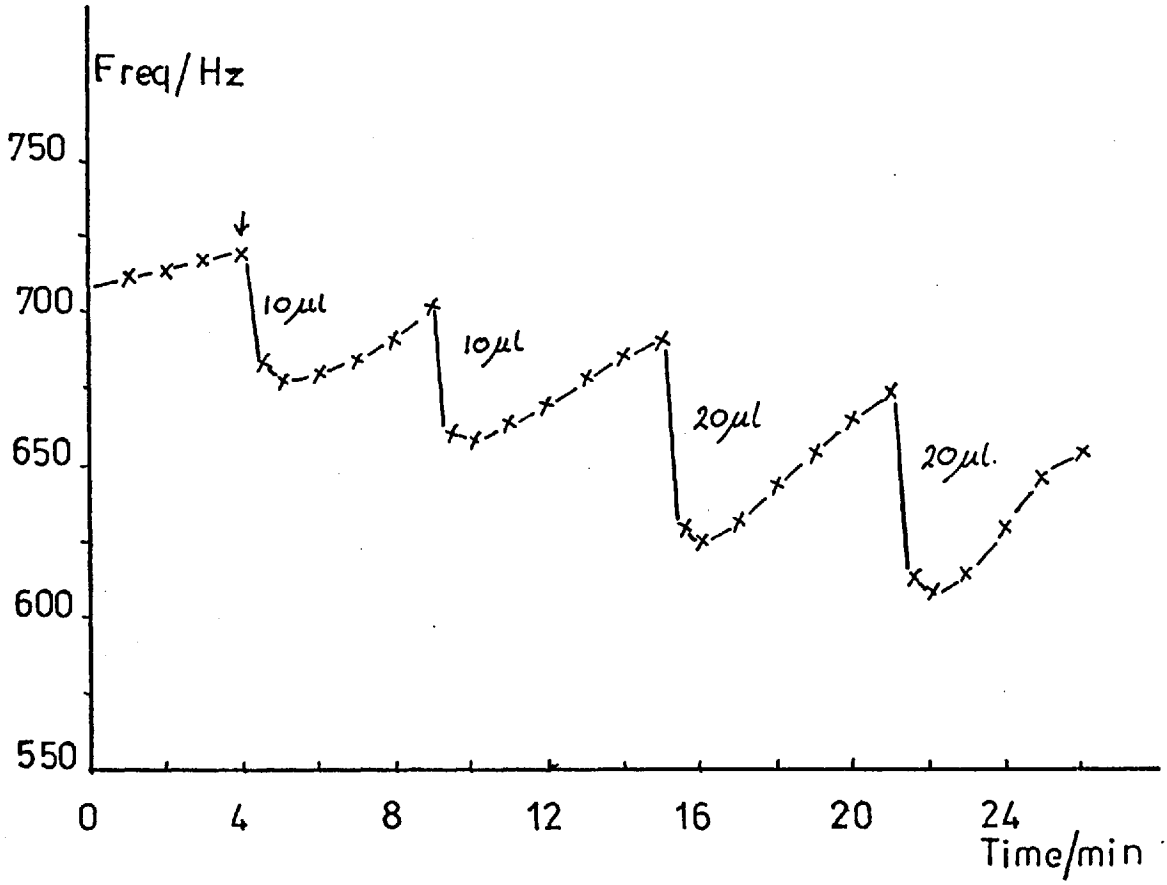

Figure 69 Peak Profiles for Liberated Mercury

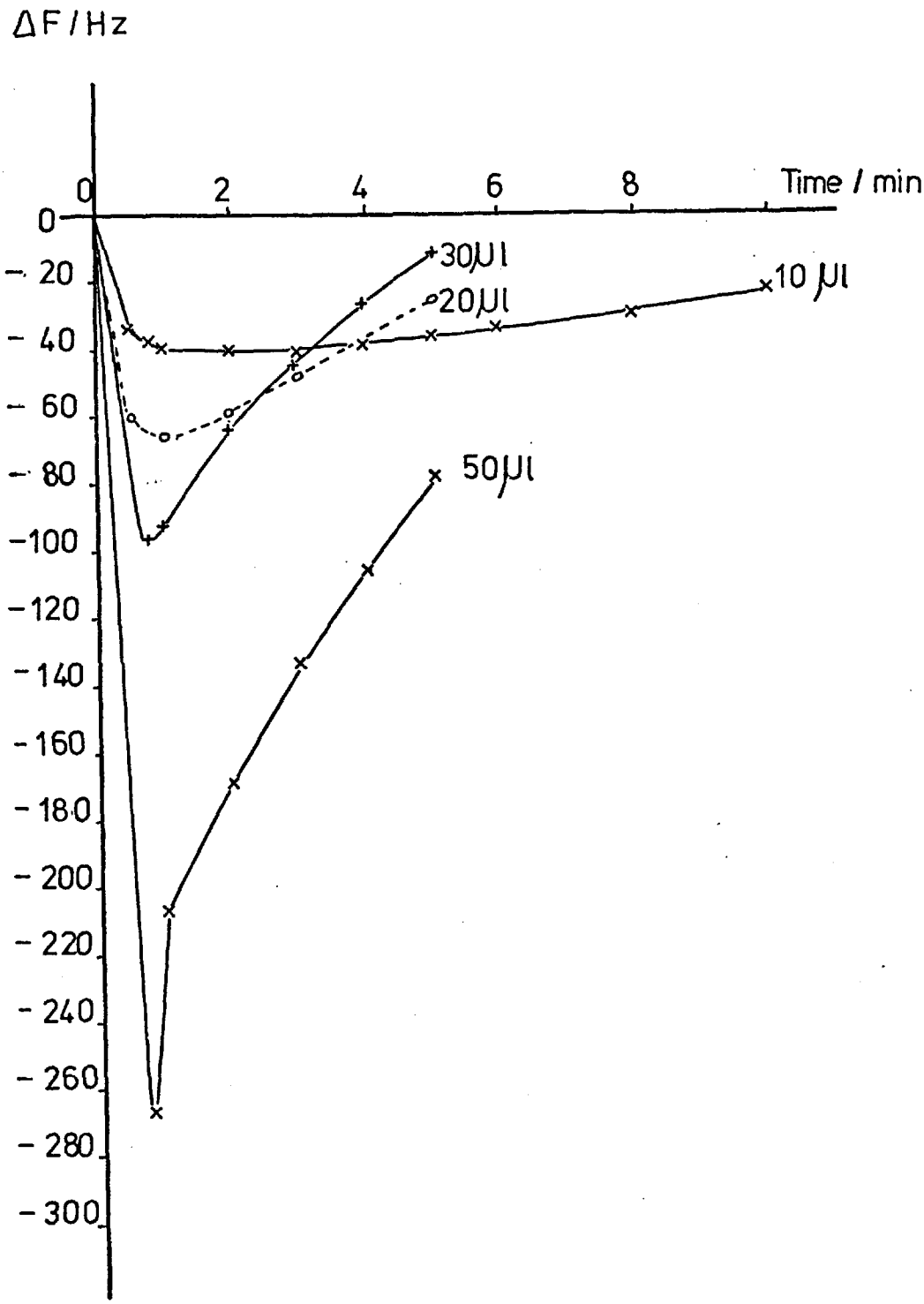

Figure 70 Peak Profiles for Liberated CO_2

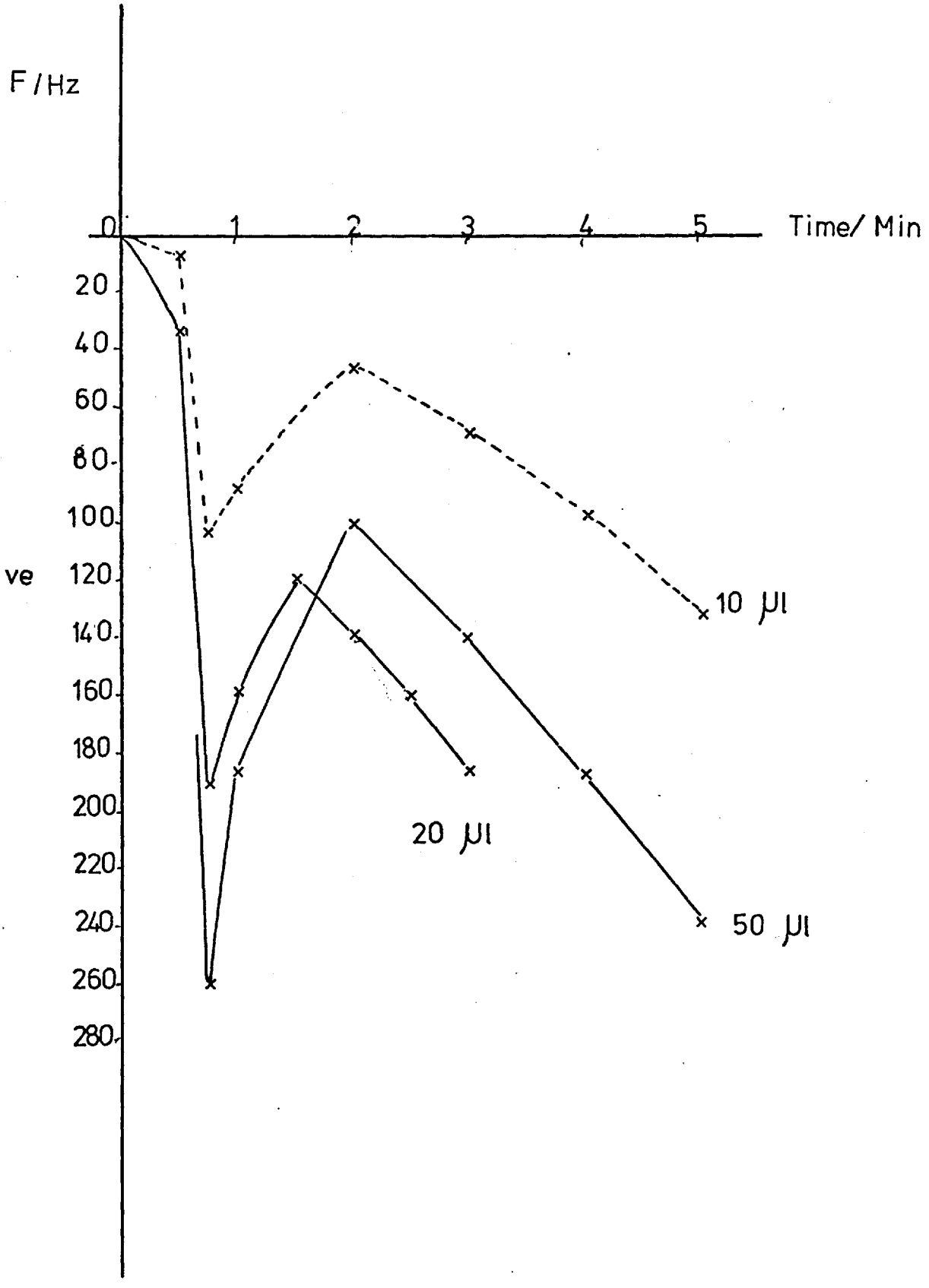

The results are given in Table 59

Table 59 The Effect of Flow Rate on Response

		ΔF_c = - 9068 Hz
Flow Rate /cm^3/min	Injection Size/µl	Response/Hz
25	10	- 137, - 98
	20	- 192, - 185
	30	- 246, - 222, - 233
	50	- 337, - 313
10	10	- 135, - 129
	20	- 210, - 238
	30	- 253
	50	- 349, - 275, - 303
	5	- 77

Reduction of the flow rate was found to have little effect on the response, which would indicate that the critical point in the system is the reaction furnace. If considerable dilution was occurring in the gas line between the reaction furnace and the cell, a faster flow rate should enhance the response.

The maximum frequency drop occurs after 45s with this system as compared with 15s with the diethanolamine system, and this suggests that a sample'hold-up' is occurring in the reaction furnace.

7.5 The Effect of Gas Pressure on the Response

A crystal coated on one electrode was calibrated at a carrier gas pressure of 1.4×10^4 N/m^2 and 3.5×10^4 N/m^2, keeping the flow rate constant at 25 cm^3/min.

The results are given in Table 60 and Figure 71.

Figure 71 Effect of Carrier Gas Pressure on Response

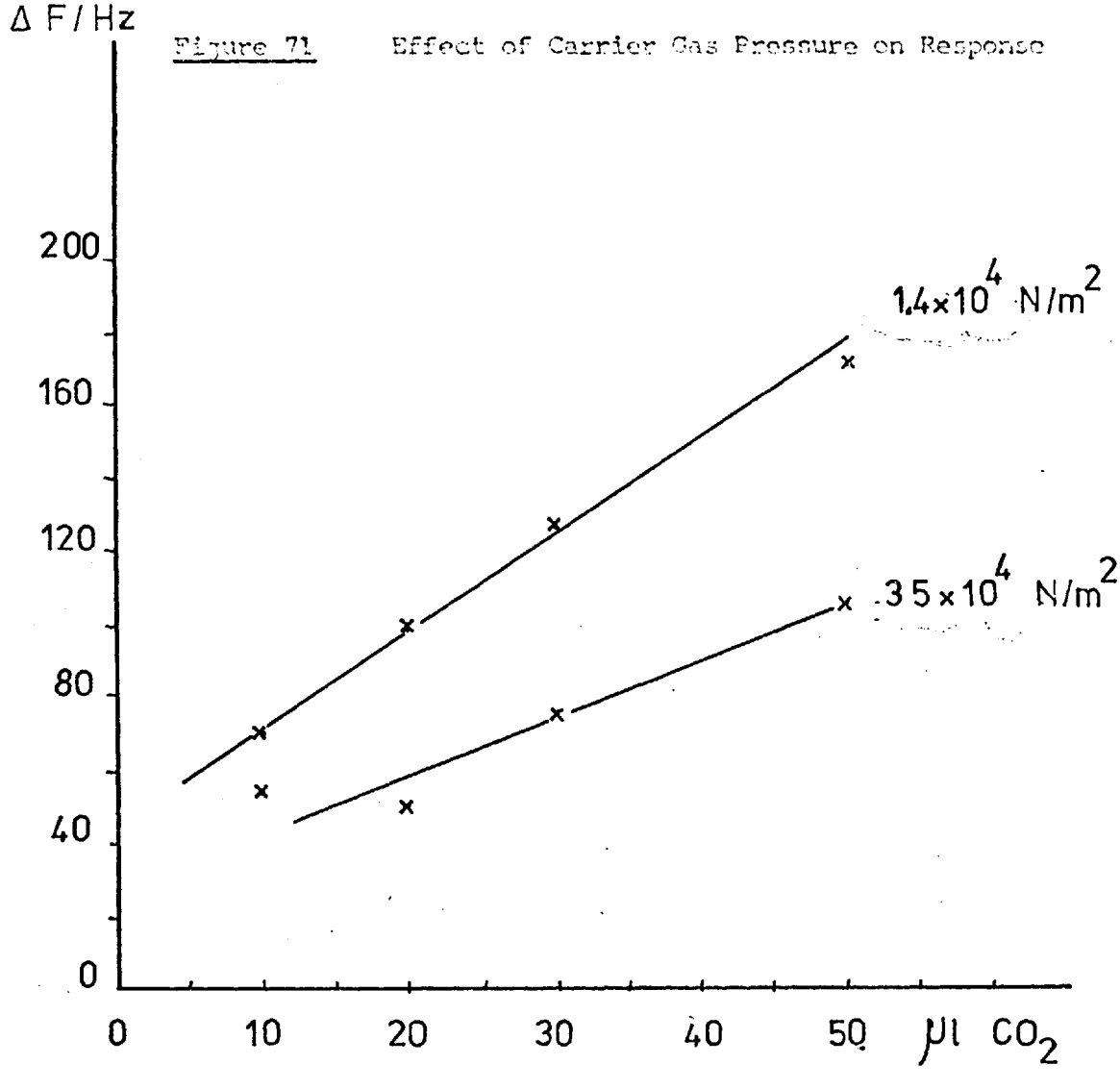

Table 69 The Effect of Pressure on the Response

$\Delta F_c = -25050$

Pressure/ N/m^2	Injection Size/Ul	Response/Hz
1.4×10^4	10	- 75, - 62
	20	- 96, -100
	30	-128, -126
	50	-167, -173
	100	-231, -245
3.5×10^4	10	- 57, - 54
	20	- 50, - 51
	30	- 72, - 79
	50	-108, -100
	100	-167

Both plots are linear and the best responses are obtained for the lower gas pressure.

7.6 Sensitivity

The best sensitivity obtained during this study was 77 ppm. However, this was for a crystal which was only coated on one electrode, and had it been coated on both sides the sensivity should be improved by a factor of 2. The use of long sample presentation should improve it still further.The value of 77 ppm is below the recommended exposure limit of 100 ppm for an 8 hour exposure. If all the parameters were optimised, the system is of potential use for pollution monitoring.

Chapter 8 Conclusion

In the preceding chapters, the development of the piezo-electric quartz crystal and its application to atmospheric pollution monitoring have been discussed. The range and versitility of the crystal detector was shown by a brief review of the current literature. Consideration of the literature revealed that the area of CO and CO_2 had not been covered, and consequently, this study was devoted to the application of the crystal detector to the determination of these two gases.

A working experimental system is described for both static and dynamic studies. For the dynamic studies nitrogen was used as a carrier gas, and the gas samples were injected into it, through an injection port. It was envisaged that eventually, this carrier gas/ sample injection system would be replaced by air pumped through the system. Owing to the necessity of injecting the sample,'real air' samples could not, unfortunately, be analysed, since the dilution by the carrier gas rendered the final concentrations of CO and CO_2 below the detection limits for the coatings. The coatings did prove sensitive enough for atmospheric levels of the gases and should give a reasonable method for their detection once the nitrogen is replaced by air. ie. 10 µl of concentrated CO_2 was diluted to 5000 ppm in the cell, which means that 10 µl air sample,containing approximately 300 ppm CO_2 would be diluted to 1.5 ppm.

The experimental system proved to be reliable and was free from mechanical failure. The only problem encountered was with the electrical system - the soldered connections between the oscillator circuit and the coaxial cable to the digital counter, tended to work

loose, owing to continual movement of the circuit and leads during the removal and replacement of the crystal in the cell. The crystal was the most fragile piece of the equipment and was most at risk during the coating technique for solids, when it was removed from the base for coating. The crystal had to be replaced in the phosphor-bronze clips with tweezers and great care had to be exercised during this procedure to prevent the edges of the crystal from snapping. Once in the cell, the crystal was well protected and had an indefinite lifetime.

The coatings caused the main problems in the study, in particular, the solid coatings. The solid coatings were the hardest to apply to the crystal and it was very difficult to obtain reproducible coatings. The solids deposited from solution, gave rise to irregular deposits which were often in the form of a ring with minimal coverage at the centre.Attempts to fill in the centre of these rings by depositing a further aliquot of the sample into the ring, proved unsuccessful, and usually caused the crystal to stop oscillating. The use of latex to glue solids to the crystal was more reliable, in that similar areas of deposition could be obtained. The main disadvantage was that only a limited quantity of the solid would adhere to the latex, but often exceeded the conditions required for the oscillation of the crystal. Coatings on latex, were not studied extensively, since it was found that the solids used gave little,or no,interaction with CO or CO_2.

The gas chromatography liquid stationary phases were far more successful. The coatings were easier to apply and gave better responses towards the gases. The main problems associated with these coatings was a tendency to bleed from the coating and to creep across the electrodes. Studies were carried out to investigate the effect of

temperature on the drift of the crystal. The drift was a function of the bleed rate of the coating and temperature, and lowering the temperature affected the drift pattern of the coating. In general, there was an improvement in the drift at lower temperatures, which is to be expected from a consideration of the vapour pressure of the liquids. The coating bleeds from the crystal in order to exert a vapour pressure in the cell.The equilibrium between the liquid and the vapour is disturbed by the carrier gas which causes an enhancement of the drift. The vapour pressure is inversely proportional to the temperature, and hence lowering the temperature has a favourable effect. This may,however, create other problems with regard to the response of the coating. Diethanolamine gave a lower response at lower temperatures for CO_2 , but triethanolamine gave an improved response towards CO_2. In both cases the recovery time for the coating was longer at the lower temperatures.

In general, the liquid stationary phase coatings were found to be more suitable for the following reasons:-

1) Liquid phases are easier to apply and are more reproducible than solids.
2) Liquid phases are more easily removed from the crystal when tailoring the frequency change on coating.
3) The sensitivity is usually better for liquid phases.
4) The reactions usually undergone by gas chromatography substrates are reversible.
5) Liquid coatings are not so likely to give rise to the high frequency effect.

The two main coatings studied were diethanolamine and triethanolamine. Both coatings could detect CO_2 , and the latter could determine levels well below atmospheric concentrations.

CO was determined below the threshold level by converting it to CO_2, using the mercury oxide reduction technique, followed by analysis of the CO_2 using a crystal coated with diethanolamine.

The equations relating the frequency change to added mass were derived, and applied to the coatings. The basic assumption made in deriving the equations was that the coating was a thin uniform layer. In practice, this was difficult to achieve particularly with the solid coatings. The solid coatings gave rise to an anomalous high frequency effect, whereby either on coating or sample presentation the frequency change was an increase instead of the expected decrease, predicted from the equations. The results of several experiments into the high frequency effect are given, and it is suggested that the cause of the effect may lie partly with the mass/area of the deposit. It seems likely that a critical mass/area of the deposit is reached and the crystal changes from being 'mass' controlled to being 'stiffness' controlled.

The high frequency effect may have a direct application to crystal detectors. Although, the author found that the high frequency response corresponded in magnitude to the expected low frequency response, a co-worker found that the response was improved by the high frequency effect.(88)

The best sensitivity obtained for each coating is given below.

Coating	Gas	Concentration/ppm
I_2O_5	CO	113
NaOH	CO_2	64
Triethanolamine	CO_2	256
Diethanolamine	CO_2	4
	CO	77

The sensitivity was found to be dependent on the mass of the coating, the area of the coating and the number of sides of the crystal that are coated, the temperature and the gas flow. If the mass of the coating is maximised and the area minimised, on both electrodes of the crystal then the sensitivity will be improved. Parameters such as temperature and flow rate need to be optimised for each coating/pollutant system. The triethanolamine/CO_2 system could be improved by operating at lower temperatures with the use of a water cooled cell. As has already been mentioned, the diethanolamine/HgO/CO system could be considerably improved by the use of a crystal coated on both electrodes with diethanolamine and by using long sample presentation.

By optimisation of the diethanolamine system, detection limits below the ppm level should be obtainable for CO_2 ,and below 10 ppm for CO. In absolute units this is, for a 10 μl injection and a 2 cm^3 cell, a detection limit of 7.9×10^{-3} mg/l for CO_2 and 9.7×10^{-2} mg/l for CO.

The main disadvantage for the diethanolamine system was that the lifetime of the coating was of the order of a few days and the sensitivity decreased rapidly from day to day. The use of spraying techniques to provide a reproducible coating techniques would overcome this problem. Once coatings can be made in a reproducible manner the crystal could be freshly coated each day with only the minimum time spent on calibration.

With both of the coatings there is the problem of interferents. No study was made of the interferents, but a few are quoted from the literature. For triethanolamine, ammonia interferes at concentrations of 1000 ppm, nitrogen dioxide at 1 ppm, sulphur dioxide at 1 ppb,(79) carbon monoxide at 6600 and moisture in trace amounts. Moisture interferes with diethanolamine and it is reasonable to expect that

sulphur dioxide and nitrogen dioxide will also interfere. It is possible to filter these pollutants from the atmosphere and it is not envisaged that this would cause too much of a problem.

The object of the study was to find a suitable coating for use with the crystal detector which would give reproducible responses towards CO and CO_2 . Triethanolamine has been proved to be suitable for analysing CO_2 in high concentrations. Diethanolamine gives greater sensitivity towards CO_2 and can be used in conjunction with the HgO reduction method for CO.Although limited work was carried out with the HgO reduction method it has been shown to have potential for atmospheric CO pollution monitoring.Both of the coatings could also be used as gas chromatography detectors.

The main area for further study with the quartz crystal detector is in the field of the coatings. There is a need for specific coatings and probably the best method of selecting them would be to screen potential coatings for a range of gases. It might be possible to tailor coatings to ensure a greater degree of specificity, as for example was attempted by adding solids to triethanolamine. The possibility of using polymers with specific properties and the chemical treatment of the quartz or gold to give sorption sites could be studied. Greater control over the form of the coating - area, mass, shape, thickness etc.- is needed, and until a coating can be made reproducible, the crystal detector is limited in its applications.

The other area for study is the high frequency effect. The actual cause needs to be determined so that it is predictable and may then have an application to crystal detectors, whereas,at the moment, it is to be avoided.

Errata

Page	
2	Line 14 for are read area.
25	Line 22 for is the removed read is then removed.
26	Line 9 for dection limit read detection limit.
38	Line 9 for that Y cut crystals read than Y cut crystals.
49	Line 1 for are of read area of.
98	Line 17 for srystal read crystal.
108	Line 24 for rection read reaction.
119	Line 8 for pastle read pestle.
172	Line 30 for prepaing read preparing.

Bibliography

1. Bach,W., "Atmospheric Pollution", McGraw-Hill Problem Series in Geography, McGraw-Hill, New York, 1972.
2. Haagen-Smit,A.J., Sci. Amer., 210, (1964), 25.
3. World Health Organisation, "Air Pollution", W.H.O., Monograph Series No. 46, W.H.O., Geneva, 1961.
4. Seiler,W. and Junge,C., J. of Geophys. Res., 75, (1970), 2217.
5. Newell,R.E., Sci. Amer., 224, (1971), 32.
6. Hamblin,L., "Pollution: The World Crisis", Tom Stacey Ltd., London 1970.
7. Commoner,B., "Science and Survival", Ballantine Books, New York, 1963, quoting, President's Science Advisory Committee, "Restoring the Quality of Our Environment", Washington, D.C.: Government Printing Office, Nov. 1965.
8. Parker,A., Proc. Inst. Chem. Engrs., 3, (1954), 99.
9. Laverick,B., Ed. "Industrial Pollution Control Yearbook 1976", Industrial Newspapers Ltd.,Redhill, 1976.
10. Patty,F.A., Ed. "Industrial Hygiene and Toxicology", Volume II, Interscience, New York, 1962.
11. Henderson, et al., J. of Ind. Hyg., 3, (1921), 79, 137.
12. Jones,G.W., et al., U.S.Bureau of Mines Reports of Investigations, Serial 2539, Oct. 1923.
13. Jech,J. and Ubl,Z., Chemical Abstracts 82, (1975), 102644, quoting Cesk. Hyg., 19(10), (1974), 470.
14. Lawther,P.J. et al., Ann. Occup. Hyg., 5, (1962), 241.
15. Betteridge,D. and Hallam,H.E., "Modern Analytical Methods", The Chemical Society Monographs for Teachers No. 21,

London, 1972.

16. Smith, R.G., et al, Health Lab. Sci., 10, (1973), 349.

17. Palanos, P.N., Anal. Instrum. 10, (1972), 117.

18. Dubois,L. and Monkman, J.L., Mikrochim. Acta, 2, (1970), 313.

19. Fensom, A., Anal. Abstrs., 21, (1971), 3819, quoting, Lab. Pract. 20(1), 49, 52.

20. Scheinberg, I.S., Brit. Pat. 1,369,067, date applied 20.10.71.

21. Bell, D.R., et al, Anal. Chim. Acta, 77, (1975), 245.

22. Lysys, I., et al, Anal. Chem. 31, (1959), 902.

23. Lambert, J.L. and Wiens, R.E., Anal. Chem. 46, (1974), 929.

24. Cole, J.W., et al, Anal. Chim. Acta, 2, (1948), 115.

25. Narita, H., Chemical Abstracts, 82, (1975), 102703, quoting Japan 7427,477, 18.7.74.

26. Katz,M., et al, Canad. J. Chem., 34, (1956), 1719.

27. Lindsley,C.H. and Yoe,J.H., Anal. Chim. Acta, 3, (1949), 445.

28. Lamb,A.B., et al, J. of Ind. Engr. Chem. 12, (1920), 213.

29. Mond,L., et al, J. Chem. Soc., 57, (1890), 749.

30. Komofuchi,Y. and Takahashi,Y., Chemical Abstracts, 81, (1974), 158207, quoting Japan Kokai (1974), 18,785.

31. Ciuhandu,G. and Bockel,V. Anal. Abstrs. 21, (1971), 3453. quoting Chim. Analyt. 52(5), (1970), 525.

32. Agranov, K.I., et al, Anal. Abtrs., 24, (1974), 2269. quoting Prib. Sist. Upr. (1973), 3, 37.

33. Holm-Jensen,I. Anal. Chim. Acta, 29, (1963), 365.

34. Van Nieuwenburg,C.J. and Hegge,L.A., Anal. Chim. Acta 5, (1951), 68.

35. Bates,R.G. and Hetzer,H.B., Anal. Chem. 33, (1961), 1285.

36. Swick,R.W., et al, Anal. Chem. 24, (1952), 2000.

37. Vurek,G.G., et al., Anal. Chem. 47, (1975), 765.

38. Scarano,E. and Calcagno,C., Anal. Chem. 47, (1975), 1055.

39. Snoek,O.I. and Gouverneur,P., Anal. Chim. Acta, 39, (1967), 463.

40. Cady,W.G., "Piezoelectricity", McGraw-Hill,New York, 1946.

41. Mason,W.P., "Piezoelectric Crystals and Their Application to Ultrasonics", Van Nostrand, New York, 1950.

42. Heising, R.A., "Quartz Crystals for Electrical Circuits." Van Nostrand, New York,1946.

43. King,W.H., Research and Development,20(5), (1969), 28.

44. Khan,G.M., Rev. Sci. Instrum. 43,(1972), 117.

45. Sauerbrey,G.Z., Z.Physik, 155, (1959), 206.

46. Sauerbrey, G.Z., Z.Physik, 178, (1964), 457.

47. King,W.H., Anal. Chem. 36, (1964), 1735.

48. Eschback,H.L. and Kruidhof,E.W., Vac. Microbal. Tech. 5, (1965), 207.

49. Janghorbani,M. Ph.D. Thesis,Oregon State University,1972.

50. Stockbridge,C.D., Vac. Microbal. Tech. 5, (1965), 193.

51. Lostis,P., Ph.D. Thesis 1958, quoted from Edmonds,T.E., Ph.D. Thesis University of London, Imperial College, 1975.

52. King,W.H., Research and Development, 20(4), (1969), 28.

53.Van Dyke,K.S., U.S.Patent. 2,571,171, Oct. 1951.

54. Lostis,P. Ph.D. Thesis, Faculty of Science, University of Paris, 1958.

55. Lostis,P. J.Phys. Rad. 20, (1959), 25S.

56. Oberg,P. and Lingensjo,J., Rev. Sci. Instrum. 30, (1959), 1053.

57. McKeown,D., Rev. Sci. Instrum. 32, (1961), 133.

58. Unterkofler,G.J. and Verderber,R.R., Rev. Sci. Instrum. 34, (1963),820.

59. Klerk,J. and Kelly,E.F., Rev. Sci. Instrum. 36, (1965), 506.

60. Haller,I. and White,P., Rev. Sci. Instrum. 34, (1963), 677.

61. Monchy,C., VIDE 27 (1972), 264, 10RN162.

62. Shiojiri,M., et al, Jap. J. Appl. Physics, 8, (1969), 783.

63. King,W.H. and Corbett,L.W., Anal. Chem. 41, (1969), 580.

64. Fischer,W.F. and King,W.H., Anal. Chem. 39, (1967), 1265.

65. Littler,R.L., U.S.Patent, 3,253,219 May 24the 1966.

66. Wade,W.H. and Slutsky,L.J., Vac. Microbal. Tech., 2, (1962), 115.

67. Slutsky,L.J. and Wade,W.H., J.Chem. Phys. 36, (1962), 2688.

68. Stockbridge,C.D., Vac. Microbal. Tech. 5, (1965), 147.

69. Wade,W.H. and Allen,R.C., J.Colloid Interface Sci., 27, (1968), 722.

70. Florio,J.V., J.Apl. Physics., 39, (1968), 3121.

71. King,W.H., Vac. Microbal. Tech. 8, (1971), 183.

72. King,W.H., U.S.Patent 3,427,864 Feb. 18th 1969.

73. King,W.H., U.S.Patent 3,266,291 Aug. 16th 1966.

74. King,W.H., U.S.Patent 3,164,000 Jan. 5th 1965.

75. King,W.H. U.S.Patent 3,260,104 Jul. 12th 1966.

76. Crawford,H.M., et al, Anal. Instrum. (1964) 105

77. Crawford,H.M., U.S.Patent 3,327,519 Jun. 27th 1967.

78. Gjessing,D.T., et al., Electron. Lettrs., 3, (4), (1967), 157.

79. Williamson,J.A. and Janzen,D.W., Analysis Instrum. 10, (1972), 175.

80. Guilbault, G.G. et al.,Environ. Lettrs. 2 , (1971), 35.

81. Lopez Roman,A. and Guilbault,G.G., Analyt. Lettrs. 5(4), (1972), 225.

82. Frechette,M.W., et al., Anal. Chem. 45, (1973), 1765.

83. Frechette,M.W. and Fasching,J.L., Environ. Sci. Tech. 7, (1973),1135.

84. Karmarkar,K.H. and Guilbault,G.G., Anal. Chim. Acta, 71, (1974),419.

85. Karmarkar,K.H., et al., Environ. Lettrs. 8(4), (1975), 345.

86. Cheney,J.L. and Homolya,J.B., Analyt. Lettrs., 8(3), (1975), 175.

87. Hartigan,M.J., Ph.D. Thesis University of Rhode Island, 1971.

88. Street,D.C., Ph.D. Thesis University of London, Imperial College, 1975.

89. Pribil,R. Private Communication.

90. Karmarkar,K.H., et al., Anal. Chim. Acta, 81, (1976), 265.

91. Karmarkar,W.H. and Guilbault,G.G., Anal. Chim. Acta, 75, (1975),111

92. Bristow,Q., J. Geochem. Explor., 1, (1972), 55.

93. Scheide,E.P. and Taylor,J.K., Environ. Sci. Tech., 8, (1974), 1097.

94. Scheide,E.P. and Taylor,J.K., Anal. Chem. (1976), 296A.

95. Note. Environ. Sci. Tech. 9(10), (1975), 902.

96. Karasek,F.W. and Gibbins,K.R., J. of Chromat. Sci., 9, (1971), 535.

97. Karasek,F.W. and Tiernay,J.M., J. of Chromat., 89, (1974), 31.

98. Guilbault,G.G. et al., Anal. Chim. Acta, 58, (1972), 421.

99. Guilbault,G.G., Anal. Chim.Acta, 39, (1967), 260.

100.Scheide,E.P. and Guilbault,G.G., Anal. Chem. 44, (1972), 1764.

101.Edmonds,T.E., Ph.D. Thesis University of London,Imperial College 1975.

102.Earp,R.B.W., Ph.D. Thesis University of Alabama 1966.

103.Janghorbani,M. and Freund,H., Anal. Chem. 45, (1973), 325.

104.Janghorbani,M. and Freund,H. Anal. Chem. 46, (1974), 621.

105.Olin,J.G., et al., Amer. Ind. Hyg. Assoc., 32, (1971), 209.

106.Olin,J.G. and Sem,G.J., Atmos. Environ. 5, (1971), 653.

107.Chuan,R.L., Anal. Meths.Appl.Air Pollution Meas.(1974), 163.

108.Mieure,J., Ph.D. Thesis University of Texas, 1968.

109.Mieure,J. and Jones,J.L., Talanta, 16, (1969), 149.

110.Jones,J.L. and Mieure,J., Anal. Chem. 41, (1969), 484.

111.King,W.H., U.S.Patent 3,329,004 Jul. 4th 1967.

112.Buck,R.P., et al., Anal. Chem. 37, (1965), 116.

113.King,W.H., Environ.Sci. Tech., 4, (1970), 1136.

114.Saltzman,B.E. and Wartburg,A.F., Anal. Chem. 37,(1965), 1261.

115.Saltzman,B.E., Anal.Chem., 33, (1961), 1100.

116.Warner,A.W. and Stockbridge,C.D., Vac. Microbal. Tech. 3, (1963),53.

117.Warner,A.W. and Stockbridge,C.D., Vac. Microbal. Tech. 2, (1962),71.

118.Behrndt,K. and Love,R.W., Vacuum, 12(1), (1962), 87.

119.Smith,W.L. and Spencer, W.J., Rev. Sci. Instrum. 34, (1963), 268.

120. Wade,W.H. and Slutsky,L.J., Rev. Sci. Instrum., 33, (1962),213.

121. King,W.H. and Camilli,C.T., Anal. Chem. 40, (1968), 1330.

122. Stockbridge,C.D., Vac. Microbal. Tech., 5, (1965), 179.

123. Stockbridge,C.D., Vac. Microbal. Tech. 5, (1965), 147.

124. Stockbridge,C.D. and Warner,A.W., Vac. Microbal. Tech. 2, (1962), 93.

125. Danckwerts,P.V. and McNeil,K.M., Trans. Instn. Chem. Engrs. 45, (1967), T32.

126. Newling,W.B.S. and Marsh,J.D.F., Instn. Gas Engrs. 3, (1963), 143.

127. Danckwerts,P.V., "Gas-Liquid Reactions", McGraw-Hill,London, 1970.

128. Beckman,A.O. et al., Anal. Chem. 20, (1948),674.

129. McCullough,J.D. et al., Anal. Chem. 19, (1947), 999.

130. Hunt,F.V. "Electroacoustics", Harvard Monographs in Applied Science No. 5, J.Wiley, New York, (1954).

131. Berezkin,V.G. and Gorshunov,O.L., Anal. Abtrs. 15(8), (1968), 4532 quoting Zh. Analit. Khim. 21 (12), (1966),1487.